Transcriptomic characterization of endothelial cells from HHT and PAH patients carrying ALK1 mutations to propose new therapeutic approaches for these two vascular diseases

Tala Al Tabosh

THÈSE

Pour obtenir le grade de

DOCTEUR DE L'UNIVERSITÉ GRENOBLE ALPES

École doctorale : CSV- Chimie et Sciences du Vivant
Spécialité : Biologie cellulaire
Unité de recherche : Biologie et Biotechnologie pour la Santé

Caractérisation transcriptomique des cellules endothéliales de patients HHT et HTAP porteurs de mutations ALK1 pour proposer de nouvelles approches thérapeutiques pour ces deux maladies vasculaires

Transcriptomic characterization of endothelial cells from HHT and PAH patients carrying ALK1 mutations to propose new therapeutic approaches for these two vascular diseases

Présentée par :

Tala AL TABOSH

Direction de thèse :

Sabine BAILLY DIRECTRICE DE RECHERCHE, Université Grenoble Alpes	Directrice de thèse
Agnès CASTAN Université Grenoble Alpes	Co-encadrante de thèse

Rapporteurs :

Carine LE GOFF
CHARGE DE RECHERCHE HDR, INSERM délégation Paris Ile-de-France Centre Est
Elisa ROSSI
MAITRE DE CONFERENCES HDR, Université Paris 5 - René Descartes

Thèse soutenue publiquement le **31 mai 2023**, devant le jury composé de :

Sabine BAILLY DIRECTRICE DE RECHERCHE, INSERM délégation Auvergne-Rhône-Alpes	Directrice de thèse
Carine LE GOFF CHARGE DE RECHERCHE HDR, INSERM délégation Paris Ile-de-France Centre Est	Rapporteure
Elisa ROSSI MAITRE DE CONFERENCES HDR, Université Paris 5 - René Descartes	Rapporteure
Julien THEVENON PROFESSEUR DES UNIVERSITES - PRATICIEN HOSPITALIER, Université Grenoble Alpes	Président
David-Alexandre TREGOUET DIRECTEUR DE RECHERCHE, INSERM délégation Nouvelle-Aquitaine	Examinateur

Invités :

Alexandre Guilhem
Praticien hospitalier, Hospices Civils De Lyon
Agnès Castan
INGENIEUR DE RECHERCHE, INSERM UMR 1292

Acknowledgements

I would like to express my deep gratitude to Dr. Carine Le Goff and Dr. Elisa Rossi for evaluating my thesis manuscript, as well as Dr. Julien Thevenon, Dr. David-Alexandre Tregouet and Dr. Alexandre Guilhem for accepting to evaluate my thesis work.

I would also like to thank the members of my comité de suivi de thèse Dr. Eva Faurobert, Dr. Eric Sulpice and Dr. Nadia Cherradi for their valuable input during our annual meetings, as well as all members of the VA Cure consortium for their involvement and regular scientific feedback. Huge thanks to Dr. Sophie Dupuis-Girod, Dr. Christophe Guignabert and Dr. Ly Tu for giving me access to patient samples and for the scientific exchanges. This project would not have been possible without you.

To my supervisors Dr. Sabine Bailly and Dr. Agnès Castan, thank you very much for your tremendous support throughout my PhD. Thank you for being closely involved and always available and ready to help whenever needed. Thank you for the weekly meetings and for the random chats that turn into long scientific discussions. I have learned a lot from you throughout these years at many levels, lessons that I will hopefully always retain. I would also like to acknowledge your assistance with the cell culture and isolations whenever I was away. Agnès, thank you for always being optimistic and encouraging at moments when nothing seemed to work. You helped me get back on track more than once. Sabine, I would like to express my admiration to your dedication to research; you are truly inspiring. It has been a pleasure working with both of you, and I thank you for making it a memorable experience.

I would also like to thank Dr. Jean-Jacques Feige for encouraging me to join BAL team for my PhD and welcoming me afterwards. I extend my gratitude to all previous and current BAL team members for the wonderful working environment and team spirit they provided. I particularly thank Dr. Emmanuelle Tillet for her scientific and technical advices. Thank you very much Emma for all your help and for your reassuring words on multiple occasions. Claire, thank you for teaching me ECFC isolation early during my PhD and for being very kind, humble and caring. Aude and Nicolas R, thank you as well for teaching me HUVECs and mouse EC isolations. Nicolas R, thank you for your scientific insights, your readiness to help whenever needed and for your refreshing sense of humor. Lisa, thank you for the technical help, but more importantly for being so sweet and caring. I would also like to thank a lot Christophe Battail, Hequn Liu and Dzenis Koca for the bioinformatics analyses. Thank you very much for your patience, time and effort. Finally, thanks a lot to my fellows along this journey, Martina and Mohammad. You made this path so much easier and more enjoyable. Yasmin, although you have only joined us recently, but it has been a delight sharing the office with you and getting to know you.

Moreover, thanks to all BCI members for the welcoming and friendly atmosphere, in particular Catherine Picart, Nadia Cherradi, Nadia Alfaidy, Odile, Laurent, Josiane, Daniel, Mariela, Cathy, Caroline, Christine, Constance, and cell culture roommates Jean, Charlotte, Adria and Laura. Thanks as well to Paul and Laura for the help with the InCell Analyzer, Véronique Collin for the help with the flow cytometry experiments, Isabelle Zanotti for the administrative help on

multiple occasions and for being very caring. Special thanks to Soha and Roland for all the support and nice memories.

At the personal level, I would like to thank Alaa, my companion throughout these years abroad, who stood by me through thick and thin. Thank you for being my family here and for the wonderful memories that I shall always cherish. This experience would not have been the same without you. Rasha, the thousands of miles between us could not stop you from being always there for me. Thank you very much for all the emotional support and for being my all-time best friend. Ouidade and Hadj, you treated me like family even when I was a complete stranger to you. I don't know how to thank you enough for the kindness you offered.

I would also like to thank my older siblings, Layal, Bilal and Amani. I know I don't say that often, but I deeply appreciate everything you have done for me. They say friends are the family you choose, but if I could pick my family I would always choose you. Big thanks to my extended family, Mohammad Hallak, Nivine, Houssam, Ahmad, uncle Mohammad and tante Iman for all the love. And of course special thanks to my lovely niece Hayyouya and my crazy nephews Aboudy, Taha, Malek and Adam for making my life sweeter. I love you all so much.

Last but not least, thank you a million times mom and dad for everything. I can never repay you for what you've done for me. Everything I am, and everything that I have accomplished, I owe it to you!

Table of Contents

List of Figures

List of Tables

Abbreviations

Act: Activin

Acvlr1: Activin A Receptor Like Type 1

ADM: Adrenomedullin

ALK: Activin receptor-Like Kinase

ANGPT: Angiopoietin

AVM: Arteriovenous Malformation

BAMBI: BMP and Activin Membrane-Bound Inhibitor

BMP: Bone Morphogenetic Protein

BMPER: Bone Morphogenetic Protein-binding Endothelial Regulator

BRE: BMP responsive element

COUP-TFII: Chicken Ovalbumin Upstream Promoter-Transcription Factor II

Cre: Cyclization Recombinase

DEG: Differentially Expressed Gene

DLL4: Delta-Like Ligand 4

E: Embryonic day

EC: Endothelial Cell

ECFC: Endothelial Colony-Forming Cell

ECM: Extracellular Matrix

EndMT: Endothelial to Mesenchymal Transition

ENG: Endoglin

ERK: Extracellular Signal–Regulated Kinase

Eph: Ephrin

EMA: European Medicines Agency

ET-1: Endothelin-1

ETV: ETS Variant Transcription Factor 1

FDA: Food and Drug Administration

FDR: False Discovery Rate

FC: Fold Change

FGF: Fibroblast Growth Factor

FOXC2: Forkhead Box Protein C2

FRT: Flippase Recognition Target

FSS: Flow Shear Stress

GDF: Growth Differentiation Factor

GI: Gastrointestinal

GOF: Gain-Of-Function

GS: Glycine/Serine

GSEA: Gene Set Enrichment Analysis

HES: Hairy and Enhancer of Split

HHT: Hereditary Haemorrhagic Telangiectasia

HMVEC: Human Microvascular Endothelial Cell

HPAH: Heritable Pulmonary Arterial Hypertension

HUVEC: Human Umbilical Vein Endothelial Cell

ID: Inhibitor of Differentiation or Inhibitor of DNA binding

IKK: IκB kinase

IL: Interleukin

IPAH: Idiopathic Pulmonary arterial Hypertension

JAG1: Jagged1

JAM: Junctional Adhesion Molecule

JNK: c-Jun amino terminal Kinase

JP: Juvenile Polyposis

KLF2: Krüppel-like factor 2

KD: Knockdown

KO: Knockout

LFC: Log_2 Fold Change

LFNG: Lunatic Fringe O-Fucosylpeptide 3-Beta-N-Acetylglucosaminyltransferase

LPS: Lipopolysaccharide

LSEC: Liver sinusoidal Endothelial Cell

MAPK: Mitogen-Activated Protein Kinase

mTOR: Mammalian Target of Rapamycin

mPAP: Mean Pulmonary Arterial Pressure

NFkB: Nuclear Factor Kappa Beta

NO: Nitric Oxide

NOS3/eNOS: endothelial Nitric Oxide Synthase

Nrp: Neuropilin

PAEC: Pulmonary Artery Endothelial Cell

PAH: Pulmonary Arterial Hypertension

PASMC: Pulmonary Arterial Smooth Muscle Cell

PlGF: Platelet Growth Factor

PDGFB: Platelet-Derived Growth Factor Beta Polypeptide

PI3K: Phosphoinositide-3 Kinase

PK: Protein kinase

PTEN: Phosphatase and TENsin Homolog

PVR: Pulmonary Vascular Resistance

RBC: Red Blood Cell

R-SMAD: Receptor-Regulated SMAD

RVSP: Right Ventricle Systolic Pressure

RUNX: Runt-Related Transcription Factor 1

(sc)RNA-seq: single cell RNA-sequencing

SHH: Sonic Hedgehog

SMAD: Suppressor of Mothers Against Decapentaplegic

SOX: SRY-Box Transcription Factor

S1PR1: Sphingosine-1-Phosphate Receptor;

TBX: T-box

TIE2: Tyrosine Kinase with Immunoglobulin-like and EGF-like domains 2

TGF-β: Transforming Growth Factor β

TNFα: Tumour Necrosis Factor alpha

VEGF: Vascular Endothelial Growth Factor

VEGFR: Vascular Endothelial Growth Factor Receptor

VPF: Vascular Permeability Factor

vSMC: Vascular Smooth Muscle Cell

vWF: Von Willebrand Factor

WT: Wild-Type

Thesis summary

Activin receptor-Like Kinase 1 (ALK1) is a type I TGF-β family receptor that is predominantly expressed on endothelial cells (ECs) and binds with high affinity to bone morphogenetic proteins 9 and 10 (BMP9 and BMP10), inducing the phosphorylation of Smad1/5 transcription factors that subsequently regulate target gene expression. ALK1-mediated signaling generally promotes vascular quiescence, and heterozygous loss-of-function mutations in *ACVRL1* (encoding ALK1) are associated with the development of a rare genetic vascular disease called hereditary hemorrhagic telangiectasia (HHT). Very rarely, mutations in *ACVRL1* have also been described in heritable pulmonary arterial hypertension (hPAH). Haploinsufficiency is the current model for these two diseases.

The aim of this work was to characterize the transcriptomic response of primary *ALK1*-mutated ECs to BMP9 and BMP10 stimulation, in order to better understand the pathogenic molecular mechanisms underlying these two diseases and identify potential therapeutic targets.

Endothelial colony-forming cells (ECFCs) and microvascular endothelial cells (MVECs) carrying heterozygous loss-of-function *ALK1* mutations were isolated from cord blood of newborn HHT donors and explanted lungs of PAH patients, respectively. RNA-sequencing was performed on each type of cells compared to control counterparts following an overnight stimulation with BMP9 or BMP10. In both EC control models, BMP9 and BMP10 stimulations induced very similar transcriptomic responses with nearly no differentially expressed genes (DEGs) between BMP9 and BMP10 stimulation. Surprisingly, comparison of the transcriptome between control and *ALK1*-mutated ECFCs revealed very similar profiles, both at the baseline and upon stimulation with BMP9 or BMP10. Consistently, control and *ALK1* mutated ECFCs displayed a similar activation level of Smad1/5 by BMP9, which could not be explained by a compensation in cell-surface ALK1 levels. On the other hand, *ALK1*-mutated PAH HMVECs, derived from a sick environment, revealed, already at the baseline, a strong transcriptional dysregulations compared to controls, with >1200 DEGs. Two-factor differential expression analysis, which takes into account the two involved variables (*ALK1* genotype and BMP stimulation), identified 44 protein-coding genes with impaired regulation by BMP9 in *ALK1*-mutated HMVECs, but none in *ALK1*-mutated ECFCs. We focused on 6 of them (*LFNG*, *JAG2*, *TNFRSF1B*, *SLC6A6*, *SOX13* and *CEBPG)* and found that at least one, *LFNG,* encoding lunatic fringe, which is a modulator of Notch signaling, could be validated by RT-qPCR on *ALK1*-mutated HMVECs, ECFCs and HUVECs (Human Umbilical Vein ECs; isolated from HHT newborns).

This work reveals that *ALK1* heterozygosity does not impair Smad1/5 activation nor strongly affect the transcriptomic response to BMP9 or BMP10, which were shown to exert equivalent transcriptomic roles *in vitro*. Nevertheless, deeper bioinformatic analysis highlighted few genes exhibiting impaired regulation by BMP9/BMP10 even in newborn cells. The paucity of transcriptomic dysregulations in mutated ECFCs indicates that the overt changes observed in mutated HMVECs cannot be solely attributed to *ALK1* heterozygosity, but might additionally involve second hits (somatic mutation/ inflammation/ angiogenesis) potentially present in the

sick lungs of endstage PAH patients. In conclusion, these findings challenge the haploinsufficiency model for HHT and PAH, and favor the notion that a second hit might be necessary for driving vascular pathogenesis, while highlighting few potential therapeutic targets (like *LFNG*) that could be highly sensitive to reductions in functional ALK1 levels and might act as priming events for early disease onset.

Résumé de thèse

Activin receptor-Like Kinase 1 (ALK1) est un récepteur de la famille des TGF-β exprimé principalement dans les cellules endothéliales (CE) et qui lie avec une grande affinité les BMP (Bone Morphogenetic Protein) 9 et 10 (BMP9 et BMP10), induisant la phosphorylation des facteurs de transcription Smad1/5 qui régulent ensuite l'expression de gènes cibles. Le rôle de la signalisation ALK1 est de contribuer à la quiescence vasculaire. Les mutations hétérozygotes perte de fonction du gène *ACVRL1* (codant pour ALK1) sont associées au développement de deux maladies vasculaires rares : la télangiectasie hémorragique héréditaire (HHT) et, plus rarement, l'hypertension artérielle pulmonaire héréditaire (HTAP) dont l'haploinsuffisance est le modèle actuel. L'objectif de ce travail est de caractériser la réponse transcriptomique de CE primaires mutées pour *ALK1* après stimulation par BMP9 et BMP10, afin de mieux comprendre les mécanismes moléculaires pathogènes et d'identifier des cibles thérapeutiques potentielles.

Des CE formant des colonies (ECFC) et des CE microvasculaires (HMVEC) portant des mutations hétérozygotes perte de fonction pour ALK1 ont été respectivement isolées à partir du sang de cordon de donneurs nouveau-nés HHT et de poumons explantés de patients atteints d'HTAP. Chaque type cellulaire, ECFC et HMVEC a été stimulé pendant 18h avec du BMP9 ou du BMP10, l'ARN a ensuite été séquencé et les niveaux d'expression comparés à ceux de cellules témoins saines. Dans les deux modèles EC, les stimulations BMP9 et BMP10 ont induit des réponses transcriptomiques très similaires avec peu de gènes différentiellement exprimés (DEGs) entre les deux ligands. La comparaison du transcriptome entre les ECFC témoins et mutés par *ALK1* a également révélé des profils similaires, au niveau basal et lors de la stimulation avec du BMP9 ou du BMP10. De plus, les ECFC témoins et mutés activent de la même manière la voie de signalisation Smad1/5 en réponse au BMP9, et ce résultat n'a pas pu être expliqué par une compensation des niveaux d'ALK1 à la surface cellulaire. En revanche, les HMVEC HTAP mutées, issues d'un environnement malade, présentent de fortes dérégulations transcriptionnelles par rapport aux témoins, avec plus de 1200 DEGs à l'état basal. Une analyse de l'expression différentielle à deux facteurs, prenant en compte les deux variables (génotype et stimulation), a permis d'identifier 44 gènes codant pour des protéines avec une régulation différentielle dans les HMVEC mutées, mais aucun dans les ECFC mutées. Je me suis intéressée à 6 d'entre eux (*LFNG*, *JAG2*, *TNFRSF1B*, *SLC6A6*, *SOX13* et *CEBPG). Parmi eux,* j'ai validé LFNG, codant pour lunatic fringe, un modulateur de la voie de signalisation Notch, dans les cellules HMEVCs, ECFCs et HUVECs (CE de la veine ombilicale de nouveau-nés isolées de couples HHT) mutées pour *ALK1.*

Ce travail a révélé que l'hétérozygotie *ALK1* n'altère pas l'activation de Smad1/5 ni n'affecte fortement la réponse transcriptomique à BMP9 ou BMP10. Une analyse bioinformatique plus approfondie a cependant mis en évidence quelques gènes avec une régulation altérée dans les cellules de nouveau-nés, ce qui indique que les changements observés dans les HMVEC mutées ne sont probablement pas uniquement dus à l'hétérozygotie d'*ALK1*, mais pourrait impliquer d'autres facteurs (mutation somatique/inflammation/angiogenèse). En conclusion, ces résultats remettent en question le modèle d'haploinsuffisance pour HHT et l'HTAP, et

favorisent l'idée qu'un second facteur pourrait être nécessaire pour conduire à la pathogenèse vasculaire, tout en mettant en évidence quelques cibles thérapeutiques potentielles qui pourraient être très sensibles à la réduction des niveaux fonctionnels d'ALK1 et pourraient agir en tant qu'événements déclencheurs pour l'apparition précoce de la maladie.

Introduction

1. The blood vascular system

1.1. Vascular components and architecture

The proper functioning of all body organs fundamentally relies on the adequate supply of oxygen, nutrients and metabolites, accompanied by the removal of metabolic waste products. The cardiovascular system fulfills this role and ensures the nourishment of tissues via the blood circulation that is transferred through a vast network of blood vessels, under the pumping action of the heart. The blood vasculature is made up of five structurally distinct vessel types that carry out specific functions:

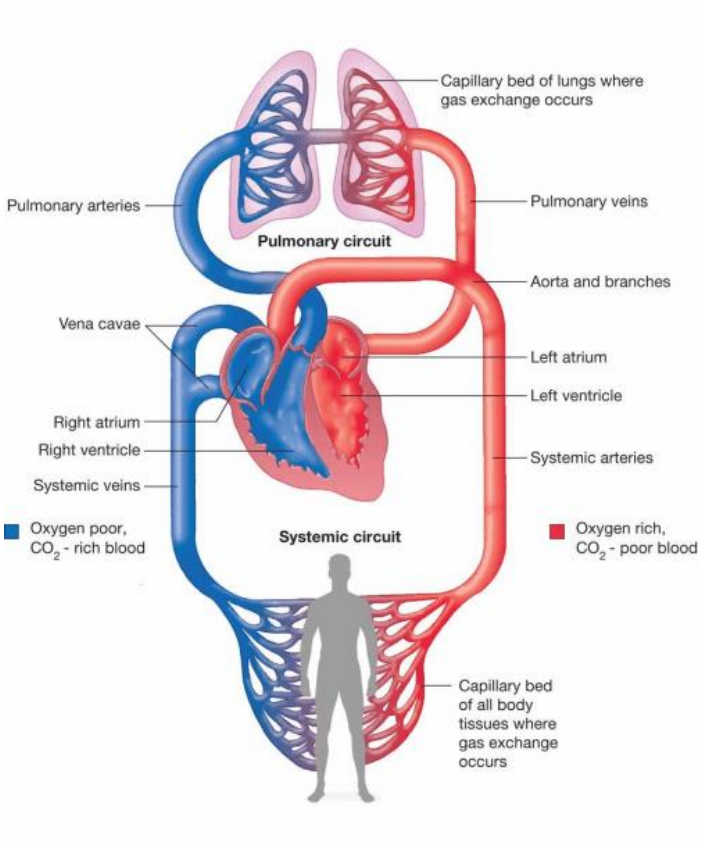

Figure 1. The systemic and pulmonary circulation systems. *The blood circulatory system is composed of the pulmonary circuit that ensures oxygenation of the blood and disposal of carbon dioxide (CO_2) in the lungs and the systemic circuit that distributes the oxygenated, CO_2-poor blood to all vascularized tissues under the pumping action of the heart. Image taken from https://difference.guru/difference-between-pulmonary-and-systemic-circulation/*

(1) arteries, which pump oxygenated blood away from the heart (with the exception of the pulmonary and umbilical arteries),
(2) arterioles, which are smaller ramifications of arteries and are the main regulators of vascular tone in response to changes in blood flow,
(3) capillaries, which are the smallest vessels and represent the sites of gaseous, nutrient and metabolic waste exchange between blood and tissues,
(4) venules, which are post-capillary small veins that receive deoxygenated blood following nutrient and oxygen exchange in tissues,
(5) veins, which are formed by converging venules and carry deoxygenated blood back to the heart (with the exception of pulmonary and umbilical veins).

Oxygen-poor blood collected from the tissues is returned through veins to the right atrium of the heart and then transferred to the right ventricle, where it gets pumped to the lungs through the pulmonary artery for oxygen replenishing (pulmonary circulation). Oxygen-rich blood returning through the pulmonary vein from the lungs into the left atrium is then transferred to the left ventricle, which pumps blood into the tissues through arteries (systemic circulation; Figure 1)[1].

In order to support each of their respective functions, the 5 types of blood vessels display different structural features, in terms of lumen diameter and wall architecture (Figure 2). Except for capillaries, blood vessel walls are composed of three layers:

(1) the innermost tunica intima, formed by a monolayer of endothelial cells (ECs), which come in direct contact with blood at the luminal side and are surrounded by a basement membrane on the basolateral one,

(2) the middle tunica media, composed of a variable number of circumferential vascular smooth muscle cell (vSMC) layers in addition to collagen and elastic fibers and

(3) the outermost tunica adventitia, also composed of collagen and elastic fibers in a loose connective tissue, in addition to fibroblasts in the large vessels, and is responsible for maintaining vessel integrity[1].

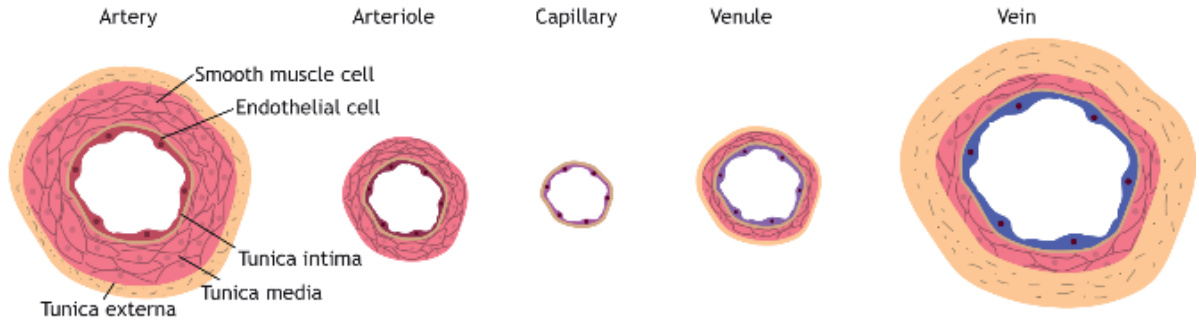

	Artery	Arteriole	Capillary			Venule	Vein
			Continuous	Fenestrated	Sinusoidal		
Pressure	↑ ↑ ↑ ↑	↑ ↑	↑			–	↑↑
Oxygen	↑↑↑	↑↑↑	↑			~	~
Velocity	↑↑↑	↑	~			↑	↑↑
Diameter/ lumen (in µm)							
Human	~4000/2000	~30/10	~8/6			~20/16	~5000/4000
Mouse	~150/50	~18/9	~5/4			~14/12	~250/150
Primary rheological function	Supply of oxygenated blood	Major site of vascular resistance	Demarcation, passive water and solute exchange	Accelerated fluid and solute exchange	Free fluid and solute exchange	Reabsorption of interstitial fluid	Collection of deoxygenated blood

Figure 2. Key structural and functional characteristics of different types of blood vessels. *With the exception of capillaries, the walls of blood vessels are composed of three layers: the tunica intima (single endothelial cell layer), tunica media (layers of smooth muscle cells) and the outermost tunica externa or adventitia composed of connective tissue and fibroblasts. To accommodate high pressure of blood received by the heart, arterial walls have more layers of smooth muscle cells in the tunica media, yet smaller tunica externa compared to veins. Compared with arterioles, venules have a thicker tunica externa, but a poorly developed tunica media, generating thinner walls and a larger lumen compared with arterioles. A comparison of rheological and functional characteristics of different blood vessels is provided. Image adapted from "Understanding angiodiversity: insights from single cell biology" by Jakab and Augustin, Development, 2020.*

The thickness of the vSMC layer of the tunica media and the relative abundance of elastic fibers varies considerably between the different types of vessels and even within arteries, which are either classified as elastic or muscularized arteries. Arteries generally possess narrower lumens, but thicker, more muscularized walls compared to veins, in order to maintain and withstand the high pressure of blood pumped by the heart. Arteries closer to the heart are more elastic, i.e. contain more elastic tissue and less vSMCs, compared to other arteries in order to maintain a relatively constant pressure gradient in response to the heart's constant pumping action[2].

On the other hand, because of the extensive branching of the vascular tree, veins receive low-pressure non-pulsatile blood flow from the venules, and thus require thinner, less elastic and muscularized walls. However, to prevent backflow of low-pressure venous blood, especially in lower and upper limbs where blood has to be delivered upwards, veins contain bicuspid valves that transiently open and shut, ensuring unidirectional flow. In addition, contracting muscles surrounding the veins, such as the skeletal muscles of the legs and contracting thoracic and abdominal muscles during respiration, aid in pumping venous blood towards the heart[2]. The walls of arterioles and venules are also composed of the three aforementioned tunics, but with much thinner media and adventitia compared to larger vessels (Figure 2).

On the contrary, capillaries lack the tunica media and adventitia described for other vessels, and are composed of a single endothelial layer, surrounded by a basement membrane. Instead of vSMCs, capillaries are surrounded by a discontinuous layer of contractile mural cells called pericytes. These cells provide physical support to the capillaries, controversially regulate capillary blood flow and take on different tissue-specific roles such as maintenance of the blood-brain-barrier, immune regulation and tissue regeneration[3]. Knowing that the flow rate of blood is inversely proportional to vessel diameter, and because the sum of the diameters of all capillaries within a capillary bed is larger than that of the feeding artery, blood flow drops as arteries branch into arterioles and further into capillaries. Thus, blood reaches the capillaries with a very low flow rate. This drop in flow rate, together with the thin wall architecture and the large surface area of the capillary, facilitate the efficient exchange of gases and metabolites between blood and the surrounding tissue through passive diffusion and pinocytosis. In order to further support tissue-specific functions and physiological needs, capillaries in different tissues

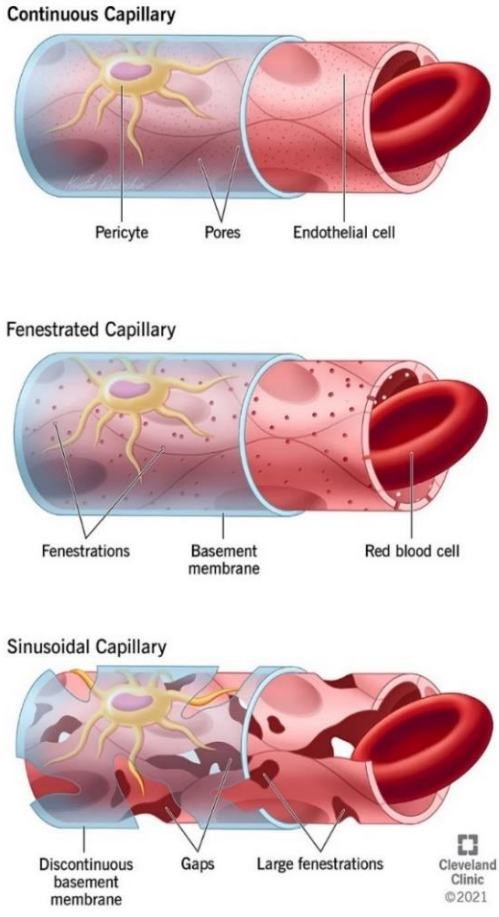

Figure 3. The three different types of capillaries. *Depending on the required tissue-specific vascular permeability, capillaries can be either continuous, fenestrated or sinusoidal, displaying different structural features. Image taken from https://my.clevelandclinic.org/health/body/21788-continuous-capillaries*

can exhibit different structural features. Depending on the level of required exchange in each tissue and consequently the degree of endothelial permeability, capillaries can be classified as continuous, fenestrated or sinusoidal[4] (Figure 3). Continuous capillaries are the least permeable and the most common type of capillaries, found for example in the lungs, heart, skin and skeletal muscles. ECs within continuous capillaries are closely attached to one another through tight junctions, but still exhibit small intercellular clefts that allow the passage of small molecules such as gases and ions across the capillary wall. Exceptionally, cerebral continuous capillaries lack these clefts and form tighter junctions at the blood-brain-barrier in order to further limit the access of molecules and protect the brain from harmful substances[4]. On the other hand, fenestrated capillaries exhibit, in addition to the aforementioned clefts, transendothelial fenestrations, that are around 60nm-wide pores that allow the passage of larger molecules. These fenestrae are particularly important in organs with active absorption and filtration functions, such as the intestinal mucosa and the kidneys, as well as in endocrine glands. In most fenestrated capillaries, the fenestrae are covered by a diaphragm composed of radially-disposed fibrils with only 5nm-wide openings, thus restricting permeability to only water and small solutes like small peptide hormones and steroids. On the other hand, kidney glomerular ECs and liver sinusoidal ECs (LSECs) have exceptional non-diaphragmed, open fenestrations. Unlike glomerular ECs that maintain a well-organized basement membrane, LSECs have a discontinuous basal lamina. Fenestrations in LSECs were also found to cluster together, forming large sieve plates. Therefore, LSECs form the third type of capillaries, called discontinuous or sinusoidal, with characteristic wide open pores. These unique features of LSECs makes the hepatic microcirculation the most porous endothelial barrier, supporting its critical scavenger role. Discontinuous capillaries can also be found in the spleen and bone marrow, allowing homing of hematopoietic progenitors to these tissues, which together with the liver represent hematopoietic sites at different stages during development[4].

1.2. Development of the blood vascular system

Being essential for the growth of all other systems, the vascular system is one of the earliest to develop during embryogenesis. The fascinating, intricate vascular network is formed through two collaborating mechanisms, termed vasculogenesis and angiogenesis. Once the developed vasculature fulfills all metabolic tissue needs, it becomes quiescent with a very low turnover rate and an estimated half-life of 6 years for normal ECs of the heart[5]. During adulthood, the quiescent endothelium is only reactivated under specific physiological conditions, such as wound healing, placentation and endometrial regeneration after menstruation, and in many pathological settings including tumorigenesis[6]. In the two upcoming sections, a description of the events taking place during vasculogenesis and angiogenesis, in addition to insights on the underlying molecular mechanisms are provided.

1.2.1. Vasculogenesis

The earliest stage of blood vessel development relies on vasculogenesis, which is a process involving a series of cell differentiation and spatial organization events leading to the formation of the primary vascular plexus. This process starts with the differentiation of stem

cells into vascular endothelial growth factor receptor 2-expressing (VEGFR2+) mesoderm under the influence of bone morphogenetic protein 4 (BMP4), Notch and Wnt signaling and via upregulation of the erythroblast transformation-specific variant transcription factor 2 (ETV2)[7]. ETV2 also induces differentiation of the VEGFR2+ mesoderm into hemangioblasts[7], the common precursors of hematopoietic and endothelial progenitors, which migrate into the yolk sac. There, under the action of basic fibroblast growth factor-2 (FGF2), hemangioblasts form aggregates that differentiate into hematopoietic and endothelial precursors. The latter, called angioblasts, localize peripherally, surrounding the hematopoietic precursors, giving rise to the blood islands. These islands then fuse to form the primitive plexus (Figure 4). Angioblasts also migrate to initiate vascular plexus formation at distant sites. In organs that do not receive angioblasts, such as the brain, angiogenesis takes over to supply this tissue with blood vessels. In the presence of VEGF, angioblasts further differentiate into endothelial cells that expand and interact with each other to form a primitive network[8,9]. This network then undergoes remodeling and maturation steps, which require interactions with extracellular matrix (ECM) components through integrins on the endothelial surface and recruitment of mural cells[9]. This gives rise to a vascular network composed of differentiated arteries, capillaries and veins, under the control of several molecular players described later in this chapter. Interestingly, with the identification of circulating endothelial progenitors in adulthood, it became evident that vasculogenesis can also occur postnatally, during which these progenitors migrate to sites of active vessel formation in response to physiological or pathological pro-angiogenic cues[8,9]. However, the main mechanism governing blood vessel formation in adults is angiogenesis.

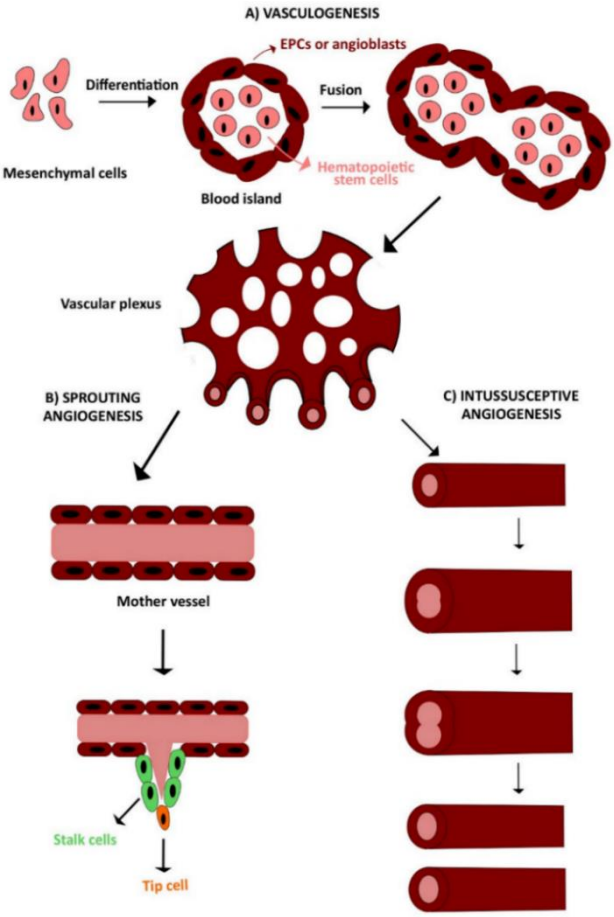

Figure 4. Vasculogenesis (A) and Angiogenesis (B-C) : central processes in vascular development. *(A) Schematic representation of vasculogenesis, defined by de novo vessel formation from aggregated endothelial precursors (EPCs or angioblasts) that assemble in the blood islands. Fusion of multiple blood islands then gives rise to the early vascular plexus from which primtive blood vessels are generated.* ***(B,C)*** *The primary vascular network expands through sprouting angiogenesis with nascent sprouts led by migrating tip cells and elongated by proliferating stalk cells* ***(B)*** *and through intussuseptive angiogenesis charcterized by splitting of a vessel in two* ***(C).*** *Image taken from "Endothelial TRPV1 as an Emerging Molecular Target to Promote Therapeutic Angiogenesis" by Negri et al, Cells, 2020.*

1.2.2. Angiogenesis

Following the formation of the primary vascular networks during embryogenesis, the vasculature further expands to support fetal and neonatal growth. This process of forming new blood vessels from pre-existing ones is called angiogenesis and also involves EC proliferation and migration, accompanied with cell and ECM reorganization. However, unlike in vasculogenesis, where vascular networks are formed *de novo* from precursor cells, during angiogenesis, new microvessels are generated from pre-existing ones either by splitting or by sprouting [8,10] (Figure 4). Sprouting angiogenesis is a tightly regulated process involving diverse molecules and signaling pathways that govern every step, starting from induction of sprout formation until assigning arterial/venous identity to newly-formed mature vessels[9]. Some key pathways involved in this process are introduced in the following section.

1.2.2.1. Key signaling pathways controlling sprouting angiogenesis

1.2.2.1.1. Vascular endothelial growth factor (VEGF) pathway

VEGF-mediated signaling is the main molecular driver of vascular development, regulating virtually all underlying key events, including the early differentiation of angioblasts during vasculogenesis and the induction of sprouting during developmental, but also pathological angiogenesis. The discovery of VEGF dates back to the early 1983, when it was first identified by Senger et al as vascular permeability factor (VPF)[11]. Six years later, two groups independently purified VEGF from different sources[12,13], gave it its current name and provided its sequence[14], which turned out to be identical to that of the previously described VPF[15].

VEGF-A is the prototypical member of the VEGF family, which later expanded to include 4 other members in mammals: placental growth factor (PlGF), VEGF-B, VEGF-C and VEGF-D. All 5 members mediate their cellular responses by binding to their cognate cell membrane-bound tyrosine kinase receptors called VEGFR1-3. The three receptors show partially overlapping expression patterns, with VEGFR1 being mostly found in monocytes and macrophages, VEGFR2 in vascular ECs and their embryonic precursors, and VEGFR3 in lymphatic ECs[16].

VEGF-A is the most important pro-angiogenic member of the family, and its responses in ECs are mostly

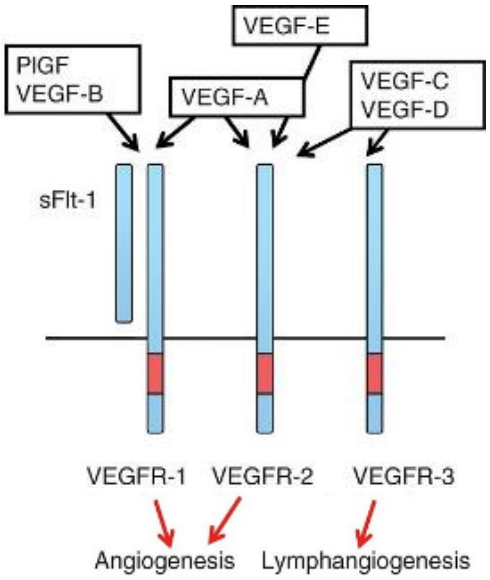

Figure 5. Specificity of VEGF ligand-receptor interactions. *VEGF-A binds VEGFR-1 and VEGFR-2, playing a major role in vasculogenesis and angiogenesis. sFlt-1, the soluble form of VEGFR-1, has an anti-angiogenic role. PlGF and VEGF-B also bind VEGFR1 and are respectively involved in placental angiogenesis and vascular survival under pathological conditions. VEGF-C and VEGF-D bind mainly to VEGFR3, regulating lymphangiogenesis, and to a lesser extent to VEGFR2. Finally, the viral VEGF-E binds to VEGFR2, promoting angiogenesis. Image adapted from "Vascular Endothelial Growth Factor (VEGF) and Its Receptor (VEGFR) Signaling in Angiogenesis: A Crucial Target for Anti- and Pro-Angiogenic Therapies" by Shibuya, Genes and Cancer, 2011*

conveyed through VEGFR2. Heterozygous and homozygous deletion of *Vegfa* and *Vegfr2* in mice, respectively, leads to embryonic lethality with hematopoietic and endothelial defects[17–19]. Different VEGF-A isoforms, generated by alternative splicing of exons 6 and 7, were identified, including $VEGF_{121}$, $VEGF_{165}$, $VEGF_{189}$ and $VEGF_{206}$. These isoforms display different affinities for their neuropilin (Nrp) co-receptors and to heparan sulfates of the basement membrane, influencing their spatial distribution in tissues[20]. Among them, $VEGF_{165}$ is the most physiologically relevant and the most abundant isoform in tissues[21]. Interestingly, some isoforms with splice sites in the last 6 amino acids of the terminal exon (exon 8) were even shown to play anti-angiogenic roles. The latter are named "b isoforms" and are denoted with a "b" preceded by the number of amino acids (VEGFxxxb)[22].

VEGF-A can also bind VEGFR1 and with higher affinity than VEGFR2, but this receptor has low kinase activity, making it a decoy receptor[23]. Alternative splicing of *VEGFR1* results in a soluble form of the receptor, known as sFlt-1 that is produced by various cell types and plays an anti-angiogenic role[24]. On the contrary, VEGF-A does not bind VEGFR3. Instead, this receptor, which is enriched in the lymphatic vasculature, binds VEGF-C and VEGF-D, promoting lymphangiogenesis. Proteolytically processed VEGF-C and VEGF-D can also play a minor angiogenic role by binding VEGFR2[24]. The remaining 2 family members, PlGF and VEGF-B, can only bind VEGFR1 and unlike other members, are both dispensable for embryonic vascular development[56] (Figure 5). However, PlGF is later involved in the development of the placental vasculature[25], and VEGF-B in driving vascular survival under pathological conditions[26] and promoting fatty acid uptake in ECs[27]. In addition to the 5 mammalian ligands of the VEGF family, VEGF-E has been described as a pro-angiogenic VEGF-related protein encoded by the Orf virus genome that specifically binds VEGFR2[28] (Figure 5). Other than VEGFRs, VEGF ligands also bind to co-receptors Nrp1 and Nrp2, which enhance VEGF signaling activity in ECs. Interestingly, these multifunctional co-receptors form complexes with a variety of receptors and are thus involved in many different signaling pathways, including those of class 3-semaphorins, platelet-derived growth factor and transforming growth factor β[29].

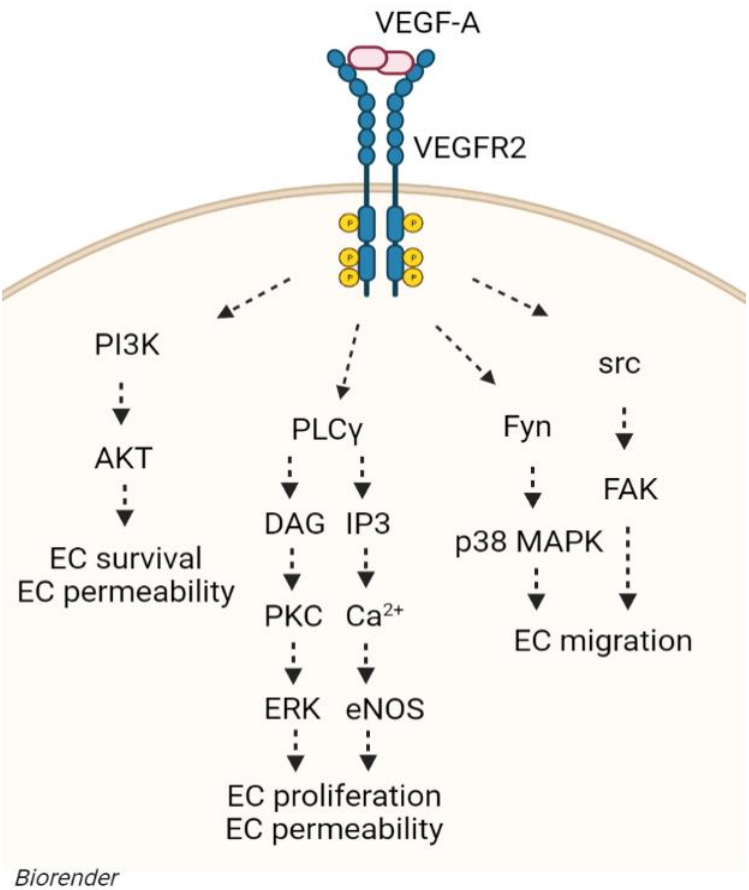

Figure 6. Key signaling pathways downstream VEGF-A-VEGFR2. *MAPK: mitogen-activated protein kinase. Remaining abbreviations are detailed in the main text. Image generated using Biorender.*

In response to hypoxia, the hypoxia inducible factor 1α (HIF-1α) binds to its response element in the promoter of VEGF-A (herein referred to as

VEGF), increasing its expression[30]. Consequently, VEGF binds to VEGFR2 on the surface of ECs, activating several pro-angiogenic signaling molecules that increase EC proliferation, migration, survival and permeability[24]. Binding of a VEGF dimer to VEGFR2 results in receptor dimerization and activation through transautophosphorylation on several tyrosine (Y) sites, including Y951, Y1054, Y1059, Y1175 and Y1214[16]. Some of these p-Y form docking sites for SH2 domain-containing proteins such as phospholipase Cγ (PLCγ), phosphoinositide 3-kinase (PI3K), SH2 domain containing adaptor protein B (SHB) and others. Binding of PLCγ to p-Y1175 leads to its phosphorylation and activation[31]. In turn, activated PLCγ hydrolyzes phosphatidylinositol (4,5)-bisphosphate (PIP2), producing diacylglycerol (DAG) and inositol 1, 4, 5-trisphosphate (IP3). DAG then activates PKC leading to the activation of the mitogenic RAF/MEK/ extracellular signal-regulated kinase (ERK) cascade that increases EC proliferation[32] (Figure 6). On the other hand, IP3 activation induces the intracellular release of Ca^{2+}, activating endothelial nitric oxide synthase (eNOS) and thus increasing the synthesis of the vasodilator nitric oxide (NO) and enhancing vascular permeability[33] (Figure 6). In parallel, activation of PI3K results in the production of membranous PIP3 that leads to recruitment and phosphorylation of protein kinase B (PKB/AKT) by phosphoinositide-dependent kinases 1 and 2[16]. Subsequently, activated AKT phosphorylates multiple downstream effectors, including Mammalian target of rapamycin (mTOR) and eNOS, increasing vascular permeability and pro-apoptotic BAD and caspase 9, leading to their inhibition and promoting cell survival[16] (Figure 6). Activation of the proto-oncogene non-receptor Tyrosine kinases Src or Yes was also proposed to increase vascular permeability by opening intercellular adherens junctions through direct or indirect phosphorylation of vascular endothelial cadherin (VE-cadherin)[16]. Src is also one of the several effectors mediating the effect of VEGF on cell migration. Src phosphorylates p-Y1175-bound SHB, which binds phosphorylated focal adhesion kinase (FAK) leading to regulation of cell attachment and migration[16]. Fyn, a member of the Src kinase family, is also recruited to phosphorylated VEGFR2 where it binds to the adaptor molecule NCK1 bound to p-Y1214. Fyn/NCK1/PAK2 complex then leads to the activation of CDC42/MEKK1/MEK3/p38 pathway that promotes EC migration[34] (Figure 6).

1.2.2.1.2. Angiopoietin-1-Tie2 pathway

Angiopoietins 1–4 (Ang1–4) constitute another family of angiogenic growth factors, whose cellular activities are mediated through the tyrosine kinase receptor Tie2, predominantly expressed on ECs. Ang1 is a Tie2 agonist enhancing the structural integrity of vessels, while Ang2 mostly functions as a Tie2 antagonist. Murine Ang3 and human Ang4 are orthologues that also bind Tie2, but their role is less characterized[35].

Ang1, the best studied member, is secreted by mural cells and acts as a vessel stabilizing agent through binding to Tie2[36]. Both *Ang1*- and *Tie2*-deficient mice display embryonic lethality and similar vascular remodeling defects defined by decreased sprouting, vessel dilation, reduced mural cell coverage and vessel rupturing. Ang1-Tie2 signaling promotes EC survival by activating the anti-apoptotic PI3K/AKT axis[37]. Ang1-Tie2 signaling also reduces vascular permeability by strengthening intercellular endothelial junctions. Specifically, Ang1-Tie2 signaling was shown to decrease phosphorylation levels of the junctional proteins VE-cadherin and platelet endothelial cell adhesion molecule 1 (PECAM1) and support their localization into junctions[38]. This pathway also displays anti-inflammatory properties, by inhibiting VEGF-induced expression of the pro-inflammatory adhesion molecules ICAM-1 and VCAM-1[39].

On the other hand, Ang2 acts as a natural antagonist of Tie2 in a context-dependent manner, and transgenic mice overexpressing *Ang2* display similar phenotypes to *Ang1*- and *Tie2*-deficient mice. Under hypoxic conditions, ECs secrete intracellularly-stored Ang2, which antagonizes Tie2 signaling, leading to vascular destabilization[40,41]. This feature is essential during the activation phase of sprouting angiogenesis. Afterwards, the decrease in Ang2 secretion shifts the Ang1/Ang2 balance back to the former, promoting vessel maturation. Tie1 is another receptor modulating Ang signaling, likely indirectly through interacting with Tie2. Loss of Tie1 *in vivo* increases vascular density and disrupts vascular integrity, highlighting its role in maintaining vascular quiescence[42,43]. In lymphatic ECs (LECs), which express low levels of Tie1, the resulting low Tie1-Tie2 interaction promotes an agonistic activity of Ang2 through binding Tie2 and activating the PI3K/AKT pathway, resulting in increased LEC survival and proliferation[44]. Interestingly, gain of function mutations in the gene coding the catalytic subunit of PI3K (*PIK3CA*) are responsible for 75.5% of lymphatic malformation cases[45]. In addition, activating somatic mutations in both *PIK3CA*[46] and *TIE2*[47], leading to excessive endothelial proliferation, are a common cause of venous malformations. Altogether, this highlights the importance of this pathway in maintaining vascular homeostasis.

1.2.2.1.3. Platelet-derived growth factor (PDGF-BB)-PDGFRβ pathway

As indicated by its name, platelet derived growth factor was initially purified from platelets, but was later found out to be secreted by a variety of cells[48]. PDGF is a potent chemoattractant, survival factor and mitogen of cells of mesenchymal origin, including pericytes, smooth muscle cells and fibroblasts[49,50]. Through its action on fibroblasts, PDGF is considered an essential promoter of wound healing[48].

There are five isoforms of PDGF that are either homodimeric (PDGF-AA, -BB, -CC and -DD) or heterodimeric (PDGF-AB) and signal through 2 structurally-related receptor tyrosine kinases PDFGRα and PDGFRβ. All five isoforms of PDGF contain a conserved PDGF/VEGF homology, domain, and just like for VEGF, PDGF binding to its receptor induces dimerization and autophosphorylation followed by signal transduction involving ERK and PI3K/AKT effectors[51], among others. PDGF-BB is secreted by ECs during angiogenesis and is responsible for recruiting and inducing the proliferation of PDGFRβ-expressing vSMCs and perciytes, which cover the nascent vessels[49]. Hence, PDGF is a key vessel maturation factor during both embryogenesis and wound healing.

1.2.2.1.4. Notch pathway

The Notch pathway is a master regulator of vascular sprouting and arteriovenous specification[52]. In mammals, this signaling pathway is mediated through 4 receptors (named Notch1 to Notch4) and 2 different families of ligands: (1) Delta-like ligands (Dll), including Dll1, Dll3 and Dll4 and (2) Jagged ligands (Jag), including Jag1 and Jag2. Endothelial cells express all Notch receptors and ligands at variable levels, with Notch1, Notch4, Dll4 and Jag1 displaying higher expression levels than others[52]. Both Notch ligands and Notch receptors are transmembrane proteins that mostly signal through trans-activation, whereby a ligand on one cell binds to its receptor on the adjacent cell, activating Notch signaling in the receptor

presenting cell. Then, ligand binding promotes sequential proteolytic cleavage events on the Notch receptor leading to the release of the Notch intracellular domain (NICD) by γ-secretase. NICD then translocates to the nucleus, where it forms a transcriptional complex with recombination signal binding protein for immunoglobulin kappa J region (RBPJk), also known as CSL, and the co-activator mastermind-like (MAML) that together regulate target gene expression[52] (Figure 7A).

The extracellular domain of Notch receptors contains several epidermal growth factor–like (EGF) repeats that are heavily glycosylated by various enzymes[53]. Among those are the 3 mammalian fringes, namely manic, lunatic and radical fringe, which represent a family of b-1,3-N-acetyl-glucosaminyltransferases. These fringes transfer N-acetyl-glucosamine moieties to O-linked fucose residues on the Notch receptor[53], enhancing the activation of Notch1 by Dll ligands while inhibiting activation by Jag ligands[54–56] (Figure 7B).

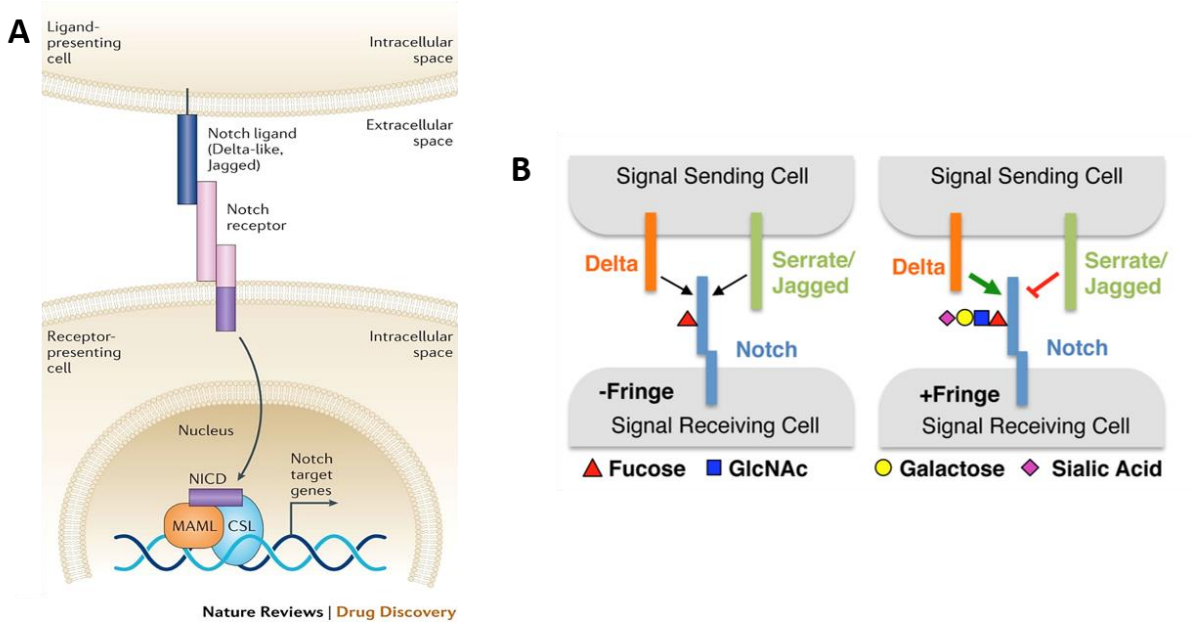

Figure 7. Activation of Notch signaling. A, *Notch receptor is activated upon binding to its ligand on an adjacent cell. Ligand binding leads to cleavage of Notch intracellular domain (NICD) that translocates to the nucleus, forms a transcriptional complex with CSL and MAML leading to regulation of Notch target genes.* ***B,*** *Before glycosylation by fringes, the Notch receptor can be activated by both Delta or Serrate/Jagged ligands. However, upon transferring N-acetyl-glucosamine (GlcNAc) to O-fucosylated sites on the extracellular domain of Notch receptor by fringes, activation of the receptor by Delta ligands is strengthened while that by Serrate/Jagged ligands is inhibited. Images taken/adapted from "Therapeutic modulation of Notch signalling — are we there yet?" by Andersson and Lendahl, Nature Reviews Drug Discovery, 2014 (**A**) and "Deciphering the Fringe-Mediated Notch Code: Identification of Activating and Inhibiting Sites allowing Discrimination between Ligands" by Kakuda et al, Developmental Cell, 2017 (**B**).*

Notch signaling is required for regulating key mechanisms during sprouting angiogenesis, namely controlling vascular branching by regulating tip/stalk cell ratios, and promoting arterial specification[52], both of which will be described in an upcoming section.

1.2.2.1.5. BMP9/BMP10-ALK1 pathway

Bone morphogenetic proteins 9 and 10 (BMP9 and BMP10) and their high affinity receptor activin receptor-like kinase 1 (ALK1) are members of the transforming growth factor-β (TGF-β) superfamily of signaling molecules. BMP9/BMP10 signaling through ALK1 in ECs is a key promoter of vascular quiescence[57]. This signaling pathway has a separate chapter dedicated to it.

1.2.2.2. Sprouting angiogenesis

Sprouting angiogenesis is the process involving the formation and extension of endothelial sprouts from pre-existing vessels, followed by anastomosis, perfusion and stabilization. This is a biphasic process involving an activation and a maturation phase[9], which are described below.

1.2.2.2.1. Activation Phase

In response to hypoxia during development or wound healing, starved parenchymal cells secrete the master proangiogenic factor VEGF to recruit adequate blood supply by directing blood vessel formation towards the hypoxic region[9] (Figure 8A). The spatial distribution of VEGF in the surrounding microenvironment promotes the differentiation and is sensed by endothelial tip cells at the vascular front through their long filopodial protrusions rich in the VEGF receptor, VEGFR2[58]. Consequently, tip cells respond by initiating directional migration towards the VEGF gradient[59] (Figure 8C). This migration is preceded by ECM degradation via matrix metalloproteinases and urokinase-type plasminogen activator, which clears the way for migrating ECs to invade the surrounding tissue, in addition to VEGF-induced increase in vascular permeability through NO-mediated vasodilation[9] (Figure 8B). The roles of these changes are to weaken EC-EC and EC-matrix interactions and to allow the extravasation of plasma proteins that build a provisional scaffold for migrating ECs[9]. VEGF or hypoxia (independently of VEGF) also loosen the interactions of ECs with mural cells[40], by enhancing the production of the Tie2 antagonist, Ang2, from ECs[60]. Once the stage is set, tip cells start to migrate through interactions of cell surface integrins, particularly αvβ3, with ECM components[61,62]. The level of this integrin is normally low in the quiescent endothelium, but NO, whose production is enhanced by VEGF, maintains adequate levels of αvβ3[63]. Then, as the leading tip cell migrates, the angiogenic sprout extends by means of VEGF-induced proliferation of trailing stalk cells[64] (Figure 8D). The growing sprouts extend until tip cells at the front interact with each other through their filopodia and fuse to form nascent vessels (Figure 8E). At this stage, cell migration stops, and lumen formation takes place through a complex process involving cell repulsion within EC cords, junctional rearrangement and changes in cell shape[9].

The molecular differences between tip and stalk cells provide instructions on how to interpret and respond to the VEGF signal. While tip cells respond to the gradient of VEGF by initiating cell migration, stalk cells respond to the local VEGF concentration by inducing proliferation[59]. Maintaining the proper equilibrium of tip to stalk cell ratios during sprouting angiogenesis is of outmost importance to ensure efficient, controlled branching. To date, several players have been implicated in regulating tip/stalk cell specification, of which Dll4-mediated Notch signaling is the most studied[52]. In response to proangiogenic VEGF signals, tip cells respond by

upregulating the Notch ligand Dll4, acquiring an invasive, migratory phenotype[65,66]. Binding of Dll4 to Notch1 on the adjacent, trailing cells activates Notch signaling and confers a stalk cell phenotype on these cells, making them less sensitive to proangiogenic VEGF signals. This effect was attributed to Notch1-mediated upregulation of target genes of the Hes/Hey family of transcription factors, which in turn downregulate *DLL4* and the VEGF receptors *KDR* (VEGFR2) and *FLT4* (VEGFR3), while upregulating the levels of the decoy receptor *FLT1* (VEGFR1)[65,66]. Imbalances in Notch signaling were reported to cause excessive or inadequate sprouting. For instance, reduction of Dll4-mediated Notch signaling during embryonic or developmental angiogenesis, either by genetic or pharmacological means, resulted in tip cell overrepresentation, leading to exaggerated sprouting[65,67–70]. On the other hand, enhanced Dll4-Notch activation reduced tip cell specification and vascular density[67]. In addition to Dll4, Jag1 was also found to be involved in regulating tip/stalk cell specification. While tip cells express high levels of Dll4 and low or no Jag1 expression, stalk cells show inverse regulation of these 2 ligands. Jag1 on stalk cells was found to act as an antagonist, where high levels of Jag1 competed with the low levels of the more potent ligand Dll4 for binding to Notch1 on tip cells, but Jag1 did not promote Notch activation. The inability of Jag1 to activate Notch signaling in tip cells was attributed to the post-translational modification of Notch1 by fringes[54]. Complete loss of lunatic fringe phenocopied Dll4 deletion in the developing retina model, highlighting an importance of this fringe in modulating Dll4-mediated effects on tip cell specification[54].

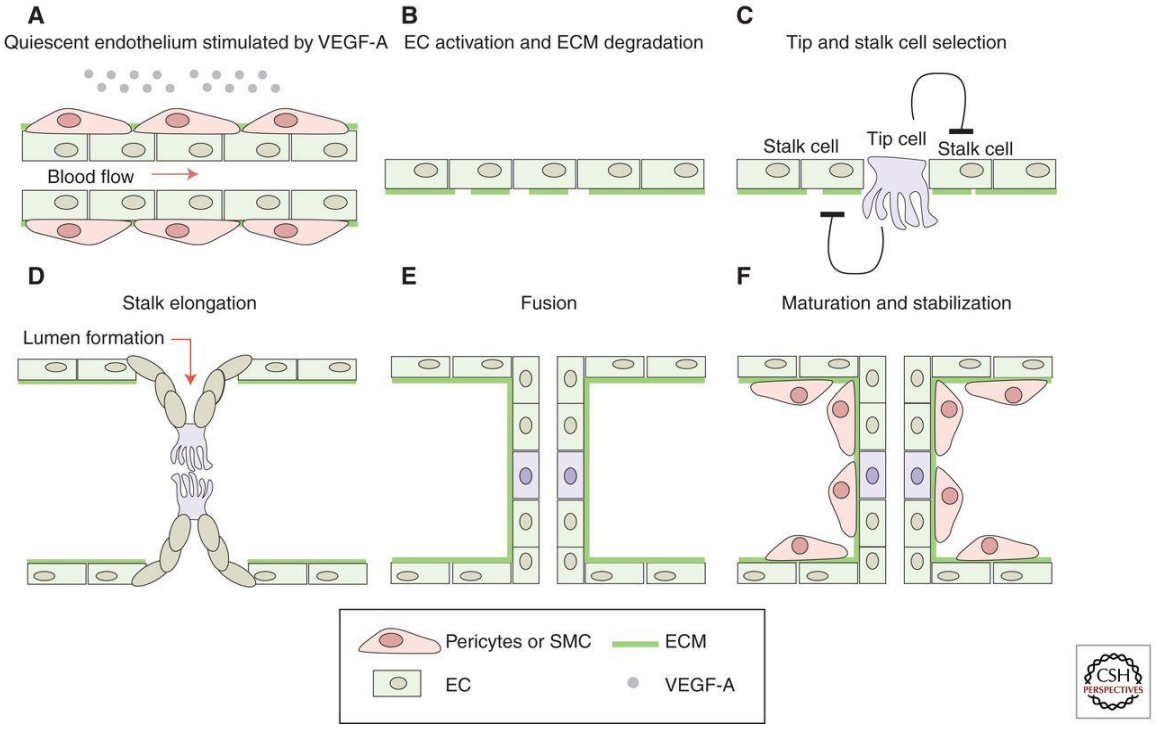

Figure 8. Sprouting angiogenesis: a multistep process. (A) *Under local hypoxic conditions, the hypoxic tissue secretes VEGF-A to activate angiogenesis, which starts with the degradation of the extracellular matrix (ECM)* ***(B)*** *accompanied with the selection of tip cells and stalk cells* ***(C)****. Tip cells on the leading front of the sprout migrate in the direction of the VEGF-A gradient that is sensed through their extensive filopodia, and the trailing stalk cells ensure elongation of the sprout by actively proliferating, while maintaining connection with the original vessel* ***(D)****. The sprout continues to elongate until it fuses with another (anastomosis), forming a nascent lumenized vessel* ***(E)*** *that becomes perfused, leading to enhanced tissue oxygenation. Consequently, VEGF-A production declines and the nascent vessel undergoes maturation and stabilization through secretion of new ECM components and recruitment of mural cells* ***(F)****. Image taken from "VEGF and Notch in tip and stalk cell selection" by Blanco and Gerhardt, Cold Spring Harbor Perspectives in Medicine, 2013.*

Similar to Notch-mutant animal models, mice deficient in ALK1 display strong hypersprouting in their developing retinas[71], and others deficient in its downstream mediators display hypersprouting from the dorsal aorta accompanied by an increase in tip cells[72], pointing to a role of ALK1 signaling in tip/stalk cell specification. Indeed, activated ALK1 and Notch were found to synergistically upregulate stalk cell-enriched Notch targets *HES1*, *HEY1*, *HEY2* and *FLT1* (VEGFR1) while downregulating the expression of the tip cell marker *APLN*[71,72]. Interestingly, blocking both signaling pathways resulted in an exacerbated hypersprouting phenotype compared to the separate targeting of each, and activation of ALK1 signaling in the retinas of pharmacologically Notch-inhibited mice drastically decreased the number of tip cells and normalized vascular sprouting[71].

Other players regulating tip/stalk cell selection include Nrp1, a co-receptor for diverse ligands, including class 3 semaphorins and VEGF-A. This tip cell-enriched receptor was shown to be important for tip cell function and guidance[73] and emerged as an active repressor of stalk cell phenotype in tip cells. On the other side, Notch activation in stalk cells downregulates Nrp1, relieving its inhibitory effect on stalk cell phenotype[74].

In addition to the aforementioned actors, a number of classical axon guidance molecules and their receptors, including ephrins, semaphorin/plexin and slit/robo families, were shown to display tip- or stalk-cell specific expression and to act as repulsive or attractive cues that reinforce tip/stalk cell specification[75].

1.2.2.2.2. Maturation phase

The newly formed vessel is leaky, fragile and requires maturation and stabilization to become fully functional (Figure 8F). This involves cessation of EC proliferation and migration, formation of a new basement membrane, recruitment of mural cells to the nascent vessel and finally determination of arterial/venous identity[76]. These complex processes are orchestrated by a plethora of tightly regulated signaling molecules.

To begin with, BMP9, the high-affinity ligand of the endothelial-enriched receptor ALK1, is a known endothelial quiescent factor that inhibits EC proliferation and migration[77]. Hence, BMP9, and its closely-related family member BMP10, could be the players responsible for establishing vascular quiescence of the activated endothelium[57]. The stationary, non-proliferative ECs establish intercellular adherens and tight junctions under the action of Ang1-Tie2 signaling[78].

At the level of structural stabilization, TGF-β1, binding to its ALK5 receptor on ECs and fibroblasts, protects the provisional matrix from degradation by suppressing the secretion of proteolytic enzymes while enhancing the synthesis of protease inhibitors. TGF-β1 in fibroblasts also increases the synthesis and secretion of ECM components that make up the basement membrane of the new vessel[79]. TGF-β1 is additionally involved in promoting mural cell coverage of the growing sprout. Following the recruitment and proliferation of mural cell progenitors driven by PDGF-B, whose expression is limited to ECs in areas of immature capillaries and growing arteries[49], TGF-β1 promotes their differentiation into pericytes and vSMCs, both of which are important elements of the mature vasculature[80,81]. Pericytes enwrap capillaries to provide structural support for these thin-walled vessels and also carry out numerous tissue-specific functions, as mentioned previously[3]. On the other hand, vSMCs are mostly components of larger vessels and are responsible for modulating vascular tone in

arteries and arterioles. By contracting or relaxing, vSMCs modify the caliber of the blood vessel, thus adjusting local blood flow according to physiological needs and controlling total peripheral resistance[1]. In addition to PDGF-B, sphingosine-1-phosphate-1 (S1P1), secreted by platelets and multiple cell types, can escape from leaky vessels, leading to recruitment of mural cells that express its receptor (endothelial differentiation sphingolipid G-protein-coupled receptor-1)[82].

Finally, as blood flow kicks in, areas with excessive vascular density undergo vascular pruning of unnecessary vessels, giving rise to a more differentiated vascular network[10]. Blood flow is also implicated in reinforcing arterial specification. For instance, arterial flow upregulates the arterial-specific ligand ephrin-B2[83–85] that binds to its venous-specific ephrin receptor B4 (EPHB4), leading to arterial-venous cell repulsion that aids in maintaining vessel identity during development[86].

Early observations of the restricted expression of Notch receptors and ligands to the arterial versus venous endothelium highlighted the involvement of this pathway in arterialization[87]. This hypothesis was later consolidated by several *in vivo* studies demonstrating aberrant arterial-venous specification in different Notch-defective mouse and zebrafish models[88–90]. As this aberrant differentiation is a hallmark of the development of arteriovenous malformations (AVMs), which are abnormal direct shunts between arteries and veins, some of these models readily developed AVMs[90,91]. In addition, Notch signaling was also found to strongly upregulate the arterial-specific[86] ephrin-B2 ligand while suppressing vein-restricted EphB4 receptor in the early vasculature[88,92], and *EFNB2* (encoding ephrin-B2)- and *EphB4*-mutant mice phenocopied AVM formation of Notch1 activation[93].

While blood flow plays a role in arterial specification, initiation of this specification goes back to the early angioblast level, before the onset of flow, where observations in zebrafish pointed to the presence of different angioblast populations giving rise to arterial versus venous ECs. Those at the origin of arterial ECs were shown to possess higher VEGF and sonic hedgehog (SHH) signaling, favoring arterial identity[94]. Mechanistically, in the presence of high VEGF concentrations, VEGFR2 activation is believed to activate Wnt signaling and upregulate the transcription factors *SOX7*, *SOX17* and *SOX18*, which altogether increase Notch activation. In turn, Notch signaling increases the expression of arterial-specific genes, including *EFNB2*. In parallel, strong VEGF-VEGFR2 signaling also activates ERK1/2-dependent signaling, favoring arterial identity[95]. On the other hand, signaling through low VEGF levels can alternatively activate the PI3K-AKT downstream signaling axis, which antagonizes ERK1/2 signaling. Venous ECs also display an enrichment of chicken ovalbumin upstream promoter-transcription factor II (COUP-TFII) that downregulates Notch signaling, inhibiting arterial specification[95]. In line with arterial and venous ECs deriving from different angioblast populations, different blood islands in chicken embryos selectively expressed either the arterial VEGF co-receptor Nrp1 or the venous co-receptor Nrp2[96].

In addition to the aforementioned factors, a recent study using Fluorescent Ubiquitination-based Cell Cycle Indicator (FUCCI)-based cell cycle reporter mice proposed a role of cell cycle stage in promoting arteriovenous specification. This work revealed that ECs in remodeling veins and arteries are enriched in different cell cycle stages, namely early G1 and late G1,

respectively. Notably, these different stages permit the differential activation of BMP versus TGF-β signaling, respectively. In turn, BMP signaling (specifically BMP4) upregulates venous markers while TGF-β signaling favors arterial gene expression[97].

1.2.2.3. Intussusceptive angiogenesis

A different, non-sprouting mode of angiogenesis is defined by splitting of pre-existing vessels to generate new, smaller ones. This phenomenon was first observed in 1986 by Caduff et al in pulmonary capillaries in rat[98], but was later found out to be a common feature of vascular growth in many vascular beds and different species[42,99]. Interestingly, intussusceptive angiogenesis was also detected in small arteries and veins, and was shown to play a role in vascular pruning and in altering the branch angle of bifurcating vessels, thus also establishing it as a mechanism of vascular remodeling[100].

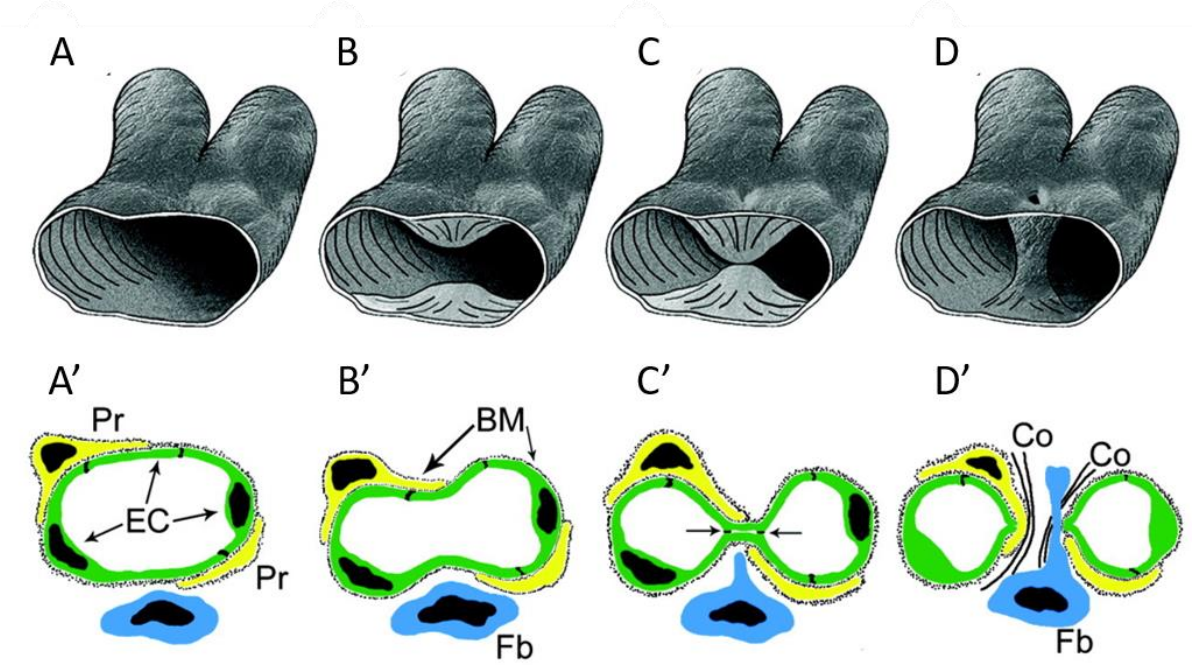

Figure 9. Intussusceptive angiogenesis: a multistep process. *Three-dimensional (A-D) and two-dimensional (A'-D') schematic representations of the steps of intussusceptive angiogenesis are shown. (A-B, A'-B') Intussusception begins with the intraluminal protrusion of opposing capillary walls. After formation of the intussusceptive pillar (C,C'), the endothelial (EC) bilayer and the basal membranes (BM) are centrally perforated as fibroblasts (Fb) and pericytes (Pr), which produce collagen fibrils (Co) (d,d') infiltrate the pillar splitting the capillary into two. Image adapted from "Intussusceptive angiogenesis: Its emergence, its characteristics, and its significance" by Burry et al, Developmental Dynamics, 2004.*

Rigorous electron microscopic investigations in lung sections of rats by the same group uncovered the mechanism behind intussusceptive angiogenesis[99]. This process was found to involve an initial step of intraluminal protrusion of ECs facing each other in the capillary wall, giving rise to an intussusceptive pillar. This was followed by the formation of new junctional complexes that seal the two newly-formed channels. Finally, infiltration of interstitial components to the pillar, including pericytes and collagen-secreting myofibroblasts, aided in the separation of the two channels from each other. As this process continued to occur longitudinally, the pillar grew in size, ultimately splitting the whole capillary into two[99] (Figure

9). Unlike sprouting angiogenesis, whereby the underlying molecular mechanisms were extensively studied, those regulating intussusceptive angiogenesis remain largely unknown.

2. BMP9/10-ALK1 signaling pathway

2.1. TGFβ superfamily ligands

The transforming growth factor-β (TGF-β) superfamily comprises 33 cytokines in humans, presented in Figure 10, that regulate extremely diverse cellular processes involved in embryonic development, tissue homeostasis and regeneration. These processes include cell differentiation, proliferation, adhesion, migration, communication, survival and ECM remodeling. In line with its systematic functions, this family of cytokines is highly ubiquitous, with almost every cell in the human body expressing and responding to at least one of its members[101,102].

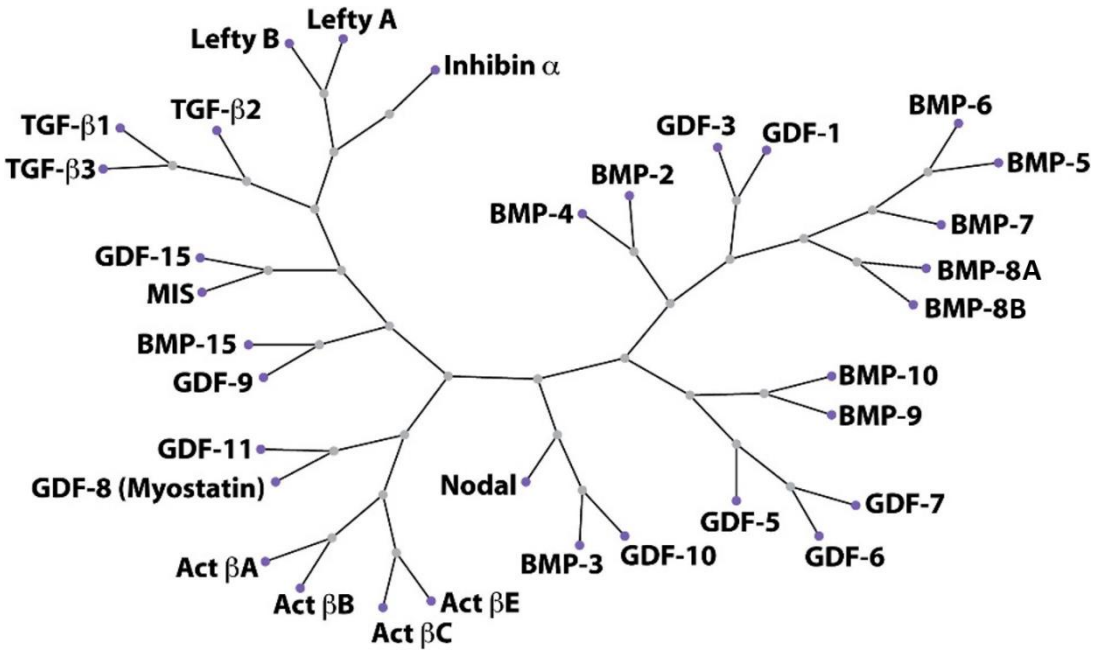

Figure 10. Phylogenetic tree of the 33 TGF-β superfamily ligands in humans. *The tree was generated through alignment of the C-terminal mature domains. Image adapted from "Structural studies of the TGF-βs and their receptors" by Hinck, FEBS Letters, 2012.*

All members of the TGF-β superfamily are structurally-related, sharing a conserved cystine knot structure, but are mostly subdivided into 2 major subfamilies based on differences in sequence similarity and signaling properties: the TGF-β subfamily and the bone morphogenetic protein (BMP) subfamily. The former includes the 3 TGF-β ligands (TGF-β1, TGF-β2 and TGF-β3), activins (A and B), nodal, myostatin and a number of growth and differentiation factors (GDFs). On the other hand, the BMP subfamily comprises all 10 BMPs (named BMP2-10 and BMP15), Anti-Mullerian hormone and the remaining GDFs[101].

As indicated by their name, BMPs were originally isolated from bones and were identified as inducers of ectopic cartilage and bone formation[103–106]. However, as the pleiotropic functions of BMPs, extending beyond the limits of bones to the kidneys, pancreas, cardiovascular system and others, were progressively uncovered, the name "body" morphogenetic proteins was alternatively proposed for this group of ligands[107].

2.2. TGFβ superfamily receptors

TGF-β superfamily ligands elicit a classical membrane-to-nucleus signal through transmembrane receptor complexes composed of two type I and two type II serine/threonine kinase receptors, in addition to a co-receptor that lacks any enzymatic activity. In humans, TGF-β superfamily receptors comprise 7 type I receptors, called activin receptor-like kinase (ALK) 1-7, 5 type II receptors (ActRIIA, ActRIIB, BMPRII, AMHRII and TGFBRII) and the two high molecular weight glycoprotein co-receptors, betaglycan and endoglin[101]. These co-receptors, comprising a very short cytoplasmic domain of around 40 amino acids, lack any enzymatic activity but play a role in potentiating the responses to selected ligands, such as the 3 TGF-β isoforms by betaglycan and BMP9 and BMP10 by endoglin[108].

2.3. Intracellular signaling

2.3.1. Canonical Smad signaling

2.3.1.1. Classes of Smad proteins

Mothers Against Decapentaplegic (Smads) are a family of transcription factors that mediate signaling in response to activated TGF-β family receptors[109]. This family of transcription factors comprises 3 classes of proteins with structural and functional differences: (1) receptor-regulated Smads (R-Smads) comprising Smad1, Smad2, Smad3, Smad5 and Smad8, (2) the common mediator (co-Smad) Smad4 and (3) inhibitory Smads (I-Smads) Smad6 and Smad7. The classical structure of R-Smads and Smad4 consists of two conserved globular domains called Mad homology (MH)1 (N-terminal) and MH2 (C-terminal) that are connected by a divergent linker region (Figure 11)[109]. The MH1 domain is mainly responsible for DNA binding, while MH2 mediates interactions with various proteins such as the type I receptor (for R-Smads), other Smads and nuclear transcriptional partners[109] (Figure 11). In addition, R-Smads possess a Ser-Ser-Xxx-Ser (SSXS) motif in their C-terminal extremities that is phosphorylated by activated type I TGF-β family receptors, leading to activation of R-Smads as described below. On the other hand, I-Smads are structurally distinct from R-Smads and Smad4. The MH1 domain and the C-terminal type I receptor phosphorylation site are missing in Smad6 and Smad7, while the rest of the MH2 domain is conserved (Figure 11). This allows Smad6 and Smad7 to compete with R-Smads for receptor binding, but without being phosphorylated themselves[109].

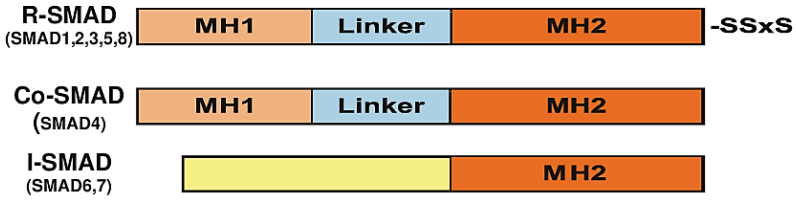

Figure 11. Main functional domains in the different classes of Smad proteins. *The 3 classes of Smads are Receptor-associated (R)-Smads, Common (Co)-Smad and Inhibitory (I)-Smads. R-Smads, which include Smad1,2,3,5 and 8 and the co-Smad, Smad4 are composed of two Mad homology (MH) domains (N-terminal MH1 and C-terminal MH2) that are joined by a linker region. R-Smads additionally harbor the Ser-Ser-Xxx-Ser (SSXS) motif in their C-terminal extremities. On the contrary, I-Smads lack the MH1 domain and SSXS motif. Image adapted from "The complex pattern of SMAD signaling in the cardiovascular system" by Euler-Taimor and Heger, Cardiovascular Research, 2005.*

2.3.1.2. Initiation of the Smad signal

Upon binding of the dimeric ligand to its specific receptor complex, the constitutively active type II receptor phosphorylates the type I receptor on serine and threonine residues located in the glycine- and serine-rich (GS) region, which is a 30 amino acid regulatory region just before the kinase domain of type I receptors. Consequently, the phosphorylated type I receptor becomes activated and phosphorylates R-Smads on their C-terminal SSXS motifs[110]. Depending on the activated type I receptor, two different groups of R-Smads can be implicated. In response to TGF-β subfamily ligands, the type I receptors ALK4, ALK5 or ALK7 phosphorylate Smad2/3, while in case of BMPs, ALK1, ALK2, ALK3 or ALK6 rather activate Smad1/5/8[110] (Figure 12). Phosphorylation of R-Smads' SSXS motif generates a docking site that allows the binding of Smad4, which is a common mediator of both TGF-β and BMP ligand subfamilies. In the absence of an activating signal, R-Smads, are predominantly cytoplasmic. However, phosphorylation of their SSXS motif allows the nuclear accumulation of R-Smads, by decreasing their affinity to cytoplasmic anchors that consequently allows their interaction with Smad4 and nuclear transcription factors[111]. Non-phosphorylated R-Smads can still enter the nucleus at low levels by interacting with the nuclear pore complex, but are transcriptionally inert. Smad4, on the other hand, undergoes continuous nucleocytoplasmic shuttling in unstimulated cells and displays equivalent distribution between the two compartments. Binding of Smad4 to the phosphorylated R-Smad homo- or heterodimer, whether in the cytoplasm or in the nucleus, enables its nuclear accumulation, potentially by masking the nuclear export sequence of Smad4[111,112]. In the nucleus, the Smad complex binds Smad-binding elements in the promoters of target genes and regulates their expression levels, as explained below.

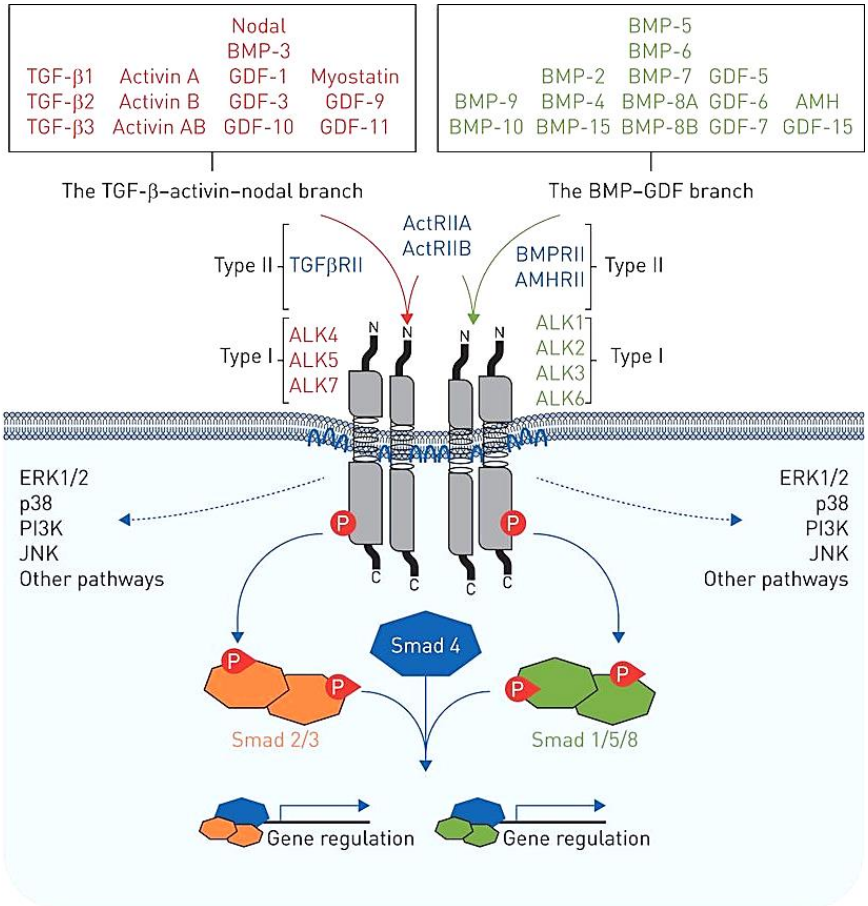

Figure 12. TGF-β superfamily ligands signal through one of two main Smad signaling branches. *The TGF-β-activin-nodal branch activates Smad2/3 mediators, while the BMP-GDF signaling branch activates Smad1/5/8. The specific type I and type II receptors involved in each signaling branch as well as some non-canonically activated pathways are specified in the figure. Image adapted from "Targeting transforming growth factor-β receptors in pulmonary hypertension" by Guignabert and Humbert, European Respiratory Journal, 2021.*

2.3.1.3. Factors shaping transcriptomic response specificity

It is noteworthy that each TGF-β superfamily ligand modulates the expression of a somewhat unique set of target genes, in accordance with the functional diversity of these ligands. So how is this ligand-gene set coupling specified? The first line of selectivity relies on the differential expression of different TGF-β superfamily receptors in different cell types, the bioavailability and local concentration of each ligand and its affinity to the different receptor combinations expressed by the cell. However, as the downstream response of any TGF-β family receptor complex is mostly mediated through either the activation of Smad2/3 or Smad1/5/8, additional factors had to be involved. Indeed, Smads bind DNA, specifically CAGA and GC-rich regions, with very low affinity that is not enough to ensure effective binding *in vivo*. By interacting with DNA-binding coactivators or corepressors, Smads form transcriptional complexes that have multiple DNA-binding sequences. These complexes then specifically bind to gene promoters containing the corresponding binding motifs in the proper orientation and separating distance and with higher affinity compared to Smads alone. Therefore, the second line of selectivity relies on the specificity of interaction between cofactors and either Smad2/3 or Smad1/5/8, but also on the pool of expressed cofactors within each cell type. These include members of transcription factor families FOX, RUNX, E2F, AP1, CREB/ATF and others. Moreover, these factors themselves can be under the control of other signaling pathways, as for FoxO for example, whose phosphorylation by various kinases leads to its extrusion from the nucleus. Hence, signals affecting these factors might also influence the Smad response. Notably, it was also shown that baseline differences in chromatin accessibility between cell types, dictated by distinct histone methylation patterns for example, influence transcriptional regulation by Smads[113]. Thus, the role of the TGF-β superfamily signals could be thought of as ensuring the accumulation of the proper Smad complex in the nucleus. Then, it is up to the cell to integrate its expressed nuclear Smad-binding partners with this complex to determine which of the many potential targets that lie in open chromatin regions get regulated.

But what about the distinct effects of two different BMPs for example on the same cell type? Morikawa et al nicely demonstrated by ChIP-seq of Smad1/5 that stimulating human umbilical vein ECs with either 1ng/mL BMP9 (strongly binds ALK1) versus a higher concentration of BMP6 (50ng/mL to accommodate for its lower affinity to its cognate receptor ALK2), resulted in the identification of mostly overlapping Smad-binding sites between the 2 ligands[113]. However, despite the fact that these 2 stimulations resulted in equivalent phospho-Smad1/5 (p-Smad1/5) levels, several BMP9-specific binding sites such as *HEY1* and *JAG1* loci were detected. By further increasing the concentration of BMP6 up to 200ng/mL, Smad1/5 binding to these BMP9-specific sites was enhanced in a BMP6 dose-dependent manner. On the other hand, common BMP6/BMP9 Smad1/5 binding sites, such as the *ID1* locus that exhibits strong Smad1/5-binding affinity, were already strongly upregulated at 20ng/mL BMP6[113]. Hence, since Smad-binding sites within the regulatory elements of different target genes can exhibit variable affinities to the Smad complex, the authors suggested that stimulations by some ligands with limited potency might not be strong enough to promote the binding of Smads to low-affinity sites. Therefore, differences in ligand affinity and potency, which are intriguingly not necessarily reflected by the level of phosphorylated Smads measured by traditional methods, can define another level of response specificity[113].

2.3.1.4. Termination of Smad signal

The duration of the active Smad signal is tightly controlled at several levels. The phosphorylated trimeric Smad complex is dephosphorylated by phosphatases in the nucleus, leading to its dissociation and the export of its individual components from the nucleus. As long as the type I receptor remains active, these Smads undergo repeated cycles of phosphorylation, assembly and nuclear import followed by the inverse events. Once the signal is terminated, the R-Smads no longer undergo phosphorylation and mostly accumulate in the cytoplasm. These repetitive cycles ensure a constant re-evaluation of receptor activity by R-Smads that accordingly control signaling duration[114]. The receptor itself can also be actively dephosphorylated by phosphatases, such as protein phosphatase 1 α that inactivates ALK1[115]. In addition, both the type I receptors and their associated Smads can be targeted for degradation by Smad E3 ubiquitin ligases Smurf1 or Smurf2[116–118]. Interestingly, the two inhibitory Smads, Smad6 and Smad7, are transcriptionally upregulated by TGF-β superfamily cytokines, but negatively regulate downstream signaling, establishing a critical negative feedback loop. Specifically, Smad7 is upregulated by TGF-β, activin, and BMP signaling and is a global inhibitor of all of these pathways, while Smad6, which is highly expressed in the cardiovascular system and is induced by BMP signaling, specifically inhibits the latter. Because Smad6 and Smad7 retain the MH2 domain[109], they can compete with R-Smads for receptor binding, but as I-Smads lack the C-terminal SSXS motif and the MH1 domain, they block downstream signaling. In addition, these inhibitory Smads were shown to inhibit signaling by competing with R-Smads for binding to Smad4 and by facilitating Smurf-dependent receptor degradation[116–118]. Another way for regulating signal duration is by manipulating the linker region of R-Smads. Phosphorylation of Ser and Thr residues in the linker regions of Smads 1, 2 and 3 by different endogenous kinases, including ERK MAP kinases and cyclin-dependent kinases, was shown to impair their nuclear accumulation and corresponding signaling activity[109].

2.3.2. Smad-independent signaling

Besides the canonical Smad signaling, TFG-β and BMP ligands have been shown to activate several signaling transducers independently of Smads, in a cell context-dependent manner. Various studies demonstrate direct activation of various mitogen-activated protein kinases (MAPKs), including c-Jun amino terminal kinase (JNK) and p38 MAPK in a TFG-β activated kinase 1 (TAK1)-dependent manner, in addition to ERK MAPK. TGF-β superfamily signaling was also shown to activate PI3K-AKT signaling, IkB kinase (IKK) and several Rho-like GTPases[119]. Most of these signal transducers could also be indirectly-activated following Smad-mediated transcriptional regulation, and in turn some of them were shown to positively or negatively regulate Smad signaling. Collectively, these pathways have been shown to mediate key TGF-β and BMP-induced functions, such as the well-known TGF-β-driven epithelial-to-mesenchymal transition (EMT) and BMP2-enhanced cell motility and invasiveness in the context of cancer. In addition, inhibition of EC migration via constitutively active ALK1 was shown by our group to be Smad-independent and to rely instead on JNK and possibly ERK pathways[120]. However, it is important to note that under different conditions or in different cell types, some of the aforementioned non-Smad transducers were either not regulated or were even inactivated by TGF-β superfamily signaling, highlighting their high context dependency[119]. Therefore, a deeper understanding of these non-Smad arms of TGF-β signaling is required to address their

potential input in the pathophysiology of diseases involving impaired TGF-β/BMP signaling and consequently considering them potential therapeutic targets.

2.4. BMP9/BMP10-ALK1 signaling axis

2.4.1. BMP9 and BMP10: high affinity ligands of endothelial receptors ALK1 and endoglin

Among the receptors of this family, the type I receptor ALK1 and the co-receptor endoglin are predominantly expressed on ECs, and their expression is upregulated in the actively angiogenic endothelium but reduced in the adult quiescent endothelium[121,122]. ALK1 expression is predominantly arterial and is higher in the pulmonary compared to the hepatic vasculature[121,123]. While endoglin shares similar expression patterns to ALK1 during early embryogenesis[122], its expression in adult mice is stronger on the venous side and is low in the lungs, skin, brain and intestine but high in the liver[124]. Both ALK1 and endoglin are present in capillaries to variable extents[121,124]. Besides ECs, endoglin is also expressed in mesenchymal stem cells, some hematopoietic progenitors and immune cells such as monocytes, macrophages and mast cells[125], and ALK1 expression was recently reported in hepatic resident macrophages called Kupffer cells[126].

Early studies demonstrated the activation of chimeras composed of ALK1 extracellular domain fused to the cytoplasmic domain of the TGF-β receptor ALK5 by TGF-β1 and TGF-β3[127] and enhanced ALK1/ALK5 complexing by TGF-β1[128]. Thus, ALK1 was first proposed as a TGF-β receptor. However, this hypothesis was debated as ALK1 and ALK5 displayed non-overlapping expression patterns *in vivo*[129] and ALK5-deleted mice do not develop the vascular defects characteristic of ALK1-deletion[130]. In addition, the same work proposing TGF-β1 and TGF-β3 as ALK1 ligands identified the presence of an additional unknown ALK1 ligand in the serum[127], which remained elusive for years. It was only in 2007 that our group and others identified BMP9 and BMP10 as the physiologically-relevant, high affinity ligands of ALK1[131–133]. These two BMPs were shown to bind ALK1 with an EC_{50} of approximately 50pg/mL[131], i.e. with much higher affinity compared to other BMPs binding to their cognate receptors ALK2, ALK3 and ALK6 (EC_{50} of around 50ng/mL). BMP9 and BMP10 were also shown to bind to other BMP type I receptors, although with much lower affinities compared to ALK1. Specifically, BMP9 was reported to bind ALK2, while BMP10 was proposed to bind ALK3 and ALK6[57]. Both BMP9 and BMP10 also bind directly and with high affinity to the homodimeric co-receptor endoglin[64,134]. Endoglin was described as a co-receptor for several other ligands, such as TGF-β1, TGF-β3, BMP2, BMP7 and activin A, but unlike for BMP9 and BMP10, binding of BMP2, BMP7 and Activin A to endoglin was indirect, necessitating the co-expression of the type I or type II receptor[135,136]. The role of endoglin is thus to capture circulating BMP9 and BMP10 and present them to the type I and type II receptors. This is important for increasing the local supply of BMP9 and BMP10, especially that these 2 ligands lack the heparin-binding region that permits other BMPs to interact with some ECM components, regulating their bioavailability[137]. As BMP9 binds directly to both ALK1 and endoglin with high affinities, it was proposed to be efficiently captured by both ALK1 and endoglin, but endoglin additionally plays a potential role in displacing the prodmain of BMP9 (presented in the next section), allowing signaling through ALK1[138]. Besides the membrane-bound form of endoglin, a soluble

circulating form (sENG) is generated upon shedding of its extracellular domain by matrix metalloproteinase-14[139]. Interestingly, sENG, mostly in a monomeric form, was demonstrated to bind BMP9 and was proposed to enhance BMP9 signaling via cell-surface endoglin instead of acting as an inhibitory ligand trap[138]. As for the type II receptors, BMP9 and BMP10 bind to the classical BMP receptors ActRIIB, BMPRII and ActRIIA, in decreasing order of affinity for BMP9, but with similar affinities for BMP10[140]. However, the 3 receptors show considerable variations in endothelial expression levels, with BMPRII being much more expressed than ActRIIA and ActRIIB in the endothelium[57]. Of note, there are several naturally occurring BMP antagonists, such as noggin, gremlin, BMPER and chordin, which mostly act as secreted BMP ligand traps, in addition to the TGF-β family pseudoreceptor BAMBI that acts as a transmembrane ligand trap[141]. Nonetheless, to date, no *in vivo* antagonists influencing BMP9 or BMP10 activity have been confirmed[57] and noggin was demonstrated to be incapable of binding BMP9 and BMP10[142].

2.4.2. Synthesis and expression of BMP9 and BMP10

BMP9 and BMP10 are two closely-related members of the TGF-β family of ligands that share a high degree of sequence similarity and bind to the same receptor complex on ECs. These 2 ligands, just like other BMPs, are first synthesized as pre-pro-proteins composed of an N-terminal signal peptide that directs them towards the secretory pathway, a prodomain that ensures proper folding and a C-terminal mature growth factor region that binds cognate receptors. Dimerization of pre-pro-proteins through the formation of a single disulfide bond linking two mature regions results in pro-proteins. The latter then undergo proteolytic cleavage by furin-like pro-protein convertases to displace the prodomains, which often remain non-covalently bound to the mature form in case of BMP9, BMP10 and some other BMPs. Interestingly, prodomains were shown to confer latency to TGF-β and some other members, but this isn't the case for BMP9 and BMP10 binding to ALK1[143]. The prodomain-bound form, in addition to the isolated mature forms of BMP9 and BMP10 can be detected in circulation and represent active signaling forms of these ligands[57] (Figure 13).

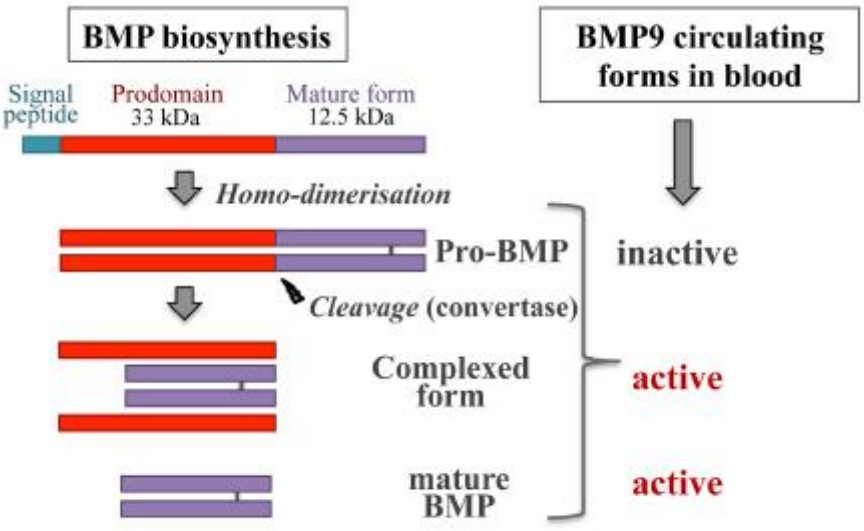

Figure 13. Schematic diagram of BMP synthesis and processing. *BMPs are first synthesized as pre-pro-proteins that dimerize via a disulfide-bond to form pro-BMPs. Pro-BMPs represent inactive precursors that are further cleaved by convertases to generate the mature active BMP and the complexed form, which is active in case of BMP9 and consists of prodomains non-covalently attached to the mature BMPs. Image adapted from "Emerging roles of BMP9 and BMP10 in hereditary hemorrhagic telangiectasia" by Tillet and Bailly, Frontiers in Genetics, 2014.*

As for their sites of expression, the right atria represent the main postnatal site of synthesis of BMP10[144], whose expression in mice starts at embryonic day (E) 8.5, whereas hepatic stellate cells are responsible for producing both BMP9, around E9.75-E10, and a low amount of BMP10[145]. Some recent reports also suggest that low levels of BMP9 could be secreted by the brain septum and by the lungs from a yet-unidentified cellular origin[146,147]. Interestingly, in addition to their homodimeric forms, our group detected biologically active circulating BMP9-BMP10 heterodimers in both mouse and human plasma and proposed hepatic stellate cells as their physiological source[145]. Heterodimerization of BMPs is a well-known phenomenon that increases the functional diversity of this family of ligands and often enhances the potency of the formed dimers. Several heterodimers, including BMP2-BMP7[148] and BMP4-BMP7[149], were shown to regulate key aspects of embryonic development that were not driven by the corresponding homodimers, and GDF9-BMP15 heterodimer was shown to synergistically enhance ovarian function in adults[150]. Regarding BMP9-BMP10 heterodimers, further work is required to unravel their physiological role.

2.4.3. Role of BMP9 and BMP10 in vascular quiescence

As previously mentioned, BMP9 and BMP10 bind receptor complexes composed of ALK1 and BMPRII, ActRIIA or ActRIIB with the help of endoglin. Unlike TGF-β and activin that have a higher affinity to and thus initially bind the type II receptor, BMP9 and BMP10 are thought to first bind endoglin, which transfers them to ALK1, forming a transient ligand-endoglin-ALK1 complex. Then, endoglin is released, allowing the interaction of ligand-ALK1 with the type II receptor[134]. However, it is noteworthy that direct binding of BMP9/10 to ALK1 and to the aforementioned type II receptors can also occur in the absence of endoglin[140], and that ALK1 overexpression rescues defective signaling caused by *Eng* deletion *in vivo*[151]. The juxtapositioning of ALK1 and the type II receptor allows the latter to phosphorylate ALK1, which in turn phosphorylates Smad1/5/8. These activated R-Smads then form a trimeric complex with Smad4 and translocate to the nucleus to regulate the expression of target genes (Figure 14), including the strong targets DNA-binding protein inhibitor 1 (*ID1*) and *ID2* and the inhibitory Smads, *SMAD6* and *SMAD7*[131] that form a negative feedback loop. The outcome of

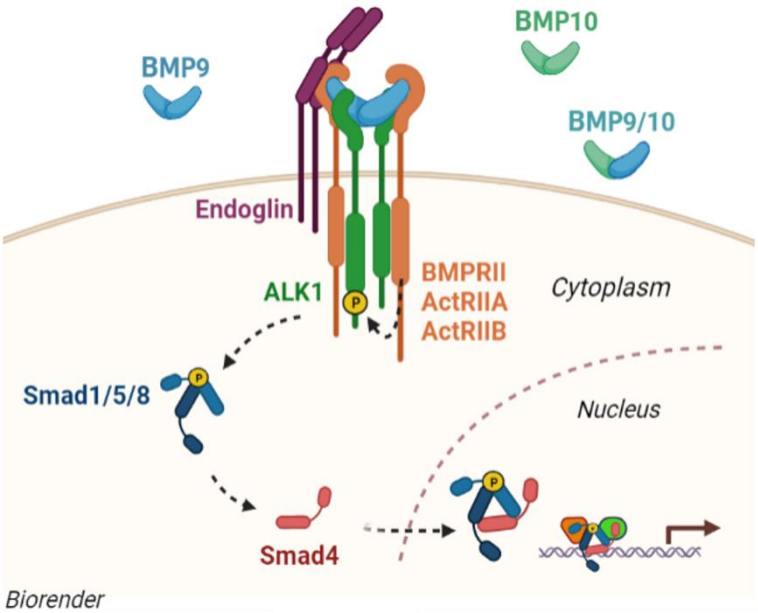

Figure 14. BMP9/10 signaling pathway in endothelial cells. *BMP9 and BMP10 homo- or hetero-dimers bind with high affinity to a receptor complex composed of ALK1, endoglin and either BMPR2, ActRIIA or ActRIIB. Ligand binding results in phosphorylation of ALK1 by the type II receptor leading to its activation. Activated ALK1 then phosphorylates R-Smads 1/5/8, which form a complex with Smad4 and accumulate in the nucleus. There, the Smad complex associates with co-activators or co-repressors to regulate target gene expression. Image generated using Biorender.*

this signaling pathway is to ensure vascular quiescence, which is a hallmark of the mature endothelium. This role had been established through various *in vitro* and *in vivo* studies summarized below. In addition, BMP9 was shown to induce Smad2 phosphorylation in an ALK5-independent manner, although with a much weaker intensity compared to p-Smad1/5/8 and only with BMP9 concentrations ≥ 1ng/mL, while p-Smad1/5/8 could already be detected with 0.1ng/mL BMP9 in pulmonary artery ECs[152,153]. This ALK1-mediated activation of Smad2 was found to depend on ActRII receptor, while Smad1/5/8 and Id responses relied on both BMPRII and ActRII. In addition, among the type II receptors, only BMPRII was important for the anti-proliferative effect of BMP9[152]. Hence, the different type II receptors were proposed to play a role in balancing the activation of predominant Smad1/5/8 and weaker Smad2 branches by BMP9-ALK1 signaling[152].

2.4.3.1. Effect on cell growth and migration

Prior to the identification of BMP9 and BMP10 as the ALK1-specific ligands, the function of ALK1 was investigated in primary ECs by expressing a constitutively active form of the receptor (ALK1ca). These studies yielded distinct conclusions. For example, one group showed that ALK1ca expression in human umbilical vein ECs (HUVECs) inhibited cell proliferation but had no impact on tube formation[154]. Another group reported enhanced migration in ALK1ca-expressing microvascular ECs[128]. Our group, however, found that ALK1ca expression inhibited both proliferation and migration of dermal HMVECs, the migration of pulmonary HMVECs and HUVECs[155], and the sprouting of ALK1ca-expressing mouse embryonic stem cells in cultured embryoid bodies[156].

Then, with the discovery of the ALK1 ligands, the role of this receptor was revisited. Our group has shown that both BMP9 and BMP10 potently suppress HMVECs proliferation and migration[131]. This was consolidated by another group demonstrating the same effects of BMP9 on FGF2-stimulated bovine aortic ECs[133], and a study reporting ALK1 and BMPRII-dependent BMP9 inhibition of human pulmonary artery ECs proliferation[152]. This growth inhibitory effect of BMP9 was validated *ex vivo* in the mouse metatarsal culture model in the presence or absence of VEGF[133]. *In vivo,* BMP9 inhibited FGF2-induced neo-angiogenesis in the mouse sponge assay and prevented blood circulation in the chorioallantoic membrane assay[157].

2.4.3.2. Effect on vascular permeability

In addition to its role on endothelial growth and migration, BMP9 was shown to modulate vascular permeability. In a hyperglycemic setting recapitulating diabetic retinopathy, BMP9 administration decreased vascular permeability *in vitro* in hyperglycemic ECs and *in vivo* in diabetic mice retinas. This effect was mediated by inhibition of VEGF-induced VE-cadherin internalization and by upregulation of the tight junctions component occludin[158]. Besides the hyperglycemic context, BMP9 also reduced vascular permeability induced by the classical permeabilizing agents tumor necrosis factor alpha (TNFα), lipopolysaccharide (LPS) and thrombin in blood outgrowth ECs and/or pulmonary artery ECs[159].

2.4.3.3. Physiological roles of BMP9 and BMP10

While the aforementioned studies highlighted the roles of BMP9 and/or BMP10 on somehow isolated aspects of angiogenesis, their global physiological roles were rather derived from Bmp9 and/or Bmp10-deficient mouse models. *Bmp9*-knockout (KO) mice of the C57BL/6 genetic background were viable, fertile and had no overt vascular defects[160–162]. However, these *Bmp9*-KO mice displayed subtle defects in their lymphatic vasculature, defined by enlarged collecting vessels, reduction in the number of lymphatic valves and consequently suboptimal lymphatic drainage[163,164]. *Bmp9* deletion in a different mouse strain, the 129/Ola, resulted in a more severe phenotype characterized by a strong reduction in fenestrations of liver sinusoidal ECs (LSECs) accompanied with inflammation and liver fibrosis[165]. Other studies also pointed out a role of BMP9 and/or BMP10 in preventing lung inflammation[162,166]. Hence, BMP9 seems to play a non-redundant role in lymphatic vasculature development and in maintaining liver homeostasis. Addressing the effect of Bmp10 loss on the lymphatics would clarify if the lymphatic phenotype observed in *Bmp9*-KO mice is due to reduction in overall ALK1 signaling due to the absence of one ligand or whether it is strictly BMP9-specific function. Similarly, the outcome of *Bmp10*-deletion on liver vasculature was not investigated, but as the liver is the site of BMP9 secretion, I would expect that the high local concentration of *Bmp9* in the liver would compensate for a reduction in BMP10. Nonetheless, if these two reported functions of BMP9 were mediated by BMP9-BMP10 heterodimers, then loss of either ligand would result in these defects.

On the other hand, *Bmp10*-KO mice die during gestation between embryonic day (E) 9.5 and 10.5 due to failed cardiac trabeculation[144]. It is noteworthy that the expression of BMP10 in mice, starting at E8.5, precedes BMP9 expression by the liver, which is detected around E9.75-E10. Hence, the absence of Bmp9 before E9.75 was suspected to be involved in this cardiac phenotype. Nevertheless, knocking in the Bmp9 gene in the *Bmp10* locus failed to prevent this phenotype, confirming a *Bmp10*-specific role in cardiac development that might be ALK1-independent[161]. To overcome embryonic lethality and investigate the effect of *Bmp10* loss on adult mouse vasculature, *Bmp10* was deleted postnatally through various methods, including inducible knockdown and administration of neutralizing Bmp10 antibodies. Until recently, several studies using these models showed that postnatal *Bmp10* deficiency alone in mice did not generate blood vasculature defects[160–162].

On the contrary, only the combined loss of both *Bmp9* and *Bmp10*, either genetically or via antibodies or ligand traps, led to overt vascular phenotypes, characterized by retinal vascularization defects (increased vascular density and arteriovenous shunting) and impaired closure of the ductus arteriosus[71,160–162,167,168]. Hence, BMP9 and BMP10 were thought to play redundant roles during postnatal angiogenesis. Nevertheless, very recent work by Paul Oh's group proposed a BMP10-specific role, where inducible *Bmp10* KO but not *Bmp9* KO mice showed AVMs in developing retinas, postnatal brain, and adult wounded skin[169]. In addition, BMP10, but not BMP9, administration, prevented retinal AVM in Bmp9/10-dKO mice[169].

2.4.3.4. Involvement of hemodynamic shear stress

The BMP9/10-ALK1 signaling pathway was shown to be a mechanosensitive pathway that is modulated by hemodynamic shear stress. *In vitro*, HUVECs exposed to increasing levels of fluid shear stress (FSS) in serum-containing medium displayed peak activation of Smad1 in response to physiological FSS levels ranging from 10 to 20 dyn/cm^2 [170]. Moreover, flow was shown to potentiate the Smad1/5/8 response to soluble BMP9 in HUVECs, by promoting ALK1-endoglin association at the cell membrane, reinforcing several aspects of the mature endothelium. Namely, flow reduced HUVECs proliferation, increased their expression of mural cell recruitment genes *PDGFB*, *TGFB1* and *JAG1* and enhanced migration of pericytes towards HUVECs exposed to flow in an HUVEC/pericyte coculture model, all occurring in an ALK1-dependent manner[171]. *In vivo*, ALK1 expression was found to be stronger in areas experiencing higher blood flow in both mice and zebrafish, suggesting its regulation by hemodynamic forces[121,123]. In zebrafish, besides promoting Alk1 expression, flow enhanced ALK1 activity by distributing its ligand bmp10. In turn, activated ALK1 signaling in nascent arteries was shown to reinforce their maturation by preventing excessive outward remodeling and endothelial proliferation, possibly through downregulating the expression of the proangiogenic chemokine receptor cxcr4a and upregulating the potent vasoconstrictor edn1 (encoding endothelin-1)[123,172]. On the other hand, in vessels harboring a primary cilium, Alk1 signaling was rather induced by low FSS levels. The strengthened signaling activity in the presence of cilia was proposed to be required for the stabilization of weakly-perfused capillaries during vascular development. Indeed, cilium-harboring ECs are more abundant during development compared to the adult vasculature, where stronger FSS levels seem to decrease the number of ciliated ECs[173].

Having explained the physiological importance of BMP9/10-ALK1 signaling in maintaining vascular quiescence, it is of no surprise that imbalances in this pathway are at the basis of vascular dysfunction. Indeed, mutations in components of BMP9/10-ALK1 pathway were identified as causative factors of two vascular diseases, namely hereditary hemorrhagic telangiectasia and pulmonary arterial hypertension. The two upcoming chapters will be dedicated for the description of these two diseases.

3. Hereditary Hemorrhagic Telangiectasia (HHT)

3.1. Brief overview

Hereditary Hemorrhagic Telangiectasia (HHT) is a genetic multisystemic disorder affecting 1 in 5,000 to 8,000 individuals worldwide[174–176]. It is inherited as an autosomal dominant trait and displays nearly complete penetrance with age albeit with variable expressivity. The disorder is described as a hemorrhagic vascular dysplasia, characterized by spontaneous, recurrent episodes of epistaxis, the most common feature of the disease, and by the development of muco-cutaneous telangiectases and visceral arteriovenous malformations (AVMs) in specific sites. Named after the physicians who first characterized it, HHT is also known as Rendu-Osler-Weber syndrome[177].

3.2. Historical background

The primary description of HHT dates back to 1864, when Henry Gawen Sutton described a hemophilia-like disorder manifested by epistaxis, internal bleeding and skin telangiectases. A year later, Benjamin Guy Babington highlighted the hereditary aspect of the disease upon reporting the occurrence of epistaxis across five generations of a family. From this point onwards, the disease was described by several others, including John Wickham Legg, but it wasn't until 1896 that HHT was differentiated from hemophilia by the French physician Henri Jules Louis Marie Rendu. Rendu reported a 52-year-old man suffering from recurrent epistaxis, similar to his mother and brother, and displaying multiple telangiectases on his face and trunk. Notably, he was the first to hypothetically link epistaxis in HHT to nasal lesions.[178] Five years later, William Osler, a highly-renowned Canadian physician and professor often described as the father of modern Hippocratic medicine,[179] credited Rendu's report and corroborated the hereditary characteristic of the disease by describing a few related cases displaying recurrent epistaxis and mucocutaneous telangiectases on the face and within the oronasal cavities. In addition, Osler reported, for the first time, that viscera in HHT patients could also be affected when he detected several dilated venules and capillaries in a gastric autopsy belonging to an HHT patient that died of gastric cancer. Frederick Parkes Weber, an English dermatologist, continued characterizing the disease. In 1907, he provided a clinical description of a series of patients, documenting the presence of several minute-sized reddish lesions on the fingers, brought to his attention by Osler[178]. In recognition of the major contributors to the description of this disease, the latter was referred to as Rendu-Osler-Weber or Osler-Weber-Rendu syndrome. In 1909, the disease was given the name "Hereditary Hemorrhagic Telangiectasia" by the American physician Frederick Moir Hanes, yet HHT is still widely known by its triple eponym[180].

3.3. Etiology

HHT is an autosomal dominant disorder caused by loss-of-function (LOF) mutations in components of the BMP9/10-ALK1 signaling pathway (Figure 15). Mutations in *ENG* (1994, chromosomal locus 9q34.11, encoding endoglin) and *ACVRL1* (1996, chromosomal locus 12q13.13, encoding ALK1) are responsible for the majority of cases and give rise to two forms of the disease, HHT1 (OMIM 187300) and HHT2 (OMIM 600376), respectively[181–185]. Collectively, over 600 pathogenic mutations in *ENG* and *ACVRL1* linked to HHT were reported in the HHT mutation database, most of which are missense mutations and deletions (http://www.arup.utah.edu/database/hht/). Other mutations include duplications, nonsense mutations, splice site variants and insertions. Mutations in *ENG* and *ACVRL1* were detected across the whole coding sequences of the two genes, thus no mutation hotspots were identified[186,187]. In addition to *ENG* and *ACVRL1,* mutations in the *SMAD4* gene (2004, chromosomal locus 18q21.2) were identified in some HHT patients, estimated to constitute 2% of total cases. These germline *SMAD4* mutations result in a combined syndrome of HHT and juvenile polyposis (JP-HHT; OMIM 175050)[186,188]. Juvenile polyposis syndrome (JP; OMIM 174900) is a rare autosomal dominant disorder characterized by the development of multiple hamartomatous polyps in the gastrointestinal tract and the increased predisposition to gastrointestinal cancers[189]. Based on the *SMAD4* mutation repository constructed by ARUP laboratories, at least 26 different *SMAD4* mutations were described in patients with the combined JP-HHT syndrome, most of which are missense mutations and deletions mainly concentrated at the MH2 domain of Smad4[190]. Another rare form of HHT, HHT5 (OMIM #615506), has been described in few cases carrying mutations in *GDF2* (chromosomal locus 10q11.22, encoding BMP9). However, due to the atypical site of telangiectases detected in these patients, particularly on the upper limbs and trunk, and their abnormally large size in one of the cases, their condition was described as a vascular-anomaly syndrome having a phenotypic overlap with HHT[191–194].

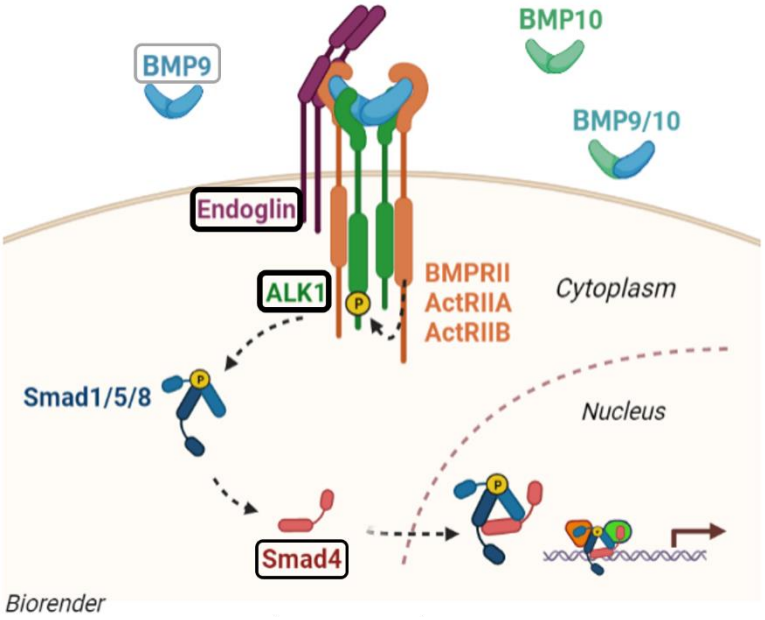

Figure 15. HHT is caused by mutations in components of BMP9/10 signaling pathway. *More than 90% of HHT cases are caused by mutations in genes encoding either endoglin or ALK1 (in intense black boxes), while around 2% are caused by SMAD4 mutations (thin black box). Some patients with mutations in the gene encoding BMP9 (think grey box) were found to present an HHT-like phenotype. Image generated using Biorender.*

Besides the components of BMP9/10-ALK1 signaling, two additional HHT-linked chromosomal loci have been identified in some families presenting classical HHT features: 5q31.3–5q32 and

7p14, responsible for HHT3 (OMIM 601101) and HHT4 (OMIM 610655) forms respectively. Nonetheless, the corresponding affected genes for both loci remain ambiguous[195,196]. Despite the identification of all aforementioned loci in HHT patients and the recent advances in molecular genetic testing, the genetic basis for around 5% of clinically diagnosed patients remains unknown[187]. Although the absence of molecular diagnosis could sometimes be linked to limitations in variant detection, there might still be room for identifying new loci implicated in HHT pathogenesis. In accordance, in 2018, Jiang et al reported an overrepresentation of rare mutations in *DROSHA*, which is a critical enzyme for miRNA processing, in clinically diagnosed HHT patients lacking mutations in the typical HHT-mutated genes[197]. Interestingly, this group also demonstrated that endothelial-specific Drosha-deficient zebrafish and mice developed vascular defects resembling those of HHT patients[197]. In addition, *EPHB4* loss-of-function variants were very recently reported in few individuals presenting atypical HHT manifestations and HHT-like liver abnormalities[198].

3.4. Diagnostic criteria

As decided by the scientific advisory board of the HHT Foundation International Inc., the clinical diagnosis of HHT is based on the four Curaçao Criteria (Figure 16), which are: spontaneous and recurrent nose bleeds, multiple mucocutaneous telangiectases at characteristic sites, visceral lesions including gastrointestinal (GI) telangiectases and arteriovenous malformations, and a family history of the disease (in first-degree relatives)[199]. Initially, manifesting two of these symptoms was considered sufficient for the clinical diagnosis of HHT[200]. Later on, in order to limit over-diagnosis within HHT families, where an unaffected first-degree relative of a patient may be falsely diagnosed on the sole basis of epistaxis or misinterpreted cutaneous vascular lesions, the diagnosis was agreed to be considered definite only when at least three out of the four criteria were satisfied. Conversely, the diagnosis is said to be possible or suspected with only two fulfilled criteria, and unlikely with less than that. These clinical diagnostic criteria are particularly beneficial when diagnosing older adults, but can be insufficient for properly diagnosing children or young adults, as telangiectases and epistaxis might have a late

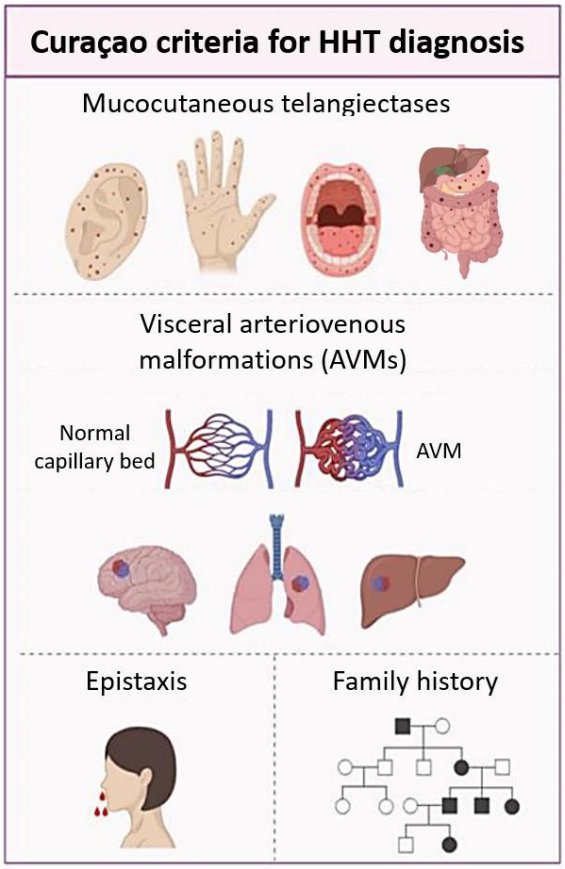

Figure 16. HHT diagnosis is based on the 4 Curaçao criteria. *These consist of: (1) mucocutaneous telangiectases in the ears, hands, nose, mouth and gastrointestinal tract, (2) arteriovenous malformations in visceral organs such as the brain, lungs and liver, (3) epistaxis and (4) family history of the disease. Image adapted from "Review of Pharmacological Strategies with Repurposed Drugs for Hereditary Hemorrhagic Telangiectasia Related Bleeding" by Albiñana et al, Journal of Clinical Medicine, 2020.*

onset and usually worsen with age[199,201,202]. In such cases, clinicians may resort to genetic testing for validating or rejecting a suspected diagnosis[199,201].

3.4.1. Epistaxis

The most common clinical manifestation in HHT patients is epistaxis, affecting more than 90% of patients in different populations[203–205]. The severity and frequency of this symptom greatly vary from one patient to another, ranging from mild, self-limited intermittent dripping of blood to continuous nasal bleeding that interferes with the patient's daily activities. The mean onset age of epistaxis in HHT patients is 12 years, but this symptom can appear as early as at 5 years of age[203]. HHT1 patients are reported to experience an earlier onset of epistaxis compared to HHT2 patients[206]. By the age of 20, more than half of HHT patients have already experienced epistaxis, and most patients report an increased severity with age[203,205,207]. Another factor affecting severity is seasonal change, as some patients experience worsened severity during the winter, when the humidity levels drop. These patients are thus advised to use humidifiers and to apply topical moisturizers to the nasal mucosa, providing moderate relief[203]. On average, the frequency of epistaxis in HHT patients is 18 episodes per month with a mean bleeding duration of 7.5 minutes[203]. The severity level and the frequency of epistaxis needed to fulfil the diagnostic criterion are not specified, yet nose bleeds must occur spontaneously and repeatedly to be regarded in the proper diagnosis of HHT[199].

3.4.2. Telangiectases

HHT-associated telangiectases are circular pinhead-sized red or purple vascular lesions that appear near the surface of the skin or on mucous membranes. These lesions can be distinguished by blanching during diascopy, i.e. momentarily disappearing upon slight compression due to prevention of blood flow to that region[205,208]. In HHT patients, multiple telangiectases commonly appear at characteristic sites in the body, mainly in the nose, in the oral cavity, on the lips, on fingers and in the GI tract[209] (Figures 16 and 17).

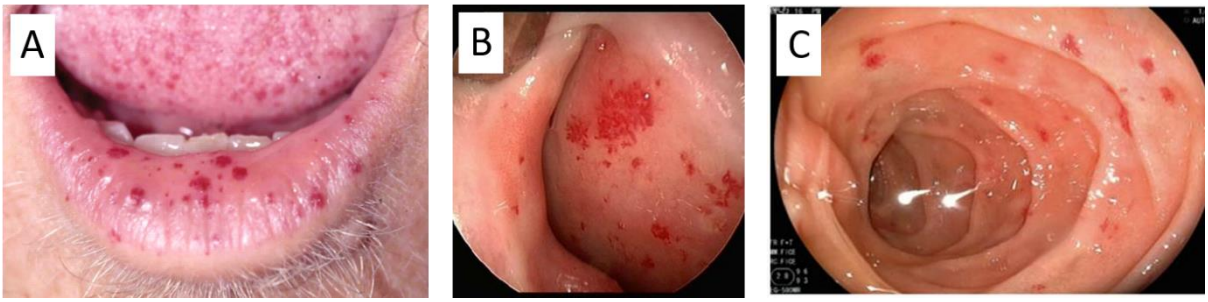

Figure 17. Typical telangiectases of HHT patients. A, *Telangiectases on the lip and tongue of an HHT patient.* ***B-C,*** *Endoscopic views of telangiectases in the nasal septum (**B**) and small intestine (**C**) of HHT patients. Images taken from " The pulmonary vascular complications of hereditary haemorrhagic telangiectasia" by Faughnan et al, European Respiratory Journal, 2009 (**A**), "Manifestations of hereditary hemorrhagic telangiectasia in children and adolescents" by Folz et al, Eur Arch Otorhinolaryngol, 2006 (**B**), "Diagnosis and treatment of patients with hereditary hemorrhagic telangiectasia (Rendu-Osler-Weber syndrome) at a university hospital in Colombia" by Mosquera-Klinger et al, Revista colombiana de Gastroenterología, 2019 (**C**).*

Mucous telangiectases in the nose and GI tract are highly prone for rupture leading respectively to epistaxis and GI bleeding. While epistaxis occurs in the majority in HHT

patients, GI bleeding only affects around 25%, most of which are older than 40 years old[201]. As a consequence of chronic bleeding of telangiectases, mostly of the nasal ones, patients commonly develop iron-deficiency anaemia[201]. On the other hand, dermal and oral telangiectases might bleed upon trauma but are generally only a cosmetic concern[208]. In a study describing the clinical profiles of 324 HHT patients, telangiectases were found in 74% of the cases[205], and other studies suggest even a higher prevalence[210]. These lesions are not apparent at birth but gradually develop, usually in the third decade, and generally increase in number and size with time[205,210].

Histologically, cutaneous telangiectases appear as focal dilatations of post-capillary venules in the upper plexus due to an increase in both luminal diameter and vascular wall thickness[211]. They are also associated with pericytes that exhibit atypical, prominent stress fibers. Interestingly, the dilatation of these venules was suggested to be the earliest morphologic event in AVM formation. According to 3D reconstructions of fully developed lesions in the mid- and lower dermis, the dilated venules connect with enlarged arterioles through capillary segments which subsequently disappear, leading to direct arteriovenous connections that are perivascularly infiltrated by lymphocytes. Mucosal telangiectases were not thoroughly investigated but were assumed to share the same organization as cutaneous ones[211].

3.4.3. Arteriovenous malformations

Last but not least, HHT is characterized by the development of visceral AVMs. These are direct connections between arteries and veins that bypass the interconnecting capillary network (Figures 16 and 18). AVMs in HHT patients affect vital organs including the lungs, liver, brain and spinal cord at various frequencies[199]. Hepatic involvement in HHT is very common, touching up to 74% of patients, but is asymptomatic in most cases. HHT-associated hepatic vascular malformations include diffuse telangiectases, which could develop into larger shunts. These shunts could involve different vessels and are thus classified as arteriovenous, arterioportal or portovenous shunts[212]. While aterioportal shunts connecting the hepatic artery to the portal vein can result in portal hypertension, arteriovenous shunts connecting the hepatic artery to the hepatic vein can lead to high-output cardiac failure[212,213]. Direct shunting of oxygenated blood from the hepatic artery to the hepatic vein, bypassing the liver, reduces effective hepatic perfusion and decreases systemic vascular resistance, leading to a higher cardiac output that gradually results in left heart failure[213]. Consequently, orthotopic liver transplantation is required for some patients with severe hepatic involvement[212]. Pulmonary AVMs are also relatively common, affecting up to 50% of patients. On the other hand, brain

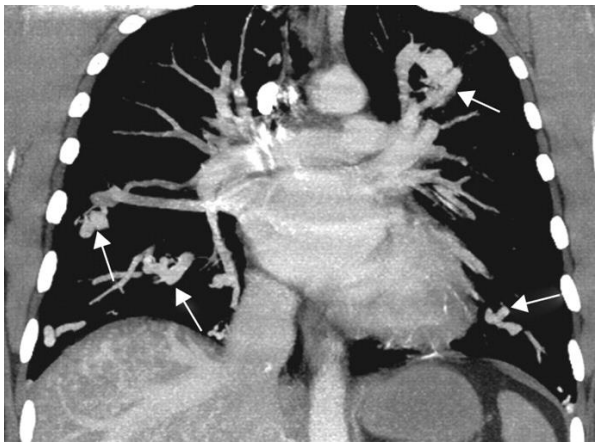

Figure 18. Pulmonary AVMs in an HHT patient. *Computed tomography of the chest of an HHT patient during severe haemoptysis showing numerous bilateral pulmonary AVMs (white arrows). Image taken from "Near-fatal haemorrhage from pulmonary arteriovenous malformation in HHT with increased cardiac output" by Cottin el al, European Respiratory Review, 2009.*

AVMs occur in only 10-20%, and spinal cord AVMs are the least common, reported in less than 1% of patients[214]. Interestingly, a clear correlation exists between the genotype of the patient and the location of developed AVMs, with HHT1 patients being more prone to develop pulmonary and cerebral AVMs while HHT2 patients more frequently presenting hepatic ones[206,210,215,216].

These abnormal connections are problematic for two reasons. First, AVMs are tortuous and fragile structures that allow the conduit of high pressured arterial blood into the veins, whose walls cannot normally accommodate this pressure. Consequently, at rare occasions, AVMs spontaneously rupture, leading to life-threatening internal hemorrhages in the aforementioned sites. Second, AVMs can give rise to a variety of complications due to shunting of blood *per se*. For example, focal loss of capillaries in pulmonary AVMs can impair the normal gaseous exchange leading to insufficient blood oxygenation. Moreover, pulmonary AVMs can provide a direct route to the systemic circulation for bacteria and small emboli that are normally filtered by the pulmonary capillaries, increasing the risk of brain abscesses and embolic strokes[214]. On the other hand, hepatic AVMs can give rise to high output cardiac failure due to excessive blood flow through the hepatic artery-hepatic vein shunt[212]. As for brain AVMs, these can undermine the critical blood-brain barrier, supporting neuronal dysfunction and seizures[217]. Therefore, AVMs are a major concern for HHT patients.

3.5. Current hypotheses behind lesion development

3.5.1. Haploinsufficiency

The fact that HHT causal *ENG* and *ACVRL1* mutations lead to loss of function of the corresponding protein product and that these mutations are inherited in an autosomal dominant manner raised plausible postulations that HHT vascular defects are caused by haploinsufficiency of the mutated gene product. This implies that a single wildtype (WT) copy of *ENG* or *ACVRL1* is not sufficient for producing enough functional protein to maintain the WT phenotype. This hypothesis was corroborated with several reports demonstrating a reduction in endoglin levels in HHT1 patient-derived cells. Endoglin protein expression levels of HHT1-derived HUVECs in addition to peripheral blood activated monocytes and endothelial colony forming cells (ECFCs) were found to be significantly lower than in healthy counterparts[218–220]. Functional analysis in endoglin overexpressing cells revealed that many mutants couldn't reach the plasma membrane, and some even exerted dominant negative effects by heterodimerizing with WT endoglin in the endoplasmic reticulum and trapping it intracellularly[221,222]. On the other hand, some mutants retained normal cell surface expression, but were functionally inactive due to lost ability to bind BMP9[221]. In all cases, *ENG* mutations found in patients with a definite clinical diagnosis resulted in less functional endoglin at the cell membrane.

Unlike most *ENG* mutations that result in decreased endoglin expression, HHT2-derived ECs and cells exogenously expressing ALK1 missense mutants did not necessarily display a reduction in cell surface ALK1 level compared to controls[219,220,223]. This is in line with the high prevalence of non-sense or frameshift mutations leading to premature termination codons in

case of *ENG* mutations, versus a higher occurrence of missense mutations in case of *ACVRL1* (http://arup.utah.edu/database). Mutations that did decrease cell surface ALK1 expression were either nonsense mutations or mutations that impaired ALK1 trafficking to the plasma membrane, while most other mutants (mut) were kinase dead and some could not bind BMP9[224]. In all cases, the mutations resulted in a partial or complete abolishment of ALK1-mediated signaling compared to exogenous WT ALK1-overexpressing cells[220,224,225]. In contrast to a study by our group[224], Gu et al and Fernandez-Lopez et al reported a dominant negative effect for some missense mutants upon their co-transfection with WT ALK1 in luciferase reporter cells[220,225]. However the authors of these studies used TGF-β, not BMP9 or BMP10, as the inducer for luciferase activity under the control of BMP responsive element (BRE). Since TGF-β activates Smad1/5/8 through binding heterodimeric ALK5/ALK1 complexes, the authors were testing the collective activity of ALK5/WT ALK1 and ALK5/mut ALK1 instead of WT ALK1/mut ALK1. So, all ALK5/mut ALK1 complexes will fail to activate BRE luciferase leading to a decrease in overall activity. Moreover, while the relative amounts of co-transfected WT and mutated ALK1 plasmids were not reported by Fernandez-Lopez et al, Gu et al introduced twice as much mutated ALK1 compared to the WT-encoding plasmid. This could lead to overrepresentation of the mutated form on the cell surface, which is not physiologically relevant and might explain the further decrease in luciferase activity in some co-transfected cells that was interpreted as a dominant negative effect[225]. In the functional analysis study performed by our group, equal amounts of WT and mutated ALK1 plasmids were co-transfected into mouse fibroblasts and BRE luciferase activity was measured in response to BMP9. As a result, luciferase activity was reduced in co-transfected cells compared to cells transfected with an equal total amount of only WT ALK1, but was similar to activity induced by cells expressing only the WT ALK1 portion (half the total amount)[224]. All in all, despite the discrepancies regarding the dominant negative effect, all ALK1 mutations that were believed to be causative of HHT led to reduced signaling activity when transiently co-expressed with WT ALK1.

In line with these studies, mice constitutively heterozygous for mutations in *Eng* or *Acvrl1* ($Eng^{+/-}$ or $Alk1^{+/-}$) exhibit reduced expression of the affected gene and present few HHT-like vascular lesions, including nosebleeds, telangiectases and dilated vessels with reduced vSMC coverage[226–228]. Nevertheless, these defects had a low penetrance, were unpredictable and occurred after a long delay starting from 3 months in $Eng^{+/-}$ mice and 7 months in $Alk1^{+/-}$ mice up until 2 years old. Interestingly, most lesions were detected in heterozygous 129/Ola inbred mice or mice in a mixed C57BL/6-129/Ola genetic background, while heterozygous deletion in C57BL/6 was much less penetrant, indicating an involvement of modifier genes in pathogenesis[226–229].

3.5.2. Need for a 2nd hit

Despite the initial studies summarized above, the haploinsufficiency model presents some limitations when explaining the cause of HHT vascular lesions. HHT is caused by germline LOF mutations in *ENG* or *ACVRL1* that are expressed by all vascular beds in the body, yet vascular malformations appear focally and strictly in characteristic locations[201]. In addition, related

patients carrying the same mutation can display different manifestations of the disease, which might be due to modifier genes or other causes[230]. These discrepancies suggest that additional local factors in each patient might be involved in driving the formation of these vascular defects. Some *in vivo* studies propose a role of environmental triggers in HHT pathogenesis[231]. For instance, $Eng^{+/-}$ mice, in the highly sensitive 129/Ola genetic background, which had abnormal fragile vessels in the eyelids displayed hemorrhages from these vessels only following local inflammation[229]. In line with that, endoglin was shown to play a role in leukocyte trafficking and extravasation that was impaired in $Eng^{+/-}$ mice compared to controls[232,233]. Similarly, 8-10 week old mice heterozygous for *Eng* or *Alk1* in the less penetrant C57BL/6 background, which don't normally show any vascular defects until several months later, developed cerebrovascular dysplasia upon local delivery of VEGF-encoding viral vectors in their brains, while WT mice treated with the same vectors had normal angiogenesis[234,235]. Hence, inflammatory and/or angiogenic stimuli can act as drivers of vascular dysplasia in susceptible heterozygous *Eng* or *Acvrl1* mutated vessels.

In addition to heterozygous mice, *Eng* or *Acvrl1* null mice were shown to readily and consistently develop AVMs when stimulated with pro-angiogenic or inflammatory signals[236–238]. To overcome embryonic lethality and gain insights on HHT pathogenic mechanisms in neonates or adults, several inducible knockout models of *Eng* or *Acvrl1* were developed using various tamoxifen-inducible Cre drivers. Inducible deletion of *Eng* or *Acvrl1* in the brain of adult mice with an established, mature endothelium resulted in minimal effects on the vasculature. On the contrary, additional local overexpression of VEGF in the brains of these mice drastically increased vascular dysplasia and induced AVM formation[239,240]. Subsequent administration of the anti-VEGF monoclonal antibody bevacizumab resulted in regression of the established dysplastic vessels[241]. Similarly, *Eng* or *Acvrl1* deletion in adult mice resulted in dermal AVMs only after wounding, and the malformation was restricted to the site of the wound[236,242]. Wounding itself elicits a healing response involving inflammation and the formation of new blood vessels, and as such is thought to provide environmental triggers supporting AVM development. Indeed, injection of VEGF or LPS into the skin of *Acvrl1* KO mice mimicked the effect of wounding in terms of dermal AVM development[238]. Moreover, blocking VEGF in *Acvrl1* KO mice using the VEGF-neutralizing antibody G6.31 effectively prevented new AVM development triggered by both LPS and wounding, highlighting angiogenesis as an essential element for driving AVM formation in the response to wounding[238]. Interestingly, this work also revealed that VEGF was required for all stages of AVM development, which were described as an initiation, maturation and maintenance phase, and blocking VEGF at any of these stages had positive therapeutic impacts to variable extents[238]. In addition, endothelial-specific inducible deletion of *Eng* in adult mice failed to produce any AVMs in the vital organs, but did give rise to AVMs in the cartilage of the pelvic symphysis. Interestingly, this peculiar tissue naturally expresses high levels of endogenous VEGF. Consequently, systemic anti-VEGFR2 treatment in these mice blocked AVM formation[243]. Similarly, earlier deletion of *Eng*, *Acvrl1 or Smad4* in neonates reproducibly results in AVM formation in the developing retina[171,244–246], which is a unique tissue characterized by postnatal vascularization through angiogenesis during the first week of life in mice[247].

On the other hand, it is important to note that some studies reported the spontaneous formation of AVMs in adult inducible *Acvrl1* KO mice, in the absence of apparent environmental triggers, especially in the GI tract within one week, followed by death[236,242].

While this might seem to contradictory, it could be that subtle inflammation induced by the gut microbiota is involved in lesion development. Furthermore, spontaneous brain AVMs were also reported in some conditional non-inducible *Eng* or *Acvrl1* KO models. Deletion of *Eng* from vSMCs and elongating ECs using the SM22a-Cre line cells[248] resulted in reproducible brain AVMs by 5 weeks of age shortly followed by death in more than half of the mice[237]. Similarly, *Acvrl1* deletion using the endothelial-specific L1-Cre induced early postnatal cerebral AVMs followed by death by postnatal day (P) 5[236]. In both cases, gene deletion occurred since gestation, yet mice survived beyond embryonic stages. This could be explained by variable degrees of activities of the Cre lines used and in the case of SM22α-Cre the fact that it doesn't target all ECs. The development of these seemingly spontaneous shunts might have commenced prenatally during active embryonic angiogenesis, or it might have been triggered early postnatally as the murine brain vasculature was shown to maintain a certain level of microvascular expansion during the first postnatal month characterized by endothelial sprouting, cell proliferation and vessel elongation[249].

3.6. HHT treatment

3.6.1. Current treatments

Current HHT treatments aim to reduce the risk and severity of bleedings, while managing the resulting anemia[250]. Epistaxis, the most common HHT symptom, can occur at any time, repetitively and can last for hours. This causes a great deal of discomfort for patients and poses serious psychological and social limitations on patients' personal and professional lives. Several measures are used in practice to limit HHT-related epistaxis, and treatment plans are usually stepwise and tailored to bleeding severity in each patient[250]. The simplest treatment relies on the use of topical moisturizers, typically saline, to keep the nasal mucosa hydrated[250]. Reducing mucosal dryness in the nose caused by turbulent airflow using various moisturizing agents helps prevent the cracking and bleeding of nasal telangiectases and was shown to significantly reduce epistaxis severity[251,252]. If not sufficient, the antifibrinolytic agent traxenamic acid, which slows down the breakdown of clots, can be taken orally to prevent or manage HHT-related epistaxis[250]. The effectiveness of this agent in reducing epistaxis severity has been validated in two randomized control trials, with minimal adverse events[253,254]. Although no increased risk of thrombosis was associated with tranexamic acid in HHT patients, its use is avoided in patients with high risk or history of thrombosis[250]. In patients showing no improvements with moisturizers or traxenamic acid, ablative therapies such as laser photocoagulation, electrocautery, radiofrequency ablation, coblation and injection sclerotherapy are used to seal or collapse the abnormal hemorrhagic nasal vessels, but these approaches only provide temporary improvement[250,255]. More severe cases are treated with septodermatoplasty, i.e. replacement of anterior nasal mucosa with a split-thickness skin graft, typically from the thighs[250,256]. Patients with recurrent epistaxis despite treatment typically undergo multiple and various procedures to manage their bleeding. In extreme cases, where epistaxis becomes life-threatening and other treatment options fail, patients are proposed surgical full nasal closure that effectively stops bleeding, but leads to obligatory mouth breathing and loss of olfaction[250,257,258].

Treatment options for GI bleedings in HHT patients are more limited, including argon plasma coagulation during diagnostic endoscopy and antifibrinolytics[250]. For both epistaxis and GI

bleeding, moderate to severe cases are currently proposed systemic anti-angiogenic therapies[250], as described in the following section. Epistaxis and GI bleeding, separately or collectively, often lead to iron-deficiency anemia, which is treated with iron supplementations or red blood cell transfusions[250].

Regarding visceral AVMs, pulmonary AVMs and some accessible brain AVMs are surgically resected or undergo embolization to stop blood from flowing into the lesions and reduce the occurrence or risk of bleeding[177,250,259]. Asymptomatic liver AVMs are left untreated, and embolization is not recommended for symptomatic ones due to high risk of serious complications. Patients with severe hepatic involvement are thus referred to orthotopic liver transplantation[250].

While most of the aforementioned treatments provide temporary relief, they are by no means curative as they do not address the underlying pathophysiology, and symptoms continue to worsen with age. Even following liver transplantation, disease was found to be recurrent with new hepatic lesions developing several years following the transplantation[260]. To date, there are no FDA or EMA-approved drugs for HHT, despite it being the second most common bleeding disorder worldwide (after Von Willebrand disease), but significant advances have been made in the last decade[261].

3.6.2. Future treatments

Individual case reports of HHT patients treated with bevacizumab (humanized anti-VEGF antibody) for cancer treatment and immunosuppressors with anti-angiogenic properties following organ transplantation drastically improved HHT symptoms[262–264]. These initial observations, the relative ease of drug repurposing, in addition to the large body of preclinical studies highlighting the involvement of angiogenesis in lesion development, triggered the launch of several clinical trials assessing anti-angiogenic therapies in HHT[252,265–270]. The most prominent therapy so far is intravenous bevacizumab, for which a phase III clinical study was completed (NCT03227263; pending results)[271]. In addition, following promising results from several case reports and small cohorts from separate treatment centers, an international, retrospective study evaluating the efficacy and safety of systemic bevacizumab in alleviating bleeding in 238 HHT patients across 12 treatment centers was implemented. This study, known as InHIBIT-Bleed, defined intravenous bevacizumab as a safe and effective treatment modality for managing HHT chronic bleeding as it led to general improvements in mean hemoglobin levels, reduction in RBC units transfused and iron infusions and decreased average epistaxis severity scores[261]. On the other hand, applying bevacizumab as a nasal spray was not more effective than placebo[252]. Other anti-angiogenic agents recently tested include the tyrosine-kinase inhibitors Sorafenib, Pazopanib and Nintedanib. Case reports using each of these inhibitors reported improved epistaxis severity or GI bleeding and a number of clinical trials have addressed or are currently evaluating their efficacies[271].

PI3K-AKT signaling pathway is a key signaling hub promoting EC survival and proliferation downstream of several angiogenic factors, such as VEGF and Ang1, and is activated by blood flow[272]. BMP9/BMP10 signaling normally counterbalances these proangiogenic triggers by reducing the phosphorylation and thus activating an inhibitor of this pathway called phosphatase and TENsin homolog (PTEN). However, in the context of defective BMP9/BMP10 signaling, PI3K-AKT pathway was found to be overactivated in cutaneous telangiectasia

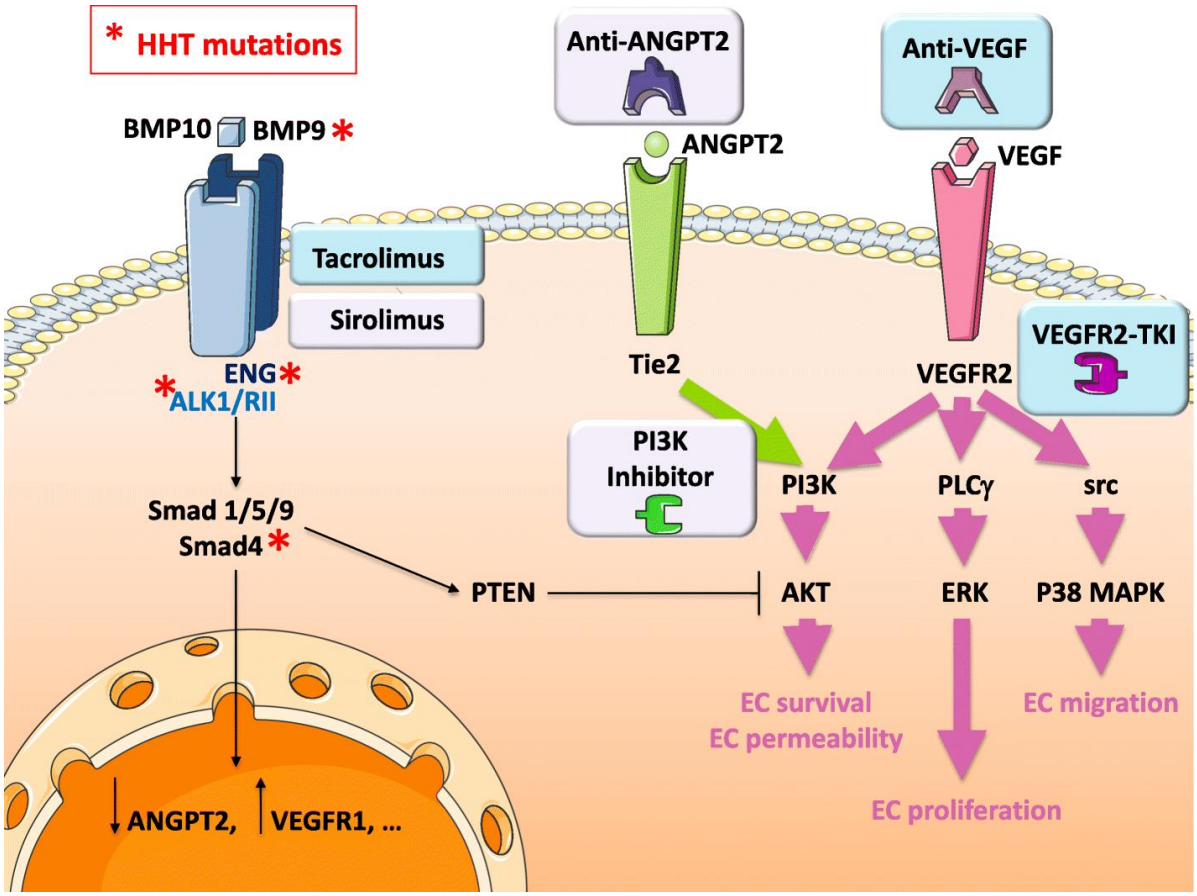

Figure 19. Signaling therapeutic targets for future treatments for HHT. *Mutations in components of the BMP9/BMP10 signaling pathway (red asterisks) result in reduced downstream signaling combined with increased activity of VEGF and ANGPT2 signaling pathways. A number of drugs targeting these pathways are currently in use in clinical trials (blue boxes) or under evaluation in preclinical studies (gray boxes) for HHT treatment. Image taken from "Future treatments for hereditary hemorrhagic telangiectasia" by Robert et al, Orphanet Journal of Rare Diseases, 2020.*

biopsies from HHT2 patients[273] and in the vascular lesions of several HHT mouse models[246,274]. Interestingly, blocking PI3K-AKT signaling in these mice by genetic or pharmacological means not only prevented, but also reversed HHT-associated vascular dysplasia[246,273,274]. In addition, mTOR signaling downstream AKT was found to be overactivated in BMP9/BMP10-immunoblocked mice, and blocking it reduced vascular defects in these mice[275]. In line with that, several case reports of HHT patients treated with the immunosuppressor sirolimus (rapamycin, mTOR inhibitor) showed great reduction of nosebleeds and anemia[271]. Of note, combining Sirolimus with the kinase inhibitor Nintedanib, which targets the receptors of PDGF, FGF and VEGF, displayed a synergistic effect in preventing and reversing vascular malformations, bleeding and anemia in 2 different HHT mouse models[275]. Inhibiting mTOR or MEK pathways, but not eNOS or MAPK pathways downstream VEGFR2 was also effective in preventing the formation of vascular defects in *Eng* mutant zebrafish[276]. Interestingly, in addition to inhibiting mTOR signaling, Sirolimus was detected in a screen of FDA-approved drugs for activators of BMP signaling as one of the 3 top hits[277]. The number one hit, in two independent screens for the same purpose, was Tacrolimus (FK506)[277,278]. Tacrolimus was then shown to potently activate Smad1/5/8 signaling in ALK1-mutated ECs and BMP9/10-immunoblocked mice, and to block VEGF-induced AKT activation, collectively leading to reduction in vascular dysplasia[278]. Following these studies, clinical trials assessing the effect of tacrolimus on bleeding in HHT patients revealed a positive impact on epistaxis or GI bleeding,

hemoglobin levels and transfusion needs upon oral administration or during (but not after) local application as a nasal ointment[279,280].

While these novel therapies, summarized in Figure 19, proved promising in terms of management of HHT-associated bleeding and subsequent anemia, their effects on patient AVMs are still poorly defined. Moreover, using systemic anti-angiogenic drugs during active growth (before maturity) could be troublesome, as extension of the vascular network is essential for supporting the increasing metabolic demands of developing tissues. Hence, there is still room for improvement, and better understanding of the mechanisms leading to vascular dysplasia in HHT might uncover other dysregulated knobs that can be safely targeted for therapeutic purposes.

4. Pulmonary arterial hypertension (PAH)

4.1. Brief overview

Pulmonary arterial hypertension (PAH) is a rare vascular disease affecting around 50 subjects/million in European countries[281]. It is a devastating disorder associated with poor prognosis and a mean survival of 2.8 years when left untreated[282]. As indicated by its name, PAH is characterized by an elevated mean pulmonary arterial pressure (PAP), exceeding 20 mmHg at rest, associated with high pulmonary vascular resistance (PVR, >2 Wood Units) and a normal pulmonary arterial wedge pressure (≤15 mmHg), measured by right heart catherization[283]. This progressive disease affects distal muscular-type pulmonary arteries and arterioles, which become vasoconstricted in patients and whose walls undergo intense pathological thickening and stiffening. Consequently, the arterial lumen gradually becomes occluded, resulting in an increased PVR and a subsequent elevation in PAP[284] (Figure 20). These changes compromise normal gaseous exchange in the lungs, resulting in dyspnea, angina, fatigue, dizziness and syncope. More importantly, the sustained elevation in PAP progressively leads to right heart failure and eventually death[285]. The similarity of initial symptoms of PAH with other common respiratory conditions and the progressive nature of the disease lead to a delayed proper diagnosis of typically more than 2 years[286]. Unfortunately, no cures for PAH have been identified to date, other than lung transplantation in eligible cases. To slow disease progression, patients are commonly treated with vasodilators, but still generally experience progressive functional decline with high mortality rates[287,288].

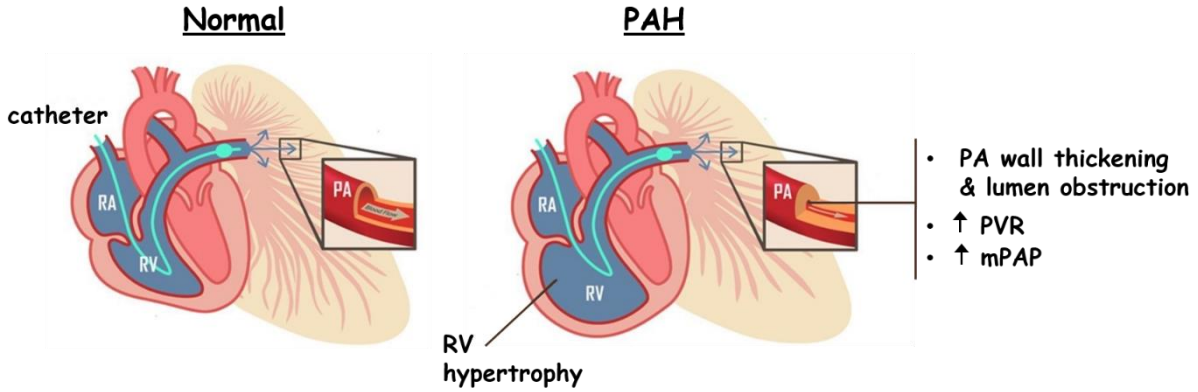

Figure 20. Defining features of PAH pathophysiology. *In PAH patients, the walls of small pulmonary arteries (PA) undergo extensive remodeling leading to lumen obstruction, elevated pulmonary vascular resistance (PVR) and mean pulmonary artery pressure, measured by right heart catherization. Elevated PVR and mPAP progressively lead to right ventricular hypertrophy and failure. Image adapted from "Pulmonary Arterial Hypertension" by Lai et al, Circulation Research, 2014.*

4.2. Pulmonary arteries in normal and PAH lungs

4.2.1. Structural features of normal pulmonary arteries

Physiologically, the pulmonary circulation, which is responsible for replenishing deoxygenated blood received from the right ventricle with oxygen in the lungs, is a high-flow, low-resistance and low-pressure system. Similar to the systemic circulation, this system receives the entirety of the cardiac output but circulates it with remarkably lower resistance and pressure values. These unique hemodynamic characteristics of the pulmonary circulation are mainly attributed to two important traits. First, the small arteries and pre-capillary arterioles in the lungs are highly compliant, due to their distinctively thin walls. The large pulmonary arteries that are in close proximity to the heart are classified as elastic-type arteries, whose medial layers contain a high level of elastic fibers. This feature enables them to maintain a relatively stable pressure gradient as the heart pumps blood into the lungs. As these elastic arteries branch into smaller ones (cross-sectional diameter below 500µm), they give rise to "muscular-type arteries" that are less elastic and more muscularized. However, pulmonary muscular-type arteries are less muscularized and have wider lumens than their systemic counterparts. In addition, the muscular layer is gradually minimized as the pulmonary arterial tree progresses distally into the lungs. Finally, the pre-capillary arterioles are barely muscularized and lack the elastic laminae. Consequently, distal pulmonary arteries and pre-capillary arterioles are less resistant to flow than their systemic counterparts due to their wider lumens and can easily distend in response to increased flow rates due to their weakly muscularized thin walls, helping them maintain low levels of vascular resistance. Second, the pulmonary circulation comprises a relatively non-perfused vascular reservoir that can be readily recruited and employed when needed. Because of these properties, the pulmonary vasculature circulates blood at low pressure, which is important for proper gaseous exchange, and can withstand rapid increases in cardiac output that are experienced during strenuous exercise without strongly affecting PAP[284,289].

4.2.2. Pathological features of PAH pulmonary arteries

PAH lungs are characterized by abnormally high PVR and mean PAP, which interfere with proper gaseous exchange and impose right ventricular strain. The hypertensive lungs of PAH patients and animal models present a set of vascular abnormalities specifically affecting muscular-type arteries and arterioles. These vessels display defects in all 3 tunics of their walls, collectively leading to the progressive obstruction of their lumens (Figures 21 and 22A). Early events in PAH vascular pathogenesis include endothelial dysfunction, characterized by a plethora of irregularities. These comprise an imbalance in the levels of secreted vasodilators and vasoconstrictors in favor of the latter, reduced anticoagulant properties, increased production of reactive oxygen species, impaired DNA repair, cancer-like metabolic changes characterized by increased rate of aerobic glycolysis (Warburg effect), endothelial-to-mesenchymal transition (EndMT) characterized by an upregulation of mesenchymal markers at the expense of endothelial markers, enhanced expression of pro-inflammatory adhesion molecules and local dysregulated secretion of various chemokines and growth factors[290,291].

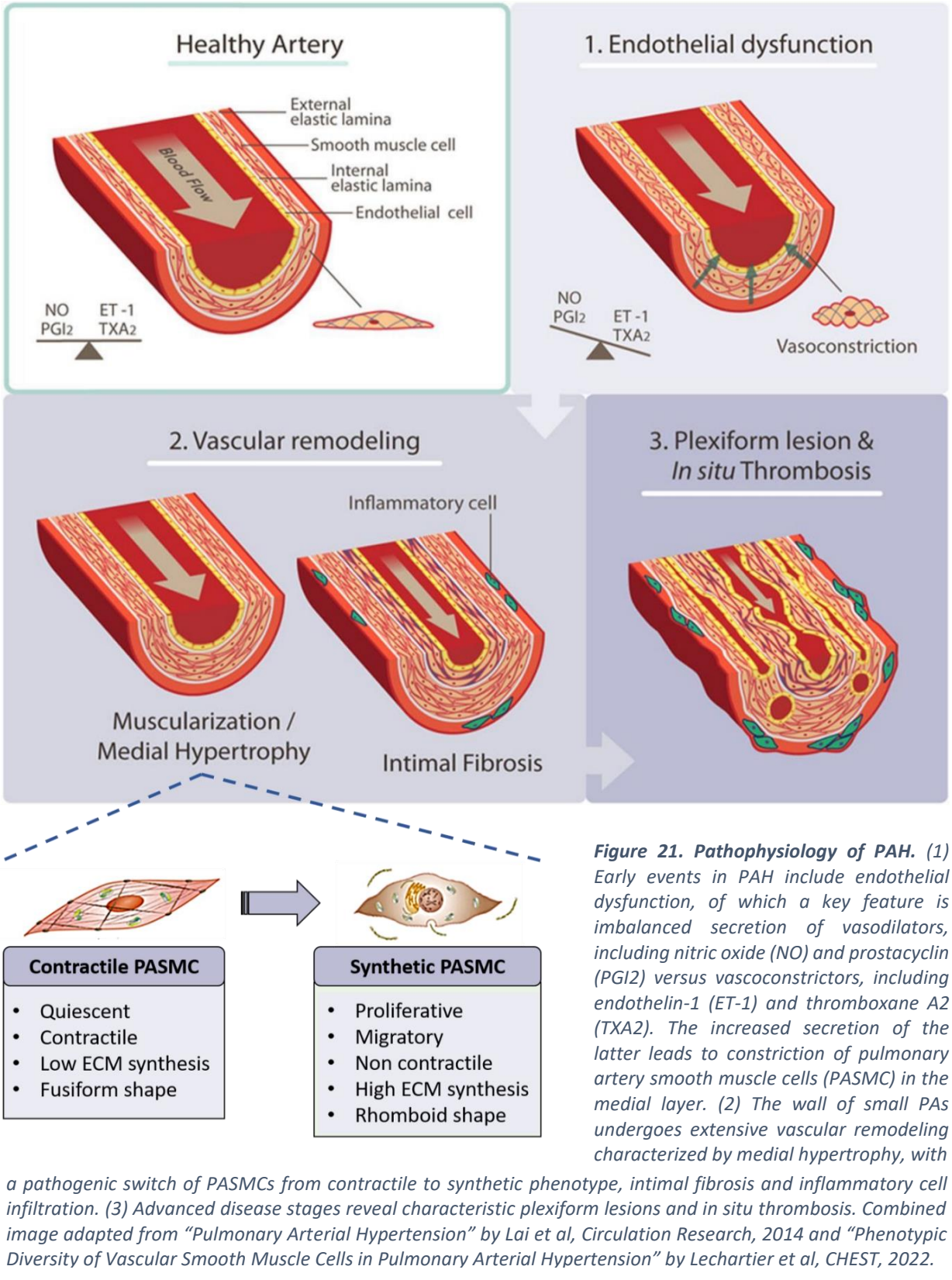

Figure 21. Pathophysiology of PAH. *(1) Early events in PAH include endothelial dysfunction, of which a key feature is imbalanced secretion of vasodilators, including nitric oxide (NO) and prostacyclin (PGI2) versus vascoconstrictors, including endothelin-1 (ET-1) and thromboxane A2 (TXA2). The increased secretion of the latter leads to constriction of pulmonary artery smooth muscle cells (PASMC) in the medial layer. (2) The wall of small PAs undergoes extensive vascular remodeling characterized by medial hypertrophy, with a pathogenic switch of PASMCs from contractile to synthetic phenotype, intimal fibrosis and inflammatory cell infiltration. (3) Advanced disease stages reveal characteristic plexiform lesions and in situ thrombosis. Combined image adapted from "Pulmonary Arterial Hypertension" by Lai et al, Circulation Research, 2014 and "Phenotypic Diversity of Vascular Smooth Muscle Cells in Pulmonary Arterial Hypertension" by Lechartier et al, CHEST, 2022.*

These abnormalities facilitate chronic pathogenic vascular remodeling that gradually leads to narrowing of the vascular lumen. The most common structural feature of PAH lungs is medial thickening of small pulmonary arteries (Figures 21 and 22B) and muscularization of normally non-muscularized arterioles. An artery is said to present medial thickening when the diameter

of its medial layer surpasses 10% of its total cross-sectional diameter, which occurs due to medial hyperplasia and hypertrophy[284]. This process is accompanied by a pathogenic switch of vSMCs from the mature contractile phenotype to the dedifferentiated synthetic phenotype exhibiting enhanced proliferation, migration, and ECM synthesis capacity (Figure 21). This last feature increases matrix deposition in the vascular wall, contributing to its stiffening[292]. Medial thickening can occur as an isolated event, considered early and potentially reversible as occurs in pulmonary hypertension associated with high altitudes, or is more commonly accompanied by other changes described below[293].

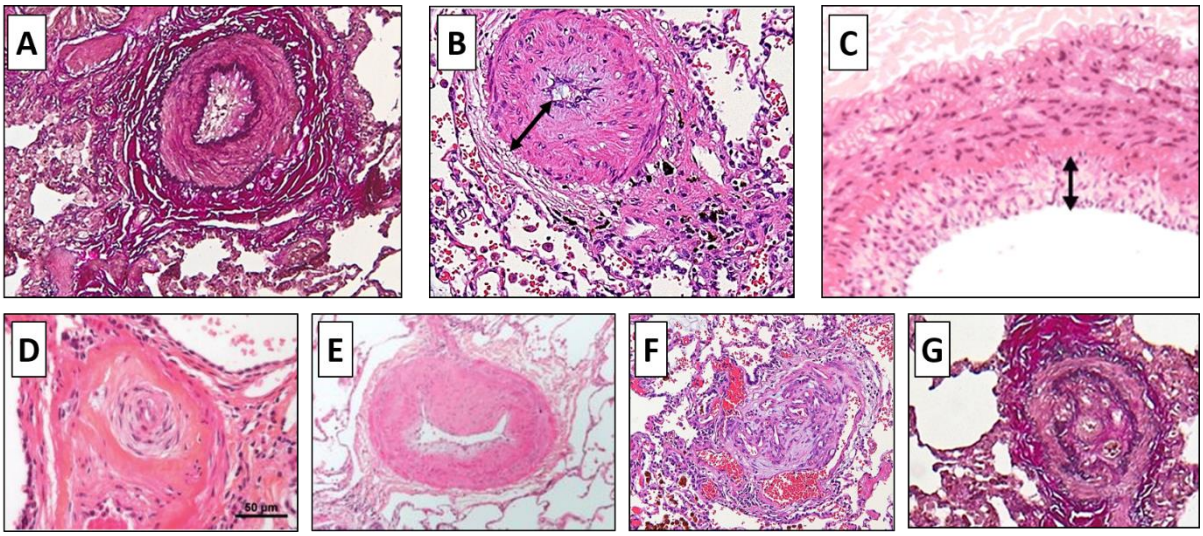

Figure 22. Histological representations of classical pulmonary artery lesions in PAH*. Haematoxylin-and-eosin staining of PAs displaying (A) some intimal fibrosis, marked medial hypertrophy and adventitial fibrosis, (B) medial hypertrophy (delimited by arrow), (C) neointimal proliferation (delimited by arrow), (D) concentric intimal laminar fibrosis composed of multiple concentrically arranged fibrous layers, (E) eccentric intimal fibrosis, (F) plexiform lesion comprised of slit-like vessels lined by endothelium and surrounded by loose fibrous tissue. (G) Elastic van Gieson staining showing an organized and re-canalized thrombus with multiple lumens. Images taken from "Diagnosis and management of pulmonary hypertension over the past 100 years" by van Wolferen et al, Respiratory Medicine, 2007, "Recent advances in pulmonary arterial hypertension" by Wilkins et al, F1000Research, 2018 and "Pathology and pathobiology of pulmonary hypertension: state of the art and research perspectives" by Humbert et al, Eur Respir J, 2019.*

The intima layer also plays an active role during PAH-associated vascular remodeling. ECs of small arteries and arterioles in PAH lungs display excessive apoptosis with the emergence of apoptotic-resistant highly proliferative cell populations[294,295] (Figure 22C). In addition, the gradual occlusion of the pulmonary arteries by vasoconstriction and medial thickening results in hemodynamic changes that were proposed to act as an additional necessary trigger for the formation of neointimal lesions. These represent new vascular structures mainly composed of migrating and proliferative vSMCs and fibroblasts with enhanced deposition of ECM components. Together, these elements accumulate between the endothelium and the medial layer and worsen lumen occlusion[296]. Abnormally proliferating fibroblasts and myofibroblasts in the intima also give rise to fibrotic intimal lesions that may be either uniform (concentric, Figure 22D) or focal (eccentric, Figure 22E)[293]. Fibrotic intimal lesions are also commonly associated with fibrosis of the adventitia, thus additionally implicating this final layer in PAH.

Furthermore, PAH lungs reveal an obliteration of pre-capillary arteries due to excessive vascular pruning leading to patterns of vascular rarefaction[290]. At late stages, PAH pulmonary arteries additionally develop plexiform lesions, which are the most typical manifestations of

PAH lungs[293]. These complex lesions involve monoclonal masses of apoptosis-resistant hyperproliferative ECs, as well as fibroblasts and ECM components that completely block the vascular lumen[297] (Figures 21 and 22F). In situ thrombosis is also a common feature of PAH lungs (Figures 21 and 22G) and some patients reveal elevated plasma levels of D-dimers and fibrinopeptides A and B, indicative of excessive coagulation[293]. In addition to changes in the different vascular components, the complex pathobiology of PAH was found to involve an immune arm, as excessive perivascular infiltration of various inflammatory cells was reported in PAH lung sections and animal models[290]. All in all, PAH pathogenesis is a complex process involving various malfunctioning vascular components that participate in increasing wall stiffness and lumen occlusion of distal pulmonary arteries and arterioles through vasoconstriction, abnormal vascular remodeling and thrombosis.

4.3. Clinical classification of PAH

Pulmonary hypertension (PH), affecting around 1% of the world population, is an umbrella term encompassing a wide variety of conditions commonly characterized by an elevated mean PAP, such as PH due to left heart disease, obstructive lung disease or hypoxia due to high altitudes. These conditions are clinically classified into 5 groups, of which the first is PAH[283]. In turn, PAH is further subdivided into several categories based on the underlying cause. As defined during the 6th World Symposium on Pulmonary Hypertension in 2018, these categories are: (1) idiopathic PAH with an unknown underlying cause, (2) heritable PAH caused by genetic mutations, (3) PAH induced by toxins and drugs such as methamphetamines and the structurally related anorexigens, (4) PAH associated with other diseases such as connective tissue and congenital heart diseases, (5) PAH with features of venous/capillary involvement and (6) persistent PH of the newborn (Figure 23)[283,298].

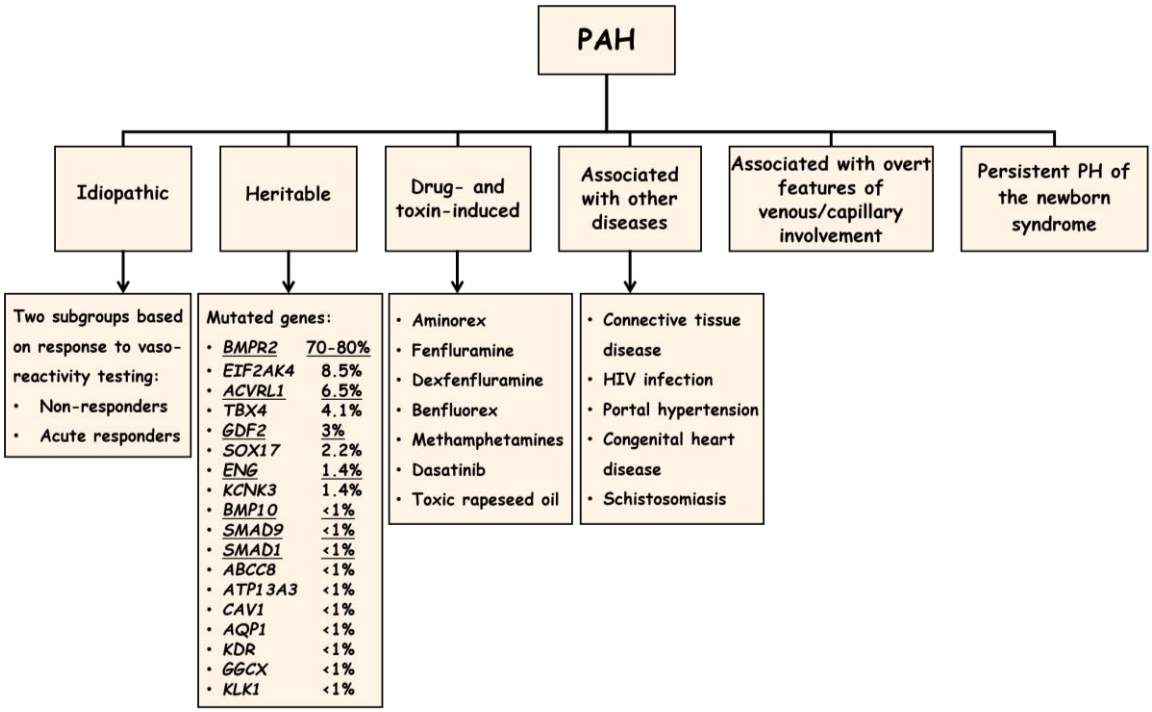

Figure 23. Updated clinical classification of PAH based on underlying etiology. *The 7 subcategories of PAH, as defined in the 6th World Symposium on Pulmonary Hypertension, as well as lists of mutated genes in heritable form with their respective prevalence, drugs and toxins definitely associated to PAH and diseases responsible for PAH are presented. Mutated genes encoding components of the BMP9/BMP10 signaling pathway are underlined.*

4.4. Heritable PAH

4.4.1. Genetic basis

The heritable PAH (HPAH) group comprises familial (≥2 clinically diagnosed family members with or without a detected germline mutation, making up around 3.9-6% of all PAH cases[285,299]), but also sporadic (initially idiopathic) cases in which PAH-associated mutations were identified. Familial and sporadic PAH cases are assigned to the HPAH group when they are not additionally associated with other PAH subcategories[300].

The first identified PAH-mutated gene was *BMPR2*, encoding one of the three type II TGF-β superfamily receptors that can mediate BMP signaling and in particular BMP9/BMP10 signaling in ECs. Mutations in this gene were later identified in at least 70% (Figure 23) and 11-40% of familial and sporadic HPAH cases, respectively[282]. These mutations reveal an autosomal dominant inheritance, but exhibit incomplete penetrance of 42% in females and only 14% in males[301]. The majority of identified *BMPR2* pathogenic mutations in PAH patients are nonsense, frameshift or splice-site mutations, whose corresponding transcripts are predicted to be degraded by nonsense-mediated mRNA decay. In addition, large deletions or duplications affecting ≥1 exon, which significantly distort protein structure, are also common[300]. Therefore, haploinsufficiency is expected to be the molecular mechanism in these cases. Missense mutations, often in the kinase domain of BMPRII, also occur and some are expected to act as dominant negatives[300]. In all cases, PAH-predisposing pathogenic *BMPR2* mutations lead to loss of function of the protein product.

In the last 2 decades, rare mutations in several other genes have been linked to PAH (Figure 14), many of which encode components of the endothelial-specific BMP9/BMP10 signaling pathway. These included: *ACVRL1*, *GDF2* (encoding BMP9), *ENG*, *BMP10*, *SMAD1*, *SMAD9* (encoding Smad8) and *CAV1* (encoding caveolin 1, a component of caveolae that is indispensable for BMPRII plasma membrane localization[302,303])[300] (Figure 23). Therefore, the BMP9/BMP10 pathway seems to be heavily implicated in PAH pathogenesis, and that's what drew our attention to this disease (Figure 24).

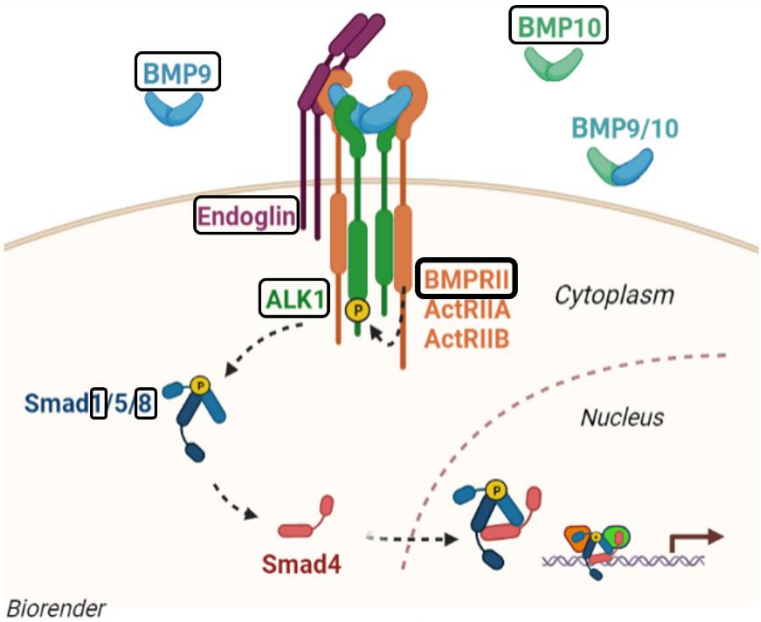

Figure 24. BMP9/BMP10 signaling components are mutated in heritable PAH. *Around 80% of HPAH patients are caused by mutations in the gene encoding BMPRII (in thick black box). Several other components of the BMP9/BMP10 pathway have been reported to be mutated in patients with PAH, including: endoglin, ALK1, BMP9, BMP10, Smad1 and Smad8 (in thin black boxes). Image generated using*

4.4.2. Pathogenesis

4.4.2.1. Reduction of BMPRII expression and signaling in PAH patients

For a very long time, the molecular mechanisms underlying the aforementioned vascular abnormalities have been largely obscure. The identification of PAH-causing *BMPR2* mutations, despite occurring in only a subset of PAH patients, provided important mechanistic insights into PAH pathogenesis. BMPRII expression is high in normal lung vasculature and displays a predominantly endothelial expression pattern with a more focal and weaker expression on vSMCs[304]. The lungs of PAH patients carrying *BMPR2* mutations were found to exhibit a reduced BMPRII expression and weakened canonical downstream signaling in terms of Smad1/5 activation and downstream expression of Id proteins in pulmonary artery (PA) SMCs and ECs[304–310]. On the other hand, the effect of *BMPR2* mutations in patient PASMCs on non-canonical MAPK signaling is controversial, with studies from the same group showing either a decrease in BMP4-mediated ERK1/2 phosphorylation or no change in ERK1/2 and p38 activation[305,306]. On the contrary, in PAECs, BMPRII silencing led to constitutive activation of Ras/Raf/ERK1/2 pathway, which normally enhances EC proliferation[311]. Interestingly, reduced BMPRII expression and signaling was also reported in idiopathic PAH patients not carrying any *BMPR2* mutations, pointing to a common mechanism in PAH pathogenesis regardless of the mutation status[304,305,310]. Several mechanisms explaining the decrease in BMPRII expression or signaling activity in PAH patients in the absence of *BMPR2* mutations have been proposed. These include downregulation of BMPRII expression by miRNAs under different conditions, such as hypoxia (miR-21, miR-125a) and interleukin (IL)-6 stimulation (miR-17/92), TNF-α stimulation or by estrogen receptor signaling, which is consistent with the higher disease prevalence in female patients compared to males. Interestingly, disturbed blood flow was also associated with a reduced expression of BMPRII in the systemic vasculature[312]. Since PAH lungs display impaired hemodynamics with many occlusions, it is possible that disturbed flow can further suppress BMPRII in the pulmonary vasculature. Furthermore, BMPRII signaling can be weakened through upregulation of its antagonist gremlin1 by the vasoconstrictor endothelin-1 (ET-1), whose production is increased by dysfunctional ECs in PAH lungs[312]. A recent study even attributed reduced BMPRII expression in PAECs and PASMCs of idiopathic patients to the decrease in the expression level of the chromatin remodeler SIN3a[313]. In line with those studies, ubiquitous heterozygous or homozygous BMPRII-deficiency *in vivo* was shown to induce spontaneous PH or exacerbate it in response to chronic hypoxia. This was also the case when BMPRII was targeted specifically in ECs or vSMCs in various transgenic animal models, in accordance with the heavy implication of these cell types in PAH vascular lesions[282].

4.4.2.2. Functional consequences of BMPRII deficiency

To date, the pathogenic mechanisms underlying PAH pathogenesis are still not fully elucidated, but a clear link has been established between loss of BMPRII signaling in response to several BMPs on one hand and the disrupted proliferation and apoptosis of vascular cells on the other one. For instance, BMP2, BMP4 and/or BMP7, which preferentially bind BMPRII as the type II receptor[314], were shown to inhibit the proliferation of rat and human PASMCs in

an Id1/Id3-dependent manner[306,307,315,316] and to induce apoptosis of human PASMCs accompanied with downregulation of the anti-apoptotic protein Bcl-2[308]. However, in PASMCs from PAH patients, these BMP-induced anti-proliferative and pro-apoptotic effects were reduced[306,308,316], in accordance with the characteristic medial hyperplasia in PAH lungs.

At the level of the endothelium, EC apoptosis is a hallmark of PAH lungs and is later on accompanied by increased proliferation of apoptosis-resistant ECs. Indeed, BMP signaling, either via BMP2 and BMP7 that bind ALK2, ALK3 or ALK6 or via BMP9 that binds ALK1, was shown to enhance PAEC survival by conferring protection from apoptosis[159,317]. In line with that, silencing BMPRII increased basal apoptotic levels in PAECs in one study[317] and reduced the protective effect of BMP9 against pro-apoptotic stimuli in another[159]. In parallel, BMP9 inhibited the proliferation of control PAEC and mouse pulmonary EC, but surprisingly had an opposite effect on BMPRII-deficient ECs, which showed enhanced proliferation in response to BMP9 due to prolonged canonical Smad1/5/8 signaling[318]. In addition, silencing BMPRII in human PAECs, without exogenous BMP stimulation, was sufficient to promote cell proliferation and migration through constitutively activating Ras/Raf/ERK1/2[311]. Furthermore, in line with the inhibitory effect of BMP9 on vascular permeability (described in Chapter 2), reduced BMPRII signaling was shown to increase endothelial permeability both *in vitro* and *in vivo*, enhancing inflammatory cell transmigration, which is required for the observed excessive infiltration of inflammatory cells in PAH lungs[159,319,320]. All in all, BMPRII, which mediates signaling of various ligands, is essential for the proper functioning of the pulmonary vasculature, and reduction in its expression and activity predisposes to PAH.

The subsequent identification in PAH patients of LOF germline mutations in *ACVRL1* and *ENG*, which are not expressed by vSMCs, and their ligands BMP9 and BMP10, further emphasized the specific role of BMP9/BMP10 signaling axis in PAH pathophysiology. In other words, ECs with defective BMP9/BMP10 signaling are probably enough to drive PAH pathogenesis. These cells can then project their abnormalities on neighboring cells through defective intercellular communications. In line with that, pulmonary ECs from idiopathic PAH patients were found to secrete excessive amounts of cytokines and growth factors that can act on neighboring vSMCs in a paracrine manner. These include the mitogenic vascoconstrictors ET-1 and angiotensin II and the growth factor FGF-2[291]. Moreover, BMP9 and BMP10 were shown to suppress the basal expression and secretion of CCL2, an important chemokine for monocyte and macrophage chemotaxis, in control human PAEC in a BMPRII and ALK1-dependent manner[321]. More generally, RNA-sequencing analysis of the lungs of double BMP9/BMP10 KO mice compared to controls identified massive dysregulations in genes related to inflammation and immunity. This means that deficient endothelial BMPRII signaling might also drive defective communication with immune cells, enhancing their recruitment[162].

4.4.2.3. Need for 2nd hits

BMP9/BMP10 signaling is required for preventing abnormal pulmonary vascular remodeling characteristic of PAH. Nevertheless, it is important to note that carriers of PAH-predisposing mutations display a low PAH penetrance, meaning that not all pathogenic mutation carriers will develop PAH[285,299]. This can be clearly appreciated in HHT patients with *ENG* or *ACVRL1* mutations, as most of these patients don't present PAH symptoms. This implies that additional events on top of the germline heterozygous mutation might be needed for PAH manifestation.

Accordingly, both genetic and environmental hits have been proposed to play a role in driving PAH pathogenesis.

Recently, *FHIT*, a tumor suppressor gene encoding fragile histidine triad diadenosine triphosphatase, was identified as a potential *BMPR2* modifier gene that is consistently downregulated in PAH patients with different etiologies[322]. This gene is highly expressed in the lungs and is a chromosomal fragile site gene that is readily mutated and downregulated in response to environmental insults[323]. In turn, FHIT downregulation was shown to reduce BMPRII expression, and its loss *in vivo* exacerbated chronic-hypoxia-induced PH[322]. Interestingly, BMPRII dysfunction in lung ECs was strongly associated with increased susceptibility to DNA damage, suggestive of impaired DNA repair responses. In turn, excessive DNA damage resulted in reduced BMPRII expression levels, constituting a vicious cycle[324]. This can facilitate the generation of somatic mutations in *FHIT* for example, but also in other genes that could be important for vascular homeostasis. Somatic mutations leading to loss of heterozygosity of BMPRII in PAH are not common, but a patient with germline *BMPR2* mutation was reported to harbor a somatic deletion of the gene encoding Smad8, which itself is infrequently mutated in PAH[325]. Collectively, these studies suggest that additional genetic hits that further suppress BMPRII expression or signaling below a critical threshold might serve as drivers of PAH pathogenesis.

Environmental triggers, such as inflammation, can also play a role in that sense. LPS administration to *BMPR2*-mutated patient PASMCs was shown to further suppress BMPRII signaling compared to untreated mutated cells[307], and TNF-α was found to reduce BMPRII expression and promote its cleavage post-translationally[326]. BMPRII deficiency, in turn, promoted exaggerated responses to inflammatory stimuli in both *BMPR2*-mutated patient cells and *BMPR2*-KO cells[327,328]. *In vivo*, chronic LPS administration induced PH in heterozygous *Bmpr2* KO mice but not in WT littermates, whereas amelioration of the exaggerated inflammatory response inhibited PAH development[327]. Therefore, while inflammation is known to be involved in advanced disease stage, it might also be a driver of PAH onset.

4.5. PAH treatments

4.5.1. Current treatments

Currently approved therapies for PAH aim to slow down clinical worsening by reducing pulmonary artery vasoconstriction. These therapies target 3 central pathways that regulate pulmonary vascular tone and are dysregulated in PAH patients: the ET-1, NO and prostacyclin pathways (Figure 25). Physiologically, these 3 pathways result in the release of vasoconstrictors or vasodilators from ECs that directly act on neighboring vSMCs via paracrine signaling to regulate their contractility.

Endothelin-1 is one of the most potent vasoconstrictors that also promotes vSMC proliferation. It is produced by ECs, and to a lower extent by vSMCs and other cell types and exerts its effects by binding to two different G-protein coupled receptors called ETA and ETB. ETA is primarily expressed on vSMCs and mediates ET-1's action as a vasoconstrictor. On the other hand, ETB is expressed by both ECs and vSMCs and mediates opposing outcomes in the 2 cell types: while ET-1 binding to ETB on vSMCs also promotes vasoconstriction, its binding

on endothelial ETB can exert vasodilatory and antiproliferative effects by reducing its bioavailability with respect to vSMCs and promoting synthesis of the vasodilators NO and prostacyclin by ECs[329]. Interestingly, ET-1 is more expressed in the lungs than other organs, and its levels were found to be elevated in hypertensive lungs[330] and plasma of PAH patients[331]. The levels of ET receptors were also found to be increased in the distal arteries of pulmonary hypertensive patients[332]. As such, approved treatments for PAH include the selective ETA inhibitor ambrisentan and the dual ETA/ETB inhibitors bosentan, which was the first approved oral treatment for PAH, and more recently, its derivative macitentan, all of which improved hemodynamics and exercise capacity in patients[287] (Figure 25).

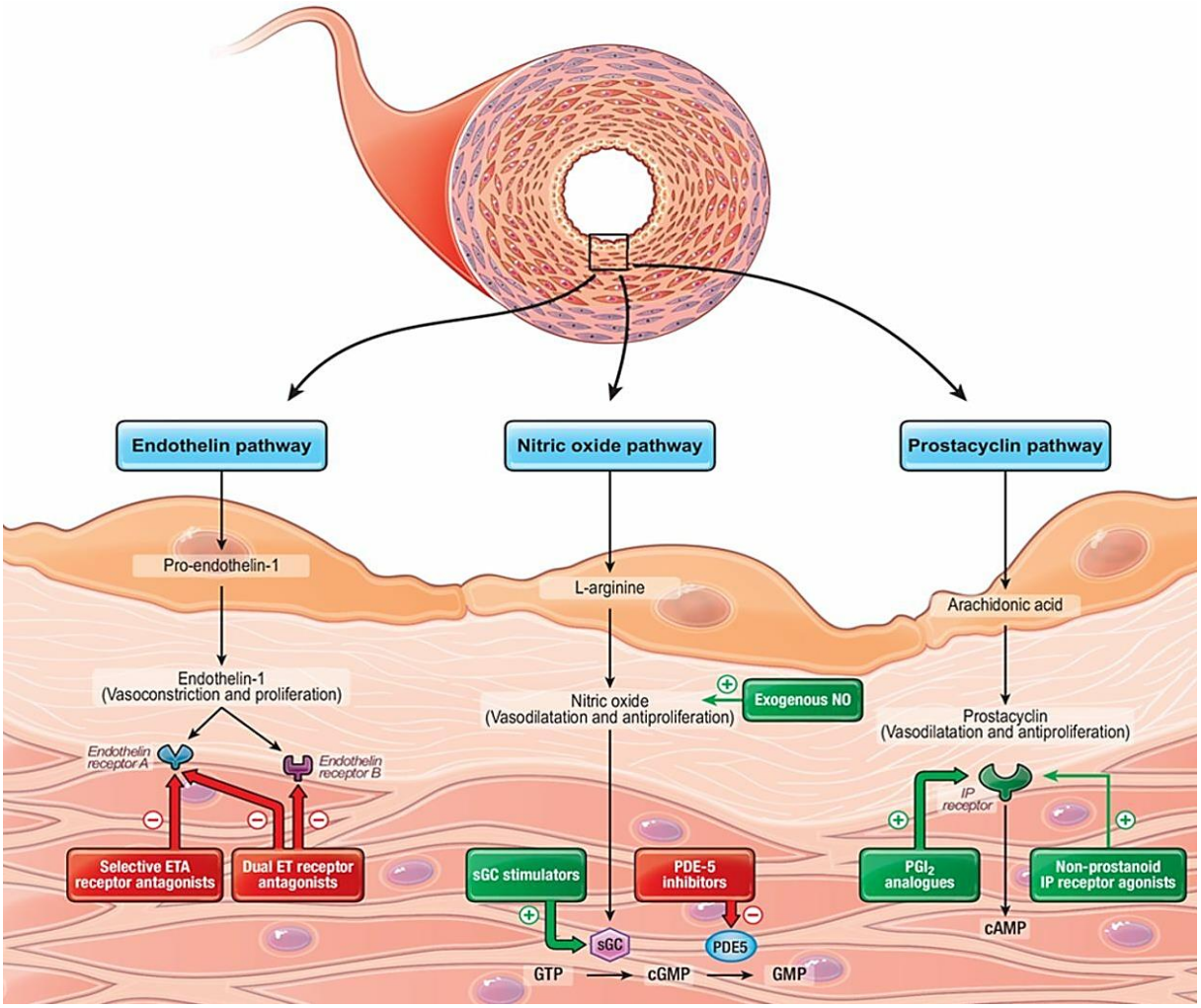

Figure 25. The three key vasomotor pathways targeted by current PAH therapies. *Endothelial dysfunction in pulmonary arterial hypertension (PAH) results in reduced production of endogenous vasodilatory molecules (nitric oxide and prostacyclin) and the upregulation of the vasoconstrictor endothelin-1 (ET) that also promotes smooth muscle cell proliferation. Inhibitors of ET pathway include selective and nonselective ET receptor antagonists; the nitric oxide (NO) pathway can be targeted by direct administration of exogenous NO, inhibition of phosphodiesterase type-5 (PDE-5), or stimulation of soluble guanylate cyclase (sGC); and the prostacyclin pathway can be activated by administratering prostanoid analogues or nonprostanoid I-prostanoid (IP) receptor agonists. Image taken from "Advances in Therapeutic Interventions for Patients with Pulmonary Arterial Hypertension" by Humbert et al, Circulation, 2014.*

Nitric oxide is an endogenous vasodilator produced in ECs by endothelial NO synthase (eNOS) upon l-arginine oxidation and also presents anti-proliferative and anti-thrombotic effects. Gaseous NO released from the endothelium diffuses to the underlying medial layer, where it binds and activates soluble guanylyl cyclase (sGC) in vSMCs. This enzyme converts guanosine triphosphate (GTP) to cyclic guanosine monophosphate (cGMP), which promotes vSMC relaxation. As a regulatory mechanism, cGMP is degraded by phosphodiesterase 5 (PDE5) that is highly expressed in vSMCs[288]. In PAH patients, NO bioavailability was found to be reduced, either due to downregulation of eNOS expression or to its reduced activity[333]. Hence, the NO-sGC-cGMP pathway represents an attractive target for enhancing vasodilation in PAH lungs, and indeed several drugs targeting different aspects of it have shown beneficial outcomes and were approved for PAH patients[287] (Figure 25). These include the sGC stimulator riociguat, which enhances cGMP synthesis by (1) sensitizing sGC to NO and stabilizing their interaction and (2) by directly stimulating sGC via an NO-independent manner. Other approved drugs include sildenafil and tadalafil, which are PDE5 inhibitors[287]. In addition, direct administration of NO by inhalation is approved for treating PAH due to persistent PH in newborns, but its complex delivery system hampers its universal use for other patients[287].

Prostacyclin is a potent vasodilator belonging to the prostanoid family of signaling molecules and is produced mainly in ECs from arachidonic acid by prostacyclin synthase. Following its release from ECs, prostacyclin binds to its specific I-prostanoid (IP) receptor on underlying vSMCs, promoting adenylyl cyclase activation. The latter catalyzes the conversion of adenosine triphosphate (ATP) to cyclic adenosine monophosphate (cAMP), which leads to vSMC relaxation and subsequent vasodilation. By the same mechanism, prostacyclin also inhibits vSMC proliferation, platelet aggregation and thrombosis and promotes anti-inflammatory effects[333]. In PAH patients, the expression of both prostacyclin synthase and prostacyclin receptor were found to be reduced in pulmonary arteries, and deletion of the prostacyclin receptor in mice exacerbated chronic hypoxia-induced PH[334,335]. The first approved treatment for PAH was intravenous administration of synthetic prostacyclin, known as epoprostenol. This treatment is associated with improved survival in patients with severe PAH. However, due to its very short half-life of approximately 3 minutes, it requires continuous infusion through a permanent central venous catheter, whose handling necessitates proper patient education and vigilance to avoid complications[287]. Other approved prostacyclin analogues for PAH include iloprost and treprostinil that can be administered through multiple routes (Figure 25). It is noteworthy that besides the specific IP receptor, the 3 aforementioned prostacyclin analogues can bind various prostanoid receptors with variable affinities. This has implications on both drug potency and adverse side effects, especially that prostanoid receptors are widely distributed throughout the body[288]. A newer agent, selexipag, is a nonprostanoid IP receptor agonist that is highly selective for the IP receptor, and its active metabolite has a longer half-life than prostacyclin analogues (9-14 hours), limiting its adverse events and permitting a reasonable administration regimen of twice daily, respectively[336,337]. Selexipag was recently shown to improve PVR and exercise capacity in PAH patients and was associated with better survival[338].

To sum up, PAH patients are currently treated with different agents that aim to restore normal vascular tone. While the aforementioned approved vasodilatory agents have all, to some extent, provided beneficial effects in terms of cardiopulmonary hemodynamics, exercise capacity and/or rate of disease progression, the disease does progress in spite of these treatments and they are rarely associated with lower mortality rates. The limited long-term

effectiveness of current treatments highlights the need for exploring new therapeutic modalities that can effectively block or preferably, reverse disease progression.

4.5.2. Future treatment perspectives: restoration of BMPRII signaling

Our enhanced understanding of the involvement of BMPRII signaling in PAH pathogenesis supports restoration of normal BMPRII signaling as a potential curative approach for PAH. Indeed, several studies have highlighted the utility of normalizing this pathway for improving clinical outcomes. As a direct proof of concept, Reynolds et al tested the outcome of BMPRII overexpression in the lungs of two different non-genetic rat models of PH (induced by monocrotaline or chronic hypoxia) that exhibit reduced lung BMPRII expression levels. The targeted adenoviral delivery of *BMPR2* gene to the pulmonary endothelium successfully improved mean PAP and PVR in these models[339]. Other ways for restoring BMPRII expression levels included the use of specific antagomiRs against miRNAs that repress BMPRII levels[340], ribosomal read through-inducing drugs to promote the full protein expression of BMPRII variants with truncating nonsense mutations[341], chemical chaperones that enhance cell membrane trafficking of specific missense-mutated BMPRII variants[342] and lyososmal inhibitors to prevent BMPRII lysosomal degradation[310,343]. These methods succeeded in increasing BMPRII levels and downstream signaling, to varying extents, and had beneficial outcomes on disease phenotype *in vitro* and/or *in vivo*. Moreover, as described in the previous chapter, tacrolimus (FK506) was identified as a potent activator of Smad1/5/8 signaling[277]. Low-dose tacrolimus treatment was capable of reversing PH in 3 *in vivo* models (EC-specific *Bmpr2* KO mice, monocrotaline-treated rats and rats exposed to sugen with hypoxia) and stabilized 3 patients with end-stage PAH[277,344]. Consequently, the safety and tolerability of tacrolimus were validated in a randomized placebo-controlled clinical trial that additionally revealed improvements of BMPRII expression levels and clinical endpoints in a subset of tacrolimus-treated patients[345]. Therefore, BMPRII signaling restoration seems to hold a real potential for treating PAH. Nonetheless, as BMPRII expression is not limited to the pulmonary vasculature, and since BMPRII-signaling mediates the various biological functions of many BMPs, caution should be warranted when systemically manipulating such a universal signaling axis. A safer alternative would be local administration of therapy, or specific targeting of the endothelium, which could also have therapeutic benefits for HHT. As such, Long et al showed in 2015 that administration of BMP9, that predominantly binds endothelial ALK1, attenuated disease development in several PH animal models, raising hopes for the use of BMP9 or receptor agonists for PAH treatment[159]. Nevertheless, subsequent studies by our group and collaborators strikingly uncovered protective effects of the loss of BMP9, but not BMP10, against PH development and progression in relevant animal models, which was associated with a decrease in ET-1 expression specifically in *Bmp9*KO mice[162,346]. In addition, a more recent study on PAH pulmonary microvascular ECs revealed that BMP9 treatment supported EndMT, which is a known feature of dysfunctional ECs in PAH, and that this effect was exacerbated by IL6[347]. BMP9 was also shown in a separate study to promote the proliferation of PAH BMPR2-mutated ECs via prolonged signaling response[318]. Therefore, while a large body of evidence supports the notion of enhancing BMPRII signaling in pulmonary vasculature as a therapeutic approach for PAH, its execution might not be as simple as initially anticipated.

It is noteworthy that deficiency in BMPRII in the pulmonary endothelium disrupts the balance between the growth-inhibitory Smad1/5/8 signaling and the growth-promoting Smad2/3 signaling by activins binding to ActRIIA[348]. Thus, a novel therapeutic approach aiming to restore this balance and normalize cellular proliferation is currently being tested for PAH patients[349–351]. This is based on the use of sotatrercept, which is a first-in-class fusion protein composed of the extracellular domain of ActRIIA fused to human IgG1 Fc domain. Sotatercept acts as a ligand trap for TGF-β superfamily members, including activins, some BMPs and growth differentiation factors. By sequestering free activins, sotatercept was found to balance these 2 signaling axes and reduce proliferation of ECs and vSMCs *in vitro*, while reversing pulmonary vascular and right ventricular remodeling in preclinical PH models[348]. Consequently, sotatercept was very recently tested in clinical trials on PAH patients receiving background therapy, resulting in reduced PVR and improved exercise capacity[349–351].

5. Gene expression analyses in the scope of HHT and PAH

Both HHT and HPAH can arise from LOF mutations in the BMP9/BMP10 signaling pathway. Intriguingly, these two vascular diseases have very different manifestations, with HHT affecting various specific vascular beds that display excessive vasodilation, while PAH being confined to the small pulmonary arteries that become largely constricted. Interestingly, despite these differences, the same germline *ACVRL1* mutations could be detected in HHT and HPAH patients, and some of these patients even develop both diseases[352–354]. To date, it remains largely ambiguous what determines which pathology develops downstream these mutations, but we do know that deficiency in this signaling pathway can have detrimental effects on the vasculature. As reviewed in Chapters 3 and 4, both diseases require new therapeutic avenues that place the BMP9/BMP10 signaling pathway at their core. The development of such therapeutic approaches, whether in HHT or PAH, relies heavily on our understanding of the downstream effectors of this pathway. Since a main outcome of BMP9/BMP10 signaling is regulation of target gene expression, transcriptomic profiling of BMP9 and/or BMP10-stimulated control (CTL) ECs and ECs defective in BMP9/BMP10 signaling can help unravel key effectors mediating EC dysfunction and lesion development. These effectors might serve as potential therapeutic targets to stop disease progression or even reverse it. Using microarrays and with the advent of bulk RNA-sequencing (RNA-seq), and more recently single cell RNA-sequencing (scRNA-seq) technologies, a number of studies have addressed the transcriptomic profiles of HHT or PAH patient-derived cells or tissue homogenates in comparison to CTLs. Some studies also assessed the response of CTL or patient (PT) cells to BMP9 and BMP10. Studied PT-derived cells included ECs and peripheral blood mononuclear cells for both HHT and PAH, in addition to PASMCs and fibroblasts for PAH. Aligned with the focus of my thesis, this chapter is dedicated for providing an overview of the aforementioned transcriptomic studies strictly involving ECs, as the BMP9/BMP10-ALK1 pathway is mainly limited to the endothelium (summarized in Table 1).

5.1. Introduction to utilized EC models

Different types of EC models have been used to study vascular dysfunction in the scope of HHT and PAH. In general, a commonly used model is human umbilical vein ECs (HUVECs), which are derived from the single vein of umbilical cords. Their wide use is attributed to their high accessibility, limited by the number of births, and the ease, success and non-invasiveness of the employed isolation procedure[355]. In the context of PAH, pulmonary artery ECs (PAECs) and HMVECs respectively isolated from the large arteries and microvessels of the lungs have been commonly employed as *in vitro* models[159,347,356,357], limited by the access to patient explanted lungs during transplantation events. In this case, CTL counterparts are usually derived from unused healthy donor explanted lungs[356,357]. Alternatively, ECFCs, formerly known as blood outgrowth ECs, have become popular candidates for studying EC dysfunction due to their non-invasive isolation method from adult peripheral blood or umbilical cord blood[358]. These cells represent a unique population of circulating EC progenitors that give rise to mature ECs capable of promoting postnatal angiogenesis and vascular repair at sites of damage. ECFCs are distinct from mature circulating ECs shed from the injured vasculature and from early EC progenitors that are of hematopoietic origin and do not give rise to mature ECs[358,359].

Table 1. List of transcriptomic studies on human endothelial cells addressing BMP9/10 response and/or comparing HHT or PAH transcriptomes to those of controls

Study category	Reference	Transcriptomic approach	Cell type	Treatment
Transcriptomic studies on CTL ECs upon BMP9/BMP10 stimulation	Morikawa M et al, 2011[113]	microarray	CTL HUVECs	stimulated or not with 1ng/mL BMP9 for 2hrs
	Long L et al, 2015[159]	microarray	CTL PAECs and CTL ECFCs	stimulated or not with 1ng/mL BMP9 for 4hrs
	Salmon RM et al, 2020[360]	microarray	CTL PAECs	stimulated or not with 0.3ng/mL of prodomain-bound BMP9 or BMP10 for 1.5hrs
	Peacock HM et al, 2020[361]	bulk RNA-sequencing	CTL HMVECs	treated or not for 2hrs with either: 1) 200 pg/mL BMP9 at static conditions 2) 30 dyn/cm^2 shear stress with the ALK1-ligand trap ALK1-Fc 3) 30 dyn/cm^2 shear stress in combination with low BMP9 concentration (1 pg/mL)
Transcriptomic studies on HHT-derived ECs	Thomas B et al, 2007[362]	microarray	CTL/HHT1/HHT2 HUVECs	none
	Fernandez-Lopez A et al, 2007[363]	microarray	CTL/HHT1/HHT2 ECFCs	none
Transcriptomic studies on HPAH/IPAH-derived ECs	Rhodes CJ et al, 2015[357]	bulk RNA-sequencing	CTL/IPAH PAECs	none
	Asosingh K et al, 2021[356]	single cell RNA-sequencing	CTL/IPAH PAECs	none
	Szulcek R et al, 2020[347]	bulk RNA-sequencing	CTL/IPAH-HPAH HMVECs	stimulated or not with 1ng/mL BMP9 for 1.5hrs or 24hrs

CTL: control, EC: endothelial cell, BMP: Bone Morphogenetic Protein, HPAH: heritable pulmonary arterial hypertension, IPAH: Idiopathic pulmonary arterial hypertension, HUVEC: Human Umbilical Vein Endothelial Cell, PAEC: Pulmonary Artery Endothelial Cell, ECFC: Endothlial Colony-Forming Cell, HMVEC: Human Microvascular Endothelial Cell, hrs: hours,

5.2. Characterization of the normal transcriptomic response to BMP9/BMP10

By combining ChIP-seq and microarray expression data, Morikawa et al unraveled a list of putative direct BMP9 target genes in HUVECs[113]. Gene expression analysis of serum-starved HUVECs stimulated or not with 1ng/mL BMP9 for 2hrs identified 108 upregulated and 37 downregulated genes with a |fold change| (|FC|) > 2. The resulting gene expression profiles were combined with mapping data from ChIP-seq of Smad1/5-bound chromatin in HUVECs stimulated with 1ng/mL BMP9 for 1.5hrs[113]. As a result, 70 of the 108 upregulated genes and 9 of the 37 downregulated ones were shown to be directly bound by Smad1/5 and considered putative direct BMP9 targets in ECs. The list of 70 upregulated targets was provided, and the 10 top upregulated targets in decreasing order of FC were: *SMAD6*, Notch targets *HEY2* and *HEY1*, *ID2*, *SMAD7*, *NOG*, *C8orf4* encoding the endothelial inflammatory regulator TC1[364], *FZD1* and *ID1*[113]. The authors did not perform functional or pathway enrichment analysis using this list of targets, but by scanning through the list one can appreciate an overrepresentation of genes related to Notch signaling pathway (*HEY2*, *HEY1*, *LFNG*, *HES1, JAG1* and *NRARP*), in addition to some belonging to Wnt signaling (*FZD1* and *FZD8*), several transcription factors (*GATA2*, *GATA3*, *GATA6*, *RUNX1T1*, *SOX18* and *FOXC1*), the well-known mechanosensitive flow-induced transcription factor *KLF4*[365] and its related members *KLF10* and *KLF3,* membrane-bound solute transporters (*SLC6A6* and *SLC38A2*) and of course canonical BMP signaling targets (*SMAD6*, *ID2*, *SMAD7*, *ID1, ID3* and *BMPR2*)[77].

Following this short descriptive gene expression analysis, a few other studies have examined BMP9 transcriptomic responses in CTL ECs at greater depth. Long et al used microarray to explore gene expression changes in PAECs and ECFCs in response to BMP9[159]. PAECs or ECFCs in low serum (0.1%) medium were either left untreated or were stimulated for 4hrs with 1ng/mL BMP9. BMP9 stimulation induced considerable transcriptional changes in both cell types, with 1883 statistically significant regulated targets in PAECs (adjusted p-value < 0.05, no LF threshold), including *ID1*, *ID2* and *BMPR2*. The upregulation of BMPRII was validated at the mRNA and protein level in BMP9-treated PAECs. Generally applicable gene set enrichment analysis for common pathways and cellular processes highlighted TGF-β signaling as the only significant BMP9-upregulated pathway and identified apoptotic cell signaling as a downregulated one. Functionally, BMP9 was shown to inhibit apoptosis and hyperpermeability that were induced by inflammatory factors in CTL PAECs and ECFCs, but also in HPAH patient-derived ECFCs with heterozygous *BMPR2* mutations. Interestingly, both the upregulation of BMPRII and the anti-apoptotic effects of BMP9 on CTL PAECs were dependent on BMPRII and Smad1 or Smad5, highlighting the importance of the canonical Smad signaling in mediating these effects of BMP9. Nevertheless, the dependence on BMPRII also highlights that only cells sustaining a BMPRII expression level sufficient for signaling are to benefit from BMP9 supplementation. In this study, BMP9 also reversed PH development in several PH rodent models, without inducing heterotopic ossification. As a conclusion of this study, BMP9 administration was proposed as a therapeutic approach for PAH[159], but this was later questioned[162,346] as described previously in the last section of Chapter 4.

Another interesting transcriptomic study on CTL PAECs was published by Salmon et al in 2020, this time using prodomain-bound forms of BMP9 and BMP10 (pro-BMP9 and pro-BMP10)[360]. This study demonstrated that the BMP9 and BMP10 prodomains do not interfere with the ligands' binding to ALK1 nor with their signaling potencies, as pro-BMP9 and pro-BMP10 exhibited similar sub-nanomolar ALK1 binding affinities and *ID1* mRNA induction when compared to their respective mature forms. In addition, similar to their mature forms[366], pro-BMP10 exhibited a slightly higher ALK1 binding affinity compared to pro-BMP9[360]. Nevertheless, microarray analysis on CTL PAECs in low serum (0.1%) treated with 0.3ng/mL of pro-BMP9 or pro-BMP10 for 1.5hrs compared to PBS-treated CTLs revealed similar transcriptomic changes between the 2 ligands when compared to CTLs. Notably, the 2 ligands shared the same top 9 upregulated genes (adjusted p-value < 0.05; *SMAD6*, *ID1*, *SMAD7*, *NOG*, *PTGS2,* encoding prostaglandin-endoperoxide synthase 2, the EndMT-associated transcription factor *SNAI1*[367], *ATOH8*, whose loss mimics PAH phenotype *in vivo*[368], *HEY2* and *C8orf4*) and the same 3 top downregulated ones (*ADM*, encoding the vasodilator adrenomedullin, *C10orf10,* also called DEPP Autophagy Regulator 1 and the tumor suppressor gene *PLK2*). Both ligands also induced a significant downregulation of the pro-angiogenic chemokine receptor *CXCR4* and upregulation of the canonical BMP target *ID3*, the Notch signaling family members *LFNG* and *NRARP* and the transcription factors *FOXC2*, *GATA2* and *GATA6*. Although a different number of significantly regulated genes was identified with pro-BMP9 (48) and pro-BMP10 (110) compared to CTLs, direct comparison of gene expression profiles between the 2 revealed no significant transcriptional differences, demonstrating that low dose pro-BMP9 and pro-BMP10 act as functionally equivalent transcriptional regulators in PAECs[360].

All of the aforementioned studies investigated BMP9 (or BMP10) transcriptional responses under static (no flow) conditions. Nevertheless, as described in Chapter 2, flow-induced shear stress, is known to potentiate the Smad1/5/8 response to soluble BMP9 in ECs[171]. In addition, shear stress itself activates downstream pathways that can modulate the levels of transcription factors present within the nucleus, such as KLF2 and KLF4[365]. It is thus reasonable to speculate that shear stress might modify the levels of Smad-binding partners, hypothetically interfering with BMP9 signaling. For those reasons, Peacock et al examined transcriptional changes in CTL HMVECs in response to BMP9 alone, FSS alone, or both in order to identify transcriptional changes by BMP9 that exclusively occur in the presence of shear stress[361]. As such, HMVECs in low-serum medium (0.1%) were treated for 2hrs with either (1) 200 pg/mL BMP9 at static conditions, (2) 30 dyn/cm^2 shear stress with the ALK1-ligand trap ALK1-Fc or (3) 30 dyn/cm^2 shear stress in combination with low BMP9 concentration (1 pg/mL), and each condition was compared to cells treated with ALK1-Fc under static conditions. The BMP9 doses were selected such that the high BMP9 dose condition induces a similar Smad1/5/8 signaling level (assessed by *ID1* induction) as the combined low BMP9 dose with shear stress. Interestingly, using RNA-seq, 61 genes were shown to be differently regulated ($|FC| \geq 2$ and adjusted p-value < 0.05) in the presence of both BMP9 and FSS compared to each alone. This indeed confirms that shear stress plays additional roles in modulating BMP9 transcriptional responses besides potentiating the signal. Among these 61 targets, the authors focused on three involved in arteriovenous identity, which are *GJA4* encoding the endothelial gap junction component connexin 37, *SEMA3G*, and *UNC5B*. In accordance with previous reports[113,360], their expression levels were increased by BMP9 under static conditions. However, their levels were rather decreased when low dose BMP9 was

combined with shear stress, and shear stress alone had no impact on their regulation. This strongly highlights the importance of taking shear stress into account when studying transcriptional regulation in ECs. Nevertheless, while the authors shed the light on the 61 genes that were differently regulated when combining BMP9 and shear stress, they did not point out how many genes were commonly and similarly regulated between the conditions. In the absence of such piece of information, one cannot disregard the potential of studies assessing transcriptional regulations under static conditions, but it would be important to check whether an interesting finding can be reproduced in the presence of shear stress, which is more physiologically relevant. Another interesting finding of this study was that BMP10 can exert distinct transcriptional roles than BMP9 under shear stress[361]. While both BMP9 and BMP10 upregulated *GJA4* under static conditions, only BMP10 maintained this upregulation in the presence of shear stress. In fact, under shear stress condition, the upregulation of *GJA4* by BMP10 was even more pronounced than at the static state, and this translated in an overall increase of *GJA4* expression in HMVECs exposed to normal serum conditions in the presence of shear stress. To better characterize the transcriptional regulation of *GJA4* by BMP9, Smad1/5-silenced HMVECs were stimulated with BMP9 with or without shear stress. While BMP9 failed to induce *GJA4* expression in the absence of Smad1/5 under static conditions, its level was increased under shear stress. This implies that under shear stress, upregulation of *GJA4* by BMP9 is likely mediated through non-canonical signaling, which could be mitigated in the presence of Smads. Hence, the authors proposed that the difference in *GJA4* regulation under shear stress between BMP9 and BMP10 could be a reflection of stronger activation of non-Smad signaling by BMP10 compared to BMP9, possibly due to differences in their binding affinities to type II receptors. Whether this hypothesis holds true remains to be validated, but such mechanisms do seem rational in explaining the recently described BMP10-specific role in the development of proper arteriovenous networks[169].

5.3. Transcriptomic profiling of HHT-derived ECs

In 2007, two independent gene expression studies using microarrays on cultured HHT ECs were published[362,363]. Thomas et al. studied HUVECs isolated from 3 CTL, 4 HHT1 and 3 HHT2 newborns in low serum medium[362]. Using an FC threshold of <0.67 or >1.5 and a false discovery rate (FDR) < 10%, they identified 70 non-redundant differentially expressed genes (DEGs) in HHT1 HUVECs and 396 in HHT2 HUVECs compared to CTLs. Functional clustering of these DEGs using NCBI Entrez database highlighted an enrichment of genes related to development, cell-cell signaling, signal transduction, cell growth or maintenance, cell adhesion and metabolism. In terms of molecular function, most seemed to be either enzymes, receptors or signal transducers. Among the identified DEGs, 70 involved in cell adhesion or growth, signal transduction, TGF-β signaling, development and vascular remodeling were selected for individual validation by reverse transcription polymerase chain reaction (RT-PCR) on a larger cohort of CTL (10) and HHT (12 HHT1 and 5 HHT2) HUVECs. As such, 50 genes were validated to be dysregulated in HHT1 or HHT2, including some which were found significantly modulated in both groups by RT-PCR, despite their initial non-redundancy by microarray analysis. Accordingly, hierarchical clustering using expression data of selected DEGs was able to separate CTL from HHT cells, but could not distinguish between the two HHT subgroups. Among the validated DEGs, *TNFSF4*, encoding TNF ligand superfamily member 4 that promotes T cell adhesion to the endothelium and T cell activation was the most upregulated in HHT HUVECs. Other top upregulated genes included the key angiogenic players *VEGFR2*,

NOTCH4 and the chemokine receptor *CXCR4*. Genes encoding the VEGF co-receptors Nrp1 and Nrp2, Ephrin-B2 and the chemokines CXCL1 and CXCL2 were also upregulated in HHT HUVECs compared to CTLs. In parallel, several ECM components were dysregulated, with a strong upregulation in nidogen 2 and a downregulation of elastin and collagen III alpha1[362]. Collectively, the aforementioned changes seem consistent with the increased vascular density in *Alk1* or *Eng* KO mouse retinas and the fragility of affected vessels in HHT patients.

The other study, by Fernandez-Lopez et al, assessed gene expression changes of ECFCs isolated from the peripheral blood of healthy donors or HHT patients[363]. The transcriptomic profiles of ECFCs from 1 HHT1 patient carrying nonsense *ENG* mutation, 1 "HHT2n" carrying nonsense *ACVRL1* mutation and 1 "HHT2m" with a missense *ACVRL1* mutation were each compared to that of a single CTL using microarray. 277 downregulated and 63 upregulated genes (no FC threshold, adjusted p-value < 0.05) were commonly identified in all 3 patients compared to the CTL. These genes were found to be involved in metabolism, cell adhesion, cell migration, cytoskeleton, DNA and RNA regulation, cell cycle and survival, leukocyte transmigration and inflammation, signal transduction and angiogenesis. RT-PCR analysis validated a few selected DEGs including those coding for eNOS, cell cycle molecules cyclin B2 and cell division cycle 25B, the adhesion molecules VE-cadherin and PECAM1 and Ang2, which were all upregulated in HHT ECFC compared to CTLs, and the TGF-β target plasminogen activator inhibitor 1, which was downregulated[363]. Hence, these 2 studies showed that endoglin- or ALK1-mutated HHT HUVECs or ECFCs display transcriptional alterations that are relevant to HHT pathogenesis. Nonetheless, both studies were not strict with the DEG selection criteria in terms of both FC and statistical thresholds for the first and the absence of a FC threshold for the second. This might lead to a higher identification of false positives. Additionally, comparing patient cells to only a single CTL in the study by Fernandez-Lopez et al can be tricky[363], as it doesn't take into account normal inter-individual heterogeneity between healthy subjects.

5.4. Transcriptomic profiling of PAH-derived ECs

Lung transplantation in end-stage PAH patients provides researchers with valuable material for studying PAH remodeled vasculature. Consequently, multiple groups have assessed the transcriptome of whole explanted PAH lung homogenates using microarrays or bulk RNA-seq[369]. However, given that microarray and bulk RNA-seq analyses do not distinguish between different cell types, this approach is very tricky, since intrapulmonary arteries represent only a small portion of the lung. Consequently, gene expression changes in other types of cells can mask changes occurring in the vascular cells[369]. As a more refined approach, some groups resorted to laser capture microdissection in order to specifically isolate and study small pulmonary arteries[369], but these samples would still consist of several cell types. Finally, at the most specific level, a few groups have selectively isolated ECs from the explanted lungs or circulating ECs from the blood of PAH patients to characterize them at the phenotypic and molecular levels. As BMP9/BMP10 signaling is the main focus of my work, and since BMPRII deficiency is commonly observed in HPAH and idiopathic PAH (IPAH) patients, this section will describe the transcriptomic studies performed on ECs from these 2 PAH subgroups.

In 2015, Rhodes et al performed the first RNA-seq on PAECs isolated from IPAH and CTL donor lungs[357]. Using a fold difference threshold ≥ 50%, they identified 23 DEGs, of which 12 had a

p-value below 0.1. Among those 12, 10 were validated by RT-PCR to be significantly dysregulated in IPAH PAECs compared to CTLs. Notably, *EFNA1*, encoding the ephrin ligand ephrin-A1 was downregulated in IPAH PAECs compared to CTLs. In addition, the mRNA levels of *COL4A1* and *COL4A2*, encoding the 2 α chains of collagen IV that is a major constituent of endothelial basement membranes, as well as its corresponding protein expression level were significantly reduced in IPAH PAECs. To relate BMPRII dysfunction to the expression changes of these genes, the authors assessed their expression levels in BMPRII-silenced CTL PAECs versus control siRNA-treated cells. *BMPR2* Knockdown (KD) cells mimicked IPAH cells in terms of upregulation of *DNAJB4* (encoding a chaperone known to stabilize E-cadherin[370]), *HMGA1* (encoding an oncogenic and pro-inflammatory chromatin remodeling protein[371,372]) and *NOS3* (encoding endothelial NO synthase) and downregulation of *EFNA1*, *COL4A1* and *COL4A2*. The upregulation of *HMGA1* in IPAH and *BMPR2* KD cells is in agreement with different studies describing heightened inflammatory responses in PAH (described in chapter 4). On the other hand, the unexpected increase of *NOS3* was proposed by the authors to reflect an uncoupling of the production of NO and peroxynitrite, which was reported in specific cases[373]. Knowing that ephrin-A1 can modulate collagen IV secretion from ECs, secreted collagen IV levels were measured in the conditional medium of *BMPR2* KD cells and were found to be lower than those from CTLs. Functionally, the authors showed that collagen IV and ephrin-A1 are required for EC adhesion, migration and tube formation *in vitro.* In parallel, mice deficient in *EFNA2*, the receptor of ephrin-A1, developed more severe PH when exposed to hypoxia and sugen 5416 compared to WT mice[357]. Altogether, this study uncovered some gene dysregulations in PAECs from IPAH patients lacking any *BMPR2* mutations, and showed that most could be reproduced in BMPRII deficient PAECs. This study also highlighted ephrin-A1 and collagen IV as important players in PAH EC dysfunction[357].

It is noteworthy that while Rhodes et al chose to address the IPAH ECs as PAECs, which usually correspond to ECs isolated from large proximal pulmonary arteries, the cells that they used were rather isolated from small arteries in peripheral lung tissue[357]. It is important to make the distinction between the two types of cells since it is the small arteries and arterioles which constitute the main site of pathogenic vascular remodeling in PAH. It would thus be more relevant to study cells isolated from small peripheral PAs for a better understanding of PAH pathogenic mechanisms. However, this doesn't rule out endothelial dysfunction in larger arteries, as was recently shown using scRNA-seq on PAECs isolated from the main PA and its first 4 branches in CTL and IPAH lungs[356]. This study by Asosingh et al revealed that PAECs isolated from large PAs are vastly heterogenous and can be subgrouped into at least eight unique clusters, for both CTL and PAH samples, with varying expression profiles[356]. Most identified clusters were assigned as either displaying a proliferative (with upregulated genes required for cell proliferation), angiogenic (with upregulated genes involved in cell adhesion, migration and angiogenesis) or quiescent phenotype (with downregulated genes related to cell cycle and proliferation) in comparison with the remaining clusters. While CTL and PAH PAECs shared several similar groups, more proliferative and angiogenic clusters were identified on the PAH side[356], in accordance with the enhanced endothelial proliferation characteristic of small PAs in PAH lungs.

Another interesting RNA-seq study, published during my PhD in 2020, was carried out by Szulcek et al on HMVEC from peripheral lungs sections of 4 IPAH patients and 1 HPAH patient carrying a *BMPR2* mutation[347]. Following contradictory reports regarding the therapeutic benefit of BMP9 treatment for PAH patients (described in the last section of chapter

4)[159,162,346], the same group that showed potential benefit of BMP9 treatment in PAH models[159] decided to characterize the transcriptomic response of CTL and PAH patient-derived ECs to BMP9. Instead of assessing gene expression patterns under complete medium with growth factors and 5% serum as in the study by Rhodes et al[357], this group analyzed cells in low serum condition (1%) without additional growth factors, stimulated or not with 1 ng/mL BMP9 for 90mins and for 24hrs. The short 90min BMP9 stimulation induced the regulation of 2431 and 1706 in CTL and PAH HMVECs respectively (|FC|>2), with 1358 DEGs shared between the two groups. This shows that PAH cells seem to display moderately impaired responses to BMP9. However, this impairment was much more pronounced at the 24hr time point, where BMP9 regulated the expression of only 100 genes in the PAH HMVECs versus 1874 genes in CTL cells, potentially pointing to an altered negative feedback in PAH HMVECs. Nevertheless, gene set enrichment analysis (GSEA) highlighted a strong enrichment of genes related to EndMT in CTL BMP9-treated cells that persisted in PAH HMVECs. Subsequently, phenotypic and functional analyses of BMP9-treated CTL and PAH HMVECs revealed that BMP9 promoted EndMT and decreased barrier function strictly in PAH cells, warning against its use in PAH patients. GSEA also highlighted a negative enrichment of gene sets related to apoptosis, hypoxia and IL6/JAK/STAT3 signaling following BMP9 stimulation in CTL HMVECs, which were not anymore negatively enriched in BMP9-treated PAH HMVECs. Interestingly, these gene sets all shared *IL6*, whose mRNA and protein expression levels were respectively found elevated in PAH HMVECs and PAH patient sera compared to CTLs. In addition, the EndMT phenotypic switch in PAH HMVECs was found to be exacerbated by IL6, while blocking it using a neutralizing IL6 antibody effectively prevented BMP9-induced EndMT in PAH HMVECs. Thus, the authors proposed to continue investigating the therapeutic potential of BMP agonists while considering anti-inflammatory add-on therapy for PAH patients exhibiting elevated IL6 levels[347].

To sum up, some studies have compared the transcriptomes of HHT ECFCs or HUVECs to CTLs, but not in response to BMP9 or BMP10, and used non-stringent criteria for selection of DEGs[362,363]. Others assessed the response of CTL ECs to BMP9[159,368], one study compared the responses of low dose pro-BMP9 to pro-BMP10 in CTL ECs[360], and one study compared the response of CTL ECs to BMP9 in the presence of absence of shear stress[361]. The only study comparing the response of patient and CTL cells to BMP9 was performed on HMVECs from 4 IPAH patients and one HPAH patient with a *BMPR2* mutation[347]. Therefore, to the best of my knowledge, there are no studies assessing BMP9 and BMP10 responses in ECs with heterozygous *ACVRL1* mutations.

Aims

Mutations in the endothelial BMP9/BMP10 signaling pathway give rise to two distinct vascular diseases with no currently identified cures. The first disease, HHT, is caused by heterozygous LOF mutations mostly in genes coding the type I receptor ALK1 or the co-receptor endoglin. Mutations in the same genes can also give rise to HPAH, albeit at a very low frequency. On the other hand, mutations in BMPR2 are found in HPAH which has never been described in HHT. Currently available treatments for HHT and PAH do not block disease progression, because they target the outcome rather than the cause of vascular dysplasia. This is mainly due to our limited understanding of the molecular mechanisms linking the aforementioned mutations to the developed abnormalities. To tackle part of this question, my project aimed to investigate the molecular mechanisms linking heterozygous ALK1 mutations to the pathogenesis of HHT and HPAH, in order to identify new therapeutic targets. Accordingly, since ALK1 is the receptor of BMP9 and BMP10, whose binding leads to regulation of target gene expression, the focus of my project was to investigate the transcriptomic response of heterozygous ALK1-mutated ECs to BMP9 or BMP10 by RNA-sequencing.

I. As such, the first objective of my project was to isolate primary patient-derived ECs carrying heterozygous ALK1 mutations.
    a. The EC model of choice for HHT, as described shortly afterwards, was ECFCs from the cord blood of HHT and CTL newborns, in addition to HUVECs for validations.
    b. As for PAH, I had access to HMVECs isolated from the lungs of the only 2 PAH patients in France with ALK1 mutations receiving lung transplantation. These cells were generously provided by our collaborator Dr. Christophe Guignabert from The National Reference Center for PAH, Marie Lannelongue hospital, Le Plessis Robinson, France.

II. The second objective was to carry out and analyze the two RNA-sequencing studies, one for HHT-derived ECFCs and another for PAH-derived HMVECs. The aim was to identify common irregularities in the transcriptomic response of two different primary ALK1-mutated EC models to the ALK1 ligands BMP9 and BMP10, and to check whether ALK1-mutated ECs from newborns respond differently to BMP9/BMP10 compared to ECs from the sick lungs of adult patients. With that in mind, the experimental setup was designed to answer 4 main questions:
    a. Do BMP9 and BMP10 have redundant or unique roles in terms of target gene regulation?
    b. What are the molecular functions and biological processes controlled by BMP9 and BMP10 under physiological conditions?
    c. What is the impact of heterozygous ALK1 mutations on gene regulation by BMP9 or BMP10 in ECFCs isolated from newborns that don’t show signs of the disease?
    d. What is the impact of heterozygous ALK1 mutations on gene regulation by BMP9 or BMP10 in HMVECs isolated from sick lungs of adult PAH patients?

Results and Methodology

All main results of my project and the associated materials and methods are provided in the manuscript draft below that is currently in the submission process. Few preliminary results are presented after the manuscript draft.

Clarification regarding the choice of utilized cellular models

As explained in the introduction chapter 4, PAH is a very rare disease affecting around 50 individuals per million. Among these cases, only a small subset is heritable, of which only 6% carry ALK1 mutations. Through our collaboration with Dr. Christophe Guignabert's group, we had access to HMVECs that were isolated from the lungs of the only 2 identified PAH patients in France with ALK1 mutations that had a lung transplantation. As CTLs, HMVECs isolated from non-sick sections from resected lungs of cancer patients were used. Since the mutated HMVECs were isolated from the explanted lungs of endstage PAH patients, we believe that these cells were exposed to a pathogenic microenvironment likely involving aberrant secretion of growth factors and pro-inflammatory signals characteristic of PAH lungs[290]. Consequently, some transcriptomic changes identified in these cells might be related to early pathogenic events, while others might be an outcome of long-term pathogenic remodeling. Identification of early transcriptomic dysregulations might uncover disease predisposition mechanisms and pave the way for developing therapeutic targets that block disease onset or progression. In order to dissect which of the identified transcriptomic changes can be considered as early pathogenic events, we decided to use ECs isolated from newborn HHT patients with heterozygous ALK1 mutations. HHT is a late-onset disease, whereby epistaxis, which is usually the earliest symptom to appear, begins around early teenage years[374]. With the exception of congenital cerebral and pulmonary AVMs, HHT babies are usually healthy and do not show any signs of the disease[375]. A group investigating potential vascular dysplasia in umbilical cords of 18 HHT1 newborns compared to 45 CTL newborns in terms of vessel dilatation, endothelial wall rupture and leukocytic infiltration found no abnormalities in the HHT1 (*ENG*) group, despite the lower endoglin protein levels in the assessed vessels[376]. This suggests that ECs isolated from the umbilical cord of HHT patients are good models for studying early disease pathogenesis, as this tissue does not present any vascular abnormalities at time of birth. Two different EC models can be derived from umbilical cords: (1) the widely used HUVECs from the umbilical vein and (2) ECFCs from the umbilical cord blood. As described in Chapter 5.1, circulating ECFCs are believed to play vasoregenerative roles at vascular repair sites[377]. Interestingly, Dumortier et al recently showed that several HHT patients that had undergone liver transplantation due to severe hepatic involvement demonstrated recurrence after a long delay[260]. This implies that the transplanted liver was possibly infiltrated with mutant ECs from the circulation, generating new hepatic vascular lesions. Given their ability to give rise to mature ECs, ECFCs could be the cells involved in post-operative disease recurrence in the liver of HHT patients. Therefore, we isolated ECFCs from the cord blood of HHT2 (ALK1) newborns and CTL subjects to study the effect of ALK1 heterozygosity on the transcriptomic response to BMP9 or BMP10 by RNA-seq in the context of a non-sick environment. We also isolated HUVECs from some of these newborns for validation of transcriptional targets by qPCR.

Main results and methodology

Impact of heterozygous ALK1 mutations on the transcriptomic response to BMP9 and BMP10 in endothelial cells from Hereditary Hemorrhagic Telangiectasia and Pulmonary Arterial Hypertension donors

Al Tabosh T.[1], Liu H.[1], Koca D.[1], M Al Tarrass[1], Tu L.[4,5], Giraud S.[2], Delagrange L.[2], Beaudoin M.[2], Rivière S.[6], Grobost V.[7], Rondeau-Lutz M.[8], Dupuis O.[9,10], Ricard N.[1], Tillet E[1], Machillot P[1], Salomon A.[1], Picart C.[1], Battail C.[1], Dupuis-Girod S.[1,2,3], Guignabert C.[4,5], Desroches-Castan A.[1], and Bailly S.[1]

[1]Biosanté unit U1292, Grenoble Alpes University, INSERM, CEA, F-38000 Grenoble, France; [2]Genetics Department, Femme-Mère-Enfants Hospital, Hospices Civils de Lyon, F-69677 Bron, France; [3]National Reference Center for HHT, F-69677 Bron, France; [4]Université Paris-Saclay, Faculté de Médecine, Pulmonary Hypertension: Pathophysiology and Novel Therapies, 94276 Le Kremlin-Bicêtre, France; [5]INSERM UMR_S 999 «Pulmonary Hypertension: Pathophysiology and Novel Therapies», Hôpital Marie Lannelongue, 92350 Le Plessis-Robinson, France; [6]Internal Medicine Department, CHU of Montpellier, St Eloi Hospital and Center of Clinical Investigation, INSERM, CIC 1411, F-34295 Montpellier CEDEX 7, France; [7]Internal Medicine Department, CHU Estaing, 63100 Clermont-Ferrand, France; [8]Internal Medicine Department, University Hospital of Strasbourg, 67091 Strasbourg CEDEX, France; [9]Obstetrics & Gynecology Department, Hospices Civils de Lyon, Lyon-Sud Hospital, Pierre-Bénite, France; [10]Faculty of Medicine, Lyon University, Lyon, France.

Abstract

Background: Heterozygous *ALK1* (Activin receptor-Like Kinase 1) mutations are associated with the development of two vascular diseases: hereditary hemorrhagic telangiectasia (HHT) and more rarely pulmonary arterial hypertension (PAH). Here, we aimed to understand the impact of *ALK1* mutations on BMP9 and BMP10 transcriptomic responses in endothelial cells.
Methods: Endothelial colony-forming cells (ECFCs) and microvascular endothelial cells (HMVECs) carrying heterozygous loss-of-function ALK1 mutations were isolated from the cord blood of newborn HHT donors and explanted lungs of PAH patients, respectively. RNA-sequencing was performed on each type of cells compared to control counterparts following an overnight stimulation with BMP9 or BMP10. Results were validated by qPCR on *ALK1*-mutated ECFCs and HMVECs.
Results: In control ECFCs, BMP9 and BMP10 stimulations induced similar transcriptomic responses with around 800 differentially expressed protein-coding genes (DEGs). Comparison of the transcriptome between control and *ALK1*-mutated ECFCs revealed very similar profiles, both at the baseline and upon stimulation. Consistently, control and *ALK1*-mutated ECFCs displayed a similar Smad1/5 response, which could not be explained by a compensation in cell-surface ALK1 level. Conversely, PAH HMVECs carrying heterozygous ALK1 mutations revealed strong transcriptional dysregulations compared to controls with >1200 DEGs at the baseline. Because our study involved two variables, ALK1 genotype and BMP stimulation, we performed a two-factor differential expression analysis and identified 44 genes associated with BMP9 regulation in mutated HMVECs, but none in ECFCs. Yet, the impaired regulation of at least one hit, namely *LFNG* (Lunatic Fringe), was validated by qPCR in different *ALK1*-mutated cellular models.
Conclusions: ALK1 heterozygosity does not impact the activation of the canonical Smad pathway by BMP9/10, nor causes overt transcriptional dysregulations, but could be enough to induce slight variations in the regulation of few genes, including *LFNG* involved in NOTCH signaling, which might be important in the pathogenesis of HHT and PAH.

Key words: ALK1; BMP; HHT; PAH; RNA-seq, LFNG

Introduction

Hereditary hemorrhagic telangiectasia (HHT [MIM: 187300, 600376, 175050]), also known as Osler–Weber–Rendu syndrome, is a rare genetic vascular disease characterized by the development of multiple focal vascular malformations (VMs), including muco-cutaneous telangiectases responsible for recurrent, spontaneous epistaxis and visceral arteriovenous malformations[1]. HHT is an autosomal-dominant disease presenting complete penetrance over the age of 50, but with highly variable expressivity. It is mostly caused by mutations in *ENG* (MIM: 131195) and *ACVRL1* (MIM: 601284), which account for 85% of cases, and more rarely in *SMAD4 (*MIM: 600993) accounting for less than 2%[2,3]. Additionally, mutations in *GDF2 (*MIM: 615506) were reported in few individuals presenting HHT-like symptoms[4]. The protein products of all 4 genes are components of the BMP/TGFß signaling pathway. *ACVRL1* (herein referred to as *ALK1*) encodes for the type I receptor ALK1, *ENG* for the co-receptor endoglin, *SMAD4* for a transcription factor downstream of the receptors and *GDF2* for BMP9, a high affinity ligand for this receptor complex[5]. The current signaling model is that BMP9 or BMP10 binds the co-receptor endoglin, which facilitates their binding to the signaling compex composed of the type I receptor ALK1 and a type II receptor that can either be BMPR2, ActR2B or ActR2A. Upon ligand binding, the type II receptor phosphorylates the type I receptor, which subsequently phosphorylates the transcription factors Smad1, Smad5 and Smad8, allowing their interactaction with Smad4. The formed trimeric Smad complex then translocates to the nucleus, where it binds to DNA together with other transcription factors in order to regulate the expression of many genes[6]. The receptor ALK1 and its co-receptor endoglin are mostly expressed on endothelial cells, supporting a key role for these receptors in vascular physiology[7]. It has been demonstrated that the BMP9/BMP10-ALK1-endoglin signaling pathway promotes vascular quiescence[8]. The current working model is that mutations within this signaling pathway would lead to an increase in angiogenesis. Thus, anti-angiogenic drugs, mainly blocking VEGF signaling pathway, have been proposed as a therapeutic option for HHT patients and tend to improve symptoms (bleedings and high cardiac output secondary to liver AVMs) but do not cure the disease[9,10].

HHT causal mutations result in the loss of function (LOF) of the gene product[11,12] and are inherited through an autosomal-dominant manner. Therefore, HHT has long been speculated to be caused by haploinsufficiency of the mutated *ENG* or *ALK1* gene product, with previous reports pointing at a reduction in endoglin and ALK1 expression in HHT1 and HHT2 patient-derived cells, respectively[13]. However, haploinsufficiency does not explain why vascular lesions in HHT patients occur focally in specific vascular beds[14], despite the systemic presence of the pathogenic germline mutation in all blood vessels.

In recent years, mutations in the same signaling pathway have been identified in rare cases of pulmonary arterial hypertension (PAH)[15]. PAH is characterized by a resting mean pulmonary artery pressure (mPAP) > 20 mmHg with a pulmonary artery wedge pressure ≤ 15 mmHg and elevated pulmonary vascular resistance (PVR) of > 2 Wood units[16,17]. PAH can develop sporadically, in association with risk factors such as drug, toxins or other diseases (i.e., connective tissue disease, HIV infection, portal hypertension, congenital heart disease, or schistosomiasis), or can be inherited. Although germline mutations in *BMPR2* gene are major predisposing factors for idiopathic (15-40%) and heritable (60-80%) PAH, less common or rare mutations in other genes encoding key members of the Smad1/5/8 signaling including *ALK1, GDF2 (BMP9)* and *BMP10* have been identified, underlining the critical role of this signaling pathway in PAH[15].

ALK1 mutations are responsible for nearly half HHT cases and a minority of PAH patients, and the same *ALK1* mutations can predispose to the two vascular disorders[18–20]. Despite our understanding of the genetics and downstream pathways involved in HHT and PAH, the molecular mechanisms that initiate HHT-related VMs and PAH are poorly understood[21]. Here, we aimed to understand the impact of *ALK1* mutations on the downstream BMP9/BMP10-ALK1 signaling pathway by studying the transcriptome of heterozygote *ALK1*-mutated primary endothelial cells to better understand the underlying molecular mechanisms and to propose new therapeutic approachs for these two diseases. To address this question, we used two different endothelial models carrying heterozygous LOF *ALK1* mutations:

(1) endothelial colony-forming cells (ECFCs) that were isolated from the cord blood of HHT newborns and (2) microvascular endothelial cells (HMVECs) isolated from explanted lungs of PAH patients.
We first used ECFCs, which allowed us to address the sole role of heterozygous *ALK1* mutations in cells not yet exposed to a sick microenvironment. These circulating cells, possessing vasoregenerative potential[22], are a particularly interesting model as they could be involved in endothelial cell turnover in the liver leading to new malformations. Indeed, it has been shown that some HHT patients who had received liver transplantations developed new HHT hepatic lesions several years later, leading to a second liver transplantation[23]. We also had access to *ALK1*-mutated HMVECs from the explanted lungs of two PAH patients, which is a very rare event as *ALK1* mutations occur in around 6% of patients with heritable PAH. In turn, heritable PAH patients represent only a subset of all PAH patients, which are estimated as 15-50 individuals per million[15]. The limited availability of *ALK1*-mutated HMVECs prompted us to additionally include HMVECs from 3 PAH patients with more frequent heterozygous mutations in the type II BMP9/10 receptor BMPR2*,* for validation of target genes by RT-qPCR. In order to validate some of the results, we also used human umbilical vein endothelial cells (HUVECs) derived from the umbilical cords of HHT newborns.
We performed RNA-sequencing on each type of cells compared to control counterparts, nonstimulated or following an overnight stimulation with BMP9 or BMP10. Altogether, our data support that *ALK1* heterozygosity does not impact the activation of the canonical Smad pathway by BMP9/10, nor cause overt transcriptional dysregulations in ECFCs. However, using two-factor differential expression analysis, in order to take into account the two variables (*ALK1* mutation and stimulation), we were able to highlight from HMVECs' RNA-seq analyses few genes exhibiting impaired regulation by BMP9/BMP10 in mutated cells. These included *LFNG,* encoding the NOTCH signaling modulator lunatic fringe, which was also found to be differentially regulated in *ALK1*-mutated ECFCs and HUVECs and might thus be important in the pathogenesis of HHT and PAH.

Results

Isolation and characterization of ECFCs carrying *ALK1* mutations

Control (CTL-H) and *ALK1*-mutated ECFCs (MUT-H) from newborns who have inherited heterozygous *ALK1* mutations from an HHT parent were clonally isolated from cord blood following the recommendations of the Vascular Biology Standardization Subcommittee[24]. Isolated ECFCs (3 CTL-H and 2 MUT-H, Table 1) displayed the classical endothelial cobblestone-like morphology (Suppl Figure 1A) and were VE-cadherin (CD144) positive (Suppl Figure 1B and C). These cells were also positive for the endothelial cell markers CD31 and CD146 and negative for the hematopoietic cell-specific surface antigen CD45 (Suppl Figure 1, D-F), confirming their endothelial identity. The functional activity of the two ALK1 mutants (MUT-H1; non sense mutation p.Trp141X and MUT-H2; missense mutation p.His280Asp, Table 1) was tested using the BMP response element (BRE) luciferase reporter assay (Figure 1A), as previously described by our group[12]. Our data indicate that these two *ALK1* pathogenic variants are not able to respond to a BMP9 stimulation (100 pg/mL, Figure 1A), supporting that they are both LOF mutations.

RNA-seq analysis in CTL ECFCs in response to BMP9 or BMP10 stimulation

In order to decipher the impact of *ALK1*-mutations on gene regulation in response to BMP9 and BMP10, RNA-sequencing was performed on ECFCs from 3 CTLs (CTL-H1, -H2 and -H3) and 2 *ALK1* mutated ECFCs (MUT-H1 and H2, Table 1) that were either nonstimulated (NS) or stimulated for 18hrs with BMP9 or BMP10 (10 ng/mL). The experiment was repeated three times, after which RNA extraction for all samples was performed, followed by quality control, library preparation and RNA sequencing. Principal component analysis (PCA) showed that we could discriminate stimulated (BMP9 or BMP10, blue and red shapes, respectively) from NS conditions (grey shape) in all ECFCs but could not discriminate CTL from *ALK1*-mutated ECFCs (Figure 1B).

Table 1. List of *ALK1*-mutated ECFCs and HUVECs isolated from HHT donors

ID	ALK1 mutation		Type of mutation	Domain	Cells isolated	Assays
MUT-H1	c.423G>A	p.Trp141X	Nonsense	Transmembrane	ECFC	RNA-seq, RT-qPCR, p-Smad1/5 IF, BLA, FC
MUT-H2	c.838C>G	p.His280Asp	Missense	Kinase	ECFC	RNA-seq, RT-qPCR, p-Smad1/5 IF, BLA, FC
MUT-H3	c.190C>T	p.Gln64X	Nonsense	Extracellular	ECFC/HUVEC	RT-qPCR (ECFC and HUVEC), p-Smad1/5 IF, BLA, FC
MUT-H4	c.1231C>T	p.Arg411Trp	Missense	Kinase	ECFC/HUVEC	RT-qPCR (ECFC and HUVEC), p-Smad1/5 IF, BLA, FC
MUT-H5	c.1112dup	p.Thr372HisfsX20	Frameshift	Kinase	ECFC/HUVEC	RT-qPCR (ECFC and HUVEC), FC
MUT-H6	c.1413C>G	p.Cys471Trp	Missense	Kinase	ECFC/HUVEC	BLA, FC

List of *ALK1*-mutated ECFCs and HUVECs that were isolated from newborns with their mutation, indicating the carried mutation (DNA and protein), the type of mutation, the mutated ALK1 domain and the assays in which they were used. RNA-seq: RNA-sequencing, RT-qPCR: reverse transcription quantitative polymerase chain reaction, p-Smad1/5 IF: phospho-Smad1/5 immunofluorescence, BLA: (BRE) BMP Responsive Element Luciferase Assay, FC: flow cytometry.

We first analyzed the BMP9 and BMP10 response versus (vs) NS condition in CTL ECFCs. Differential gene expression analysis using an absolute $\log_2$ fold change threshold of 1 (lLFC (BMP response/NS condition)l ≥1) and an adjusted p-value (padj) ≤0.05 (Benjamini-Hochberg procedure) (Supplementary information SI1) identified respectively 828 and 787 differentially expressed genes (DEGs) coding for proteins upon BMP9 or BMP10 stimulation (Table 2). These DEGs were nearly equally distributed between up- and down-regulated genes (Table 2). Interestingly, BMP9 and BMP10 induced a highly similar transcriptomic response evidenced by the high Pearson correlation coefficient = 0.993 when plotting the LFCs of the DEGs obtained in response to BMP9 vs those obtained in response to BMP10 (Figure 1C) and the high number of shared DEGs regulated by both ligands 81.4% (Suppl Figure 2A). This similarity was also reflected in the volcano plots of BMP9- and BMP10-stimulated vs NS ECFCs, which highlighted the same top dysregulated genes, in terms of LFC or padj (Figure 1D and E). Among these top DEGs, we detected many genes known to be regulated by BMP9 and BMP10 in other endothelial cell types (*SMAD6, SMAD7, SMAD9, ID1, ID2, ENG, HEY2*, *BMPER*, *TMEM100*, *APLN*) (Figure 1D and E). We also identified new DEGs with very similar regulation patterns between BMP9 and BMP10, including *STAT4*, *SLC40A1*, *SLC9A9*, *CLEC1B*, *CLEC3B*, *BMP4*, *KAT7*, *MPP4*, *HDDC2*, *CREBL1*, *DRC1*, *GCHFR,* and *LEFTY2* (Figure 1D and E). In accordance with the high similarity between BMP9 and BMP10 response, no DEGs could be identified when directly comparing BMP9 to BMP10-stimulated CTL ECFCs (Table 2). Additionally, gene set enrichment analysis (GSEA) using hallmark gene sets from MsigDB was performed independently on total genes (whether DEGs or not) regulated by BMP9 or BMP10 in CTL ECFCs (Supplementary information SI2). The top 20 enriched genesets identified were very similar between BMP9 and BMP10 (Figure 1F). As expected, TGFß signaling was positively enriched by BMP9 and BMP10 stimulation, but we could also identify a positive enrichment of epithelial to mesenchymal transition, protein secretion and several signaling pathways (IL6-JAK-STAT3, KRAS and MTORC1) (Figure 1F). On the other hand, many hallmarks related to cell cycle were negatively enriched (MYC-targets, mitotic spindle, G2M checkpoint and E2F targets, Figure 1F), supporting the reported role of BMP9 and BMP10 in maintaining vascular quiescence[8,25]. Together, these results demonstrate that under these stimulatory conditions, BMP9 and BMP10 induce a very similar transcriptomic response in CTL ECFCs.

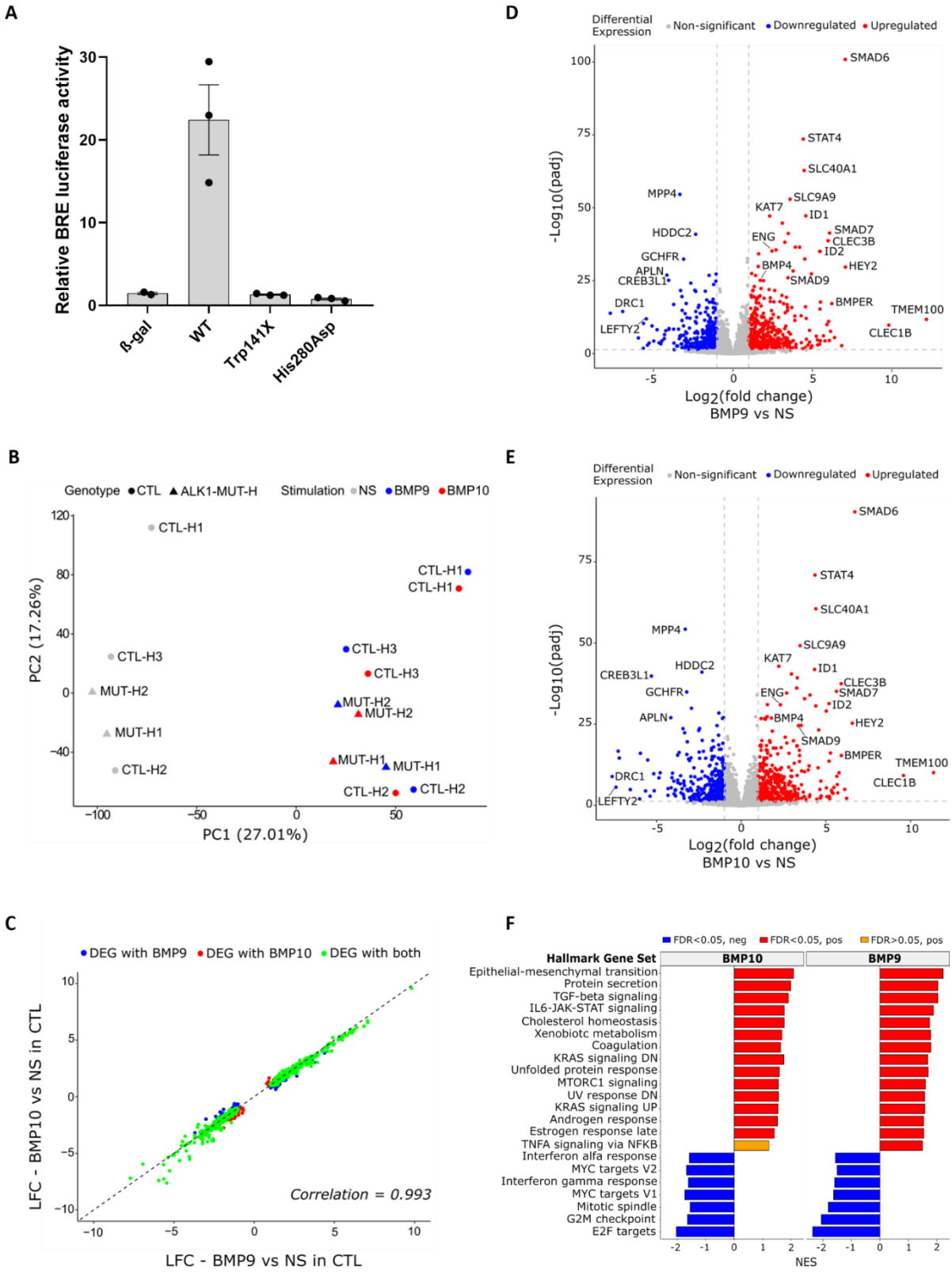

◂ Figure 1. BMP9 and BMP10 induce a similar transcriptomic response in control ECFCs

A, Relative BRE (BMP Response Element) luciferase activity measured in NIH-3T3 cells overexpressing either WT or mutant *ALK1* plasmids identified in *ALK1*-mutated ECFCs (p.Trp141X, MUT-H1) and (p.His280Asp, MUT-H2) used in the ECFC RNA-seq analysis. BRE firefly luciferase activities were normalized to renilla luciferase activity. Data shown are mean ± SEM from 3 independent experiments. **B-F,** 3 CTL (CTL-H1, CTL-H2 and CTL-H3) and 2 *ALK1*-mutated ECFCs (MUT-H1 and MUT-H2) were stimulated or not with BMP9 or BMP10 (10 ng/mL) for 18 hours. The experiment was repeated three times after which bulk RNA-seq analysis was performed. **B,** Principal component analysis (PCA) showing clustering of RNA-seq samples by treatment

(NS vs BMP9 or BMP10 stimulation) in CTL and MUT ECFCs. Each dot represents the mean of 3 experiments for 1 sample. **C,** Scatter plot comparing log_2 fold change (LFC) values of protein coding DEGs regulated in CTL ECFCs by BMP9 vs those regulated by BMP10 both compared to NS. Pearson correlation is reported. **D-E,** Volcano plot representations showing global changes in gene expression in CTL ECFCs after BMP9 **(D)** or BMP10 **(E)** stimulation. DEGs with high LFC and high statistical significance are annotated. **F,** Gene-set enrichment analysis (GSEA) performed using hallmark gene sets. The bar plot represents the top significant gene set categories enriched in CTL ECFCs upon BMP10 or BMP9-stimulation ordered using normalized enrichment scores (NES).

ALK1 heterozygosity in ECFCs does not impair the global transcriptomic response to BMP9 or BMP10

To uncover the effect of heterozygous *ALK1* mutations on gene regulation, we analyzed the basal transcriptome of MUT vs CTL ECFCs, before any stimulation, and in response to BMP9 or BMP10. In accordance with the PCA, which could not differentiate CTL from MUT ECFCs (Figure 1B), only 28 DEGs were identified between NS CTL and MUT ECFCs (Table 2). Similarly, following a BMP9 or BMP10 stimulation, only 19 and 30 DEGs were significantly differentially expressed between the two ECFC groups, respectively (Table 2).

Upon analyzing the transcriptomic response of MUT ECFCs to BMP9 or BMP10, 604 and 564 DEGs were identified, respectively (Table 2). As in CTL ECFCs, BMP9 and BMP10 induced a similar response in *ALK1*-mutated cells, with 77.2% DEGs commonly regulated by both ligands (Suppl Figure 2B) and a highly similar global regulation pattern (Pearson correlation coefficient = 0.989, Sup Figure 2C).

We next compared the log_2 fold changes of each list of target genes in stimulated CTL vs stimulated *ALK1*-mutated ECFCs and found that most regulated genes demonstrated the same regulation patterns in the two cell groups upon BMP9 or BMP10 stimulation (Pearson correlation coefficient= 0.958 and 0.962 respectively, Figure 2A and B). Consistently, we could identify in *ALK1*-mutated ECFCs the same top protein-coding genes regulated by BMP9 or BMP10 as in CTL ECFCs (*SMAD6, SMAD7, SMAD9, ID1, ID2, ENG, HEY2, BMPER, TMEM100, STAT4, APLN, SLC40A1, SLC9A9, CLEC1B, CLEC3B, BMP4, KAT7, MPP4, HDDC2, CREBL1, DRC1, GCHFR, LEFTY2;* Figure 2C and D). Altogether, these data unexpectedly show that CTL and *ALK1*-mutated ECFCs display highly similar transcriptomic profiles following BMP9 or BMP10 stimulation.

Table 2. Number of protein-coding DEGs identified by differential expression analysis in CTL and *ALK1*-mutated ECFCs and HMVECs

	ECFCs			HMVECs		
Comparison	Total DEGs	Upregulated	Downregulated	Total DEGs	Upregulated	Downregulated
CTL NS vs B9	828	456	372	704	366	338
CTL NS vs B10	787	418	369	481	225	256
CTL B9 vs B10	0	0	0	2	0	2
MUT NS vs B9	604	310	294	295	158	137
MUT NS vs B10	564	278	286	206	90	116
MUT B9 vs B10	0	0	0	0	0	0
CTL NS vs MUT NS	28	11	17	1261	528	733
CTL B9 vs MUT B9	19	6	13	1262	502	760
CTL B10 vs MUT B10	30	7	23	1164	503	661

3 CTL ECFCs and 2 *ALK1*-mutated ECFCs (MUT-H1-H2) or 3 CTL HMVECs and 2 *ALK1*-mutated HMVECs (MUT-P1-P2) were stimulated or not with BMP9 or BMP10 (10 ng/mL) for 18 hours. The experiment was repeated three times to generate technical replicates, after which bulk RNA-seq analysis was performed using DESeq2 package with an absolute log_2 fold change threshold of 1 ($|Log_2FC| \geq 1$) and an adjusted p-value ≤0.05 (Benjamini-Hochberg procedure). Data show protein coding DEGS analyzed by NS: non-stimulated, B9: BMP9-stimulated, B10: BMP10-stimulated

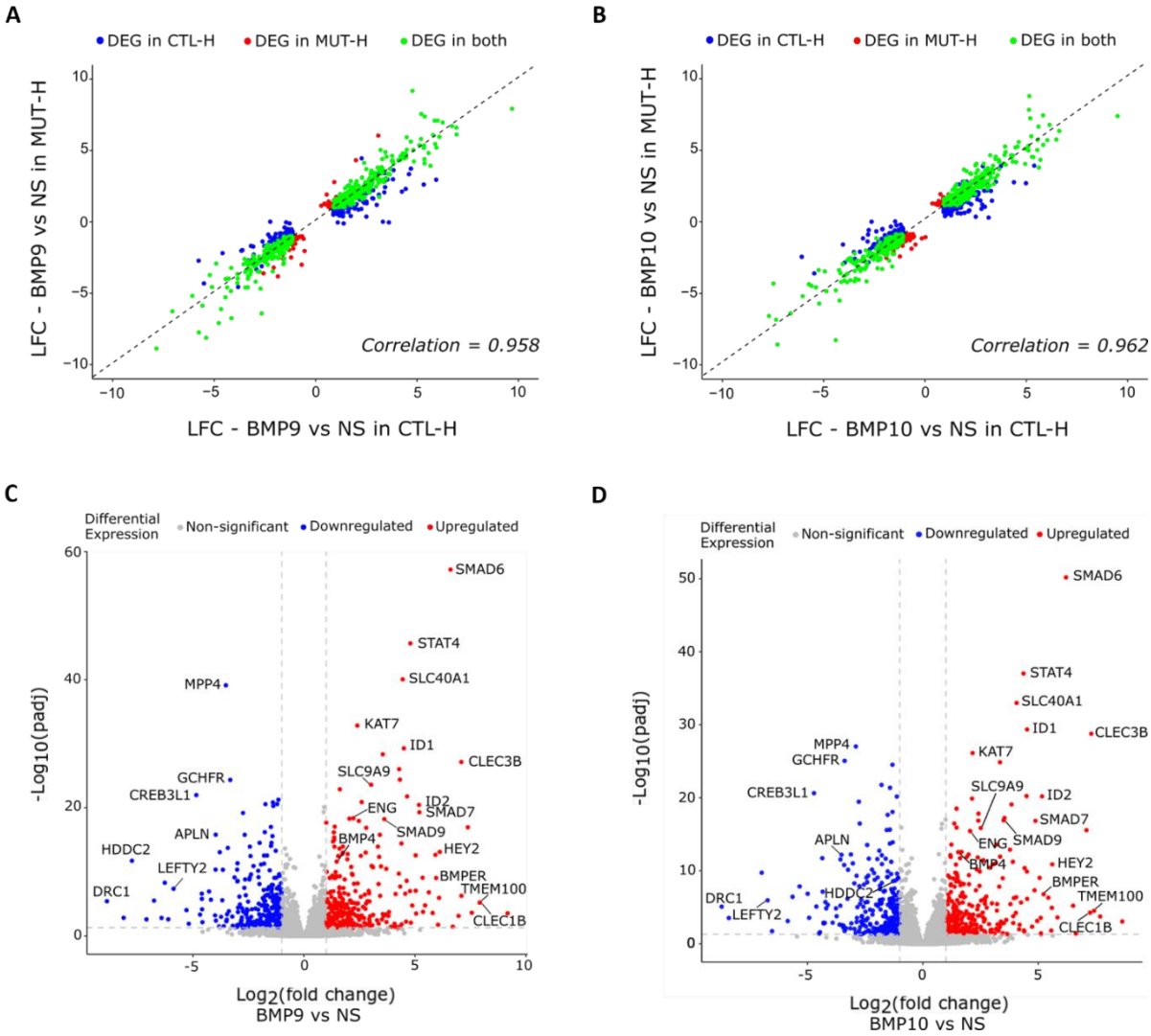

Figure 2. *ALK1* heterozygosity in ECFCs does not impair the global transcriptomic response to BMP9 or BMP10

A-D, 3 CTL (CTL-H1, CTL-H2 and CTL-H3) and 2 *ALK1*-mutated ECFCs (MUT-H1 and MUT-H2) were stimulated or not with BMP9 or BMP10 (10 ng/mL) for 18 hours. The experiment was repeated three times after which bulk RNA-seq analysis was performed. **A-B,** Scatter plots comparing log_2 fold change (LFCs) values of protein coding DEGs regulated by BMP9 **(A)** or BMP10 **(B)** in CTL ECFCs vs MUT ECFCs. Pearson correlation is reported. **C-D,** Volcano plots representations showing global changes in gene expression in *ALK1*-mutated ECFCs after BMP9 **(C)** or BMP10 **(D)** stimulation vs NS. DEGs with high LFC and high statistical significance are annotated.

ALK1 heterozygosity in ECFCs does not impair p-Smad1/5 response to BMP9

To understand this surprising result, we next investigated the status of Smad1/5 phosphorylation induced by BMP9 in a higher number of LOF *ALK1*-mutated ECFCs (n=6, Table 1, Fig1A and Suppl Figure 3). We focused on BMP9 regulation as BMP9 and BMP10 showed a similar transcriptomic response (Figure 1). MUT ECFCs stimulated with BMP9 (10 ng/mL) for one hour displayed similar levels of nuclear p-Smad1/5 immunofluorescence intensities to stimulated CTLs (Figure 3A and B). To validate this result, we performed a BRE luciferase reporter assay in CTL (n=2) and MUT (n=4) ECFCs (Table 1) stimulated with increasing doses of BMP9 (0.2-10 ng/mL) for 6 hours. Both CTL and MUT ECFCs exhibited a clear dose-dependent response to BMP9 (Figure 3C); yet, no significant differences were observed between the 2 groups (Figure 3C), which displayed identical half maximal effective concentrarions (EC_{50}: 517 pg/mL for CTL vs 514 pg/mL for MUT ECFCs; inset Figure 3C). We also quantified the mRNA levels of *ID1,* a target gene known to be strongly induced by BMP9, and found no

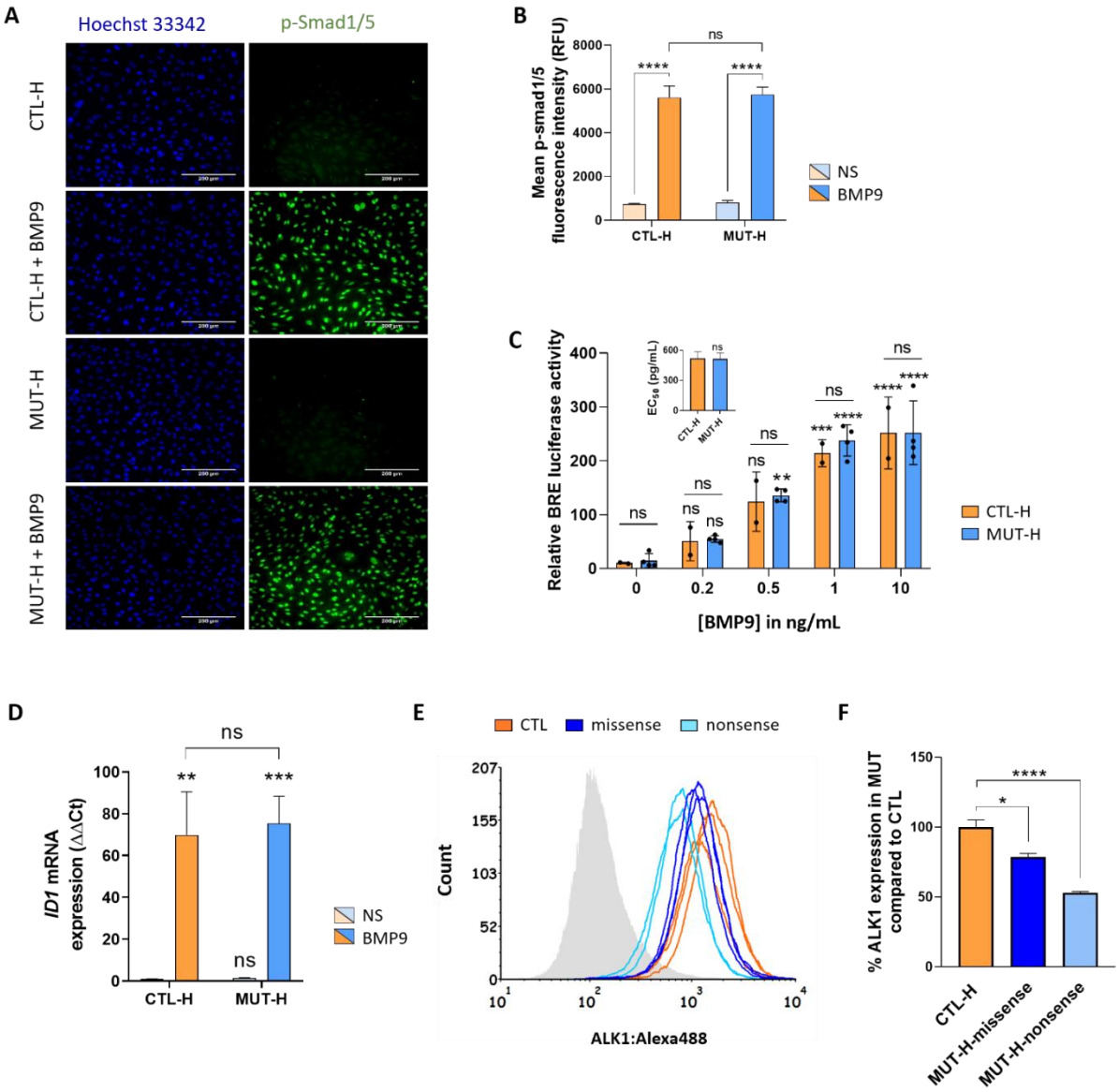

Figure 3. *ALK1* heterozygosity in ECFCs does not impair the p-Smad1/5 response to BMP9

A-B, 3 CTL and 6 MUT ECFCs (MUT-H1-H6) were stimulated with BMP9 (10ng/mL) for 1hr then fixed and immunostained for phospho-Smad1/5 (p-Smad1/5). Cells were stimulated in duplicates and at least 16 different fields were imaged in each well. **A,** Representative p-Smad1/5 immunostainings in 1 CTL and 1 MUT ECFC in the absence or presence of BMP9 for 1hr. The nuclei were counterstained using Hoechst 33342. **B,** p-Smad1/5 fluorescence was quantified in the nuclei using IN Carta Image Analysis Software. Data presented are mean relative fluorescent intensity (RFU) ± SEM of 3 independent experiments. **C,** 2 CTL and 4 MUT (MUT-H1-H4) ECFCs were transiently transfected with pGL3(BRE)2-luc and pRL-TK-luc. Cells were then either non-treated or stimulated with increasing concentrations of BMP9 (0.2, 0.5, 1, 10ng/mL) for 6 hours. Firefly luciferase activities were normalized to renilla luciferase activities. Data shown are mean ± SD from 1 representative experiment of 4, and each point corresponds to one donor. The inset represents the calculated BMP9 EC_{50} for CTL and MUT ECFCs. **D,** RT-qPCR quantification of I*D1* mRNA expression normalized to HPRT level in 4 CTL and 4 MUT (MUT-H1-H4) ECFCs following an 18hr stimulation with 10ng/ml BMP9**.** Data are mean ± SEM of 3 independent stimulations presented as ΔΔCt compared to CTL NS. **E,** Flow cytometric analysis comparing cell-surface ALK1 levels in 3 CTL vs 5 MUT ECFCs either carrying an *ACVRL1* missense mutations (MUT-H2, MUT-H4 and MUT-H6) or a nonsense mutations (MUT-H1 and MUT-H3). Isotypic control is illustrated in grey. One representative flow cytometry histogram of 3 is shown. **F,** Quantification of the ALK1 cell-surface expression by flow cytometry (in percentage of in MUT ECFCs with missense or nonsense mutations compared to CTL ECFCs). Data are means ± SEM of 3 independent experiments. Two-way Anova followed by Sidak's multiple comparisons tests were used for statistical analysis of panels B-D, except for the inset of figure C where Mann-Whitney test was used. Kruskal–Wallis test followed by Dunn's multiple comparison's test was used for F. For all panels, ns: non-significant, *P<0.05, **P<0.01, ***P<0.001 and ****P<0.0001.

difference between CTL (n=4) and MUT (n=4) ECFCs (Table 1, Figure 3D). To examine whether the similar Smad1/5 activation in MUT vs CTL ECFCs was due to a compensation in ALK1 protein levels in *ALK1*-mutated ECFCs, we assessed the levels of membranous ALK1 by flow cytometry analysis in 5 different MUT ECFCs (Table 1, Suppl Figure 3) in comparison to 3 CTL ECFCs. We found that *ALK1*-mutated ECFCs carrying a missense mutation had a slightly lower level of membranous ALK1 level than CTL ECFCs, and those carrying an *ALK1* nonsense mutation displayed a 50% reduction in the level of cell surface ALK1 (Figure 3E and F). Thus the similar Smad signalling response in CTL and *ALK1*-mutated ECFCs cannot be attributed to a compensatory level of ALK1. Altogether, these results support that *ALK1*-mutated ECFCs maintain intact activation of the canonical Smad1/5 signaling pathway in response to BMP9.

Table 3. PAH patient characteristics

ID	Affected gene	mutation		Type of mutation	Domain	Age	Gender	PAPm (mmHg)	NYHA Functional class	Therapies
MUT-P1	*ACVRL1*	c.955G>C	p.Gly319Arg	Missense	Kinase	14	Female	90	IV	bosentan, sildenafil, treprostinil
MUT-P2	*ACVRL1*	c.1450C>T	p.Arg484Trp	Missense	Kinase	19	Female	100	II	bosentan, sildenafil, epoprostenol
MUT-P3	*BMPR2*	del exon 11-13		Large deletion	kinase + cytoplasmic tail	37	Female	74	IV	bosentan, sildenafil, treprostinil
MUT-P4	*BMPR2*	c.314+3A>T		Splice site	Extracellular	14	Female		II	bosentan
MUT-P5	*BMPR2*	c.901T>C	p.Ser301Pro	Missense	kinase	26	Female	99	IV	none, transplanted immediately upon diagnosis

List of *ALK1*- and *BMPR2*-mutated HMVECs that were isolated from explanted lungs of PAH patients, indicating the carried mutation, the type of mutation and the mutated or deleted *ALK1* or *BMPR2* domain, in addition to some characteristics and treatments of the patient. PAPm: mean pulmonary arterial pressure, NYHA: New York Heart Association.

PAH patient-derived lung endothelial cells carrying *ALK1* mutations display different transcriptomic profiles compared to CTLs at the basal state

Having not detected any differences in the transcriptomic nor in the early Smad1/5 response to BMP9 or BMP10 in newborn-derived *ALK1*-mutated ECFCs, we investigated the transcriptomic response in HMVECs carrying *ALK1*-mutations derived from transplanted sick lungs of PAH patients (MUT-P1 and -P2, Table 3). The two *ALK1* mutations were missense mutations mapping to the kinase domain of ALK1 and were both confirmed as LOF mutations using the BRE luciferase assay (Figure 4A).

To delineate the transcriptomic signature of these cells, RNA-sequencing was performed, using the same experimental conditions described for ECFCs, i.e. using 3 CTLs and 2 *ALK1*-mutated HMVECs from PAH patients (MUT-P1 and -P2, Table 3) that were either stimulated overnight with BMP9 or BMP10 (10 ng/mL) or were left nonstimulated (NS). Hierarchical clustering discriminated four clusters: (1) NS and stimulated MUT-P2 samples, (2) NS and stimulated MUT-P1 samples, (3) NS CTLs and (4) BMP9 and BMP10-stimulated CTL samples (from left to right, Suppl Figure 4). This clustering showed that, unlike MUT-H ECFCs, the transcriptomes of MUT-P HMVECs were clearly different from those of CTLs. Interestingly, MUT-P HMVECs of each patient separated into two different clusters (Suppl Figure 4), highlighting variability between the two patients, which might be related to different disease stages or different treatments. The differential expression analysis (lLFCl≥1 and padj ≤0.05, Benjamini-Hochberg correction) (Supplementary information SI3) comparing NS *ALK1*-mutated and CTL HMVECs identified 1261 protein coding DEGs (Table 2), with both down-regulated (58%) and up-regulated (42%) genes. GSEA using hallmark gene sets in NS CTL vs *ALK1*-mutated HMVECs (Supplementary information SI4) revealed a positive enrichment of several gene sets involved in cell cycle (E2F targets, G2M checkpoint, MYC-targets and mitotic spindle) and a negative enrichment in genes related to various signaling

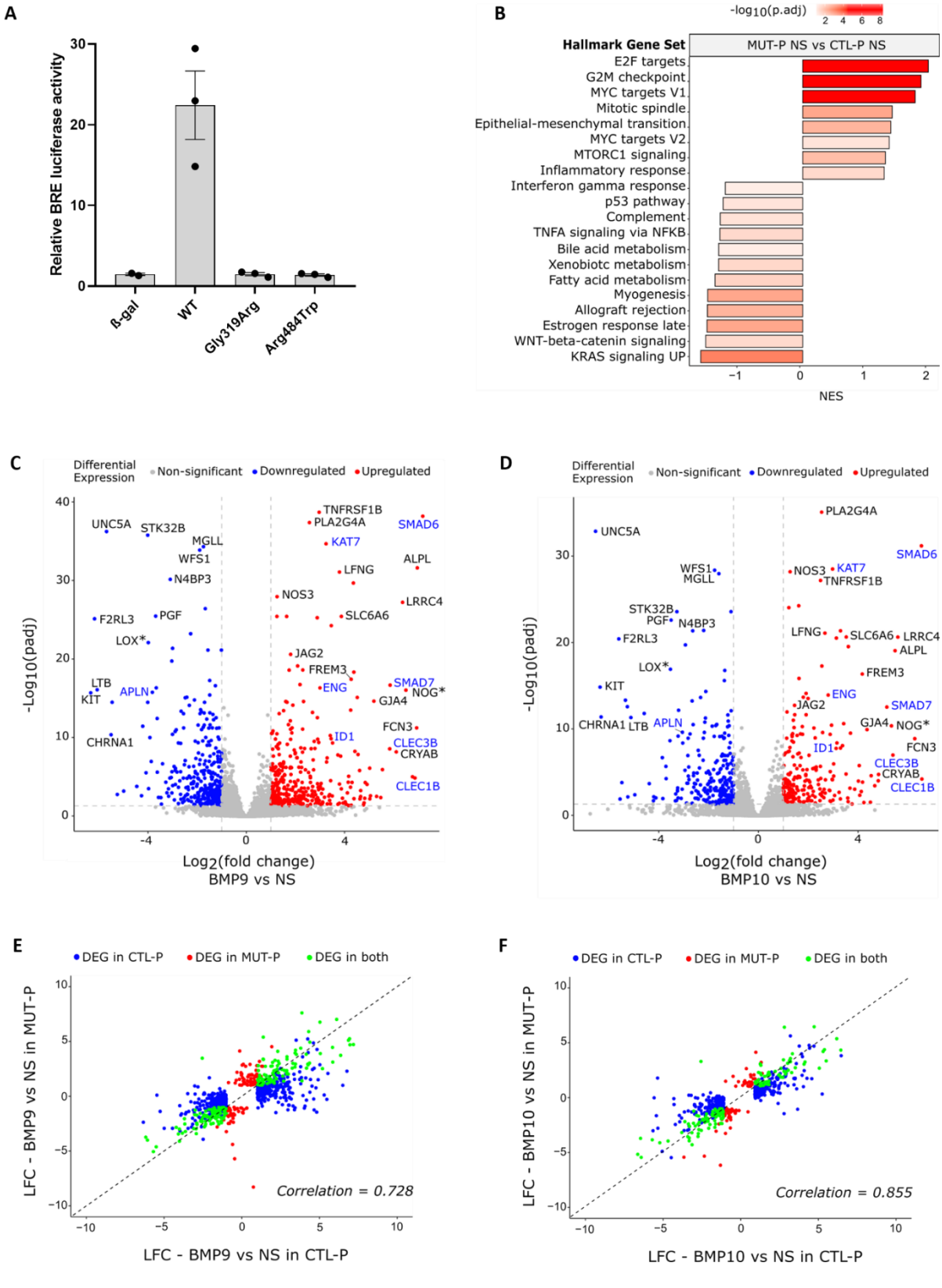

Figure 4. *ALK1*-mutated HMVECs display substantially different transcriptomic profiles compared to controls

A, Relative BRE (BMP Response Element) luciferase activity measured in NIH-3T3 cells overexpressing either WT or mutant *ALK1* plasmids identified in *ALK1*-mutated HMVECs (p.Gly319Arg, MUT-P1) and (p.Arg484Trp, MUT-P2) that are included in the HMVEC RNA-seq analysis. BRE luciferase activities were normalized to renilla luciferase activities. Data shown are mean ± SEM from of 3 independent experiments. **B-F**, 3 CTL and 2 *ALK1*-mutated (MUT-P1 and MUT-P2) HMVECs were stimulated

or not with BMP9 or BMP10 (10 ng/mL) for 18 hours. The experiment was repeated three times after which bulk RNA-seq analysis was performed. **B,** GSEA performed using hallmark gene sets. The bar plot represents the top significant gene set categories enriched in non-stimulated MUT HMVECs compared to nonstimulated CTL HMVECs. Each bar represents a hallmark gene set and bars are ordered from top to bottom by decreasing order of enrichment score (NES). **C-D,** Volcano plot representations showing global changes in gene expression in CTL HMVECs after BMP9 **(C)** or BMP10 **(D)** stimulation. DEGs with high LFC and high statistical significance are annotated. DEGs annotated in blue correspond to DEGs identified in CTL ECFCs (Fig-1D-E). **E-F,** Scatter plots comparing log_2 fold change (LFCs) of DEGs regulated by BMP9 **(E)** or BMP10 **(F)** in CTL HMVECs vs MUT HMVECs. Pearson correlation is reported.

pathways (KRAS signaling, WNT-beta-catenin signaling and TNFα signaling; Figure 4B). Together, these data show that *ALK1*-mutated HMVECs derived from diseased lungs have a severely altered basal transcriptome compared to CTL HMVECs.

BMP9 and BMP10 induce cell type-specific transcriptomic reponses

We then analyzed the BMP9 and BMP10 transcriptomic response in CTL HMVECs. Differential expression analysis identified 704 and 481 DEGs in BMP9- and BMP10-stimulated CTL HMVECs, respectively (Table 2). Although the number of DEGs was lower in BMP10-stimulated cells, the gene regulation patterns in BMP9- vs BMP10-stimulated CTL HMVECs were highly correlated (Pearson correlation coefficient = 0.844), further supporting, as for ECFCs (Fig 1C), that BMP9 and BMP10 induce a very similar transcriptomic response *in vitro*. This similarity was also reflected in the volcano plots of BMP9- and BMP10-stimulated vs NS cells, which highlighted similar top regulated genes, in terms of LFC or padj (Figure 4C and D). Interestingly, by comparing BMP9/10-regulated genes in CTL HMVECs to those in CTL ECFCs, with the limitation that these data come from two independent RNA-sequencing analyses, only a quarter of the DEGS was shared between ECFCs and HMVECs (27% for BMP9 and 26% for BMP10; Suppl Figure 5A and B). *ID1*, *SMAD6*, *SMAD7*, *ENG*, *KAT7, CLEC1B*, *CLEC3B*, and *APLN* were identified as top targets in both ECFCs (Fig 1 D and E) and HMVECs (highlighted in blue in Figure 4C and 4D). On the other hand, some top target genes, such as *LOX* and *NOG,* were specific to HMVECs (highlighted by an asterisk in Figure 4C and D).

***ALK1*-mutated HMVECs display slightly different transcriptomic responses to BMP9 and BMP10 compared to CTL HMVECs**

We next analyzed the BMP9 or BMP10 response in *ALK1*-mutated vs CTL HMVECs. BMP9 and BMP10 stimulation resulted in the regulation of 295 and 206 DEGs, respectively (Table 2). This corresponds to around 60% less DEGs compared to stimulated CTLs. This decrease in the number of DEGs suggests that *ALK1*-mutated HMVECs might possess a reduced capacity to respond to BMP9 or BMP10. When comparing the log_2 fold changes of each list of dysregulated genes in stimulated CTL vs patient HMVECs, we obtained fairly high Pearson correlation coefficients (0.728 for BMP9 and 0.855 for BMP10; Figure 4E and F). However, these correlations were lower than the ones obtained in ECFCs (Figure 2A and B), suggesting that the BMP9 and BMP10 responses in *ALK1*-mutated HMVECs might be more affected than in *ALK1*-mutated ECFCs.

Since we are simultaneously analyzing two variables (genotype and stimulation) and because there was a clear difference between CTL and MUT HMVECs at the basal level (Table 2), we performed a two-factor analysis as previously described[26] (see Materials and Methods section), considering the two factors: genotype and BMP9 or BMP10 treatment (Benjamini–Hochberg adjusted for multiple comparisons padj < 0.05). We found 44 protein-coding interaction term genes differentially regulated by BMP9 in CTL vs *ALK1*-mutated HMVECs and 15 in response to BMP10, which were all shared with BMP9 stimulation (marked by an asterisk, Suppl Figure 6). We selected 25 genes out of these 44 (highlighted in blue in Suppl Figure 6) for validation by RT-qPCR on independent BMP9 stimulations. Selection criteria were (1) to show clear visible differences in regulation between CTLs and MUTs in response to BMP9 and BMP10 and (2) have minimal interindividual heterogeneity between members of each group (CTL or MUT group; data not shown). The regulation of 24 out of the 25 selected genes (the exception being *MTUS1)*, were confirmed by RT-qPCR (data not shown), validating the robustness of the two-factor analysis.

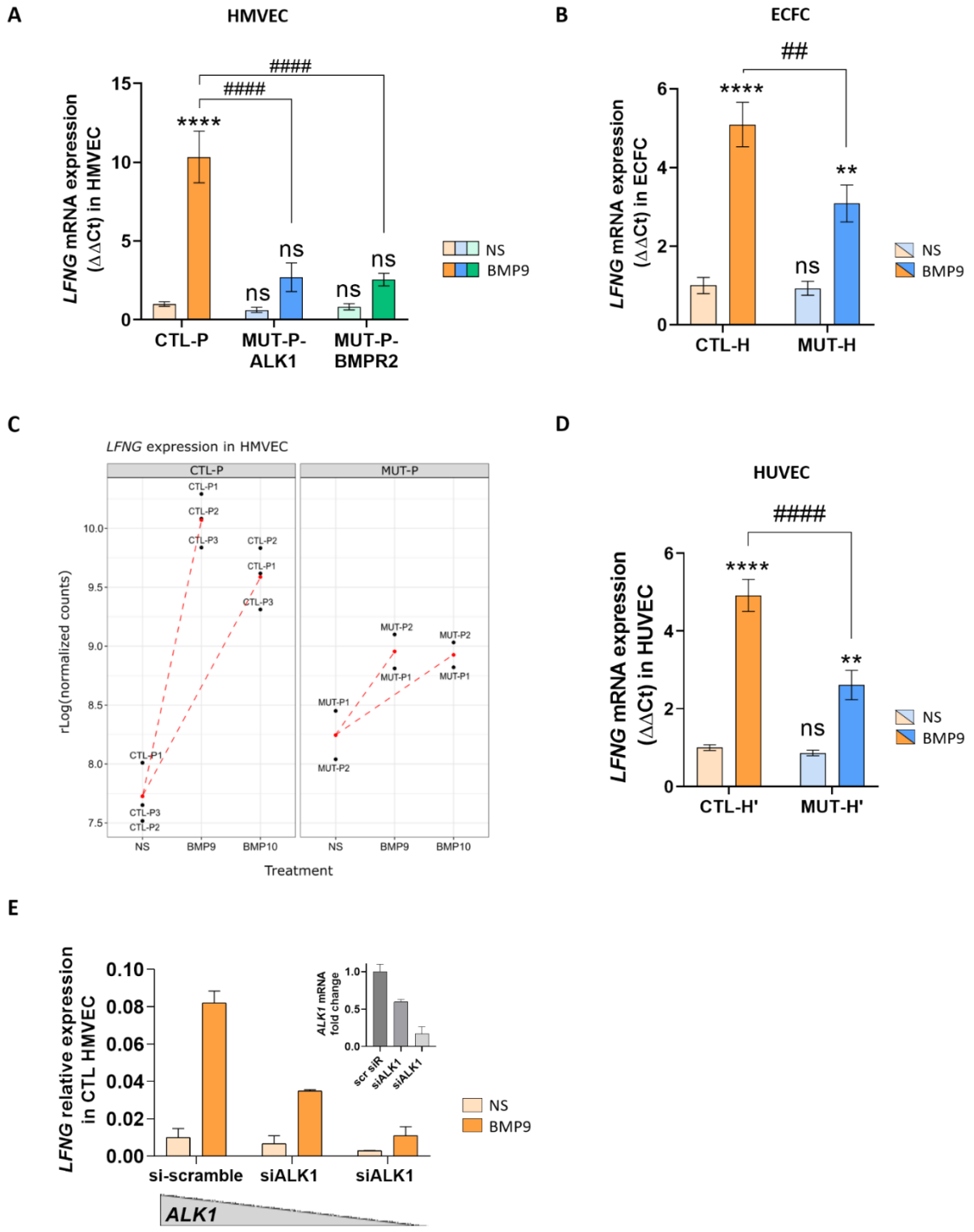

Figure 5. Regulation of *LFNG* mRNA expression by BMP9 in in CTL and *ALK1*-mutated HMVECs, ECFCs and HUVECs.

A, B, RT-qPCR quantification of the mRNA expression level of *LFNG* in 3 CTL, 2 *ALK1*-mutated (MUT-P1 and -P2) and 3 *BMPR2*-mutated HMVECs (MUT-P3-P5) **(A)**, 3 CTL and 4 *ALK1*-mutated ECFCs (MUT-H1-H4) **(B)**. *LFNG* mRNA expression level is normalized to *HPRT* mRNA expression and presented as ΔΔCt compared to mean CTL NS. Data shown are mean ± SEM of at least 3 independent stimulations. **C,** Count plot representation showing the regularized log transformed counts of *LFNG* mRNA in CTL-P and *ALK1*-MUT-P HMVECs in nonstimulated (NS) and BMP9 or BMP10 stimulated cells. **D,** RT-qPCR quantification of the mRNA expression level of *LFNG* in 3 CTL and 3 *ALK1*-mutated (MUT-H3-H5) HUVECs. *LFNG* mRNA expression level is normalized to *HPRT* mRNA expression and presented as ΔΔCt compared to mean CTL NS. Data shown are mean ± SEM of at

least 3 independent stimulations. A, B, D, Two-way Anova followed by Sidak's multiple comparisons test were used for statistical analysis of panels. ns: non-significant, **P<0.01 and ****P<0.0001 vs NS and ##P<0.01 and ####P<0.0001 vs CTL. **E,** 2 CTL HMVECs were treated either with scrambled siRNA (siScr) or 2 different concentrations of siRNA against *ACVRL1* (siALK1) to generate a gradient of ALK1 expression and then stimulated with 10ng/mL BMP9 for 18hr. *LFNG* mRNA expression normalized to *HPRT* mRNA level is presented as $2^{-\Delta Ct}$. Data shown are mean ± SD of 2 CTL HMVECs. Inset represents *ACVRL1* mRNA expression presented as ΔΔCt compared to scrambled siRNA-transfected cells.

LFNG (lunatic fringe) shows impaired regulation by BMP9 in *ALK1*-mutated HMVECs, ECFCs and HUVECs

Among the 24 genes validated, we focused on 6 of them (*LFNG*, *JAG2*, *TNFRSF1B*, *SLC6A6*, *SOX13* and *CEBPG)* as these were also identified as DEGs in response to BMP9 and BMP10 in CTL ECFCs with the same sense of regulation, making them good candidates to compare the effect of *ALK1* mutation on gene regulation by BMP9 across the different models of endothelial cells. We tested their regulation by RT-qPCR in CTL and *ALK1*-mutated ECFCs. Among these 6 genes, only *LFNG* mRNA expression was found to be significantly differentially regulated between CTL and *ALK1*-mutated cells in both HMVECs (n=2) and ECFCs (n=4) (Figure 5A, 5B and Suppl Fig 7A, 7B). As we were limited by the number of *ALK1*-mutated HMVECs available and in order to test whether mutations in the same pathway would respond similarly, we tested 3 *BMPR2*-mutated HMVECs derived from transplanted lungs of PAH patients (Table 3). As shown on figure 5A, *LFNG* mRNA upregulation by BMP9 was strongly reduced in HMVECs derived from PAH patients carrying either *ALK1* or *BMPR2* mutation compared to CTLs (10.3 folds in CTLs vs 2.7 and 2.6 folds in *ALK1*- (n=2) and *BMPR2*- (n=3) mutated cells respectively, Figure 5A). RT-qPCR analysis performed in CTL ECFCs, showed that *LFNG* mRNA expression was also significantly upregulated by BMP9 (5.1 folds, Figure 5B), altough not as strongly as in CTL HMVECs (10.3 folds, Figure 5A), and that this increase was significantly reduced in *ALK1*-mutated ECFCs (3.1 folds, n=4, Figure 5B). The results obtained by RT-qPCR in HMVECs validate the two-factor analysis generated from the RNA-seq data in HMVECs, as illustrated in the count-plot representation (Figure 5A), which shows that *LFNG* mRNA expression was significantly induced in response to BMP9 (14 folds) or BMP10 (10 folds) in CTLs, but only weakly induced in *ALK1*-mutated cells. The RNA-seq analysis performed in CTL ECFCs also identified *LFNG* as DEG, but the two factor analysis did not identify any differentialy regulated genes between BMP-stimulated CTLs and *ALK1*-mutated ECFCs. The BMP9 regulations of *JAG2*, *TNFRSF1B*, *SLC6A6*, *SOX13* and *CEBPG* mRNA expression were all confirmed by RT-qPCR in CTL HMVECs and, consistent with the two-factor analysis, their induction was repressed in *ALK1*- and *BMPR2*-mutated HMVECs, except for SLC6A6 that followed the same reduction trend but that did not reach statistical significance (Suppl Fig 7A). The BMP9 regulation of these genes was confirmed in CTL ECFCs, however their regulation in *ALK1*-mutated cells showed either similar or slightly weaker regulation by BMP9 compared to CTLs (Suppl Fig 7B). Together, these results support that *LFNG* transcriptional regulation by BMP9 could be affected by ALK1 heterozygosity but did not allow to conclude on the other interaction term genes studied.

To further test this hypothesis, we studied the BMP9 response in HUVECs, another type of endothelial cells that can be isolated from newborns. RT-qPCR for *LFNG*, *JAG2*, *TNFRSF1B*, *SLC6A6*, *SOX13* and *CEBPG* were performed on 3 CTLs and 3 LOF *ALK1*-mutated HUVECs (CTL-H' and MUT-H') stimulated or not with BMP9 for 18hrs. These genes were all induced in response to BMP9 in CTL HUVECs, although SOX13 stimulation did not reach significance (Figure 5D and Suppl Fig 7C). As for HMVECs and ECFCs (Figure 5A and B), we found a significant decrease in the level of induction of *LFNG* mRNA expression by BMP9 in *ALK1*-mutated HUVECs compared to CTLs (4.9 folds in CTL-H' and 2.6 folds in MUT-H'; Figure 5D). The BMP9 regulation of *JAG2*, *TNFRSF1B* and *SLC6A6* mRNA expressions were also found to be significantly reduced in *ALK1*-mutated vs CTL HUVECs (Suppl Figure 7C).

To further validate these results, we next set-up an experiment using a siRNA approach, where we could decrease ALK1 expression to the half, in order to mimic ALK1 heterozygosity. We found that reducing *ALK1* mRNA levels in CTL HMVECs by 50 or 90% (inset in Figure 5F), dose-dependently suppressed *LFNG* induction by BMP9 (Figure 5E). Together, these data show that *ALK1* heterozygosity could impair the BMP9 regulation of *LFNG* mRNA expression and possibly other genes, depending on the endothelial cellular model.

Discussion

To our knowledge, this is the first study assessing the BMP9 and BMP10 transcriptomic responses in endothelial cells carrying heterozygous *ALK1* mutations. In this work, we performed RNA-seq analyses on two types of primary *ALK1*-mutated cells: (1) ECFCs derived from HHT newborns, whereby ECFCs were not yet exposed to a sick environment and (2) HMVECs derived from severely ill explanted lungs of end-stage PAH patients. This work uncovered several important findings, including the fact that ALK1 heterozygosity does not impair Smad1/5 activation nor strongly affect the transcriptomic response to BMP9 nor BMP10 stimulation. Consequently, our data challenge the current model of haploinsufficiency, that needs to be reconsidered since a LOF mutation in a single *ALK1* allele does not strongly affect the transcriptomic response.

The first interesting point from this work was the comparison between BMP9 and BMP10 transcriptomic responses in endothelial cells. BMP9 and BMP10 have been identified as two high affinity ligands for ALK1 with very similar affinities. BMP9, but not BMP10, can also bind the type I receptor ALK2, yet with a much lower affinity than ALK1[27]. In addition, different affinities for the type II receptors to BMP9 vs BMP10 have been described. Here, we show that BMP9 and BMP10, despite the reported differences in receptor binding affinities, induced highly similar transcriptomic responses in both ECFCs and HMVECs. This is in accordance with recent work that compared transcriptomic regulation by precursor forms of BMP9 and BMP10 in pulmonary arterial endothelial cells using lower BMP doses[28]. Nonetheless, these *in vitro* findings do not rule out specific *in vivo* roles that can arise from differences in spatiotemporal expression patterns, as recently described[29].

Another interesting point was the use of two different endothelial cell types (ECFCs and HMVECs) for studying BMP9 and BMP10 transcriptomic responses. With the limitation that these two RNA-seq analyses were performed independently, it is interesting to note that the transcriptomic profiles of ECFCs and HMVECs in response to BMP9 or BMP10 stimulation were not largely overlapping, with only 26-27% of genes commonly regulated in both cell types. Nonetheless, BMP9 or BMP10-induced gene regulation patterns between ECFCs and HMVECs were still fairly correlated, with Pearson correlation coefficients reaching 0.71 and 0.75 for BMP9 and BMP10, respectively. This suggests that a proportion of the DEGs identified in one EC type are not detected in the other because they don't reach the set thresholds rather than displaying differential patterns of gene regulation. On the other hand, the other group of genes presenting distint regulation patterns between the two cell types indicate that the studied cells retain organotypic specificities despite being cultured *in vitro*. This specificity could be due to predetermined BMP Smad binding sites in specific endothelial subtypes as already described[30].

Among the cell type-specific targets, we identified *LOX* as a strongly downregulated target in response to BMP9 or BMP10 in HMVECs but not in ECFCs. Interestingly, *LOX*, which codes for a lysyl oxidase that is implicated in crosslinking of extracellular matrix components, was previously found to be elevated in the proliferating pulmonary endothelium of PAH patients[31]. We also detected *NOG*, encoding the strong BMP antagonist noggin[32,33] as a target upregulated by BMP9/10 in HMVECs but not in ECFCs.

This work also unexpectedly revealed similarity in the BMP9 or BMP10 response between CTL and *ALK1*-mutated ECFCs, both at the transcriptomic level and at the Smad1/5 activation level. This result is rather surprising, as it demonstrates, for the first time, that losing one functional *ALK1* allele does not considerably affect the downstream Smad signaling response. The intact activation of the pathway in mutated ECFCs was neither due to the high dose of BMP9 and BMP10 used, as similar results were obtained using low doses of BMP9 in the BRE luciferase assay on CTL and MUT ECFCs (Figure 3C), nor due to a compensation in ALK1 expression, as decreased levels of membranous ALK1 were detected in the heterozygote ECFCs (Figure 3F). Our findings thus support the hypothesis that 50% of functional membranous ALK1 is sufficient for driving normal canonical signal transduction. Our data would support the hypothesis that dimeric ALK1 signaling complexes composed of one functional ALK1 receptor and one non-funtional ALK1 receptor could be functionally active, but this point needs to be further demonstrated. This hypothesis is consistent with a previous study reporting the sole need of one functional type I receptor within the ACVR1/BMPR1 (in this case, an ACVR1 kinase active and a BMPR1 kinase inactive) to phosphorylate Smad1/5 in response to BMP2/7 heterodimers[34].

More importantly, the nearly identical transcriptomic responses to BMP9 or BMP10 between CTL and *ALK1*-mutated ECFCs suggest that haploinsufficiency might not be sufficient for the development of HHT. This result is in accordance with the recent identification of a bi-allelic loss of *ALK1* or *ENG* in at least 50% of tested cutaneous telangiectasia samples isolated from HHT patients[35], supporting the hypothesis that a second 'knudsonian' somatic hit in the other allele is necessary to drive HHT pathogenesis. This notion is not novel to the vascular anomalies field, as it was already shown for venous, glomuvenous and cerebral cavernous malformations[36,37]. These somatic mutations could explain why some lesions develop only focally in HHT patients, and how related patients, carrying the same mutation, can develop different manifestations of the disease. However, this hypothesis has not yet been validated neither in liver or lung AVMs nor in diffuse lesions.

In contrast to *ALK1*-mutated ECFCs isolated from a non-sick microenvironment, *ALK1*-mutated HMVECs isolated from the lungs of endstage PAH patients revealed strong dysregulations in gene expression compared to controls, already in non-stimulated cells (1261 DEGs, Table 2). This might not be surprising, as these cells not only harbored heterozygous *ALK1* mutations, but have also been exposed to a pathogenic, likely inflammatory environment as is usually described for lungs of PAH patients[38] and as evidenced by the enrichment in proliferation and inflammation-related gene sets in the mutated cells by our GSEA (Figure 4B). Due to these large transcriptomic differences already at the basal level, it was difficult to pinpoint which genes are differently regulated by BMP9 and BMP10 in the presence of an *ALK1* mutation, regardless of their initial differences at the basal level. Hence, using a two-factor analysis, which takes into account the two variables (genotype and BMP stimulation), we identified 44 hits and validated six of them by RT-qPCR in both *ALK1*- and *BMPR2*-mutated HMVECs (*LFNG*, *JAG2*, *TNFRSF1B*, *SLC6A6*, *SOX13* and *CEBPG*, Figure 5A and Suppl Figure 7A). Among them, *LFNG* was found to be significantly dysregulated in the three *ALK1*-mutated endothelial cell types (HMVECs, ECFCs and HUVECs), when assessed by RT-qPCR. However, its dysregulation in *ALK1*-mutated ECFCs or HUVECs was not as drastic as in *ALK1*- or *BMPR2*-mutated HMVECs. Intriguingly, the BMP9 regulation of *LFNG* was impaired in *ALK1*-mutated ECFCs, despite their normal Smad1/5 activation. One possible explanation for that, as proposed by Morikawa et al[30], is that different Smad1/5 binding sites have different affinities for Smad1/5 complex, with some high affinity sites, such as that of *ID1*, and other low affinity ones, such as those of *JAG1* and *HEY1*, thus requiring higher or more sustained levels of Smad1/5 activation or the involvement of other DNA binding protein partners for their regulation[30]. In that same study, *LFNG*'s promoter was shown by chromatin immunoprecipitation-sequencing to be bound by Smad1/5 in response to BMP9 stimulation in HUVECs[30]. *LFNG* could be one of these genes with low Smad1/5 binding affinity and/or needing other Smad binding partners, making it more sensitive to ALK1 heterozygosity. *ALK1*-mutated HUVECs, but not *ALK1*-mutated ECFCs, additionally displayed significant dysregulations in *JAG2, TNFRSF1B* and *SLC6A6* mRNA expression, suggesting that HUVECs might be more sensitive to *ALK1* LOF than ECFCs. This could be due to the fact that HUVECs are derived from a vessel environment in contrast to ECFCs, which are circulating cells.

Interestingly, *LFNG* and *JAG2* are two components of the Notch signaling pathway, which is a master regulator of tip/stalk cell differentiation and arterial specification[39]. Furthermore, multiple Notch-defective mouse models were reported to develop AVMs[40–43], which represent a major pathological feature of HHT. In addition, BMP and Notch pathways synergistically upregulate several shared transcription factors such as Hey1, Hey2 and Hes1[44,45]. Here, we report a less studied intersection point between BMP and Notch axes, through BMP9/10-mediated regulation of *LFNG*. *LFNG* codes for lunatic fringe, a glycosyl transferase that post-translationally modifies Notch1, leading to inhibition of its activation by Jagged ligands while enhancing its activation by Delta-like ligands (Dll)[46–48]. It is noteworthy that reduced activation of Dll4-mediated Notch signaling results in excessive sprouting[49] during the activation phase of angiogenesis and promotes cell cycle reentry during the maturation phase[50]. Knowing that *Alk1*-depleted HHT mouse models display hypersprouting and increased vascular density in their developing retinas[51], it is plausible that suppressed upregulation of *LFNG* by BMP9 in the presence of *ALK1*-mutations might be contributing to this phenotype by mitigating Dll4 activation.

This work provides, to our knowledge, the first *in vitro* line of evidence that *ALK1* heterozygosity on its own does not drastically impair the response of endothelial cells to BMP9 nor BMP10, neither at an early step of signal transduction (phosphorylation of Smad1/5), nor downstream at the transcriptomic level, supporting that one functional receptor could be enough for canonical signaling. We also show that the two high affinity ALK1 ligands, BMP9 and BMP10, induce highly similar transcriptomic changes *in vitro*, pointing to an overlapping function in this context. Interestingly, through deeper investigations, we could identify at least one gene, i.e. *LFNG*, whose regulation by BMP9 was weakly impaired in newborn heterozygous *ALK1*-mutated endothelial cells, but more intensely suppressed in *ALK1* or *BMPR2*-mutated HMVECs from PAH patients. Altogether, our findings suggest that heterozygous *ALK1* mutations could be priming events awaiting further triggers for driving lesion development. This requires further validation by studying the effects of angiogenic or inflammatory triggers or shear stress[52] on BMP9/10-ALK1 signaling in heterozygous *ALK1*-mutated endothelial cells, all of which were beyond the scope of this work. In parallel, future studies investigating the role of *LFNG,* and more largely the Notch signaling pathway, are needed to establish their implication in driving early HHT pathogenesis.

References

1. Shovlin CL. Hereditary haemorrhagic telangiectasia: Pathophysiology, diagnosis and treatment. *Blood Rev*. 2010;24(6):203-219. doi:10.1016/j.blre.2010.07.001

2. Gallione CJ, Repetto GM, Legius E, et al. A combined syndrome of juvenile polyposis and hereditary haemorrhagic telangiectasia associated with mutations in MADH4 (SMAD4). *The Lancet*. 2004;363(9412):852-859. doi:10.1016/S0140-6736(04)15732-2

3. Lesca G, Burnichon N, Raux G, et al. Distribution ofENG andACVRL1 (ALK1) mutations in French HHT patients. *Hum Mutat*. 2006;27(6):598-598. doi:10.1002/humu.9421

4. Wooderchak-Donahue WL, McDonald J, O'Fallon B, et al. BMP9 mutations cause a vascular-anomaly syndrome with phenotypic overlap with hereditary hemorrhagic telangiectasia. *Am J Hum Genet*. 2013;93(3):530-537. doi:10.1016/j.ajhg.2013.07.004

5. David L, Mallet C, Mazerbourg S, Feige JJ, Bailly S. Identification of BMP9 and BMP10 as functional activators of the orphan activin receptor-like kinase 1 (ALK1) in endothelial cells. *Blood*. 2007;109(5):1953-1961. doi:10.1182/blood-2006-07-034124

6. Shi Y, Massagué J. Mechanisms of TGF-β Signaling from Cell Membrane to the Nucleus. *Cell*. 2003;113(6):685-700. doi:10.1016/S0092-8674(03)00432-X

7. David L, Feige JJ, Bailly S. Emerging role of bone morphogenetic proteins in angiogenesis. *Cytokine Growth Factor Rev*. 2009;20(3):203-212. doi:10.1016/j.cytogfr.2009.05.001

8. David L, Mallet C, Keramidas M, et al. Bone Morphogenetic Protein-9 Is a Circulating Vascular Quiescence Factor. *Circ Res*. 2008;102(8):914-922. doi:10.1161/CIRCRESAHA.107.165530

9. Robert F, Desroches-Castan A, Bailly S, Dupuis-Girod S, Feige JJ. Future treatments for hereditary hemorrhagic telangiectasia. *Orphanet J Rare Dis*. 2020;15(1):4. doi:10.1186/s13023-019-1281-4

10. Dupuis-Girod S, Shovlin CL, Kjeldsen AD, et al. European Reference Network for Rare Vascular Diseases (VASCERN): When and how to use intravenous bevacizumab in Hereditary Haemorrhagic Telangiectasia (HHT)? *Eur J Med Genet*. 2022;65(10):104575. doi:10.1016/j.ejmg.2022.104575

11. Mallet C, Lamribet K, Giraud S, et al. Functional analysis of endoglin mutations from hereditary hemorrhagic telangiectasia type 1 patients reveals different mechanisms for endoglin loss of function. *Hum Mol Genet*. 2015;24(4):1142-1154. doi:10.1093/hmg/ddu531

12. Ricard N, Bidart M, Mallet C, et al. Functional analysis of the BMP9 response of ALK1 mutants from HHT2 patients: a diagnostic tool for novel ACVRL1 mutations. *Blood*. 2010;116(9):1604-1612. doi:10.1182/blood-2010-03-276881

13. Pece-Barbara N, Cymerman U, Vera S, Marchuk DA, Letarte M. Expression Analysis of Four Endoglin Missense Mutations Suggests That Haploinsufficiency Is the Predominant Mechanism for Hereditary Hemorrhagic Telangiectasia Type 1. *Hum Mol Genet*. 1999;8(12):2171-2181. doi:10.1093/hmg/8.12.2171

14. Shovlin CL, Guttmacher AE, Buscarini E, et al. Diagnostic criteria for hereditary hemorrhagic telangiectasia (Rendu-Osler-Weber syndrome). *Am J Med Genet*. 2000;91(1):66-67. doi:10.1002/(sici)1096-8628(20000306)91:1<66::aid-ajmg12>3.0.co;2-p

15. Aldred MA, Morrell NW, Guignabert C. New Mutations and Pathogenesis of Pulmonary Hypertension: Progress and Puzzles in Disease Pathogenesis. *Circ Res*. 2022;130(9):1365-1381. doi:10.1161/CIRCRESAHA.122.320084

16. Simonneau G, Montani D, Celermajer DS, et al. Haemodynamic definitions and updated clinical classification of pulmonary hypertension. *Eur Respir J*. 2019;53(1):1801913. doi:10.1183/13993003.01913-2018

17. Humbert M, Kovacs G, Hoeper MM, et al. 2022 ESC/ERS Guidelines for the diagnosis and treatment of pulmonary hypertension. *Eur Heart J*. 2022;43(38):3618-3731. doi:10.1093/eurheartj/ehac237

18. Walsh LJ, Collins C, Ibrahim H, Kerins DM, Brady AP, O Connor TM. Pulmonary arterial hypertension in hereditary hemorrhagic telangiectasia associated with ACVRL1 mutation: a case report. *J Med Case Reports*. 2022;16(1):99. doi:10.1186/s13256-022-03296-9

19. Yokokawa T, Sugimoto K, Kimishima Y, et al. Pulmonary Hypertension and Hereditary Hemorrhagic Telangiectasia Related to an *ACVRL1* Mutation. *Intern Med*. 2020;59(2):221-227. doi:10.2169/internalmedicine.3625-19

20. Girerd B, Montani D, Coulet F, et al. Clinical Outcomes of Pulmonary Arterial Hypertension in Patients Carrying an *ACVRL1* (*ALK1*) Mutation. *Am J Respir Crit Care Med*. 2010;181(8):851-861. doi:10.1164/rccm.200908-1284OC

21. Roman BL, Hinck AP. ALK1 signaling in development and disease: new paradigms. *Cell Mol Life Sci CMLS*. 2017;74(24):4539-4560. doi:10.1007/s00018-017-2636-4

22. Paschalaki KE, Randi AM. Recent Advances in Endothelial Colony Forming Cells Toward Their Use in Clinical Translation. *Front Med*. 2018;5:295. doi:10.3389/fmed.2018.00295

23. Dumortier J, Dupuis-Girod S, Valette PJ, et al. Recurrence of Hereditary Hemorrhagic Telangiectasia After Liver Transplantation: Clinical Implications and Physiopathological Insights. 2019;69(5):9.

24. Smadja DM, Melero-Martin JM, Eikenboom J, Bowman M, Sabatier F, Randi AM. Standardization of methods to quantify and culture endothelial colony-forming cells derived from peripheral

blood: Position paper from the International Society on Thrombosis and Haemostasis SSC. *J Thromb Haemost*. 2019;17(7):1190-1194. doi:10.1111/jth.14462

25. Ricard N, Ciais D, Levet S, et al. BMP9 and BMP10 are critical for postnatal retinal vascular remodeling. *Blood*. 2012;119(25):6162-6171. doi:10.1182/blood-2012-01-407593

26. Panov J, Simchi L, Feuermann Y, Kaphzan H. Bioinformatics Analyses of the Transcriptome Reveal Ube3a-Dependent Effects on Mitochondrial-Related Pathways. *Int J Mol Sci*. 2020;21(11):4156. doi:10.3390/ijms21114156

27. Scharpfenecker M, van Dinther M, Liu Z, et al. BMP-9 signals via ALK1 and inhibits bFGF-induced endothelial cell proliferation and VEGF-stimulated angiogenesis. *J Cell Sci*. 2007;120(6):964-972. doi:10.1242/jcs.002949

28. Salmon RM, Guo J, Wood JH, et al. Molecular basis of ALK1-mediated signalling by BMP9/BMP10 and their prodomain-bound forms. *Nat Commun*. 2020;11(1):1621. doi:10.1038/s41467-020-15425-3

29. Desroches-Castan A, Tillet E, Bouvard C, Bailly S. BMP9 and BMP10 : Two close vascular quiescence partners that stand out. *Dev Dyn*. 2022;251(1):158-177. doi:10.1002/dvdy.395

30. Morikawa M, Koinuma D, Tsutsumi S, et al. ChIP-seq reveals cell type-specific binding patterns of BMP-specific Smads and a novel binding motif. *Nucleic Acids Res*. 2011;39(20):8712-8727. doi:10.1093/nar/gkr572

31. Vadasz Z, Balbir Gurman A, Meroni P, et al. Lysyl oxidase—a possible role in systemic sclerosis–associated pulmonary hypertension: a multicentre study. *Rheumatology*. 2019;58(9):1547-1555. doi:10.1093/rheumatology/kez035

32. Zimmerman LB, De Jesús-Escobar JM, Harland RM. The Spemann Organizer Signal noggin Binds and Inactivates Bone Morphogenetic Protein 4. *Cell*. 1996;86(4):599-606. doi:10.1016/S0092-8674(00)80133-6

33. Gazzerro E, Gangji V, Canalis E. Bone morphogenetic proteins induce the expression of noggin, which limits their activity in cultured rat osteoblasts. *J Clin Invest*. 1998;102(12):2106-2114. doi:10.1172/JCI3459

34. Tajer B, Dutko JA, Little SC, Mullins MC. BMP heterodimers signal via distinct type I receptor class functions. *Proc Natl Acad Sci*. 2021;118(15):e2017952118. doi:10.1073/pnas.2017952118

35. Snellings DA, Gallione CJ, Clark DS, Vozoris NT, Faughnan ME, Marchuk DA. Somatic Mutations in Vascular Malformations of Hereditary Hemorrhagic Telangiectasia Result in Bi-allelic Loss of ENG or ACVRL1. *Am J Hum Genet*. 2019;105(5):894-906. doi:10.1016/j.ajhg.2019.09.010

36. Brouillard P, Vikkula M. Genetic causes of vascular malformations. *Hum Mol Genet*. 2007;16(R2):R140-R149. doi:10.1093/hmg/ddm211

37. Snellings DA, Girard R, Lightle R, et al. Developmental venous anomalies are a genetic primer for cerebral cavernous malformations. *Nat Cardiovasc Res*. 2022;1(3):246-252. doi:10.1038/s44161-022-00035-7

38. Rabinovitch M, Guignabert C, Humbert M, Nicolls MR. Inflammation and Immunity in the Pathogenesis of Pulmonary Arterial Hypertension. *Circ Res*. 2014;115(1):165-175. doi:10.1161/CIRCRESAHA.113.301141

39. Fernández-Chacón M, García-González I, Mühleder S, Benedito R. Role of Notch in endothelial biology. *Angiogenesis*. 2021;24(2):237-250. doi:10.1007/s10456-021-09793-7

40. Carlson TR, Yan Y, Wu X, et al. Endothelial expression of constitutively active *Notch4* elicits reversible arteriovenous malformations in adult mice. *Proc Natl Acad Sci*. 2005;102(28):9884-9889. doi:10.1073/pnas.0504391102

41. Krebs LT, Starling C, Chervonsky AV, Gridley T. *Notch1* activation in mice causes arteriovenous malformations phenocopied by ephrinB2 and EphB4 mutants. *genesis*. Published online 2010:NA-NA. doi:10.1002/dvg.20599

42. Krebs LT, Shutter JR, Tanigaki K, Honjo T, Stark KL, Gridley T. Haploinsufficient lethality and formation of arteriovenous malformations in Notch pathway mutants. *Genes Dev*. 2004;18(20):2469-2473. doi:10.1101/gad.1239204

43. Murphy PA, Kim TN, Lu G, Bollen AW, Schaffer CB, Wang RA. *Notch4* Normalization Reduces Blood Vessel Size in Arteriovenous Malformations. *Sci Transl Med*. 2012;4(117). doi:10.1126/scitranslmed.3002670

44. Larrivée B, Prahst C, Gordon E, et al. ALK1 Signaling Inhibits Angiogenesis by Cooperating with the Notch Pathway. *Dev Cell*. 2012;22(3):489-500. doi:10.1016/j.devcel.2012.02.005

45. Moya IM, Umans L, Maas E, et al. Stalk Cell Phenotype Depends on Integration of Notch and Smad1/5 Signaling Cascades. *Dev Cell*. 2012;22(3):501-514. doi:10.1016/j.devcel.2012.01.007

46. Kakuda S, Haltiwanger RS. Deciphering the Fringe-Mediated Notch Code: Identification of Activating and Inhibiting Sites Allowing Discrimination between Ligands. *Dev Cell*. 2017;40(2):193-201. doi:10.1016/j.devcel.2016.12.013

47. LeBon L, Lee TV, Sprinzak D, Jafar-Nejad H, Elowitz MB. Fringe proteins modulate Notch-ligand cis and trans interactions to specify signaling states. *eLife*. 2014;3:e02950. doi:10.7554/eLife.02950

48. Brückner K, Perez L, Clausen H, Cohen S. Glycosyltransferase activity of Fringe modulates Notch–Delta interactions. *Nature*. 2000;406(6794):411-415. doi:10.1038/35019075

49. Benedito R, Roca C, Sörensen I, et al. The Notch Ligands Dll4 and Jagged1 Have Opposing Effects on Angiogenesis. *Cell*. 2009;137(6):1124-1135. doi:10.1016/j.cell.2009.03.025

50. Ehling M, Adams S, Benedito R, Adams RH. Notch controls retinal blood vessel maturation and quiescence. *Development*. 2013;140(14):3051-3061. doi:10.1242/dev.093351

51. Tual-Chalot S, Mahmoud M, Allinson KR, et al. Endothelial Depletion of Acvrl1 in Mice Leads to Arteriovenous Malformations Associated with Reduced Endoglin Expression. Kaartinen V, ed. *PLoS ONE*. 2014;9(6):e98646. doi:10.1371/journal.pone.0098646

52. Baeyens N. Fluid shear stress sensing in vascular homeostasis and remodeling: Towards the development of innovative pharmacological approaches to treat vascular dysfunction. *Biochem Pharmacol*. 2018;158:185-191. doi:10.1016/j.bcp.2018.10.023

Supplementary Material

Materials and Methods

Trial design.
The study was approved by the local research ethics committee (Hospice civils de Lyon, CPP 2021-A01792-39) and by the French Medical Products Agency (ANSM). Written informed consent was obtained from all patients in accordance with national regulations. The trial was conducted in accordance with the principles of the Declaration of Helsinki[1] and Good Clinical Practice guidelines. This trial was registered with the ClinicalTrials.gov Identifier #NCT05632484. (https://clinicaltrials.gov/ct2/show/NCT05632484?cond=HHT&map_cntry=FR&draw=3&rank=12).

Primary endothelial cell isolation
Human umbilical cord blood (UCB) samples (35–110 mL) were collected in heparin-coated syringes from 6 newborns carrying HHT-linked *ALK1* mutations and 3 healthy subjects (Table 1). Isolation of endothelial colony-forming cells (ECFCs) was performed as recommended by the Vascular Biology Standardization Subcommittee[2]. UCB samples were diluted at a 1:3 ratio in RPMI 1640 medium (Gibco) supplemented with 2% fetal bovine serum (FBS; Biosera). Then, mononuclear cell (MNC) fractions were isolated through density gradient centrifugation using 1.077 g/ml Pancoll solution (Pan Biotech) followed by successive washing steps. Finally, MNC were plated in 10µg/mL fibronectin-coated 24-well tissue culture plates in microvascular endothelial cell growth medium-2 (EGM-2 MV; Lonza) with 10% FBS at a density of 5×10^6 cells/cm^2. Cells were incubated in 5% CO_2 at 37°C and the medium was changed daily during the first 7 days and every other day thereafter. Following the first passage, the serum composition was reduced to 5%. ECFCs were used up to 45 days after cord blood processing.
In parallel, human umbilical vein endothelial cells (HUVECs) were isolated, as previously described[3], from the umbilical vein of a number of newborns from which ECFCs were isolated (Table 1).
Human microvascular endothelial cells (HMVECs) were isolated from the explanted lungs of PAH patients during lung transplantation as previously described[4,5] (Table 3).

Cell culture
ECFCs, HMVECs and HUVECs were maintained in EGM-2 MV medium (Lonza). For RNA-sequencing and RT-qPCR, cells were washed twice with phosphate buffered saline (PBS) and were incubated for 18hr in EBM-2 (Endothelial Basal Medium, Lonza) with or without 10ng/ml recombinant human BMP9 (3209-BP, R&D Systems) or recombinant human BMP10 (2926-BP; R&D Systems). Murine NIH-3T3 fibroblasts were maintained in high glucose, sodium pyruvate and GlutaMAX-supplemented Dulbecco's modified Eagle medium (DMEM; Gibco) with 10% FBS (Biosera) and 1% Pen/Strep (Gibco).

Immunofluorescence
For VE-cadherin staining, ECFCs were seeded at confluency in glass Lab-Tek Chamber Slides (Thermo Fisher Scientific), fixed the next day with 4% paraformaldehyde, permeabilized with 0.1% Triton X100 in PBS, saturated with 1% bovine serum albumin (BSA; Sigma-Aldrich) in PBS and incubated at 4°C for 1h with anti-VE-cadherin (1:100; #2158; Cell Signaling Technology). For detection, the cells were subsequently incubated with alexa fluor 488 donkey anti-rabbit IgG (AB_2340620, Jackson ImmunoResearch) for 30min at room temperature. Nuclei were counterstained with Hoechst 33342 (Sigma-Aldrich) and images were acquired using Axio Imager 2 (ZEISS) and analyzed on ZEN Microscopy Software.
Phospho-Smad1/5 (p-Smad1/5) immunostaining in ECFCs was performed as previously described[6]. 20,000 cells/well were seeded in 96-well black cell culture microplate (Greiner Bio-One 655090) for 24h.Then, cells were starved for 2hr in EBM-2 and stimulated for 1hr with 10ng/mL recombinant human BMP9 (R&D Systems). Cells were then fixed with 4% paraformaldehyde, permeabilized with 0.2% Triton X100 in PBS, saturated with 3% BSA in PBS and incubated overnight at 4°C with anti-p-

Smad1/5 (1:800; #9516; Cell Signaling Technology). The cells were subsequently incubated with alexa fluor 488 donkey anti-rabbit IgG (AB_2340620, Jackson ImmunoResearch) and nuclei were counterstained with Hoechst 33342. Images were acquired using IN Cell Analyzer 2500HS widefield fluorescence microscope using a 20X objective. At least 16 different fields were imaged/well and 3 independent experiments were performed with 2 technical replicates each. To allow comparison between wells, the exposure time was kept constant across all wells. The acquired images were then analyzed using InCarta software (General Electrics Healthcare, USA).

Flow cytometry

Cells were seeded 25000 cells/cm^2 and allowed to grow for 48 hours. Cells were detached using trypsin/EDTA solution (CC-5012; Lonza) diluted at 0.000714%, resuspended in 2% BSA in PBS at 1x10^7 cells/mL and incubated with one of the following antibodies: fluorescein isothiocyanate (FITC)–conjugated mouse anti-human CD31 (clone WM59; 557508; BD Pharmingen), FITC-conjugated mouse anti-human CD45 (clone HI30; 560976; BD Pharmingen), phycoerythrin (PE)-conjugated mouse anti-human CD144 (clone 55-7H1; 560410; BD Pharmingen), PE mouse anti-human CD146 (clone P1H12; 550315; BD Pharmingen), unconjugated goat anti-human ALK1 antibody (AF370; R&D Systems) followed by alexa fluor 488 donkey anti-goat IgG (AB_2340430, Jackson ImmunoResearch) or an isotype control antibody. Ten to twenty thousand cells were analyzed on the BD FACSMelody sorter (BD Biosciences) using FCS Express Flow Cytometry Software.

Site-directed mutagenesis

Plasmids encoding the ALK1 mutations understudied were generated by polymerase chain reaction through site-directed mutagenesis of a pcDNA3-1(+) plasmid encoding WT N-terminal HA-tagged ALK1 using the QuikChange Lightning kit (Agilent) following the manufacturer's instructions. All mutated plasmids were verified by full sequencing (Eurofins). Primer sequences used for mutagenesis are listed in Suppl Table 1.

Luciferase reporter assay

NIH-3T3 cells in white 96-well culture plates (Greiner) were transfected in Opti-MEM (Invitrogen) using lipofectamine 2000 (Invitrogen) with 75ng pGL3(BRE)2-luc, 30ng pRL-TKluc and 5ng of plasmids encoding either HA-tagged WT or mutant ALK1 as previously described[7]. Five hours post transfection, cells were stimulated with or without recombinant human BMP9 (100 pg/mL) for 18 hours. For direct luciferase activity measurements in primary ECFCs, the cells were transfected in Opti-MEM using lipofectamine 3000 (Invitrogen) with 40ng pGL3(BRE)2-luc and 60ng pRL-TKluc. Three hours post transfection, ECFCs were stimulated with or without recombinant BMP9 in increasing concentrations (0.2 ng/mL–10 ng/mL) for 6 hours. Firefly and renilla luciferase activities were sequentially measured with twinlite Firefly and Renilla Luciferase Reporter Gene Assay System (Perkin Elmer) using the SPARK multimode microplate reader (Tecan) and final luciferase activities were reported as firefly luciferase activities normalized to renilla luciferase activities.

RNA sequencing and bioinformatic analysis

Cells from each donor were seeded in 3 culture vessels and were stimulated or not overnight with 10ng/ml of BMP9 or BMP10. Stimulations were repeated two or three times for each donor, generating technical replicates. After an overnight stimulation, the cells were trypsinized, spun and frozen as dry pellets at -80°C prior sending to Genewiz (https://www.genewiz.com) for RNA extraction, quality control, library preparation and RNA-sequencing. Mapped reads and sample metadata were imported into R software (version 4.0.3[8]), and loaded in DESeq2 R package (version 1.30.1[9]). Replicates were collapsed using the "collapseReplicates" function from the DESeq2 package. In order to reduce noise, genes that had less than 150 counts across all samples were filtered out. Differential gene expression analysis was performed using the DESeq2 package, and the Wald test was used to determine the significance of $\log_2$ fold change. Pairwise comparisons between conditions, as well as intercept terms for two-factor analysis, were retrieved using the "results" function from the DESeq2 package.

Regularized log transformed data was used to perform Principle Component Analysis (PCA) and to plot expression heatmaps and countplots. Heatmaps were generated using the "ComplexHeatmap" (version 2.6.2[10], R package, and hierarchical clustering was based on Euclidian distance and Complete linkage. Gene set enrichment analysis (GSEA)[11] was performed using the "clusterProfiler" R package (version 3.18.1[12]). The ordering vector for GSEA was based on the stat value of the Wald test. Gene set on which GSEA was based was "Hallmark pathways", obtained from Broad Institutes MsigDB (version 7.5.1[13]). All p-values were adjusted for multiple testing using the Benjamini-Hochberg procedure, to obtain a false discovery rate (FDR). Only protein-coding DEGs are shown in volcano and scatter plots.

RNA extraction and RT-qPCR

Cells were lysed and RNA was extracted using the NucleoSpin RNA kit (Macherey-Nagel) according to the manufacturer's instructions. 1µg RNA was reverse-transcribed using iScript cDNA Synthesis Kit (Bio-Rad) in a T100 thermal cycler (Bio-rad), and quantitative PCR was performed on 1/10 diluted cDNA samples using SsoAdvanced Universal SYBR Green Supermix (Bio-Rad) in a CFX96 Real-Time System, (Bio-Rad). Data analysis was performed with CFX Manager Software V3.1 (Bio-Rad) and relative expression levels were calculated using the delta Ct (ΔCt) method with *HPRT* serving as the housekeeping gene. Alternatively, fold changes in expression levels were calculated using the Livak's ΔΔCt method. Primer sequences used for RT-qPCR are listed in Suppl Table2.

RNA interference

CTL HMVECs (250,000 cells/well in 6-well plates) were transfected using Lipofectamine RNAiMAX Transfection Reagent (2.5µL/well, Invitrogen) with either Silencer Negative Control #1 siRNA (AM4611, Ambion) at a final concentration of 1nM or Silencer Select pre-designed siRNA directed against human ALK1 (siALK1, 4392420, siRNA ID s987, Ambion) at a final concentration of 0.0035nM or 1nM, to induce different degrees of ALK1 silencing. Lipofectamine and siRNA mixes were incubated at room temperature for 20mins followed by cell transfection in Opti-MEM (11058021, Gibco). Five hours later, an equivalent volume to Opti-MEM of EGM-2MV medium with 10% FBS was added per well to obtain 5% final composition. Forty-eight hours post-transfection, cells were stimulated or not with BMP9 10ng/mL for 18hrs to study *LFNG* regulation by BMP9 as a function of ALK1 level.

Supplementary References

1. World Medical Association. World Medical Association Declaration of Helsinki: ethical principles for medical research involving human subjects. *JAMA*. 2013;310(20):2191-2194. doi:10.1001/jama.2013.281053

2. Smadja DM, Melero-Martin JM, Eikenboom J, Bowman M, Sabatier F, Randi AM. Standardization of methods to quantify and culture endothelial colony-forming cells derived from peripheral blood: Position paper from the International Society on Thrombosis and Haemostasis SSC. *J Thromb Haemost*. 2019;17(7):1190-1194. doi:10.1111/jth.14462

3. Garnier-Raveaud S, Usson Y, Cand F, Robert-Nicoud M, Verdetti J, Faury G. Identification of membrane calcium channels essential for cytoplasmic and nuclear calcium elevations induced by vascular endothelial growth factor in human endothelial cells. *Growth Factors*. 2001;19(1):35-48. doi:10.3109/08977190109001074

4. Tu L, Dewachter L, Gore B, et al. Autocrine Fibroblast Growth Factor-2 Signaling Contributes to Altered Endothelial Phenotype in Pulmonary Hypertension. *Am J Respir Cell Mol Biol*. 2011;45(2):311-322. doi:10.1165/rcmb.2010-0317OC

5. Bordenave J, Tu L, Berrebeh N, et al. Lineage Tracing Reveals the Dynamic Contribution of Pericytes to the Blood Vessel Remodeling in Pulmonary Hypertension. *ATVB*. 2020;40(3):766-782. doi:10.1161/ATVBAHA.119.313715

6. Sales A, Khodr V, Machillot P, et al. Differential bioactivity of four BMP-family members as function of biomaterial stiffness. *Biomaterials*. 2022;281:121363. doi:10.1016/j.biomaterials.2022.121363

7. Ricard N, Bidart M, Mallet C, et al. Functional analysis of the BMP9 response of ALK1 mutants from HHT2 patients: a diagnostic tool for novel ACVRL1 mutations. *Blood*. 2010;116(9):1604-1612. doi:10.1182/blood-2010-03-276881

8. R Core Team. *R: A Language and Environment for Statistical Computing*. R Foundation for Statistical Computing; 2022. https://www.R-project.org/

9. Love MI, Huber W, Anders S. Moderated estimation of fold change and dispersion for RNA-seq data with DESeq2. *Genome Biology*. 2014;15(12):550. doi:10.1186/s13059-014-0550-8

10. Gu Z. Complex Heatmap Visualization. *iMeta*. Published online 2022. doi:10.1002/imt2.43

11. Subramanian A, Tamayo P, Mootha VK, et al. Gene set enrichment analysis: A knowledge-based approach for interpreting genome-wide expression profiles. *Proceedings of the National Academy of Sciences*. 2005;102(43):15545-15550. doi:10.1073/pnas.0506580102

12. Yu G, Wang LG, Han Y, He QY. clusterProfiler: an R package for comparing biological themes among gene clusters. *OMICS: A Journal of Integrative Biology*. 2012;16(5):284-287. doi:10.1089/omi.2011.0118

13. Liberzon A, Subramanian A, Pinchback R, Thorvaldsdóttir H, Tamayo P, Mesirov JP. Molecular signatures database (MSigDB) 3.0. *Bioinformatics*. 2011;27(12):1739-1740. doi:10.1093/bioinformatics/btr260

Supplementary Figures

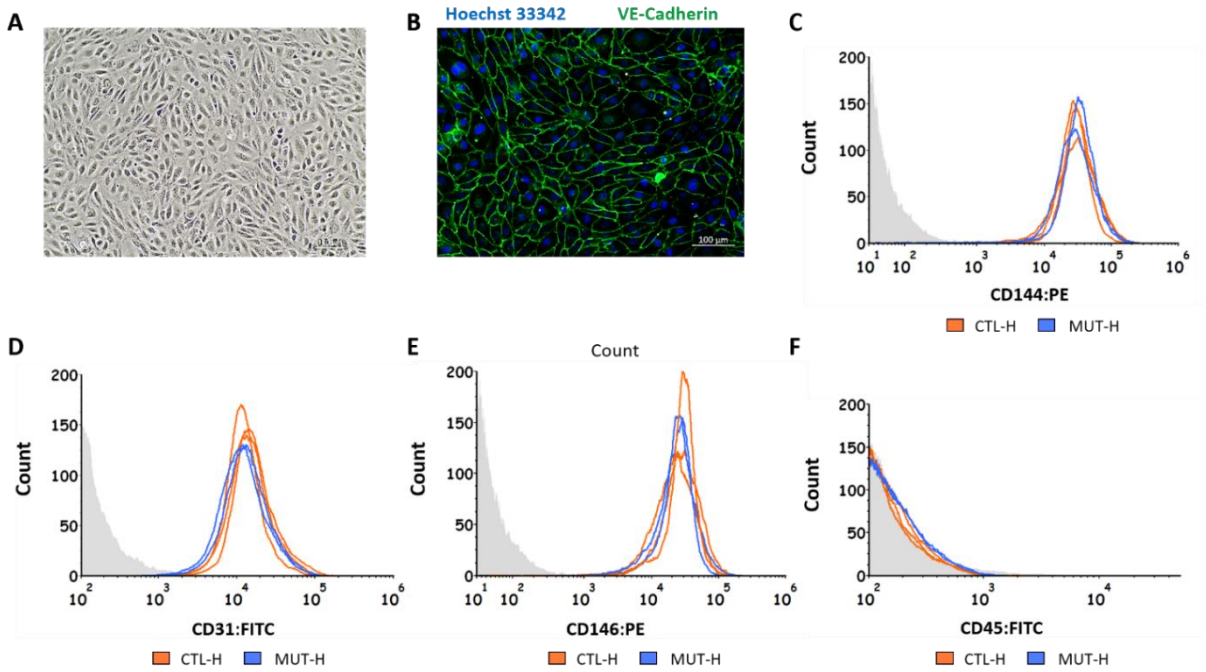

Supplemntary figure 1. Characterization of isolated ECFCs from CTL and *ALK1*-mutated donors

A, Representative phase contrast image of isolated ECFCs displaying the characteristic endothelial cell cobblestone morphology. **B,** Representative immunostaining of the endothelial cell marker VE-cadherin on ECFCs. The nuclei were counterstained using Hoechst 33342. **C-F,** Flow cytometric analysis of surface antigens on ECFCs, showing that the isolated cells are positive for the endothelial cell markers CD144 (VE-cadherin, **C**), CD31 (PECAM-1, **D**) and CD146 (S-Endo 1 antigen, **E**) but not for the leukocyte common antigen CD45 **(F)**. Isotypic CTL is represented in grey, 3 CTL ECFCs in orange and 2 mutated ECFCs (MUT-H1-H2, Table 1) in blue.

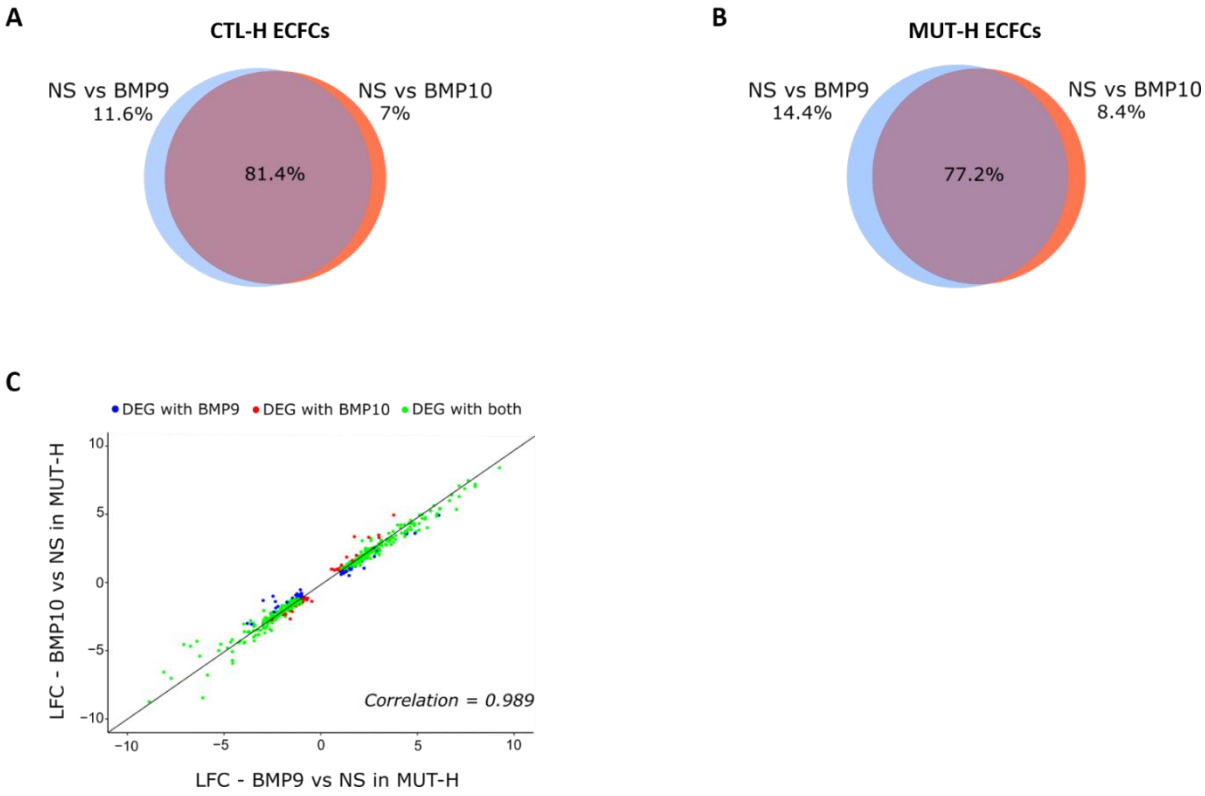

Supplementary Figure 2. BMP9 and BMP10 induce a similar transcriptomic response in CTL and *ALK1*-mutated ECFCs
A, B, Venn diagram demonstrating the percentage of common and specific protein coding DEGs induced by BMP9 and BMP10 vs NS in CTL ECFCs (**A**) and in MUT ECFCs (**B**). **C,** Scatter plot comparing log_2 fold change (LFC) values of DEGs that are regulated in MUT ECFCs by BMP9 vs NS vs those regulated by BMP10 vs NS cells. Pearson correlation is reported.

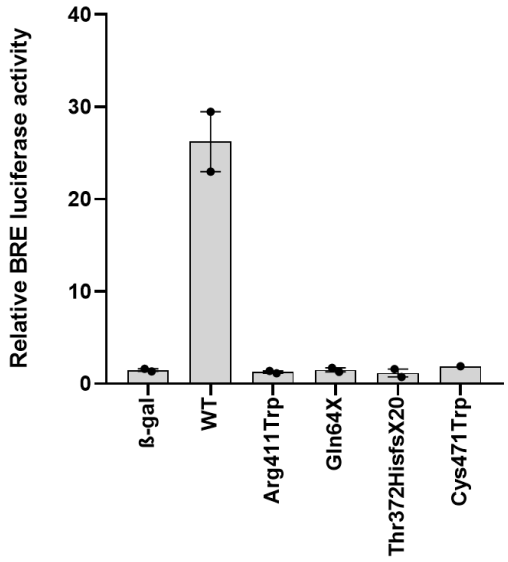

Supplementary Figure 3. BRE luciferase activity of ALK1 mutations identified in ECFCs and HUVECs
Relative BRE (BMP Response Element) luciferase activity measured in NIH-3T3 cells overexpressing either WT or mutant *ALK1* plasmids identified in *ALK1*-mutated ECFCs or HUVECs that are included in different experiments (p.Gln64X: MUT-H3, p.Arg411Trp: MUT-H4, Thr372HisfsX20: MUT-H5, Cys471Trp: MUT-H6, Table 1). Firefly luciferase activities were normalized to renilla luciferase activities. Data shown are mean ± SEM from of 2 independent experiments.

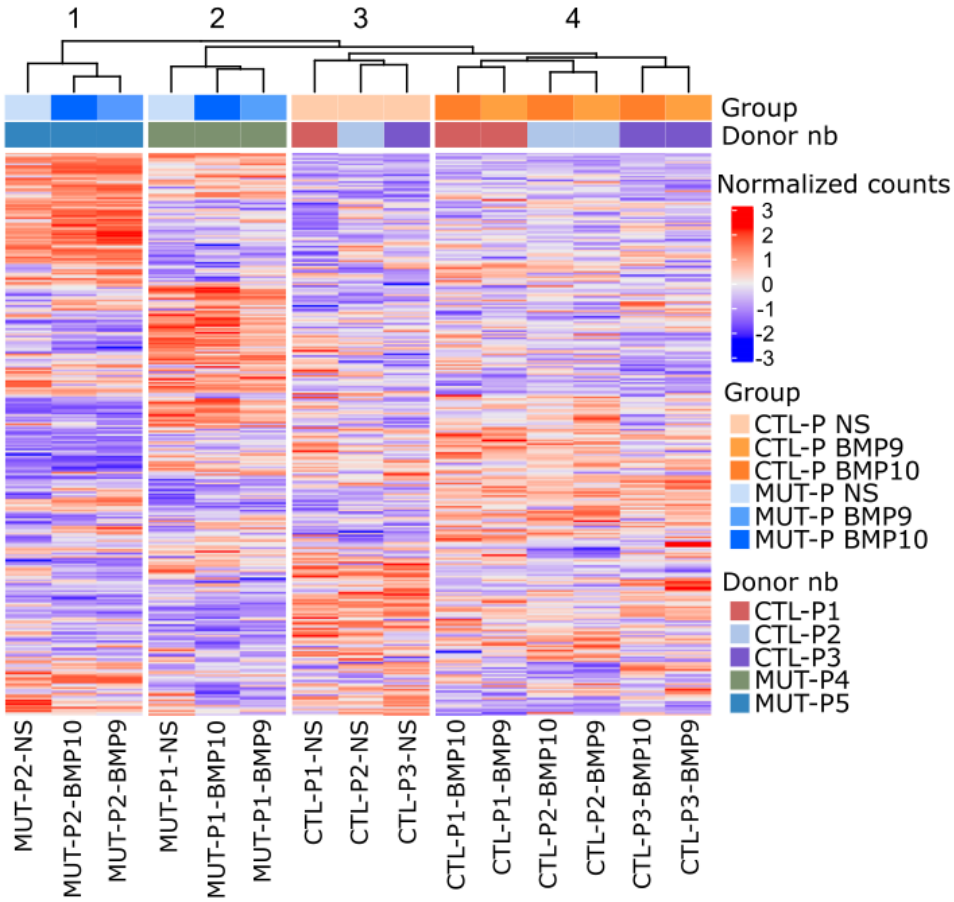

Supplementary Figure 4. Hierarchical clustering of HMVEC transcriptomic data

3 CTL and 2 *ALK1*-mutated (MUT-P1-P2) HMVECs were stimulated or not with BMP9 or BMP10 (10 ng/mL) for 18 hours. The experiment was repeated three times after which bulk RNA-seq analysis was performed. Heatmap demonstrating hierarchical clustering based on Euclidian distance applied on all genes across all groups of samples. The samples are separated into 4 clusters: (1) non-stimulated and stimulated MUT-P2 samples, (2) non-stimulated and stimulated MUT-P1 samples, (3) non-stimulated CTL samples and (4) BMP9 and BMP10-stimulated CTL samples. The color code reflects the expression level of a given gene across different samples, with red signifying higher expression and blue signifying lower expression.

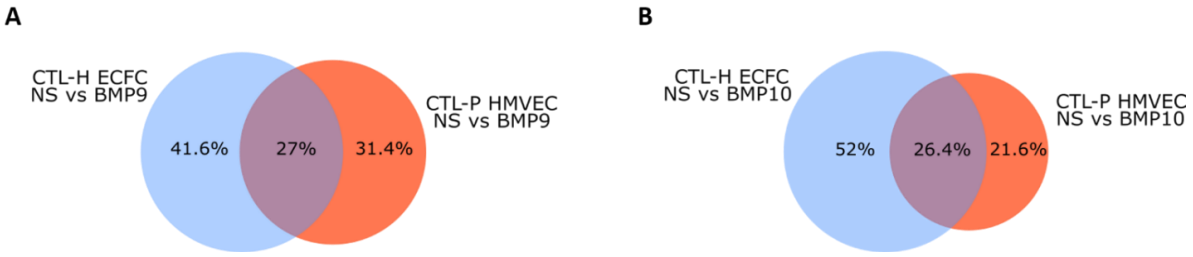

Supplementary Figure 5. BMP9 and BMP10 induce specific transcriptomic changes in CTL ECFCs versus CTL HMVECs
Venn diagrams demonstrating the percentage of common and specific protein coding DEGs between CTL ECFCs and CTL HMVECs in response to BMP9 **(A)** or BMP10 **(B)** vs NS counterparts.

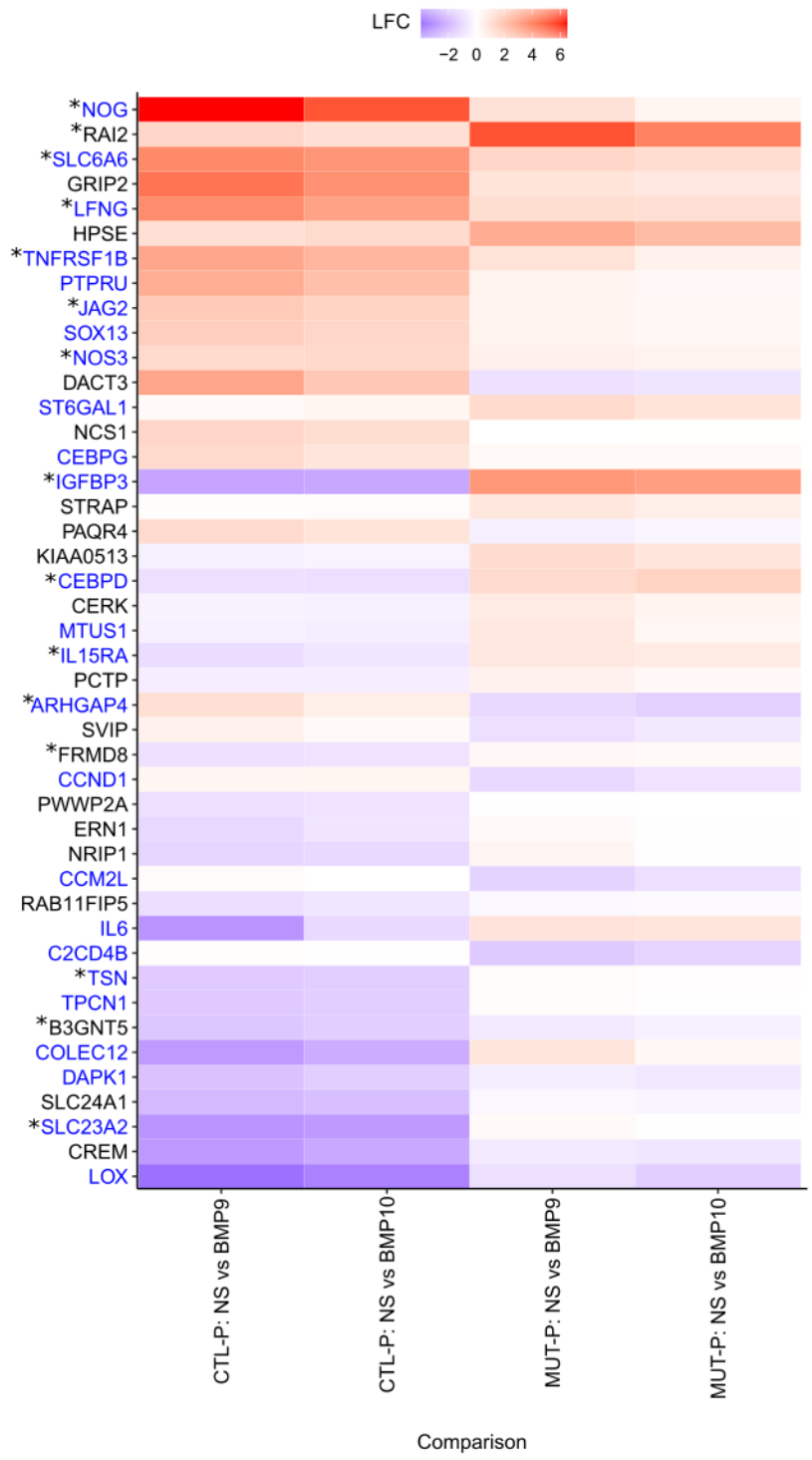

Supplementary Figure 6. Regulation patterns of hits identified by the two-factor analysis in *ALK1*-mutated HMVECs. Heatmap demonstrating the log fold changes of the 44 protein-coding interaction genes, which were identified by the two-factor analysis as significantly differentially regulated by BMP9 or BMP10 between control and *ALK1*-mutated HMVECs. Genes identified as significantly differentially regulated by both BMP9 and BMP10 are marked by an asterisk and those that were selected for validation by RT-qPCR are marked in blue.

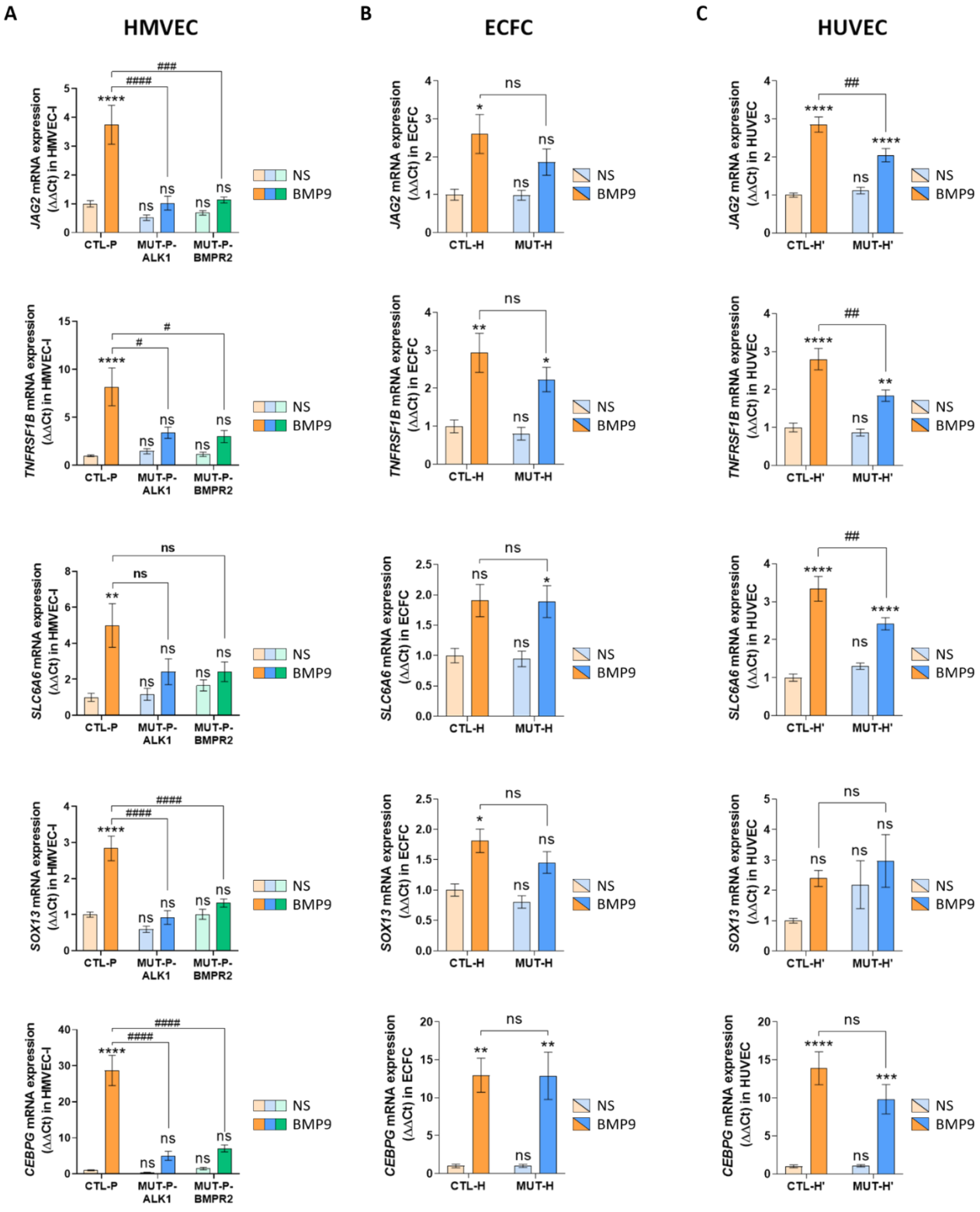

Supplementary Figure 7. RT-qPCR validation of genes identified by two-factor analysis in *ALK1*-mutated HMVECs, ECFCs and HUVECs

RT-qPCR quantification of the mRNA expression levels of *JAG2, TNFRSF1B*, *SLC6A6*, *SOX13* and *CEBPG* performed in 3 CTL, 2 *ALK1*-mutated (MUT-P1-P2) and 3 *BMPR2*-mutated HMVECs (MUT-P3-P5) **(A)**, 3 CTL and 4 *ALK1*-mutated ECFCs (MUT-H1-H4) **(B)** and 3 CTL and 3 *ALK1*-mutated HUVECs (MUT-H'3-H'5) **(C)**. Target gene expression levels are normalized to *HPRT* mRNA expression presented as ΔΔCt compared to mean CTL NS. Data are mean ± SEM of at least 3 independent stimulations. Two-way Anova followed by Sidak's multiple comparisons test were used for statistical analyses. ns: non-significant, *P<0.05, **P<0.01 and ****P<0.0001 vs NS and #P<0.05, ##P<0.01, ###P<0.001 and ####P<0.0001 vs CTL.

Supplementary Tables

Supplementary Table 1. Primers allowing the generation of mutant *ALK1* constructs by site-directed mutagenesis-associated PCR designed using the QuickChange Primer Design Program (Agilent)

GenBank sequence accession number	mutation	Forward (5'-3')	Reverse (5'-3')
NM_001077401.1	p.Trp141X	CGTCGGACATGCTACAGGCCCAGGACAC	GTGTCCTGGGCCTGTAGCATGTCCGACG
	p.His280Asp	GAGCCGTGCTCGTCGTAGTGCGTGATG	CATCACGCACTACGACGAGCACGGCTC
	p.Gly319Arg	GTTTGCCCTGTGTACGGAAGATCTCCACGTG	CACGTGGAGATCTTCCGTACACAGGGCAAAC
	p.Arg484Trp	GTGTCTTCTTGATCCACAGCGCGGTGAGTCG	CGACTCACCGCGCTGTGGATCAAGAAGACAC
	p.Gln64X	CCCGATGTTCCTAGGGGTGCCTCCC	GGGAGGCACCCCTAGGAACATCGGG
	p.Arg411Trp	ATTCACGATGGTCCAGCGGGCAATCTCCC	GGGAGATTGCCCGCTGGACCATCGTGAAT
	p.Thr372HisfsX20	GTACCGCTTGGTGCCCCACTCTCGGGT	ACCCGAGAGTGGGGCACCAAGCGGTAC
	p.Arg411Gln	CATTCACGATGGTCTGGCGGGCAATCTCC	GGAGATTGCCCGCCAGACCATCGTGAATG
	p.Cys471Trp	GGGTTTGGGTACCACCACTCCCGCATCAT	ATGATGCGGGAGTGGTGGTACCCAAACCC

Supplementary Table 2. Primers for quantitative RT-qPCR designed using Primer-Blast on GenBank sequences. All listed primer pairs, except for those of *SLC6A6*, are separated by at least one intron on the corresponding genomic DNA or span an exon-exon junction.

Gene	GenBank sequence accession number	Forward (5'-3')	Reverse (5'-3')
ID1	NM_181353.3	CTGCTCTACGACATGAACGGC	TGACGTGCTGGAGAATCTCCA
LFNG	NM_001040167	CTTCATCGCTGTCAAGACCAC	GCCTCATCTTCCCCGTCAGT
JAG2	NM_002226	GTCGTCATCCCCTTCCAGTTC	ATTCGGGGTGGTATCGTTGT
TNFRSF1B	NM_001066	CATGCCGGCTCAGAGAATAC	CTCACAGGAGTCACACACGG
SLC6A6	NM_001134367	ATGGGTGATGCTGAGAGCTG	CGCGAAGGAAGCGGTAATTT
SOX13	NM_005686.3	AGAAGTGGTGCCAGCCATAG	TCTGCTAGGCTCTCTTGGGT
CEBPG	NM_001252296.2	CACTTCGCAGGCATAGTTGG	TCTCCCTTGCCAACACAGAA
ACVRL1	NM_001077401.1	CACGGACTGCTTTGAGTCCT	TCTGCTGATCCACACACACC

Preliminary results

1. Characterization of LFNG regulation dynamics by BMP9/BMP10 in ECs

Because the transcriptomic analysis and the corresponding qPCR validations were all performed on cells treated with BMP9/BMP10 for 18hrs, we wondered whether *LFNG* is regulated by BMP9 at earlier time points. To monitor *LFNG* mRNA regulation by BMP9 with time, a single stimulation kinetics with 10ng/mL BMP9 was performed on CTL and ALK1-mutated ECFCs (3 CTLs and 4 MUTs), HUVECs (3 CTLs and 3 MUTs) and HMVECs (3 CTLs and 2 MUTs) for at least 5 time points: 1, 2, 4, 8 and 18hrs. The general regulation profile of *LFNG* mRNA was similar in CTL ECFCs, HUVECs and HMVECs, which all displayed an early stimulation peak after 1 or 2hrs of stimulation followed by another gradual increase in expression level at later time points (Figure 26A-C). In case of ECFCs, a peak induction of 5.6 folds was reached at 2hrs, and the mRNA expression level started increasing again after 4hrs, reaching a maximum of 6.2 folds at 18hrs (Figure 26A). For both HUVECs and HMVECs, the initial peak was reached already after 1hr, with a similar fold change to ECFCs in HUVECs (6 folds), but with a higher induction in HMVECs reaching 10.7 folds (Figure 26B,C). The expression level in HUVECs then started to increase again but weakly after 8hrs, while in HMVECs the 2nd increase started immediately after 2hrs, reaching a maximum of 14 folds at 8hrs and decreasing afterwards (Figure 26B,C). Thus, while differences in the speed and level of induction exist between the 3 EC types, *LFNG* in all of them seems to have an oscillating expression pattern, in accordance with its reported regulation pattern in presomitic mesoderm that is essential for proper somitogenesis[378]. In ALK1-mutated ECFCs, *LFNG* mRNA regulation

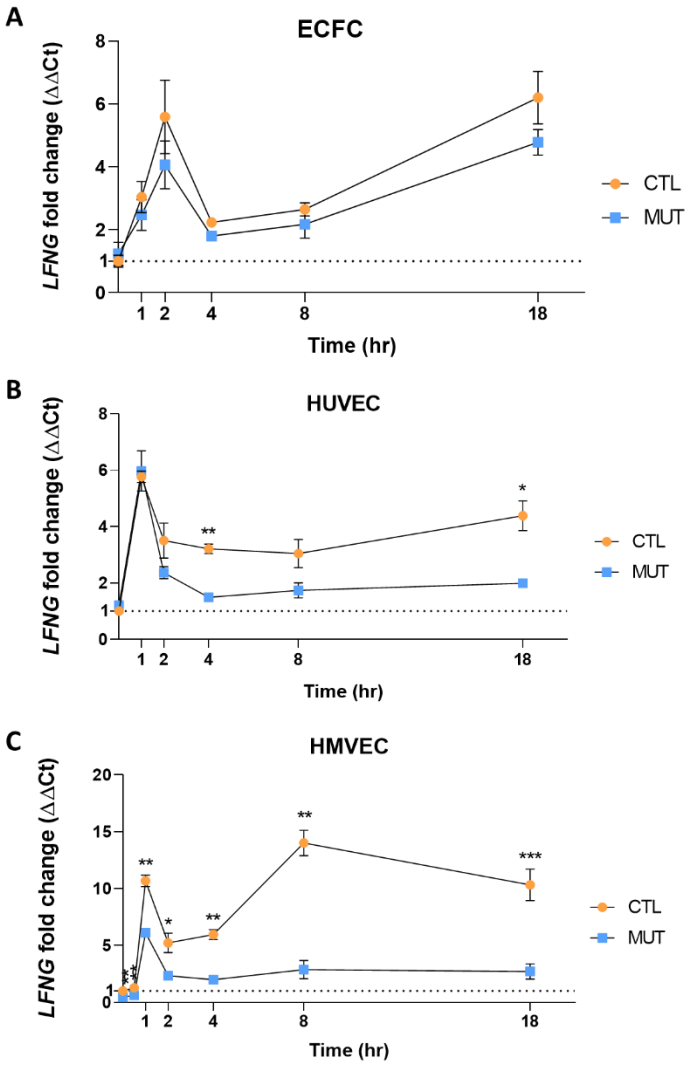

Figure 26. Characterization of LFNG regulation dynamics in different CTL and ALK1-mutated EC models. *RT-qPCR quantification of the mRNA expression level of LFNG in CTL and ALK1-mutated ECFCs (A), HUVECs (B) and HMVECs (C) in a kinetics BMP9 stimulation from 0.5 or 1hr until 18hrs. LFNG mRNA expression level is normalized to HPRT mRNA expression and presented as ΔΔCt compared to mean CTL NS at the earliest time point. Data shown are mean ± SD for cells from multiple donors. Two-way Anova followed by Sidak's multiple comparisons tests were used for statistical analysis. *p<0.05, **p<0.001 and ***p<0.0001.*

pattern at the different time points mirrored that in CTL ECFCs, but with a slightly weaker induction than CTLs. Mutated HUVECs were capable of inducing normal upregulation of *LFNG* at the early 1hr peak, while mutated HMVECs already displayed a significantly weaker increase of 6.1 folds at 1hr compared to their respective CTLs. *LFNG* induction then significantly dropped at 4 and 2hrs in mutated HUVECs and HMVECs respectively, followed by only minor inductions at the following time points. These preliminary results indicate that the cyclic regulation of *LFNG* was almost lost in mutated HMVECs. The oscillating pattern could also be impaired in mutated HUVECs, but since CTL HUVECs displayed slower induction in the second cycle compared to CTL HMVECs, longer time points would help uncover whether the induction level in mutated HUVECs will have the chance to rise again or not.

2. *Assessment of the p-Smad1/5 response to BMP9/BMP10 in ALK1-mutated ECs under flow*

Given the role of fluid shear stress (FSS) in potentiating Smad1/5/8 response to soluble BMP9[171], and since BMP9 stimulation coupled to FSS was shown to induce some unique transcriptomic changes not induced by BMP9 at static conditions[361], we wondered whether ALK1-mutated (MUT) ECFCs might respond differently to BMP9 stimulation under flow conditions compared to CTLs. Hence, as a preliminary experiment, the p-Smad1/5 response to BMP9 of ECFCs from 2 CTLs (CTL-H2 and CTL-H3) and 2 MUTs (MUT-H1 and MUT-H2), which were all included in the RNA-seq analysis, were assessed under FSS conditions by immunofluorescence. The experiment was carried out in microfluidic chips placed on a lab rocker that was set to 25 tilting degrees, performing 1 round per minute.

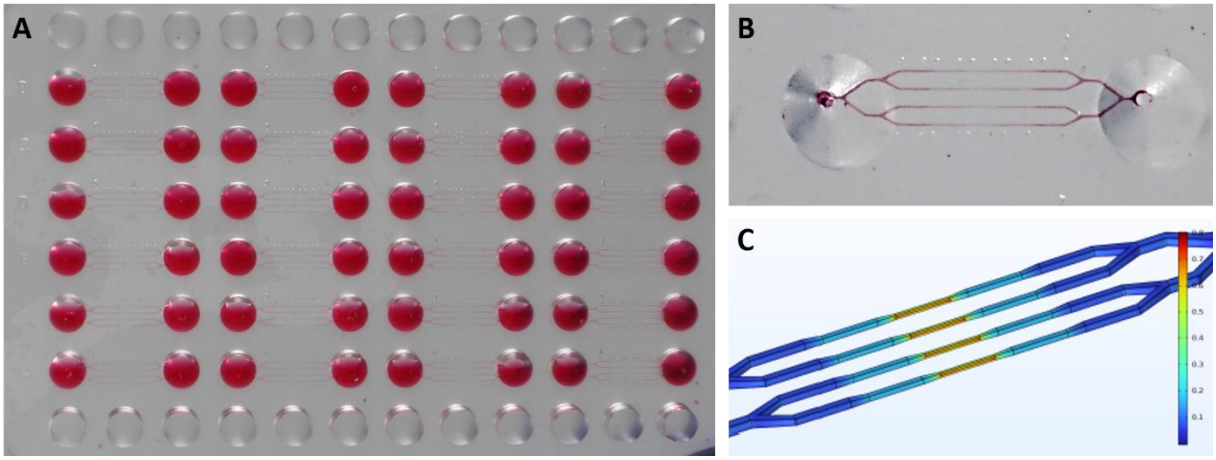

***Figure 27. Presentation of the microfluidic device used to assess BMP9 response under laminar flow**. **A**, Full microfluidic plate showing 24 separate units filled with cell culture medium. **B**, Zoom in into one unit that was previously filled with medium showing the 2 medium inlets at the ends and the 4 microfluidic branches. **C**, Graphical model of one unit highlighting the three main areas with different diameters that inversely correlate with shear stress levels. Approximate shear stress levels (in Pa) are indicated by the color code. Images provided by Tuan Nguyen from Finnadvance.*

The used microfluidic chips were fabricated by our collaborators, Finnadvance (Oulu University) within the MSCA international training network VA Cure, and this experiment was performed in our laboratory during a secondment of PhD student Tuan Nguyen from Finnadvance. The microfluidic device contains 24 separate culture units, each composed of a 4-branch microchannel connecting two media reservoirs (Figure 27A,B). The 4 branches within the same unit serve as technical replicates. Each branch has a conical shape with a varying diameter along its length (Figure 27C) ranging from 190µm (dark blue, at the 2 ends), 140µm (cyan) to 70 µm (orange, in the center). This difference in diameter generates different FSS

levels ranging from approximately 0.1Pa or 1dyn/cm^2 at the widest part (at the ends) to 0.65Pa or 6.5dyn/cm^2 at the narrowest central part (Figure 27C). CTL or MUT ECFCs were seeded in triplicates in fibronectin-coated (100µg/mL) units at a density of 120,000cells/unit in full EGM2 medium and were incubated in 5% CO2 at 37°C on a rocker allowing bi-directional flow for few days with daily change of medium. Four days later, migrating and proliferating ECs had covered the full length of the branches and formed hollow tubular structures. At this point, the cells were starved for 2hr in serum and growth-factor free EBM2, followed by 1hr stimulation (or not) with BMP9 10ng/mL, fixation by 4% paraformaldehyde and p-Smad1/5 immunostaining as described in the supplementary material of the manuscript draft. Cells were co-stained with anti-VE-cadherin (in-house mouse monoclonal antibody generously provided by Stephanie Bouillot) to label EC junctions, and nuclei were counterstained with 4',6-diamidino-2-phenylindole (DAPI). Image acquisition using CX7 microscope (thermofischer) and fluorescence quantification were performed by Emmanuelle Soleilhac at the CMBA platform* in CEA Grenoble. Both the narrowest and widest segments of the branches were assessed in order to capture the impact of 2 different FSS levels on the p-Smad1/5 response of ECs (Figure 28). Eight to 12 different fields were analyzed per donor and branch diameter, and results are presented as a function of branch diameter (Figure 29).

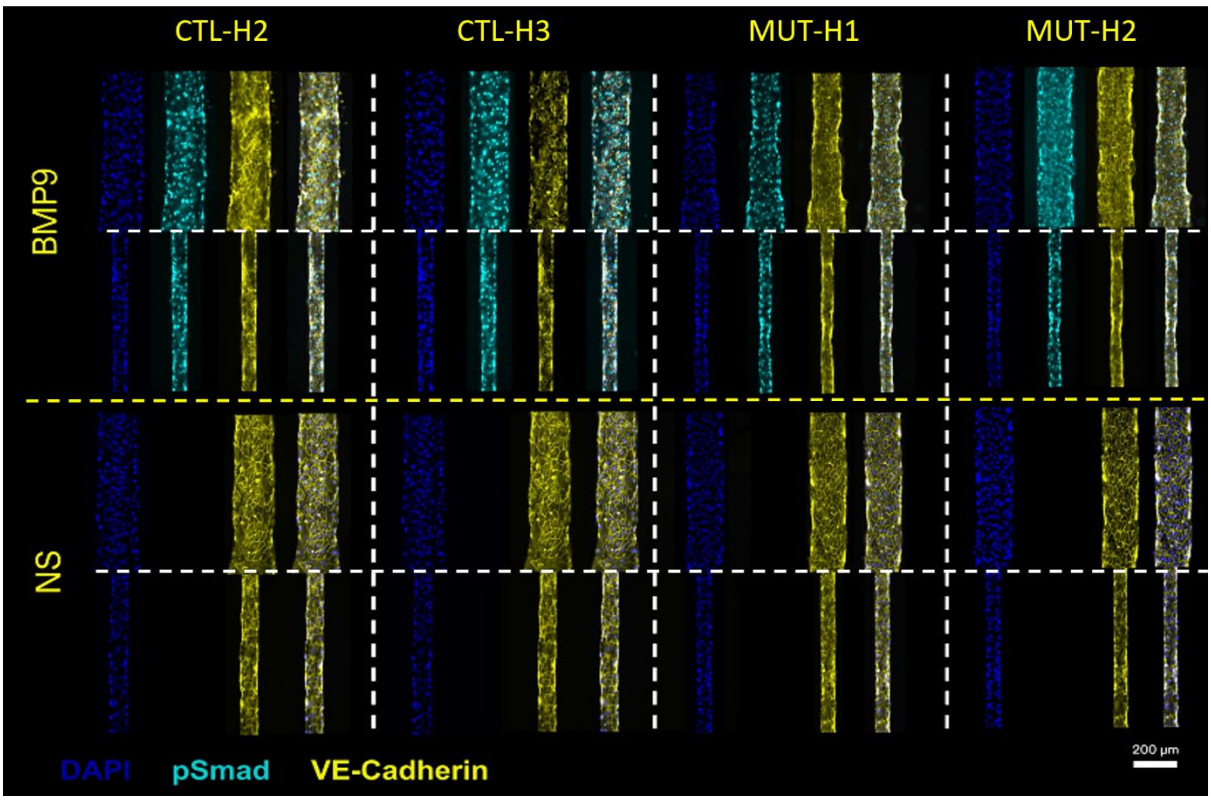

Figure 28. Smad1/5 response of BMP9-stimulated CTL and ALK1-mutated ECs under flow. *Representative p-Smad1/5 and VE-cadherin immunostainings in non-stimulated (NS) or BMP9-stimulated CTL and MUT ECFCs under flow are shown in 2 microfluidic segments of different diameters.*

As expected, in both the narrow and wide segments, BMP9 induced the phosphorylation of Smad1/5 in the 2 CTLs (Figure 28 and 29A,B). Interestingly, mean BMP9-induced p-Smad1/5 levels in each of the 2 CTLs were significantly higher in the narrow segment (higher FSS) compared to the wider one (lower FSS; Figure 29C). While BMP9 induced MUT-H2 cells carrying a missense *ACVRL1* mutation showed comparable p-Smad1/5 levels after BMP9 stimulation to the 2 CTLs, MUT-H1 cells with a nonsense mutation had a very mild, yet

**Part of this work has been performed at the CMBA platform - IRIG-DS-BGE-Gen&Chem-CMBA, CEA-Grenoble, F-38054 Grenoble, (a member of GIS-IBISA and ChemBioFrance infrastructure) supported by GRAL, a program of the Chemistry Biology Health Graduate School of Université Grenoble Alpes (ANR-17-EURE-011,12003).*

significant, induction of Smad1/5 phosphorylation in both segments (Figure 29A,B). Because of this lower induction in MUT-H1, the average p-Smad1/5 levels in BMP9-stimulated MUT ECFCs was lower than that of CTLs in both segments (Figure 29C,D).

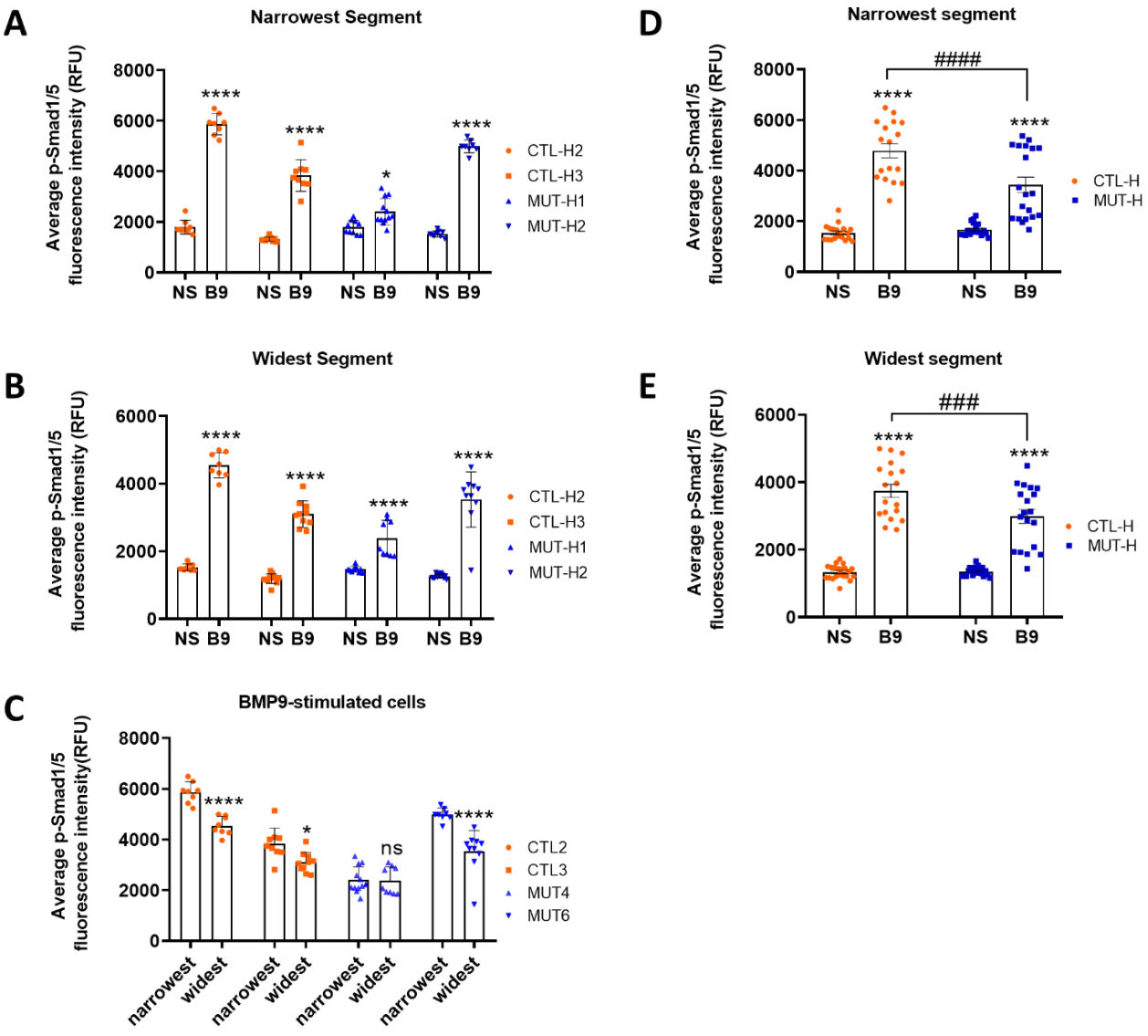

Figure 29. Effect of ALK1 heterozygosity on p-Smad1/5 response to BMP9 under flow. A-C*, Average p-Smad1/5 levels in non-stimulated (NS) and BMP9-stimulated (B9) CTL (n=2) and ALK1-mutated ECFCs (n=2) in the narrowest (**A**) and widest (**B**) segments of the microfluidic branches and side by side comparison of BMP9-induced p-Smad1/5 levels between the 2 different segments for each donor (**C**). **D-E,** Graphs representing mean p-Smad1/5 as a function of ALK1 genotype in the narrowest (**D**) and widest segments (**E**). Data shown are mean ± SD and each point corresponds to one field. Two-way ANOVA followed by Sidak's multiple comparisons tests were used for statistical analysis. ns: non-significant, *P<0.05, ###P<0.001 and ****/####P<0.0001.*

This indicates that FSS might uncover impairments in ALK1-mutated cells that are not evident under static conditions. Nevertheless, no solid conclusions must be made yet, as this experiment was performed only once and was intended to be a trial for the cell seeding and staining steps and for optimizing the parameters for automated image acquisition. Accordingly, several images had suboptimal resolution.

3. Uncovering new functions of BMP9 and BMP10 using transcriptomic data

The main findings of this project have been based on differential expression analyses of the 2 RNA-seq studies in CTL vs ALK1-mutated EC. This kind of analysis provides information on all transcriptional changes surpassing specified fold change and statistical thresholds. Nevertheless, additional valuable information can be extracted from transcriptomic data using enrichment analysis from CTL ECs stimulated with BMP9 or BMP10. We aim to exploit the generated transcriptomic data on CTL ECFCs and CTL HMVECs upon stimulation with BMP9 and BMP10 to better characterize the functions of these 2 ligands in ECs using gene set enrichment analysis. For that, several databases can be used that provide complementary information on the enriched gene sets, including the three gene ontology (GO) categories biological process (BP), molecular function (MF) and cellular component (CC). Some databases like Kyoto Encyclopedia of Genes and Genomes (KEGG) and wikipathways can also be used to provide information on enriched pathways based on transcriptional changes.

With the help of bioinformaticians, I have started performing GSEA using GO BP database on CTL ECFCs or HMVECs upon stimulation with BMP9 or BMP10. The performed analysis is not confined to DEGs identified by the differential expression analysis, but also takes into account genes with mild changes not reaching the ser LFC or statistical thresholds. Due to the high redundancy in the BP database, instead of highlighting a few enriched gene sets that give an overview of the most important functions or pathways modulated by BMP9 and BMP10, more than a thousand significantly enriched gene sets have been identified for each comparison. To overcome this high redundancy in gene ontologies and improve the interpretability of the data, two measures were taken. First, instead of using the full GO resource, GO slims database was used to perform the GSEA. GO slims are cut-down versions of the GO ontologies that contain a subset of the terms from the GO resource and give a broad overview of the ontology content without the details of the specific, fine-grained terms. This step already reduced the number of significant gene sets to a maximum of 400 in each of the 4 comparisons. Second, significantly enriched gene sets related to each other were grouped together into clusters by means of semantic similarities that are based on tree-like structure, meaning that GO terms that are close neighbors on the hierarchical tree are grouped together. For example, mitotic nuclear division, sister chromatid segregation, G2/M transition of mitotic cell cycle and around 70 more related gene sets were clustered together automatically. Following this automatic clustering by the bioinformaticians, I performed additional fine-tuning by manually joining together clusters that have a similar biological significance and providing relevant titles for all clusters. After that, I manually compared all positively and negatively enriched clusters identified in the 4 following comparisons: CTL ECFCs BMP9 vs NS, CTL ECFCs BMP10 vs NS, CTL HMVECs BMP9 vs NS and CTL HMVECs BMP10 vs NS. The identification of a specific cluster in two different EC types and by both BMP9 and BMP10 adds more power to the analysis and confidence in the results. The positively and negatively-enriched clusters that have been repeatedly identified in multiple comparisons are shown in Table 2. An enriched gene set is said to be positively or negatively enriched when the majority of genes belonging to this set are respectively upregulated or downregulated. Nevertheless, this sense of enrichment shouldn't be directly linked to an increase or decrease of a specific activity, since the upregulated genes in a positively enriched gene set for example might be inhibitors of this

pathway or function. All in all, the GSEA analyses highlighted the involvement of BMP9 and BMP10 in regulating several key processes such as cell growth and cell cycle, cell-cell and cell-matrix adhesion, actin cytoskeleton organization, lipid metabolism, and transport of various ions and molecules including carboxylic acids, proteins and carbohydrates. In addition, these analyses linked BMP9/10 signaling to several other pathways, notably Notch, Wnt, NF-κB and ERK signaling pathways.

Table 2. List of positively and negatively-enriched clusters of BP gene ontology terms that have been repeatedly identified the different EC models and under BMP9 and BMP10 stimulations

		ECFC		HMVEC	
	Cluster name	**BMP9 vs NS**	**BMP10 vs NS**	**BMP9 vs NS**	**BMP10 vs NS**
positively enriched	BMP signaling pathway	x	x	x	x
	Biomineralization	x	x	x	
	Wnt signaling pathway	x	x	x	x
	Inorganic ion homeostasis	x	x	x	x
	Cell Growth	x	x	x	x
	ERK1 and ERK2 signaling pathway	x	x	x	x
	Lipid metabolism	x	x	x	x
	Carboxylic acid transport	x	x	x	x
	Notch signaling pathway	x	x	x	
	Cell migration	x	x		
	Protein metabolism	x	x	x	x
	Glycoprotein metabolism	x	x		
	Vesicle transport	x	x		
	Carbohydrate transport	x	x		
	Response to steroid hormone			x	x
negatively enriched	Actin cytoskeleton organization	x	x	x	x
	NF-kappaB signaling	x	x	x	x
	Activation of immune response	x	x	x	x
	Cell-matrix adhesion	x	x	x	x
	Cell-cell adhesion	x	x	x	x
	Cell cycle	x	x		
	Cilium organization	x	x		
	Regulation of apoptosis	x	x		
	Nucleotide metabolism	x	x		
	G protein-coupled receptor signaling pathway	x	x		

x sign marks an enrichment of a BP cluster in a particular condition. NS: non-stimulated

Discussion

This section is dedicated to elaborate some points that haven't been brought up in the discussion section of the paper and to further develop some others that had been briefly discussed.

1. Discussion on technical points

1.1. Choice of ligand

Since BMP9 and BMP10 are the only identified ALK1 ligands[131,133], this project addressed the transcriptomic response of CTL and ALK1-mutated ECs to both BMP9 and BMP10 (individually) instead of focusing on one of them. While establishing the experimental design at the start of my PhD, the studies by Morikawa et al and Long et al were, to the best of my knowledge, the only two transcriptomic studies assessing the global gene regulation by BMP9 in ECs, and no studies were performed using BMP10[113,159]. It was thus interesting to include BMP10 and provide a side-by-side comparison of these two ligands that share high sequence similarity, have different binding affinities to the type II receptors and display both redundant and specific roles *in vivo*.

1.2. Stimulation duration

The 2 aforementioned studies assessed gene regulation by BMP9 after 2 or 4hrs of stimulation[113,159]. While this stimulation is sufficient for many direct targets, such as *ID1 and ID2*, other genes, such as *CXCL8* (IL-8) and *SELE* (E-selectin), require a longer period to display changes in mRNA expression level[152]. Hence, to capture some early and late responders and to complement already published microarray data, we assessed gene regulation after an overnight (18hr) stimulation with BMP9 or BMP10. A limitation of this late time point is that mRNA levels of some early responders might have normalized back to the basal levels and would thus be missed. In addition, some genes might be differently, even inversely regulated at different time points. Therefore, the ideal scenario would be to perform a kinetics transcriptomic study, but this would be cumbersome given the high number of conditions analyzed here. Nevertheless, in the recent study by Szulcek et al described in Chapter 5, the authors compared CTL to PAH-derived HMVECs stimulated with BMP9 for either 90mins or 24hrs and found that after 90mins stimulation 55.9% the DEGs identified in CTLs are shared with patient cells, while after 24hrs this number decreased to 4.5%[347]. This indicates that more information on dysregulated pathways or functions could potentially be derived from longer stimulation periods.

1.3. BMP dose

The concentration of BMP9 or BMP10 used in this work (10ng/mL) is higher than what was utilized by other groups[113,159,347,360]. While lower concentrations, such as 1ng/mL, are enough to induce a strong phosphorylation of Smad1/5[133], they might not be sufficient for inducing transcriptional changes in some target genes. For example, a 1ng/mL dose of BMP9 can

upregulate *SMAD6* expression, but not *EFNB2*, while a 10ng/mL further increases *SMAD6* and induces *EFNB2* expression (data not shown). Therefore, it seems that higher BMP9/10 concentrations might allow the identification of more targets. It was previously reported that BMP9, but not BMP10, can bind and activate ALK2 in mesenchymal stem cells, but with a weaker affinity than ALK1[133]. Using 10ng/mL BMP9 might thus activate ALK2 in ECs[360,379]. However, since no DEGs were identified between BMP9- and BMP10-stimulated CTL ECFCs, and only 3 were identified in HMVECs, ALK2 activation by BMP9, if any, doesn't seem to have a considerable effect on the BMP9-induced transcriptional regulation. Another limitation of this dose is that it might induce Smad2 phosphorylation, as was shown in HPAECs starting from 1ng/mL BMP9[152]. Nevertheless, the 10ng/mL dose is physiologically relevant, as it falls within the normal 2 to 12ng/mL range of circulating active BMP9 that was determined by our group using human sera and plasma samples[157]. In addition, with respect to comparisons between CTL and ALK1-mutated ECFCs, we later showed using BRE luciferase assay that ALK1-mutated cells respond similarly to CTLs even at lower BMP9 concentrations.

1.4. Number of samples

A limitation of our work was the relatively low number of samples analyzed by RNA-seq, which was 3 CTLs and 2 ALK1-mutated in each study. A higher number of samples would have clearly provided more statistical power, but it would have taken me too much time to have access to more samples. In case of ECFCs, since these cells were isolated from the cord blood of newborns, we were limited by the number of pregnant couples including an HHT patient in nearby cities. Additionally, as HHT is an autosomal dominant disease, each newborn would have only a 50% chance to inherit the HHT-causing mutation, and not all acquired blood samples give rise to EC clones. Thus, the RNA-seq study on ECFCs was launched with 3 CTLs and 2 MUTs, as no HHT childbirths were scheduled in the upcoming months of my PhD. Concerning the PAH-derived HMVECs, the two patients from whom the cells were isolated were the only 2 HPAH patients identified in France carrying an *ACVRL1* mutation that had undergone lung transplantation. Nevertheless, for each of the RNA-seq studies, the BMP9 and BMP10 stimulations (along with the non-stimulated CTL) were repeated 3 times for most samples, and twice for some, in order to generate technical replicates. Expression data from these technical replicates were then collapsed, and averaged values were used for differential expression analysis. Moreover, all qPCR validations for RNA-seq data were performed on a larger number of MUT ECFC samples, since more were isolated in the subsequent year, and HMVECs were corroborated with BMPRII-mutated HMVECs from 3 PAH patients.

2. Discussion on specific analyses

2.1. BMP9 vs BMP10

Our findings indicate that BMP9 and BMP10 induce highly similar transcriptomic regulations in both ECFCs and HMVECs, with or without ALK1 mutations. Although BMP9 and BMP10-induced DEGs did not completely overlap, LFCs of genes regulated by each ligand were very highly correlated, with Pearson correlation coefficients approaching 1. This implies that the non-overlapping DEGs obtained with each ligand do have similar regulation patterns by both

ligands, but they might not have reached the LFC or statistical threshold with one of the two ligands. The high dose of BMP9 and BMP10 used might have theoretically masked some differences in gene regulation between the 2 ligands due to differences in their binding affinities to different type II receptors[140]. However, this is unlikely to be the case since the recent study by Salmon et al (2020) similarly showed no differentially expressed genes between BMP9- and BMP10-stimulated CTL PAECs at the low dose of 0.3ng/mL[360].

2.2. Two-factor analysis

Differential expression analysis comparing CTL to MUT HMVECs at the basal, BMP9-stimulated and BMP10-stimulated states identified respectively 1261, 1262 and 1164 DEGs. The DEGs identified between CTLs and MUTs in the stimulated states could be attributed to different causes. Some of these DEGs might reflect impaired transcriptional regulation by BMP9 or BMP10 in MUTs compared to CTLs, which are interesting for understanding the effect of the ALK1 mutation on gene regulation. In contrast, others might not be targets of BMP9/10, but appeared as DEGs between CTLs and MUTs at the stimulated state because they were already DEGs at the basal level and the stimulation had little or no effect on their levels. The classical differential expression analysis normally used to compare two conditions with one variable cannot distinguish DEGs belonging to the two aforementioned cases from each other. Therefore, we utilized a more advanced differential expression analysis, called two-factor analysis that is specifically tailored to handle two variables simultaneously, in order to take into account the 2 variables of this study, namely the ALK1 genotype and the BMP stimulation. This kind of analysis has been previously applied in few transcriptomic studies[380–383]. The two-factor analysis pointed out respectively 44 and 15 protein-coding genes that were significantly differently regulated by BMP9 and BMP10 in MUTs compared to CTLs, coined “interaction term genes”. Then, plotting the normalized counts of these genes on countplots (as for *LFNG* in Figure 5C of the results section) helps illustrate the direction of regulation of every interaction term gene in each individual CTL or MUT and the difference in this regulation amplitude between CTLs and MUTs, regardless of their initial basal levels. Based on the two-factor analysis results and by examining all count plots of the identified interaction term genes, 25 were selected for individual validation using qPCR on independent stimulations of CTL, ALK1-mutated and BMPR2-mutated HMVECs, and 24 were confirmed to be significantly different using Two-way ANOVA, highlighting the robustness of the two-factor analysis. It is noteworthy that all 15 interaction term genes identified in BMP10-stimulated cells overlapped with those identified in BMP9-stimulated cells. The remaining BMP9-specific genes revealed very similar profiles in BMP10-stimulated cells in countplots, but probably did not reach statistical significance by two-factor analysis due to some variations between samples of the same group.

3. General discussion of main findings

3.1. Challenging the haploinsufficiency model

The major finding of the current work is that ALK1-mutated ECFCs isolated from newborn HHT donors have similar Smad1/5 activation and transcriptomic responses to BMP9/10 compared

to CTLs, despite the decrease in cell surface ALK1 levels. At first glance, these findings seemed contradictory to a previous study by our group reporting suppressed BRE luciferase activity in 3T3 mouse fibroblasts overexpressing a mix of WT and mutated ALK1 variants[384]. 3T3 cells co-transfected with 0.5ng expression vector coding WT ALK1 and 0.5ng of vectors coding various mutated ALK1 variants showed luciferase activities lower than cells transfected with 1ng WT, but equivalent to those transfected with 0.5ng only. Nevertheless, 3T3 cells might not express the full machinery required for maximum BMP9/10-ALK1 signaling, such as endoglin, and endothelial cells with endogenous levels of ALK1 are more relevant for testing this hypothesis than 3T3 cells exogenously overexpressing it.

Since the studied ALK1-mutated cells displayed a reduction in cell surface ALK1 expression, reaching 50% in carriers of nonsense mutations, we hypothesized that 50% functional ALK1 seems sufficient for driving normal signal transduction. As we've shown, ECFCs carrying nonsense mutations have roughly 50% the normal level of ALK1 on their surface, likely due to non-sense mediated decay of the mutant transcripts. On the other hand, cells carrying missense mutations had slightly lower levels. Cells carrying ALK1 missense mutations that do not affect plasma membrane stability and trafficking are expected to exhibit on their surface functional receptor complexes with 2 WT ALK1 receptors, non-functional complexes with 2 mutated ALK1 receptors and mixed complexes with one WT and one mutated receptor. Mechanistically, our data might support the hypothesis that a single functional ALK1 copy in the mixed complexes is sufficient to activate the signaling cascade. A similar phenomenon was observed in ACVR1/BMPR1 complexes, where the kinase activity of only ACVR1 was needed to phosphorylate Smad1/5 in response to BMP2/7 heterodimers, while that of BMPR1 was dispensable[385]. On a functional level, our findings suggest that ALK1 heterozygosity on its own might not be sufficient for driving pathogenesis. In turn, this indicates that the overt transcriptomic dysregulations observed in the ALK1-mutated cells derived from explanted lungs of end-stage PAH patients cannot be solely attributed to the heterozygous *ACVRL1* mutation, but are likely the combined outcome of the germline mutation and other factors, as proposed by the two-hit hypothesis for HHT. Along these lines, many *in vivo* studies have highlighted the role of inflammation or angiogenesis in triggering characteristic vascular malformations in HHT experimental mouse models (detailed in Chapter 3.5.2), and HHT patients benefit from anti-angiogenic bevacizumab treatment[261]. Therefore, these environmental triggers might be required for influencing and distorting transcriptional responses in ALK1-mutated cells.

Interestingly, during the course of my PhD, exciting work by the group of Douglas Marchuk provided the first ever piece of evidence backing up the two-hit hypothesis in HHT patients[386]. In this case, however, the second hit was not an environmental trigger, but a genetic one. In 9 out of 19 patient-derived cutaneous telangiectasia biopsies, low-frequency somatic mutations in *ENG* or *ACVRL1* were detected using next-generation sequencing. These somatic mutations were confirmed to occur in trans configuration in at least 7 of these samples, leading to bi-allelic loss of *ENG* or *ACVRL1*. For the remaining biopsies, the authors argued that the failure to detect somatic mutations could be attributed to the limited power of the sequencing methodology used in detecting large DNA alterations such as mitotic

recombination, large deletions and chromosome loss[386]. As such, it was hypothesized that the malformations arise when endothelial clones acquire somatic mutations in the WT allele of the affected gene leading to loss of heterozygosity[386]. This is a well-known pathogenic phenomenon in cancer, known as the Knudsonian two-hit mechanism. This hypothesis is also not new to the vascular anomalies field as it was previously shown in several familial vascular malformations, including venous, glomuvenous and cerebral cavernous malformations[387,388], and it can help explain why symptoms increase with age in HHT patients[200] since somatic mutations accumulate with time.

Prior to the aforementioned study, another group indirectly addressed the possibility of the two-hit mechanism by assessing endoglin levels in the endothelium of cerebral and pulmonary AVMs of two HHT1 patients using immunostaining. Mutations carried by both patients resulted in transient intracellular species that are not expressed on the cell membrane. Endoglin levels were found to be reduced in the vasculature of these patients but could still be detected in the AVMs. Hence, the authors disregarded the possibility of biallelic loss[389]. However, since somatic mutations occur at low frequency, and vascular malformations could arise from mosaic ECs[237,239], only a subpopulation of the ECs in the malformation are expected to completely lose endoglin. Consequently, when surrounded by *ENG*-expressing cells, this *ENG*-null subpopulation might go unnoticed by immunostaining. Moreover, although most described HHT endoglin mutants led to transient intracellular proteins, some mutations give rise to cell surface products incapable of binding BMP9. In this case, unless the somatic mutation interferes with antibody binding, the mutant could still be detected by immunostaining and the lesions might still appear to express the protein, even if it's nonfunctional. Besides immunostaining, the authors isolated DNA from the pulmonary AVM and detected both the WT copy of *ENG* and mutated copy with the reported germline mutation. Nevertheless, the sequencing technology used back then (in year 2000) might not have been sensitive enough to detect low-frequency somatic mutations in a small subpopulation of cells. Hence, the two-hit mechanism should not have been ruled out in that study. On the PAH side, no somatic mutations leading to *BMPR2* or *ACVRL1* biallelic loss in explanted lungs of patients have been reported, but this point might not have been sufficiently investigated. However, a pro-inflammatory endothelial phenotype and increased perivascular inflammatory infiltration are well-known characteristics of PAH lungs[290], in accordance with the enrichment of inflammation-related gene sets in mutated HMVECs compared to CTLs in the current work. In addition, inflammatory triggers were reported to further reduce *BMPR2* expression levels in *BMPR2*-mutated PASMCs[326] and to induce EndMT in PAH HMVECs in the presence of BMP9[347]. Therefore, similar to HHT vascular dysplasia, inflammatory triggers might serve as potential 2nd hits for promoting EC dysfunction in PAH.

3.2. Identification of genes potentially involved in early pathogenesis

Another important finding of this study is that some of the genes displaying impaired regulation by BMP9 or BMP10 in mutated HMVECs also show impaired regulation in mutated ECFCs or HUVECs, although to milder extents. These genes were *LFNG*, encoding the Notch receptor regulator lunatic fringe, *JAG2* encoding the Notch ligand Jagged 2, *TNFRSF1B*, encoding a member of the TNF-receptor superfamily and *SLC6A6* encoding a sodium-

dependent taurine and beta-alanine transporter. Interestingly, *LFNG* was the only gene showing significantly impaired regulation in both ALK1-mutated ECFCs and HUVECs. The other 3 genes were only significantly dysregulated in mutated HUVECs, with *JAG2* and *TNFRSF1B* showing a trend of weaker regulation in mutated ECFCs, while *SLC6A6* did not show any difference at all between CTL and mutated ECFCs. This suggests that although both ALK1-mutated ECFCs and HUVECs were derived from the same microenvironment from newborns that don't show any signs of HHT, and sometimes from the same newborn, mutated HUVECs are, for some reason, more sensitive to reduction in functional ALK1 than ECFCs. In all cases, the use of newborn mutated cells in our study provided an opportunity to detect few genes showing uniquely high sensitivity to reduced functional ALK1 that might be important for disease onset. While mutated HMVECs allowed the initial identification of these genes by the two-factor analysis, it is not possible to deduce from these data alone whether the interaction term genes are a cause or outcome of endothelial dysfunction in the affected lungs. However, since ECFCs and HUVECs were not isolated from a sick microenvironment, we can hypothesize that dysregulations of these genes reflect early events in pathogenesis.

The only gene that showed significant dysregulations in mutated cells of all 3 EC models was *LFNG*. The resulting protein, lunatic fringe, is a glycosyl transferase that transfers a sugar moiety to the of Notch1 receptor, leading to an enhanced activation by Dll1 or Dll4 versus a suppressed activation by Jag1[390,391]. This enzyme is known for its role during somitogenesis, as Lfng-/- mice display abnormal formation and anterior–posterior patterning of the somites[392]. Some of these mice die rapidly within few hours after birth due to breathing difficulties secondary to rib abnormalities[392]. Additionally, *LFNG* mutations have been described in two patients with spondylocostal dysostosis, which represents to a group of congenital disorders characterized by multiple vertebral segmentation defects and malformations of the ribs[393,394]. One of the two patients had a homozygous missense mutation that led to LOF of the protein product[393] and the other was a compound heterozygote with one frameshift mutation leading to a truncated protein and a LOF missense mutation[394]. Interestingly, assessment of Lfng-/- developing retinal vasculature revealed enhanced angiogenic sprouting with a higher number of tip cells per field and increased vascular area compared to WT mice[390], phenocopying Dll4+/- mice[65,66]. A similar increase in vascular sprouting and density is also observed in the retinas of inducible EC-specific Alk1-/- or Eng-/- mice[171,244,245]. All in all, this raises the hypothesis that lunatic fringe, which is a target of BMP9/BMP10-ALK1 signaling, might be involved in mediating proper vascular sprouting downstream of ALK1 by enhancing Dll4-mediated Notch activation to limit the number of tip cells and resulting nascent sprouts. This current work provides direct evidence in primary ALK1-mutated ECs that *LFNG* induction by BMP9 or BMP10 is suppressed by ALK1 heterozygosity, even in newborn ECs that otherwise reveal mostly normal transcriptomic responses to BMP9 and BMP10. However, although this induction was reduced compared to CTLs, BMP9 in mutated ECFCs and HUVECs still significantly induced *LFNG* induction, and it is not known whether the remaining lunatic fringe level is enough for efficiently modulating Notch activity. While retinal vascularization was not examined in Lfng+/- mice, these mice did not show any defects in somitogenesis and were viable and fertile[392]. In addition, neither parent of the first spondylocostal dysostosis patient who themselves carried the heterozygous *LFNG* mutation were affected[393]. This might indicate that partial loss of functional lunatic fringe is tolerable, in line with the absence of HHT phenotype in newborns from whom the cells were isolated. On the contrary, a stronger loss of *LFNG* expression, possibly due to a 2nd

hit, might play a role in promoting HHT vascular dysplasia. A lot needs to be tested before this preliminary hypothesis can be validated, but the identification of an early modified target in heterozygous-ALK1 mutated ECs might hold great potential for hindering disease progression through proper early intervention.

4. Discussion on the p-Smad1/5 response to BMP9 under flow

The reduced p-Smad1/5 response to BMP9 in MUT-H1 under flow is consistent with a very recent study showing that *ENG*-mutated ECs in 3D organ-on-chip devices with microfluidic flow display defective vascular features that were not apparent in classical static 2D assays[395]. Namely, 3D lumenized vessels formed by the mutated cells under flow had reduced vascular density coupled to decreased EC proliferation and reduced vessel diameter, both of which are inconsistent with the hyperdense and dilated retinal vessels of HHT mouse models. Vessels formed by mutated ECs in the microfluidic chips also displayed impaired pericyte coverage and were leakier than those formed by WT cells, while no differences in proliferation, migration nor barrier function were detected under static 2D conditions between the 2 groups. Therefore, the authors concluded that the used 3D microfluidic system unraveled HHT-features of mutated ECs that otherwise seemed normal[395]. However, it is important to note that this experiment was performed using ECs differentiated from induced pluripotent stem cells from only a single HHT patient that is mosaic to the *ENG* mutation, compared to isogenic WT cells from the same patient. In addition, in the 3D microfluidic assays, cells were first resuspended in EGM2 culture medium supplemented with 2U/ml thrombin, were grown in the presence of the Notch signaling inhibitor DAPT for the first 24hrs and were replenished with EGM2 supplemented with 50ng/mL VEGF on a daily basis[395]. Hence, not only did the authors provide pro-inflammatory (thrombin)[396] and pro-angiogenic (additional VEGF) triggers to the cells in the microfluidic chips, but they also interfered with Notch signaling. Given the established role of inflammatory and angiogenic triggers in driving vascular dyslasia in HHT mouse models (detailed in Chapter 3.5.2) and the dysregulation of *LFNG* and *JAG2* in our ALK1-mutated cells, it is highly plausible that these triggers could be the true drivers promoting the observed defects in vessels formed by the *ENG*-mutated cells. Of course, FSS might still play a role in that aspect, but this cannot be clearly deciphered in the presence of the aforementioned confounding factors.

Perspectives

1. *LFNG* as a therapeutic target in HHT

1.1. Further characterization of LFNG regulation by BMP9/BMP10 in vitro

Before moving forward with *LFNG* as a therapeutic target, its regulation dynamics by BMP9, and perhaps BMP10, has to be confirmed since the kinetics studies were performed only once. Additionally, it would be interesting to perform a dose response assay in order to determine the minimum dose of BMP9 or BMP10 that induces *LFNG* mRNA upregulation in the different EC models, and to check whether larger impairments in its regulation can be detected at lower BMP9/BMP10 concentrations. Finally, it is necessary to check whether changes in *LFNG* mRNA levels upon BMP9/BMP10 stimulation translate into changes at the protein expression level. For that, western blots against lunatic fringe are planned for all 3 EC types at the different time points and effective BMP doses.

1.2. Assessing LFNG expression levels in vivo and in patient samples

To investigate the outcome of BMP9/BMP10-ALK1 signaling deficiency *in vivo*, LFNG mRNA or protein expression levels can be assessed in the retinas of constitutive BMP9; tamoxifen-inducible BMP10 double KOs (*Bmp9*$^{-/-}$; R26CreERT2 *Bmp10*$^{lox/lox}$) and in the retinas of EC-specific tamoxifen-inducible *Alk1* KOs (Cdh5-CreERT2$^{+/-}$;*Acvrl1*$^{flox/flox}$), both of which are available at our lab and show defects in postnatal retinal angiogenesis. LFNG mRNA or protein expression levels in the retinas of these models can be compared to those of WT controls using RNAScope in situ Hybridization or immunostaining, respectively.

At the patient level, LFNG mRNA or protein levels can also be assessed in tissue sections from explanted lungs of HPAH patients with mutations in *BMPR2* (*ACVRL1* mutations very rare) or from explanted livers or telangiectasia biopsies of HHT patients compared to control tissue. We have already started testing lunatic fringe level by immunostaining in lung samples of PAH patients in collaboration with Dr. Christophe Guignabert's group.

1.3. Assessing the role of BMP9/BMP10 stimulation on selective Notch activation by Dll vs Jag ligands

The next step would be to assess whether changes in *LFNG* expression by BMP9/BMP10 in ECs effectively regulate differential Notch-activation by Dll vs Jag ligands. This shall be tested via luciferase assay using the Notch CSL reporter (4xCSL-luciferase; generously provided by Dr. Bruno Larrivée), using the following planned experimental design:

a. Transfect ECs with 4xCSL-luciferase reporter and allow enough time for luciferase expression.
b. Stimulate with 10ng/mL BMP9 (or lower concentration depending on the results of the dose response assay) for 1hr (HUVECs and HMVECs) or 2hrs (ECFCs) to induce *LFNG* expression. The selected durations are subject to modification based on western blot results for lunatic fringe upregulation by BMP9/BMP10 kinetics stimulation.

c. Trypsinize the cells and transfer to separate Dll- and Jag-coated wells or co-culture with separate Dll and Jag-overexpressing 3T3 cells.
d. Allow enough time for Notch activation then lyse and measure luciferase activity.

1.4. Exploring means for restoration of oscillatory LFNG expression

Interestingly, many members of the Notch signaling pathway possess oscillatory regulation patterns involving regulatory feedback loops, such as *DLL1*, *DLL4*, *HES1* and *HES7*[397,398], and this cyclic regulation of *DLL4* was proposed to allow dynamicity in the selection of tip and stalk cells during sprouting angiogenesis[398]. Therefore, we can speculate that loss of cyclic regulation of *LFNG,* whose encoded protein strengthens Dll4-mediated Notch activation, can have important implications during sprouting angiogenesis. Importantly, *in vivo* studies assessing the role of *Lfng* on somitogenesis revealed that expression of nonoscillating *Lfng* in transgenic mice could not rescue defective somite patterning induced by the loss of cyclic endogenous *Lfng*[378], strongly highlighting the importance of the oscillatory expression pattern. With that in mind, potential therapeutic strategies targeting *LFNG* should aim to restore its normal oscillatory expression pattern rather than focusing only on its overexpression. Factors regulating *LFNG* oscillation outside of the BMP9/BMP10-ALK1 signaling pathway might serve as therapeutic targets for rescuing *LFNG* regulation. In the presomitic mesoderm of mice, *Lfng* oscillation was reported to be regulated by oscillatory Hes7, and lunatic fringe in turn regulates oscillations in Notch activation, forming a continuous feedback loop[378]. However, evidence also suggests the involvement of other Notch-independent regulators of *Lfng* cyclic gene expression in the posterior paraxial mesoderm[378]. Here we show that *LFNG* oscillation can be induced by BMP9/BMP10. To gain better understanding on the regulation of *LFNG* downstream of ALK1, its expression is to be assessed in Smad4-silenced ECs. Since *LFNG* gene locus was shown by ChIP-Seq analysis to exhibit a Smad1/5 binding region in BMP9-stimulated HUVECs[113], it is expected to be Smad4-dependent. However, its regulation can be co-dependent on additional Smad-independent factors that might be targeted for normalization of *LFNG* induction. An overview of putative transcription factors regulating *LFNG* expression can be derived from determining transcription factor binding sites in the promoter region of *LFNG* (retrieved from Eukaryotic Promoter Database) using for example PROMO tool (https://alggen.lsi.upc.es/cgi-bin/promo_v3/promo/promoinit.cgi?dirDB=TF_8.3). The role of putative transcription factors can then be validated by individual silencing of suspected factors followed by assessment of BMP9-induced *LFNG* upregulation in ECs. Identification of the regulatory machinery behind *LFNG* oscillatory expression in ECs might uncover key knobs that can be targeted for promoting endogenous *LFNG* expression in its normal physiological dynamics.

2. Providing in vitro proof of concept for 2nd hit hypothesis

Since we hypothesized that ALK1-mutated HMVECs from the lungs of PAH patients might have been exposed to genetic or environmental 2nd hits, we examined whether the ALK1-mutated cells from the 2 PAH patients harbor somatic *ACVRL1* mutations using information on the *ACVRL1* reads from the RNA-seq analysis on these cells. For that and with the help of

bioinformaticians, we used Mutect2, which is a somatic variant caller that uses local haplotype assembly and realignment to detect short somatic mutations[399]. In other words, this tool scans sequenced *ACVRL1* reads and detects the presence of low frequency (i.e. somatic) short mutations such as single nucleotide variations and small insertions or deletions. Using this tool, we successfully detected the germline mutation carried by each PAH patient, at a frequency of approximately 50%, but we could not detect pathogenic low-frequency short mutations. While this could indicate the absence of somatic mutations in these cells, they might still potentially carry larger DNA changes that cannot be detected by this method. Interestingly, based on our findings and the recent identification of somatic hits in telangiectasia of HHT patients by Snellings et al[386], the group of Dr. Sophie Dupuis-Girod at the HHT reference center in Lyon has started investigating the presence of somatic mutations leading to biallelic loss of *ENG* or *ACVRL1* in samples from vascular lesions of HHT patients.

As explained previously, the 2nd hit might also be an environmental angiogenic or inflammatory trigger. Proof of concept of the 2nd hit hypothesis can be attained if ALK1-mutated ECFCs and HUVECs display abnormalities in the presence of pro-inflammatory or pro-angiogenic triggers that were not evident in the absence of those triggers. To test that, MUT ECFCs and HUVECs can be treated with pro-inflammatory (LPS, IL-6 or TNF-α) or pro-angiogenic (VEGF) triggers followed by assessment of their Smad1/5 response and the regulation of some interaction term genes in response to BMP9 or BMP10 stimulation. If in the presence of these triggers the mutated cells start to display reduced p-Smad1/5 levels in response to BMP9 or BMP10 and the induction of *LFNG*, *JAG2*, *TNFRSF1B*, *SLC6A6*, *SOX13* and/or *CEBPG* becomes weaker, this would validate that 2nd hits are required to disrupt canonical Smad signaling and transcriptional regulation of susceptible targets. Of course the response of CTL ECs in the presence of these triggers has to be assessed in parallel and should be considered as the reference point for responses in mutated cells. On the functional level, a previous study reported that the combined treatment of BMP9 and IL-6 promotes the appearance of EndMT features (reduction in peripheral VE-cadherin and gain of organized SM22α expression) in CTL HMVECs, but to a stronger extent in IPAH or *BMPR2*-mutated HPAH HMVECs[347]. However, BMP9 stimulation alone strengthened EC junctions in CTLs, but had an opposite effect on patient HMVECs[347]. Hence, assessment of cytoskeletal changes in response to BMP9/BMP10 alone or in combination with inflammatory triggers might also highlight 2nd hit- (inflammation) dependent alterations.

3. Assessment of the p-Smad1/5 response to BMP9/BMP10 in ALK1-mutated ECs under flow

The image acquisition and analysis parameters for quantifying p-Smad1/5 fluorescence levels in the microfluidic channels have been optimized following the first preliminary experiment of BMP9 stimulation under flow, with the help of Emmanuelle Soleilhac at the CMBA platform. An example of representative improved confocal fluorescence images of p-Smad1/5 and VE-cadherin staining in 3 different areas of the branches (with diameters of 70, 140 and 190µm) are presented in Figure 30. Thus, future experiments using ECFCs from a larger number of donors, as well as CTL and MUT HUVECs will provide a better view on the impact of heterozygous *ACVRL1* mutations on the p-Smad1/5 response to BMP9 under flow.

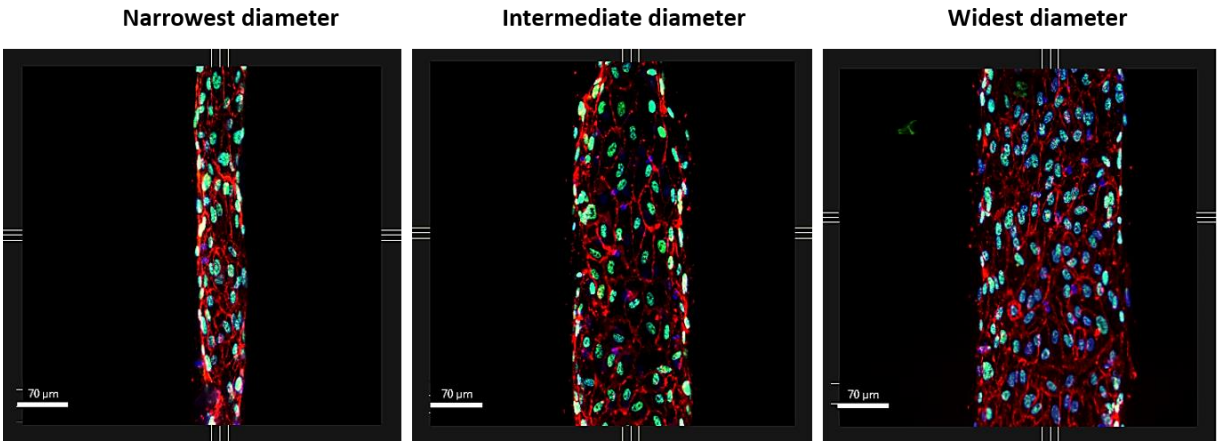

Figure 30. Confocal fluorescence imaging of ECs in microfluidic channels with optimized acquisition parameters. *Representative images of CTL ECFCs stained with VE-Cadherin (red), p-Smad1/5 (green) and nuclei counterstained with DAPI (blue) in the 3 sections of the channels with different diameters.*

Alternatively, since this system relies on bidirectional flow, and given that ECs *in vivo* polarize and migrate against the direction of flow in an ALK1- and endoglin-dependent manner[400], it could be better to employ microfluidic devices that provide unidirectional flow through pumps[361]. It would also be interesting to assess VE-cadherin by immunostaining as a marker of barrier function following the combined treatment of BMP9 and an inflammatory trigger. This would allow us to check if we can recapitulate results from static *in vitro* experiments that were proposed in the second perspective, especially that laminar shear stress under physiological levels is known to activate anti-inflammatory signals[401].

4. Uncovering new functions of BMP9 and BMP10 using transcriptomic data

After identifying the different BP GO clusters that are enriched in response to BMP9 and BMP10 in CTL ECFCs and HMVECs, focus will be shed on one or few of the identified gene set clusters for further investigation. BMP9 and/or BMP10 have already been reported to be involved in regulating cell proliferation, migration, apoptosis, barrier function, cytoskeletal organization and inflammation[57,162]. Therefore, it would be interesting to explore functions that were not previously described, such as inorganic ion homeostasis and lipid metabolism. The next step would be to first validate DEGs within these gene sets by qPCR and western blotting on independent BMP9 and BMP10 stimulations using ECFCs, HMVECs, and HUVECs, then use appropriate functional assays to confirm their roles in ECs. Double *Bmp9*/*Bmp10* KO mice available at the lab might also be used for *in vivo* validations.

References

1. Pugsley MK, Tabrizchi R. The vascular system. *Journal of Pharmacological and Toxicological Methods*. 2000;44(2):333-340. doi:10.1016/S1056-8719(00)00125-8

2. Tucker WD, Arora Y, Mahajan K. Anatomy, Blood Vessels. In: *StatPearls*. StatPearls Publishing; 2022. Accessed February 9, 2023. http://www.ncbi.nlm.nih.gov/books/NBK470401/

3. Birbrair A, Zhang T, Wang ZM, Messi ML, Mintz A, Delbono O. Pericytes at the intersection between tissue regeneration and pathology: Figure 1. *Clin Sci*. 2015;128(2):81-93. doi:10.1042/CS20140278

4. Claesson-Welsh L, Dejana E, McDonald DM. Permeability of the Endothelial Barrier: Identifying and Reconciling Controversies. *Trends in Molecular Medicine*. 2021;27(4):314-331. doi:10.1016/j.molmed.2020.11.006

5. Ricard N, Bailly S, Guignabert C, Simons M. The quiescent endothelium: signalling pathways regulating organ-specific endothelial normalcy. *Nat Rev Cardiol*. 2021;18(8):565-580. doi:10.1038/s41569-021-00517-4

6. Al Tabosh T, Al Tarrass M, Bailly S. The BMP9/10-ALK1-Endoglin Pathway as a Target of Anti-Angiogenic Therapy in Cancer. In: *Immunology and Cancer Biology*. Vide Leaf, Hyderabad; 2021. doi:10.37247/IMCAC.1.2021.21

7. Lee D, Park C, Lee H, et al. ER71 Acts Downstream of BMP, Notch, and Wnt Signaling in Blood and Vessel Progenitor Specification. *Cell Stem Cell*. 2008;2(5):497-507. doi:10.1016/j.stem.2008.03.008

8. Ribatti D, Vacca A, Nico B, Roncali L, Dammacco F. Postnatal vasculogenesis. *Mechanisms of Development*. 2001;100(2):157-163. doi:10.1016/S0925-4773(00)00522-0

9. Carmeliet P. Mechanisms of angiogenesis and arteriogenesis. *Nat Med*. 2000;6(4):389-395. doi:10.1038/74651

10. Risau W. Mechanisms of angiogenesis. *Nature*. 1997;386(6626):671-674. doi:10.1038/386671a0

11. Senger DR, Galli SJ, Dvorak AM, Perruzzi CA, Harvey VS, Dvorak HF. Tumor Cells Secrete a Vascular Permeability Factor That Promotes Accumulation of Ascites Fluid. *Science*. 1983;219(4587):983-985. doi:10.1126/science.6823562

12. Plouët J, Schilling J, Gospodarowicz D. Isolation and characterization of a newly identified endothelial cell mitogen produced by AtT-20 cells. *The EMBO Journal*. 1989;8(12):3801-3806. doi:10.1002/j.1460-2075.1989.tb08557.x

13. Ferrara N, Henzel WJ. Pituitary follicular cells secrete a novel heparin-binding growth factor specific for vascular endothelial cells. *Biochemical and Biophysical Research Communications*. 1989;161(2):851-858. doi:10.1016/0006-291X(89)92678-8

14. Leung DW, Cachianes G, Kuang WJ, Goeddel DV, Ferrara N. Vascular Endothelial Growth Factor Is a Secreted Angiogenic Mitogen. *Science*. 1989;246(4935):1306-1309. doi:10.1126/science.2479986

15. Keck PJ, Hauser SD, Krivi G, et al. Vascular Permeability Factor, an Endothelial Cell Mitogen Related to PDGF. *Science*. 1989;246(4935):1309-1312. doi:10.1126/science.2479987

16. Koch S, Claesson-Welsh L. Signal Transduction by Vascular Endothelial Growth Factor Receptors. *Cold Spring Harbor Perspectives in Medicine*. 2012;2(7):a006502-a006502. doi:10.1101/cshperspect.a006502

17. Ferrara N, Carver-Moore K, Chen H, et al. Heterozygous embryonic lethality induced by targeted inactivation of the VEGF gene. *Nature*. 1996;380(6573):439-442. doi:10.1038/380439a0

18. Carmeliet P, Ferreira V, Breier G, et al. Abnormal blood vessel development and lethality in embryos lacking a single VEGF allele. *Nature*. 1996;380(6573):435-439. doi:10.1038/380435a0

19. Shalaby F, Rossant J, Yamaguchi TP, et al. Failure of blood-island formation and vasculogenesis in Flk-1-deficient mice. *Nature*. 1995;376(6535):62-66. doi:10.1038/376062a0

20. Park JE, Keller GA, Ferrara N. The vascular endothelial growth factor (VEGF) isoforms: differential deposition into the subepithelial extracellular matrix and bioactivity of extracellular matrix-bound VEGF. *MBoC*. 1993;4(12):1317-1326. doi:10.1091/mbc.4.12.1317

21. Apte RS, Chen DS, Ferrara N. VEGF in Signaling and Disease: Beyond Discovery and Development. *Cell*. 2019;176(6):1248-1264. doi:10.1016/j.cell.2019.01.021

22. Qiu Y, Hoareau-Aveilla C, Oltean S, Harper SJ, Bates DO. The anti-angiogenic isoforms of VEGF in health and disease. *Biochemical Society Transactions*. 2009;37(6):1207-1213. doi:10.1042/BST0371207

23. Sawano A, Takahashi T, Yamaguchi S, Aonuma M, Shibuya M. Flt-1 but not KDR/Flk-1 tyrosine kinase is a receptor for placenta growth factor, which is related to vascular endothelial growth factor. *Cell Growth Differ*. 1996;7(2):213-221.

24. Shibuya M. Vascular Endothelial Growth Factor (VEGF) and Its Receptor (VEGFR) Signaling in Angiogenesis: A Crucial Target for Anti- and Pro-Angiogenic Therapies. *Genes & Cancer*. 2011;2(12):1097-1105. doi:10.1177/1947601911423031

25. Chau K, Hennessy A, Makris A. Placental growth factor and pre-eclampsia. *J Hum Hypertens*. 2017;31(12):782-786. doi:10.1038/jhh.2017.61

26. Zhang F, Tang Z, Hou X, et al. VEGF-B is dispensable for blood vessel growth but critical for their survival, and VEGF-B targeting inhibits pathological angiogenesis. *Proc Natl Acad Sci USA*. 2009;106(15):6152-6157. doi:10.1073/pnas.0813061106

27. Hagberg CE, Falkevall A, Wang X, et al. Vascular endothelial growth factor B controls endothelial fatty acid uptake. *Nature*. 2010;464(7290):917-921. doi:10.1038/nature08945

28. Ogawa S, Oku A, Sawano A, Yamaguchi S, Yazaki Y, Shibuya M. A Novel Type of Vascular Endothelial Growth Factor, VEGF-E (NZ-7 VEGF), Preferentially Utilizes KDR/Flk-1 Receptor and Carries a Potent Mitotic Activity without Heparin-binding Domain. *Journal of Biological Chemistry*. 1998;273(47):31273-31282. doi:10.1074/jbc.273.47.31273

29. Prud'homme GJ, Glinka Y. Neuropilins are multifunctional coreceptors involved in tumor initiation, growth, metastasis and immunity. *Oncotarget*. 2012;3(9):921-939. doi:10.18632/oncotarget.626

30. Iyer NV, Kotch LE, Agani F, et al. Cellular and developmental control of O_2 homeostasis by hypoxia-inducible factor 1α. *Genes Dev*. 1998;12(2):149-162. doi:10.1101/gad.12.2.149

31. Takahashi T, Yamaguchi S, Chida K, Shibuya M. A single autophosphorylation site on KDR/Flk-1 is essential for VEGF-A-dependent activation of PLC-gamma and DNA synthesis in vascular endothelial cells. *EMBO J*. 2001;20(11):2768-2778. doi:10.1093/emboj/20.11.2768

32. Takahashi T, Ueno H, Shibuya M. VEGF activates protein kinase C-dependent, but Ras-independent Raf-MEK-MAP kinase pathway for DNA synthesis in primary endothelial cells. *Oncogene*. 1999;18(13):2221-2230. doi:10.1038/sj.onc.1202527

33. Wu H mac, Yuan Y, Zawieja DC, Tinsley J, Granger HJ. Role of phospholipase C, protein kinase C, and calcium in VEGF-induced venular hyperpermeability. *American Journal of Physiology-Heart and Circulatory Physiology*. 1999;276(2):H535-H542. doi:10.1152/ajpheart.1999.276.2.H535

34. Lamalice L, Houle F, Huot J. Phosphorylation of Tyr1214 within VEGFR-2 Triggers the Recruitment of Nck and Activation of Fyn Leading to SAPK2/p38 Activation and Endothelial Cell Migration in Response to VEGF. *Journal of Biological Chemistry*. 2006;281(45):34009-34020. doi:10.1074/jbc.M603928200

35. Eklund L, Olsen B. Tie receptors and their angiopoietin ligands are context-dependent regulators of vascular remodeling. *Experimental Cell Research*. 2006;312(5):630-641. doi:10.1016/j.yexcr.2005.09.002

36. Fukuhara S, Sako K, Noda K, Nagao K, Miura K, Mochizuki N. Tie2 is tied at the cell-cell contacts and to extracellular matrix by Angiopoietin-1. *Exp Mol Med*. 2009;41(3):133. doi:10.3858/emm.2009.41.3.016

37. Kim I, Kim HG, So JN, Kim JH, Kwak HJ, Koh GY. Angiopoietin-1 Regulates Endothelial Cell Survival Through the Phosphatidylinositol 3′-Kinase/Akt Signal Transduction Pathway. *Circulation Research*. 2000;86(1):24-29. doi:10.1161/01.RES.86.1.24

38. Gamble JR, Drew J, Trezise L, et al. Angiopoietin-1 Is an Antipermeability and Anti-Inflammatory Agent In Vitro and Targets Cell Junctions. *Circulation Research*. 2000;87(7):603-607. doi:10.1161/01.RES.87.7.603

39. Kim I, Moon SO, Park SK, Chae SW, Koh GY. Angiopoietin-1 Reduces VEGF-Stimulated Leukocyte Adhesion to Endothelial Cells by Reducing ICAM-1, VCAM-1, and E-Selectin Expression. *Circulation Research*. 2001;89(6):477-479. doi:10.1161/hh1801.097034

40. Maisonpierre PC, Suri C, Jones PF, et al. Angiopoietin-2, a Natural Antagonist for Tie2 That Disrupts in vivo Angiogenesis. *Science*. 1997;277(5322):55-60. doi:10.1126/science.277.5322.55

41. Scharpfenecker M, Fiedler U, Reiss Y, Augustin HG. The Tie-2 ligand Angiopoietin-2 destabilizes quiescent endothelium through an internal autocrine loop mechanism. *Journal of Cell Science*. 2005;118(4):771-780. doi:10.1242/jcs.01653

42. Patan S, Haenni B, Burri PeterH. Evidence for intussusceptive capillary growth in the chicken chorio-allantoic membrane (CAM). *Anat Embryol*. 1993;187(2). doi:10.1007/BF00171743

43. Sato TN, Tozawa Y, Deutsch U, et al. Distinct roles of the receptor tyrosine kinases Tie-1 and Tie-2 in blood vessel formation. *Nature*. 1995;376(6535):70-74. doi:10.1038/376070a0

44. Song SH, Kim KL, Lee KA, Suh W. Tie1 regulates the Tie2 agonistic role of angiopoietin-2 in human lymphatic endothelial cells. *Biochemical and Biophysical Research Communications*. 2012;419(2):281-286. doi:10.1016/j.bbrc.2012.02.009

45. Brouillard P, Schlögel MJ, Homayun Sepehr N, et al. Non-hotspot PIK3CA mutations are more frequent in CLOVES than in common or combined lymphatic malformations. *Orphanet J Rare Dis*. 2021;16(1):267. doi:10.1186/s13023-021-01898-y

46. Limaye N, Kangas J, Mendola A, et al. Somatic Activating PIK3CA Mutations Cause Venous Malformation. *The American Journal of Human Genetics*. 2015;97(6):914-921. doi:10.1016/j.ajhg.2015.11.011

47. Limaye N, Wouters V, Uebelhoer M, et al. Somatic mutations in angiopoietin receptor gene TEK cause solitary and multiple sporadic venous malformations. *Nat Genet*. 2009;41(1):118-124. doi:10.1038/ng.272

48. Heldin CH, Westermark B. Mechanism of Action and In Vivo Role of Platelet-Derived Growth Factor. *Physiological Reviews*. 1999;79(4):1283-1316. doi:10.1152/physrev.1999.79.4.1283

49. Hellstrom M, Kal n M, Lindahl P, Abramsson A, Betsholtz C. Role of PDGF-B and PDGFR-beta in recruitment of vascular smooth muscle cells and pericytes during embryonic blood vessel formation in the mouse. *Development*. 1999;126(14):3047-3055. doi:10.1242/dev.126.14.3047

50. Kohler N, Lipton A. Platelets as a source of fibroblast growth-promoting activity. *Experimental Cell Research*. 1974;87(2):297-301. doi:10.1016/0014-4827(74)90484-4

51. Wu E, Palmer N, Tian Z, et al. Comprehensive Dissection of PDGF-PDGFR Signaling Pathways in PDGFR Genetically Defined Cells. Rutherford S, ed. *PLoS ONE*. 2008;3(11):e3794. doi:10.1371/journal.pone.0003794

52. Fernández-Chacón M, García-González I, Mühleder S, Benedito R. Role of Notch in endothelial biology. *Angiogenesis*. 2021;24(2):237-250. doi:10.1007/s10456-021-09793-7

53. Saiki W, Ma C, Okajima T, Takeuchi H. Current Views on the Roles of O-Glycosylation in Controlling Notch-Ligand Interactions. *Biomolecules*. 2021;11(2):309. doi:10.3390/biom11020309

54. Benedito R, Roca C, Sörensen I, et al. The Notch Ligands Dll4 and Jagged1 Have Opposing Effects on Angiogenesis. *Cell*. 2009;137(6):1124-1135. doi:10.1016/j.cell.2009.03.025

55. Yang LT, Nichols JT, Yao C, Manilay JO, Robey EA, Weinmaster G. Fringe glycosyltransferases differentially modulate Notch1 proteolysis induced by Delta1 and Jagged1. *Mol Biol Cell*. 2005;16(2):927-942. doi:10.1091/mbc.e04-07-0614

56. Kakuda S, Haltiwanger RS. Deciphering the Fringe-Mediated Notch Code: Identification of Activating and Inhibiting Sites Allowing Discrimination between Ligands. *Dev Cell*. 2017;40(2):193-201. doi:10.1016/j.devcel.2016.12.013

57. Desroches-Castan A, Tillet E, Bouvard C, Bailly S. BMP9 and BMP10 : Two close vascular quiescence partners that stand out. *Developmental Dynamics*. 2022;251(1):158-177. doi:10.1002/dvdy.395

58. Gerhardt H, Golding M, Fruttiger M, et al. VEGF guides angiogenic sprouting utilizing endothelial tip cell filopodia. *J Cell Biol*. 2003;161(6):1163-1177. doi:10.1083/jcb.200302047

59. Blanco R, Gerhardt H. VEGF and Notch in Tip and Stalk Cell Selection. *Cold Spring Harbor Perspectives in Medicine*. 2013;3(1):a006569-a006569. doi:10.1101/cshperspect.a006569

60. Oh H, Takagi H, Suzuma K, Otani A, Matsumura M, Honda Y. Hypoxia and Vascular Endothelial Growth Factor Selectively Up-regulate Angiopoietin-2 in Bovine Microvascular Endothelial Cells. *Journal of Biological Chemistry*. 1999;274(22):15732-15739. doi:10.1074/jbc.274.22.15732

61. Eliceiri BP, Klemke R, Strömblad S, Cheresh DA. Integrin αvβ3 Requirement for Sustained Mitogen-activated Protein Kinase Activity during Angiogenesis. *Journal of Cell Biology*. 1998;140(5):1255-1263. doi:10.1083/jcb.140.5.1255

62. Leavesley DI, Schwartz MA, Rosenfeld M, Cheresh DA. Integrin beta 1- and beta 3-mediated endothelial cell migration is triggered through distinct signaling mechanisms. *Journal of Cell Biology*. 1993;121(1):163-170. doi:10.1083/jcb.121.1.163

63. Murohara T, Witzenbichler B, Spyridopoulos I, et al. Role of Endothelial Nitric Oxide Synthase in Endothelial Cell Migration. *ATVB*. 1999;19(5):1156-1161. doi:10.1161/01.ATV.19.5.1156

64. Alt A, Miguel-Romero L, Donderis J, et al. Structural and Functional Insights into Endoglin Ligand Recognition and Binding. Kursula P, ed. *PLoS ONE*. 2012;7(2):e29948. doi:10.1371/journal.pone.0029948

65. Hellström M, Phng LK, Hofmann JJ, et al. Dll4 signalling through Notch1 regulates formation of tip cells during angiogenesis. *Nature*. 2007;445(7129):776-780. doi:10.1038/nature05571

66. Lobov IB, Renard RA, Papadopoulos N, et al. Delta-like ligand 4 (Dll4) is induced by VEGF as a negative regulator of angiogenic sprouting. *Proc Natl Acad Sci U S A*. 2007;104(9):3219-3224. doi:10.1073/pnas.0611206104

67. Siekmann AF, Lawson ND. Notch signalling limits angiogenic cell behaviour in developing zebrafish arteries. *Nature*. 2007;445(7129):781-784. doi:10.1038/nature05577

68. Scehnet JS, Jiang W, Kumar SR, et al. Inhibition of Dll4-mediated signaling induces proliferation of immature vessels and results in poor tissue perfusion. *Blood*. 2007;109(11):4753-4760. doi:10.1182/blood-2006-12-063933

69. Suchting S, Freitas C, le Noble F, et al. The Notch ligand Delta-like 4 negatively regulates endothelial tip cell formation and vessel branching. *Proc Natl Acad Sci U S A*. 2007;104(9):3225-3230. doi:10.1073/pnas.0611177104

70. Lim R, Sugino T, Nolte H, et al. Deubiquitinase USP10 regulates Notch signaling in the endothelium. *Science*. 2019;364(6436):188-193. doi:10.1126/science.aat0778

71. Larrivée B, Prahst C, Gordon E, et al. ALK1 Signaling Inhibits Angiogenesis by Cooperating with the Notch Pathway. *Developmental Cell*. 2012;22(3):489-500. doi:10.1016/j.devcel.2012.02.005

72. Moya IM, Umans L, Maas E, et al. Stalk Cell Phenotype Depends on Integration of Notch and Smad1/5 Signaling Cascades. *Developmental Cell*. 2012;22(3):501-514. doi:10.1016/j.devcel.2012.01.007

73. Gerhardt H, Ruhrberg C, Abramsson A, Fujisawa H, Shima D, Betsholtz C. Neuropilin-1 is required for endothelial tip cell guidance in the developing central nervous system. *Dev Dyn*. 2004;231(3):503-509. doi:10.1002/dvdy.20148

74. Aspalter IM, Gordon E, Dubrac A, et al. Alk1 and Alk5 inhibition by Nrp1 controls vascular sprouting downstream of Notch. *Nat Commun*. 2015;6(1):7264. doi:10.1038/ncomms8264

75. Larrivée B, Freitas C, Suchting S, Brunet I, Eichmann A. Guidance of Vascular Development: Lessons From the Nervous System. *Circulation Research*. 2009;104(4):428-441. doi:10.1161/CIRCRESAHA.108.188144

76. Ribatti D, Crivellato E. "Sprouting angiogenesis", a reappraisal. *Developmental Biology*. 2012;372(2):157-165. doi:10.1016/j.ydbio.2012.09.018

77. David L, Mallet C, Mazerbourg S, Feige JJ, Bailly S. Identification of BMP9 and BMP10 as functional activators of the orphan activin receptor-like kinase 1 (ALK1) in endothelial cells. *Blood*. 2007;109(5):1953-1961. doi:10.1182/blood-2006-07-034124

78. Thurston G, Rudge JS, Ioffe E, et al. Angiopoietin-1 protects the adult vasculature against plasma leakage. *Nat Med*. 2000;6(4):460-463. doi:10.1038/74725

79. Roberts AB, Sporn MB. Regulation of Endothelial Cell Growth, Architecture, and Matrix Synthesis by TGF-β. *Am Rev Respir Dis*. 1989;140(4):1126-1128. doi:10.1164/ajrccm/140.4.1126

80. Hirschi KK, Rohovsky SA, D'Amore PA. PDGF, TGF-β, and Heterotypic Cell–Cell Interactions Mediate Endothelial Cell–induced Recruitment of 10T1/2 Cells and Their Differentiation to a Smooth Muscle Fate. *Journal of Cell Biology*. 1998;141(3):805-814. doi:10.1083/jcb.141.3.805

81. Darland DC, D'Amore PA. TGF beta is required for the formation of capillary-like structures in three-dimensional cocultures of 10T1/2 and endothelial cells. *Angiogenesis*. 2001;4(1):11-20. doi:10.1023/a:1016611824696

82. Liu Y, Wada R, Yamashita T, et al. Edg-1, the G protein–coupled receptor for sphingosine-1-phosphate, is essential for vascular maturation. *J Clin Invest*. 2000;106(8):951-961. doi:10.1172/JCI10905

83. Atuma SS, Lundström K, Lindquist J. The electrochemical determination of vitamin A. Part II. Further voltammetric determination of vitamin A and initial work on the determination of vitamin D in the presence of vitamin A. *Analyst*. 1975;100(1196):827-834. doi:10.1039/an9750000827

84. Fang JS, Coon BG, Gillis N, et al. Shear-induced Notch-Cx37-p27 axis arrests endothelial cell cycle to enable arterial specification. *Nat Commun*. 2017;8(1):2149. doi:10.1038/s41467-017-01742-7

85. Obi S, Yamamoto K, Shimizu N, et al. Fluid shear stress induces arterial differentiation of endothelial progenitor cells. *Journal of Applied Physiology*. 2009;106(1):203-211. doi:10.1152/japplphysiol.00197.2008

86. Wang HU, Chen ZF, Anderson DJ. Molecular Distinction and Angiogenic Interaction between Embryonic Arteries and Veins Revealed by ephrin-B2 and Its Receptor Eph-B4. *Cell*. 1998;93(5):741-753. doi:10.1016/S0092-8674(00)81436-1

87. Villa N, Walker L, Lindsell CE, Gasson J, Iruela-Arispe ML, Weinmaster G. Vascular expression of Notch pathway receptors and ligands is restricted to arterial vessels. *Mechanisms of Development*. 2001;108(1-2):161-164. doi:10.1016/S0925-4773(01)00469-5

88. Lawson ND, Scheer N, Pham VN, et al. Notch signaling is required for arterial-venous differentiation during embryonic vascular development. *Development*. 2001;128(19):3675-3683. doi:10.1242/dev.128.19.3675

89. Gale NW, Dominguez MG, Noguera I, et al. Haploinsufficiency of delta-like 4 ligand results in embryonic lethality due to major defects in arterial and vascular development. *Proc Natl Acad Sci USA*. 2004;101(45):15949-15954. doi:10.1073/pnas.0407290101

90. Trindade A, Ram Kumar S, Scehnet JS, et al. Overexpression of delta-like 4 induces arterialization and attenuates vessel formation in developing mouse embryos. *Blood*. 2008;112(5):1720-1729. doi:10.1182/blood-2007-09-112748

91. Carlson TR, Yan Y, Wu X, et al. Endothelial expression of constitutively active *Notch4* elicits reversible arteriovenous malformations in adult mice. *Proc Natl Acad Sci USA*. 2005;102(28):9884-9889. doi:10.1073/pnas.0504391102

92. Shawber CJ, Das I, Francisco E, Kitajewski J. Notch Signaling in Primary Endothelial Cells. *Annals of the New York Academy of Sciences*. 2003;995(1):162-170. doi:10.1111/j.1749-6632.2003.tb03219.x

93. Krebs LT, Starling C, Chervonsky AV, Gridley T. *Notch1* activation in mice causes arteriovenous malformations phenocopied by ephrinB2 and EphB4 mutants. *genesis*. Published online 2010:NA-NA. doi:10.1002/dvg.20599

94. Kohli V, Schumacher JA, Desai SP, Rehn K, Sumanas S. Arterial and Venous Progenitors of the Major Axial Vessels Originate at Distinct Locations. *Developmental Cell*. 2013;25(2):196-206. doi:10.1016/j.devcel.2013.03.017

95. Marziano C, Genet G, Hirschi KK. Vascular endothelial cell specification in health and disease. *Angiogenesis*. 2021;24(2):213-236. doi:10.1007/s10456-021-09785-7

96. Herzog Y, Guttmann-Raviv N, Neufeld G. Segregation of arterial and venous markers in subpopulations of blood islands before vessel formation. *Dev Dyn*. 2005;232(4):1047-1055. doi:10.1002/dvdy.20257

97. Chavkin NW, Genet G, Poulet M, et al. *Endothelial Cell Cycle State Determines Propensity for Arterial-Venous Fate*. Developmental Biology; 2020. doi:10.1101/2020.08.12.246512

98. Caduff JH, Fischer LC, Burri PH. Scanning electron microscope study of the developing microvasculature in the postnatal rat lung. *Anat Rec*. 1986;216(2):154-164. doi:10.1002/ar.1092160207

99. Patan S, Alvarez MJ, Schittny JC, Burri PH. Intussusceptive Microvascular Growth: A Common Alternative to Capillary Sprouting. *Arch Histol Cytol*. 1992;55(Suppl):65-75. doi:10.1679/aohc.55.Suppl_65

100. Mentzer SJ, Konerding MA. Intussusceptive angiogenesis: expansion and remodeling of microvascular networks. *Angiogenesis*. 2014;17(3):499-509. doi:10.1007/s10456-014-9428-3

101. David CJ, Massagué J. Contextual determinants of TGFβ action in development, immunity and cancer. *Nat Rev Mol Cell Biol*. 2018;19(7):419-435. doi:10.1038/s41580-018-0007-0

102. Gordon KJ, Blobe GC. Role of transforming growth factor-β superfamily signaling pathways in human disease. *Biochimica et Biophysica Acta (BBA) - Molecular Basis of Disease*. 2008;1782(4):197-228. doi:10.1016/j.bbadis.2008.01.006

103. Urist MR. Bone: Formation by Autoinduction. *Science*. 1965;150(3698):893-899. doi:10.1126/science.150.3698.893

104. Urist MR, Huo YK, Brownell AG, et al. Purification of bovine bone morphogenetic protein by hydroxyapatite chromatography. *Proc Natl Acad Sci USA*. 1984;81(2):371-375. doi:10.1073/pnas.81.2.371

105. Urist MR, Strates BS. Bone Morphogenetic Protein. *J Dent Res*. 1971;50(6):1392-1406. doi:10.1177/00220345710500060601

106. Wang EA, Rosen V, Cordes P, et al. Purification and characterization of other distinct bone-inducing factors. *Proc Natl Acad Sci USA*. 1988;85(24):9484-9488. doi:10.1073/pnas.85.24.9484

107. Obradovic Wagner D, Sieber C, Bhushan R, Börgermann JH, Graf D, Knaus P. BMPs: From Bone to Body Morphogenetic ProteinsA report on the First International BMP Workshop: "Modern Trends in BMP Signaling," Berlin, Germany, 6 to 9 September 2009. *Sci Signal*. 2010;3(107). doi:10.1126/scisignal.3107mr1

108. Kim SK, Henen MA, Hinck AP. Structural biology of betaglycan and endoglin, membrane-bound co-receptors of the TGF-beta family. *Exp Biol Med (Maywood)*. 2019;244(17):1547-1558. doi:10.1177/1535370219881160

109. Massagué J, Seoane J, Wotton D. Smad transcription factors. *Genes Dev*. 2005;19(23):2783-2810. doi:10.1101/gad.1350705

110. Massagué J, Gomis RR. The logic of TGFβ signaling. *FEBS Letters*. 2006;580(12):2811-2820. doi:10.1016/j.febslet.2006.04.033

111. Hill CS. Nucleocytoplasmic shuttling of Smad proteins. *Cell Res*. 2009;19(1):36-46. doi:10.1038/cr.2008.325

112. Watanabe M, Masuyama N, Fukuda M, Nishida E. Regulation of intracellular dynamics of Smad4 by its leucine-rich nuclear export signal. *EMBO Rep*. 2000;1(2):176-182. doi:10.1093/embo-reports/kvd029

113. Morikawa M, Koinuma D, Tsutsumi S, et al. ChIP-seq reveals cell type-specific binding patterns of BMP-specific Smads and a novel binding motif. *Nucleic Acids Research*. 2011;39(20):8712-8727. doi:10.1093/nar/gkr572

114. Inman GJ, Nicolás FJ, Hill CS. Nucleocytoplasmic Shuttling of Smads 2, 3, and 4 Permits Sensing of TGF-β Receptor Activity. *Molecular Cell*. 2002;10(2):283-294. doi:10.1016/S1097-2765(02)00585-3

115. Valdimarsdottir G, Goumans MJ, Itoh F, Itoh S, Heldin CH, Dijke P ten. Smad7 and protein phosphatase 1α are critical determinants in the duration of TGF-β/ALK1 signaling in endothelial cells. *BMC Cell Biol*. 2006;7(1):16. doi:10.1186/1471-2121-7-16

116. Kavsak P, Rasmussen RK, Causing CG, et al. Smad7 Binds to Smurf2 to Form an E3 Ubiquitin Ligase that Targets the TGFβ Receptor for Degradation. *Molecular Cell*. 2000;6(6):1365-1375. doi:10.1016/S1097-2765(00)00134-9

117. Murakami G, Watabe T, Takaoka K, Miyazono K, Imamura T. Cooperative Inhibition of Bone Morphogenetic Protein Signaling by Smurf1 and Inhibitory Smads. *MBoC*. 2003;14(7):2809-2817. doi:10.1091/mbc.e02-07-0441

118. Ebisawa T, Fukuchi M, Murakami G, et al. Smurf1 Interacts with Transforming Growth Factor-β Type I Receptor through Smad7 and Induces Receptor Degradation. *Journal of Biological Chemistry*. 2001;276(16):12477-12480. doi:10.1074/jbc.C100008200

119. Zhang YE. Non-Smad Signaling Pathways of the TGF-β Family. *Cold Spring Harb Perspect Biol*. 2017;9(2):a022129. doi:10.1101/cshperspect.a022129

120. David L, Mallet C, Vailhé B, Lamouille S, Feige JJ, Bailly S. Activin receptor-like kinase 1 inhibits human microvascular endothelial cell migration: Potential roles for JNK and ERK. *J Cell Physiol*. 2007;213(2):484-489. doi:10.1002/jcp.21126

121. Seki T, Yun J, Oh SP. Arterial Endothelium-Specific Activin Receptor-Like Kinase 1 Expression Suggests Its Role in Arterialization and Vascular Remodeling. *Circulation Research*. 2003;93(7):682-689. doi:10.1161/01.RES.0000095246.40391.3B

122. Jonker L, Arthur HM. Endoglin expression in early development is associated with vasculogenesis and angiogenesis. *Mechanisms of Development*. 2002;110(1-2):193-196. doi:10.1016/S0925-4773(01)00562-7

123. Corti P, Young S, Chen CY, et al. Interaction between *alk1* and blood flow in the development of arteriovenous malformations. *Development*. 2011;138(8):1573-1582. doi:10.1242/dev.060467

124. Galaris G, Montagne K, Thalgott JH, et al. Thresholds of Endoglin Expression in Endothelial Cells Explains Vascular Etiology in Hereditary Hemorrhagic Telangiectasia Type 1. *IJMS*. 2021;22(16):8948. doi:10.3390/ijms22168948

125. Meurer SK, Weiskirchen R. Endoglin: An 'Accessory' Receptor Regulating Blood Cell Development and Inflammation. *IJMS*. 2020;21(23):9247. doi:10.3390/ijms21239247

126. Zhao D, Yang F, Wang Y, et al. ALK1 signaling is required for the homeostasis of Kupffer cells and prevention of bacterial infection. *Journal of Clinical Investigation*. 2022;132(3):e150489. doi:10.1172/JCI150489

127. Lux A, Attisano L, Marchuk DA. Assignment of Transforming Growth Factor ␤1 and ␤3 and a Third New Ligand to the Type I Receptor ALK-1. :10.

128. Goumans MJ. Balancing the activation state of the endothelium via two distinct TGF-beta type I receptors. *The EMBO Journal*. 2002;21(7):1743-1753. doi:10.1093/emboj/21.7.1743

129. Seki T, Hong KH, Oh SP. Nonoverlapping expression patterns of ALK1 and ALK5 reveal distinct roles of each receptor in vascular development. *Laboratory Investigation*. 2006;86(2):116-129. doi:10.1038/labinvest.3700376

130. Park SO, Lee YJ, Seki T, et al. ALK5- and TGFBR2-independent role of ALK1 in the pathogenesis of hereditary hemorrhagic telangiectasia type 2. *Blood*. 2008;111(2):633-642. doi:10.1182/blood-2007-08-107359

131. David L, Mallet C, Mazerbourg S, Feige JJ, Bailly S. Identification of BMP9 and BMP10 as functional activators of the orphan activin receptor-like kinase 1 (ALK1) in endothelial cells. *Blood*. 2007;109(5):1953-1961. doi:10.1182/blood-2006-07-034124

132. Brown MA, Zhao Q, Baker KA, et al. Crystal Structure of BMP-9 and Functional Interactions with Pro-region and Receptors. *Journal of Biological Chemistry*. 2005;280(26):25111-25118. doi:10.1074/jbc.M503328200

133. Scharpfenecker M, van Dinther M, Liu Z, et al. BMP-9 signals via ALK1 and inhibits bFGF-induced endothelial cell proliferation and VEGF-stimulated angiogenesis. *Journal of Cell Science*. 2007;120(6):964-972. doi:10.1242/jcs.002949

134. Saito T, Bokhove M, Croci R, et al. Structural Basis of the Human Endoglin-BMP9 Interaction: Insights into BMP Signaling and HHT1. *Cell Reports*. 2017;19(9):1917-1928. doi:10.1016/j.celrep.2017.05.011

135. Barbara NP, Wrana JL, Letarte M. Endoglin Is an Accessory Protein That Interacts with the Signaling Receptor Complex of Multiple Members of the Transforming Growth Factor-β Superfamily. *Journal of Biological Chemistry*. 1999;274(2):584-594. doi:10.1074/jbc.274.2.584

136. Cheifetz S, Bellón T, Calés C, et al. Endoglin is a component of the transforming growth factor-beta receptor system in human endothelial cells. *J Biol Chem*. 1992;267(27):19027-19030.

137. Nickel J, Ten Dijke P, Mueller TD. TGF-β family co-receptor function and signaling. *ABBS*. 2018;50(1):12-36. doi:10.1093/abbs/gmx126

138. Lawera A, Tong Z, Thorikay M, et al. Role of soluble endoglin in BMP9 signaling. *Proc Natl Acad Sci USA*. 2019;116(36):17800-17808. doi:10.1073/pnas.1816661116

139. Hawinkels LJAC, Kuiper P, Wiercinska E, et al. Matrix Metalloproteinase-14 (MT1-MMP)–Mediated Endoglin Shedding Inhibits Tumor Angiogenesis. *Cancer Research*. 2010;70(10):4141-4150. doi:10.1158/0008-5472.CAN-09-4466

140. Townson SA, Martinez-Hackert E, Greppi C, et al. Specificity and Structure of a High Affinity Activin Receptor-like Kinase 1 (ALK1) Signaling Complex. *J Biol Chem*. 2012;287(33):27313-27325. doi:10.1074/jbc.M112.377960

141. Ali IHA, Brazil DP. Bone morphogenetic proteins and their antagonists: current and emerging clinical uses: Targeting BMPs in human disease. *Br J Pharmacol*. 2014;171(15):3620-3632. doi:10.1111/bph.12724

142. Seemann P, Brehm A, König J, et al. Mutations in GDF5 Reveal a Key Residue Mediating BMP Inhibition by NOGGIN. Barsh GS, ed. *PLoS Genet*. 2009;5(11):e1000747. doi:10.1371/journal.pgen.1000747

143. Goumans MJ, Zwijsen A, ten Dijke P, Bailly S. Bone Morphogenetic Proteins in Vascular Homeostasis and Disease. *Cold Spring Harb Perspect Biol*. 2018;10(2):a031989. doi:10.1101/cshperspect.a031989

144. Chen H, Shi S, Acosta L, et al. BMP10 is essential for maintaining cardiac growth during murine cardiogenesis. *Development*. 2004;131(9):2219-2231. doi:10.1242/dev.01094

145. Tillet E, Ouarné M, Desroches-Castan A, et al. A heterodimer formed by bone morphogenetic protein 9 (BMP9) and BMP10 provides most BMP biological activity in plasma. *Journal of Biological Chemistry*. 2018;293(28):10963-10974. doi:10.1074/jbc.RA118.002968

146. Liu W, Deng Z, Zeng Z, et al. Highly expressed BMP9/GDF2 in postnatal mouse liver and lungs may account for its pleiotropic effects on stem cell differentiation, angiogenesis, tumor growth and metabolism. *Genes & Diseases*. 2020;7(2):235-244. doi:10.1016/j.gendis.2019.08.003

147. López-Coviella I, Berse B, Krauss R, Thies RS, Blusztajn JK. Induction and Maintenance of the Neuronal Cholinergic Phenotype in the Central Nervous System by BMP-9. *Science*. 2000;289(5477):313-316. doi:10.1126/science.289.5477.313

148. Little SC, Mullins MC. Bone morphogenetic protein heterodimers assemble heteromeric type I receptor complexes to pattern the dorsoventral axis. *Nat Cell Biol*. 2009;11(5):637-643. doi:10.1038/ncb1870

149. Suzuki A, Kaneko E, Maeda J, Ueno N. Mesoderm Induction by BMP-4 and -7 Heterodimers. *Biochemical and Biophysical Research Communications*. 1997;232(1):153-156. doi:10.1006/bbrc.1997.6219

150. Mottershead DG, Sugimura S, Al-Musawi SL, et al. Cumulin, an Oocyte-secreted Heterodimer of the Transforming Growth Factor-β Family, Is a Potent Activator of Granulosa Cells and Improves Oocyte Quality. *Journal of Biological Chemistry*. 2015;290(39):24007-24020. doi:10.1074/jbc.M115.671487

151. Hwan Kim Y, Vu PN, Choe S woon, et al. Overexpression of Activin Receptor-Like Kinase 1 in Endothelial Cells Suppresses Development of Arteriovenous Malformations in Mouse Models of Hereditary Hemorrhagic Telangiectasia. *Circ Res*. 2020;127(9):1122-1137. doi:10.1161/CIRCRESAHA.119.316267

152. Upton PD, Davies RJ, Trembath RC, Morrell NW. Bone Morphogenetic Protein (BMP) and Activin Type II Receptors Balance BMP9 Signals Mediated by Activin Receptor-like Kinase-1 in Human Pulmonary Artery Endothelial Cells. *Journal of Biological Chemistry*. 2009;284(23):15794-15804. doi:10.1074/jbc.M109.002881

153. Star GP, Giovinazzo M, Langleben D. Bone morphogenic protein-9 stimulates endothelin-1 release from human pulmonary microvascular endothelial cells. *Microvascular Research*. 2010;80(3):349-354. doi:10.1016/j.mvr.2010.05.010

154. Ota T, Fujii M, Sugizaki T, et al. Targets of transcriptional regulation by two distinct type I receptors for transforming growth factor-? in human umbilical vein endothelial cells. *J Cell Physiol*. 2002;193(3):299-318. doi:10.1002/jcp.10170

155. Lamouille S, Mallet C, Feige JJ, Bailly S. Activin receptor–like kinase 1 is implicated in the maturation phase of angiogenesis. *Blood*. 2002;100(13):4495-4501. doi:10.1182/blood.V100.13.4495

156. Mallet C, Vittet D, Feige JJ, Bailly S. TGFbeta1 induces vasculogenesis and inhibits angiogenic sprouting in an embryonic stem cell differentiation model: respective contribution of ALK1 and ALK5. *Stem Cells*. 2006;24(11):2420-2427. doi:10.1634/stemcells.2005-0494

157. David L, Mallet C, Keramidas M, et al. Bone Morphogenetic Protein-9 Is a Circulating Vascular Quiescence Factor. *Circulation Research*. 2008;102(8):914-922. doi:10.1161/CIRCRESAHA.107.165530

158. Akla N, Viallard C, Popovic N, Lora Gil C, Sapieha P, Larrivée B. BMP9 (Bone Morphogenetic Protein-9)/Alk1 (Activin-Like Kinase Receptor Type I) Signaling Prevents Hyperglycemia-Induced Vascular Permeability. *ATVB*. 2018;38(8):1821-1836. doi:10.1161/ATVBAHA.118.310733

159. Long L, Ormiston ML, Yang X, et al. Selective enhancement of endothelial BMPR-II with BMP9 reverses pulmonary arterial hypertension. *Nat Med*. 2015;21(7):777-785. doi:10.1038/nm.3877

160. Ricard N, Ciais D, Levet S, et al. BMP9 and BMP10 are critical for postnatal retinal vascular remodeling. *Blood*. 2012;119(25):6162-6171. doi:10.1182/blood-2012-01-407593

161. Chen H, Brady Ridgway J, Sai T, et al. Context-dependent signaling defines roles of BMP9 and BMP10 in embryonic and postnatal development. *Proc Natl Acad Sci USA*. 2013;110(29):11887-11892. doi:10.1073/pnas.1306074110

162. Bouvard C, Tu L, Rossi M, et al. Different cardiovascular and pulmonary phenotypes for single- and double-knock-out mice deficient in BMP9 and BMP10. *Cardiovascular Research*. 2022;118(7):1805-1820. doi:10.1093/cvr/cvab187

163. Levet S, Ciais D, Merdzhanova G, et al. Bone morphogenetic protein 9 (BMP9) controls lymphatic vessel maturation and valve formation. *Blood*. 2013;122(4):598-607. doi:10.1182/blood-2012-12-472142

164. Yoshimatsu Y, Lee YG, Akatsu Y, et al. Bone morphogenetic protein-9 inhibits lymphatic vessel formation via activin receptor-like kinase 1 during development and cancer progression. *Proc Natl Acad Sci USA*. 2013;110(47):18940-18945. doi:10.1073/pnas.1310479110

165. Desroches-Castan A, Tillet E, Ricard N, et al. Bone Morphogenetic Protein 9 Is a Paracrine Factor Controlling Liver Sinusoidal Endothelial Cell Fenestration and Protecting Against Hepatic Fibrosis. *Hepatology*. 2019;70(4):1392-1408. doi:10.1002/hep.30655

166. Li W, Long L, Yang X, et al. Circulating BMP9 Protects the Pulmonary Endothelium during Inflammation-induced Lung Injury in Mice. *Am J Respir Crit Care Med*. 2021;203(11):1419-1430. doi:10.1164/rccm.202005-1761OC

167. Ruiz S, Zhao H, Chandakkar P, et al. A mouse model of hereditary hemorrhagic telangiectasia generated by transmammary-delivered immunoblocking of BMP9 and BMP10. *Sci Rep*. 2016;6(1):37366. doi:10.1038/srep37366

168. Levet S, Ouarné M, Ciais D, et al. BMP9 and BMP10 are necessary for proper closure of the ductus arteriosus. *Proc Natl Acad Sci USA*. 2015;112(25). doi:10.1073/pnas.1508386112

169. Choi H, Kim BG, Kim YH, Lee SJ, Lee YJ, Oh SP. BMP10 functions independently from BMP9 for the development of a proper arteriovenous network. *Angiogenesis*. 2023;26(1):167-186. doi:10.1007/s10456-022-09859-0

170. Baeyens N, Nicoli S, Coon BG, et al. Vascular remodeling is governed by a VEGFR3-dependent fluid shear stress set point. *eLife*. 2015;4:e04645. doi:10.7554/eLife.04645

171. Baeyens N, Larrivée B, Ola R, et al. Defective fluid shear stress mechanotransduction mediates hereditary hemorrhagic telangiectasia. *Journal of Cell Biology*. 2016;214(7):807-816. doi:10.1083/jcb.201603106

172. Laux DW, Young S, Donovan JP, Mansfield CJ, Upton PD, Roman BL. Circulating Bmp10 acts through endothelial Alk1 to mediate flow-dependent arterial quiescence. *Development*. 2013;140(16):3403-3412. doi:10.1242/dev.095307

173. Vion AC, Alt S, Klaus-Bergmann A, et al. Primary cilia sensitize endothelial cells to BMP and prevent excessive vascular regression. *Journal of Cell Biology*. 2018;217(5):1651-1665. doi:10.1083/jcb.201706151

174. Kjeldsen AD, Vase P, Green A. Hereditary haemorrhagic telangiectasia: a population-based study of prevalence and mortality in Danish patients. *J Intern Med*. 1999;245(1):31-39. doi:10.1046/j.1365-2796.1999.00398.x

175. Puente RZ, Bueno J, Salcedo M. Epidemiology of Hereditary Haemorrhagic Telangiectasia (HHT) in Spain. *Hereditary Genet*. 2016;05(03). doi:10.4172/2161-1041.1000173

176. Bideau A, Plauchu H, Brunet G, Robert J. Epidemiological investigation of Rendu-Osler disease in France: its geographical distribution and prevalence. *Popul*. 1989;44(1):3-22.

177. Dupuis-Girod S, Bailly S, Plauchu H. Hereditary hemorrhagic telangiectasia: from molecular biology to patient care: Hereditary hemorrhagic telangiectasia. *Journal of Thrombosis and Haemostasis*. 2010;8(7):1447-1456. doi:10.1111/j.1538-7836.2010.03860.x

178. Juares AJC, Dell'Aringa AR, Nardi JC, Kobari K, Rodrigues VLMGM, Filho RMP. Rendu-Osler-Weber Syndrome: case report and literature review. *Brazilian Journal of Otorhinolaryngology*. 2008;74(3):452-457. doi:10.1016/S1808-8694(15)30582-6

179. Becker RE. Remembering Sir William Osler 100 years after his death: what can we learn from his legacy? *The Lancet*. 2014;384(9961):2260-2263. doi:10.1016/S0140-6736(14)61887-0

180. Fuchizaki U, Miyamori H, Kitagawa S, Kaneko S, Kobayashi K. Hereditary haemorrhagic telangiectasia (Rendu-Osler-Weber disease). *The Lancet*. 2003;362(9394):1490-1494. doi:10.1016/S0140-6736(03)14696-X

181. McAllister KA, Grogg KM, Johnson DW, et al. Endoglin, a TGF-P binding protein of endothelial cells, is the gene for hereditary haemorrhagic telangiectasia type. 1994;8:7.

182. Johnson DW, Berg JN, Baldwin MA, et al. Mutations in the activin receptor–like kinase 1 gene in hereditary haemorrhagic telangiectasia type 2. *Nat Genet*. 1996;13(2):189-195. doi:10.1038/ng0696-189

183. Lesca G, Burnichon N, Raux G, et al. Distribution ofENG andACVRL1 (ALK1) mutations in French HHT patients. *Hum Mutat*. 2006;27(6):598-598. doi:10.1002/humu.9421

184. Olivieri C, Pagella F, Semino L, et al. Analysis of ENG and ACVRL1 genes in 137 HHT Italian families identifies 76 different mutations (24 novel). Comparison with other European studies. *J Hum Genet*. 2007;52(10):820-829. doi:10.1007/s10038-007-0187-5

185. Prigoda NL. Hereditary haemorrhagic telangiectasia: mutation detection, test sensitivity and novel mutations. *Journal of Medical Genetics*. 2006;43(9):722-728. doi:10.1136/jmg.2006.042606

186. Richards-Yutz J, Grant K, Chao EC, Walther SE, Ganguly A. Update on molecular diagnosis of hereditary hemorrhagic telangiectasia. *Hum Genet*. 2010;128(1):61-77. doi:10.1007/s00439-010-0825-4

187. Shovlin CL, Simeoni I, Downes K, et al. Mutational and phenotypic characterization of hereditary hemorrhagic telangiectasia. *Blood*. 2020;136(17):1907-1918. doi:10.1182/blood.2019004560

188. Gallione CJ, Repetto GM, Legius E, et al. A combined syndrome of juvenile polyposis and hereditary haemorrhagic telangiectasia associated with mutations in MADH4 (SMAD4). *The Lancet*. 2004;363(9412):852-859. doi:10.1016/S0140-6736(04)15732-2

189. Calva-Cerqueira D, Chinnathambi S, Pechman B, Bair J, Larsen-Haidle J, Howe J. The rate of germline mutations and large deletions of *SMAD4* and *BMPR1A* in juvenile polyposis. *Clinical Genetics*. 2009;75(1):79-85. doi:10.1111/j.1399-0004.2008.01091.x

190. Wooderchak WL, Spencer Z, Crockett DK, McDonald J, Bayrak-Toydemir P. Repository of SMAD4 Mutations: Reference for Genotype/ Phenotype Correlation. *J Data Mining in Genom Proteomics*. 2010;01(01). doi:10.4172/2153-0602.1000101

191. Wooderchak-Donahue WL, McDonald J, O'Fallon B, et al. BMP9 Mutations Cause a Vascular-Anomaly Syndrome with Phenotypic Overlap with Hereditary Hemorrhagic Telangiectasia. *The American Journal of Human Genetics*. 2013;93(3):530-537. doi:10.1016/j.ajhg.2013.07.004

192. Balachandar S, Graves TJ, Shimonty A, et al. Identification and validation of a novel pathogenic variant in *GDF2* (BMP9) responsible for hereditary hemorrhagic telangiectasia and pulmonary arteriovenous malformations. *American J of Med Genetics Pt A*. 2022;188(3):959-964. doi:10.1002/ajmg.a.62584

193. Liu J, Yang J, Tang X, et al. Homozygous *GDF2* -Related Hereditary Hemorrhagic Telangiectasia in a Chinese Family. *Pediatrics*. 2020;146(2):e20191970. doi:10.1542/peds.2019-1970

194. Hodgson J, Ruiz-Llorente L, McDonald J, et al. Homozygous *GDF2* nonsense mutations result in a loss of circulating BMP9 and BMP10 and are associated with either PAH or an "HHT-like" syndrome in children. *Molec Gen & Gen Med*. 2021;9(12). doi:10.1002/mgg3.1685

195. Cole SG. A new locus for hereditary haemorrhagic telangiectasia (HHT3) maps to chromosome 5. *Journal of Medical Genetics*. 2005;42(7):577-582. doi:10.1136/jmg.2004.028712

196. Bayrak-Toydemir P, McDonald J, Akarsu N, et al. A fourth locus for hereditary hemorrhagic telangiectasia maps to chromosome 7. *Am J Med Genet*. 2006;140A(20):2155-2162. doi:10.1002/ajmg.a.31450

197. Jiang X, Wooderchak-Donahue WL, McDonald J, et al. Inactivating mutations in Drosha mediate vascular abnormalities similar to hereditary hemorrhagic telangiectasia. *Sci Signal*. 2018;11(513):eaan6831. doi:10.1126/scisignal.aan6831

198. Guilhem A, Dupuis-Girod S, Espitia O, et al. Seven cases of hereditary haemorrhagic telangiectasia-like hepatic vascular abnormalities associated with *EPHB4* pathogenic variants. *J Med Genet*. Published online February 22, 2023:jmg-2022-109107. doi:10.1136/jmg-2022-109107

199. Shovlin CL, Guttmacher AE, Buscarini E, et al. Diagnostic criteria for hereditary hemorrhagic telangiectasia (Rendu-Osler-Weber syndrome). *Am J Med Genet*. 2000;91(1):66-67. doi:10.1002/(sici)1096-8628(20000306)91:1<66::aid-ajmg12>3.0.co;2-p

200. Plauchu H, De Chadarévian JP, Bideau A, Robert JM. Age-related clinical profile of hereditary hemorrhagic telangiectasia in an epidemiologically recruited population. *Am J Med Genet*. 1989;32(3):291-297. doi:10.1002/ajmg.1320320302

201. Faughnan ME, Palda VA, Garcia-Tsao G, et al. International guidelines for the diagnosis and management of hereditary haemorrhagic telangiectasia. *Journal of Medical Genetics*. 2011;48(2):73-87. doi:10.1136/jmg.2009.069013

202. McDonald J, Bayrak-Toydemir P, DeMille D, Wooderchak-Donahue W, Whitehead K. Curaçao diagnostic criteria for hereditary hemorrhagic telangiectasia is highly predictive of a pathogenic variant in ENG or ACVRL1 (HHT1 and HHT2). *Genetics in Medicine*. 2020;22(7):1201-1205. doi:10.1038/s41436-020-0775-8

203. AAssar OS, Friedman CM, White RI. The Natural History of Epistaxis in Hereditary Hemorrhagic Telangiectasia: *The Laryngoscope*. 1991;101(9):977???980. doi:10.1288/00005537-199109000-00008

204. Westermann CJJ, Rosina AF, de Vries V, Coteau PA de. The prevalence and manifestations of hereditary hemorrhagic telangiectasia in the Afro-Caribbean population of the Netherlands Antilles: A family screening. *Am J Med Genet*. 2003;116A(4):324-328. doi:10.1002/ajmg.a.10002

205. Plauchu H, De Chadarévian JP, Bideau A, Robert JM. Age-related clinical profile of hereditary hemorrhagic telangiectasia in an epidemiologically recruited population. *Am J Med Genet*. 1989;32(3):291-297. doi:10.1002/ajmg.1320320302

206. Bayrak-Toydemir P, McDonald J, Markewitz B, et al. Genotype–phenotype correlation in hereditary hemorrhagic telangiectasia: Mutations and manifestations. *Am J Med Genet*. 2006;140A(5):463-470. doi:10.1002/ajmg.a.31101

207. McCaffrey TV, Kern EB, Lake CF. Management of Epistaxis in Hereditary Hemorrhagic Telangiectasia: Review of 80 Cases. *Archives of Otolaryngology - Head and Neck Surgery*. 1977;103(11):627-630. doi:10.1001/archotol.1977.00780280027001

208. Guttmacher AE, Marchuk DA, Trerotola SO, Pyeritz RE. Hereditary Hemorrhagic Telangiectasia (Osler–Weber–Rendu Syndrome). In: *Emery and Rimoin's Principles and Practice of Medical Genetics*. Elsevier; 2013:1-18. doi:10.1016/B978-0-12-383834-6.00055-0

209. Shovlin CL, Guttmacher AE, Buscarini E, et al. Diagnostic criteria for hereditary hemorrhagic telangiectasia (Rendu-Osler-Weber syndrome). :2.

210. Letteboer TGW, Mager HJ, Snijder RJ, et al. Genotype-phenotype relationship for localization and age distribution of telangiectases in hereditary hemorrhagic telangiectasia. *Am J Med Genet*. 2008;146A(21):2733-2739. doi:10.1002/ajmg.a.32243

211. Braverman IM, Keh A, Jacobson BS. Ultrastructure and Three-Dimensional Organization of the Telangiectases of Hereditary Hemorrhagic Telangiectasia. *Journal of Investigative Dermatology*. 1990;95(4):422-427. doi:10.1111/1523-1747.ep12555569

212. Harwin J, Sugi MD, Hetts SW, Conrad MB, Ohliger MA. The Role of Liver Imaging in Hereditary Hemorrhagic Telangiectasia. *JCM*. 2020;9(11):3750. doi:10.3390/jcm9113750

213. Wu P, Horwith A, Mai S, Parikh M, Tyagi G, Pai R. High-Output Cardiac Failure Due to Hereditary Hemorrhagic Telangiectasia: A Case of an Extra-Cardiac Left to Right Shunt. *Int J Angiol*. 2017;26(02):125-129. doi:10.1055/s-0035-1568878

214. Dupuis-Girod S, Cottin V, Shovlin CL. The Lung in Hereditary Hemorrhagic Telangiectasia. *Respiration*. 2017;94(4):315-330. doi:10.1159/000479632

215. Lesca G, Olivieri C, Burnichon N, et al. Genotype-phenotype correlations in hereditary hemorrhagic telangiectasia: Data from the French-Italian HHT network. *Genetics in Medicine*. 2007;9(1):14-22. doi:10.1097/GIM.0b013e31802d8373

216. Komiyama M, Ishiguro T, Yamada O, Morisaki H, Morisaki T. Hereditary hemorrhagic telangiectasia in Japanese patients. *J Hum Genet*. 2014;59(1):37-41. doi:10.1038/jhg.2013.113

217. Drapé E, Anquetil T, Larrivée B, Dubrac A. Brain arteriovenous malformation in hereditary hemorrhagic telangiectasia: Recent advances in cellular and molecular mechanisms. *Front Hum Neurosci*. 2022;16:1006115. doi:10.3389/fnhum.2022.1006115

218. Cymerman U, Vera S, Pece-Barbara N, et al. Identification of Hereditary Hemorrhagic Telangiectasia Type 1 in Newborns by Protein Expression and Mutation Analysis of Endoglin. *Pediatr Res*. 2000;47(1):24-24. doi:10.1203/00006450-200001000-00008

219. Fernandezl A, Sanzrodriguez F, Zarrabeitia R, et al. Blood outgrowth endothelial cells from Hereditary Haemorrhagic Telangiectasia patients reveal abnormalities compatible with vascular lesions. *Cardiovascular Research*. 2005;68(2):235-248. doi:10.1016/j.cardiores.2005.06.009

220. Fernandez-L A, Sanz-Rodriguez F, Zarrabeitia R, et al. Mutation study of Spanish patients with hereditary hemorrhagic telangiectasia and expression analysis of Endoglin and ALK1. *Hum Mutat*. 2006;27(3):295-295. doi:10.1002/humu.9413

221. Mallet C, Lamribet K, Giraud S, et al. Functional analysis of endoglin mutations from hereditary hemorrhagic telangiectasia type 1 patients reveals different mechanisms for endoglin loss of function. *Human Molecular Genetics*. 2015;24(4):1142-1154. doi:10.1093/hmg/ddu531

222. Förg T, Hafner M, Lux A. Investigation of Endoglin Wild-Type and Missense Mutant Protein Heterodimerisation Using Fluorescence Microscopy Based IF, BiFC and FRET Analyses. Koval M, ed. *PLoS ONE*. 2014;9(7):e102998. doi:10.1371/journal.pone.0102998

223. Abdalla SA. Analysis of ALK-1 and endoglin in newborns from families with hereditary hemorrhagic telangiectasia type 2. *Human Molecular Genetics*. 2000;9(8):1227-1237. doi:10.1093/hmg/9.8.1227

224. Ricard N, Bidart M, Mallet C, et al. Functional analysis of the BMP9 response of ALK1 mutants from HHT2 patients: a diagnostic tool for novel ACVRL1 mutations. *Blood*. 2010;116(9):1604-1612. doi:10.1182/blood-2010-03-276881

225. Gu Y, Jin P, Zhang L, et al. Functional analysis of mutations in the kinase domain of the TGF-β receptor ALK1 reveals different mechanisms for induction of hereditary hemorrhagic telangiectasia. *Blood*. 2006;107(5):1951-1954. doi:10.1182/blood-2005-05-1834

226. Bourdeau A, Dumont DJ, Letarte M. A murine model of hereditary hemorrhagic telangiectasia. *J Clin Invest*. 1999;104(10):1343-1351. doi:10.1172/JCI8088

227. Srinivasan S. A mouse model for hereditary hemorrhagic telangiectasia (HHT) type 2. *Human Molecular Genetics*. 2003;12(5):473-482. doi:10.1093/hmg/ddg050

228. Arthur HM, Ure J, Smith AJH, et al. Endoglin, an Ancillary TGFβ Receptor, Is Required for Extraembryonic Angiogenesis and Plays a Key Role in Heart Development. *Developmental Biology*. 2000;217(1):42-53. doi:10.1006/dbio.1999.9534

229. Torsney E, Charlton R, Diamond AG, Burn J, Soames JV, Arthur HM. Mouse Model for Hereditary Hemorrhagic Telangiectasia Has a Generalized Vascular Abnormality. *Circulation*. 2003;107(12):1653-1657. doi:10.1161/01.CIR.0000058170.92267.00

230. Kritharis A, Al-Samkari H, Kuter DJ. Hereditary hemorrhagic telangiectasia: diagnosis and management from the hematologist's perspective. *Haematologica*. 2018;103(9):1433-1443. doi:10.3324/haematol.2018.193003

231. Bernabeu C, Bayrak-Toydemir P, McDonald J, Letarte M. Potential Second-Hits in Hereditary Hemorrhagic Telangiectasia. *JCM*. 2020;9(11):3571. doi:10.3390/jcm9113571

232. Rossi E, Sanz-Rodriguez F, Eleno N, et al. Endothelial endoglin is involved in inflammation: role in leukocyte adhesion and transmigration. *Blood*. 2013;121(2):403-415. doi:10.1182/blood-2012-06-435347

233. Rossi E, Lopez-Novoa JM, Bernabeu C. Endoglin involvement in integrin-mediated cell adhesion as a putative pathogenic mechanism in hereditary hemorrhagic telangiectasia type 1 (HHT1). *Front Genet*. 2015;5. doi:10.3389/fgene.2014.00457

234. Xu B, Wu YQ, Huey M, et al. Vascular Endothelial Growth Factor Induces Abnormal Microvasculature in the Endoglin Heterozygous Mouse Brain. *J Cereb Blood Flow Metab*. 2004;24(2):237-244. doi:10.1097/01.WCB.0000107730.66603.51

235. Hao Q, Zhu Y, Su H, et al. VEGF Induces More Severe Cerebrovascular Dysplasia in Eng+/− than in Alk1+/− Mice. *Transl Stroke Res*. 2010;1(3):197-201. doi:10.1007/s12975-010-0020-x

236. Park SO, Wankhede M, Lee YJ, et al. Real-time imaging of de novo arteriovenous malformation in a mouse model of hereditary hemorrhagic telangiectasia. *J Clin Invest*. Published online October 1, 2009:JCI39482. doi:10.1172/JCI39482

237. Choi EJ, Chen W, Jun K, Arthur HM, Young WL, Su H. Novel Brain Arteriovenous Malformation Mouse Models for Type 1 Hereditary Hemorrhagic Telangiectasia. Brusgaard K, ed. *PLoS ONE*. 2014;9(2):e88511. doi:10.1371/journal.pone.0088511

238. Han C, Choe S woon, Kim YH, et al. VEGF neutralization can prevent and normalize arteriovenous malformations in an animal model for hereditary hemorrhagic telangiectasia 2. *Angiogenesis*. 2014;17(4):823-830. doi:10.1007/s10456-014-9436-3

239. Choi EJ, Walker EJ, Shen F, et al. Minimal Homozygous Endothelial Deletion of Eng with VEGF Stimulation Is Sufficient to Cause Cerebrovascular Dysplasia in the Adult Mouse. *Cerebrovasc Dis*. 2012;33(6):540-547. doi:10.1159/000337762

240. Walker EJ, Su H, Shen F, et al. Arteriovenous malformation in the adult mouse brain resembling the human disease. *Ann Neurol*. 2011;69(6):954-962. doi:10.1002/ana.22348

241. Walker EJ, Su H, Shen F, et al. Bevacizumab Attenuates VEGF-Induced Angiogenesis and Vascular Malformations in the Adult Mouse Brain. *Stroke*. 2012;43(7):1925-1930. doi:10.1161/STROKEAHA.111.647982

242. Garrido-Martin EM, Nguyen HL, Cunningham TA, et al. Common and Distinctive Pathogenetic Features of Arteriovenous Malformations in Hereditary Hemorrhagic Telangiectasia 1 and Hereditary Hemorrhagic Telangiectasia 2 Animal Models—Brief Report. *ATVB*. 2014;34(10):2232-2236. doi:10.1161/ATVBAHA.114.303984

243. Tual-Chalot S, Garcia-Collado M, Redgrave RE, et al. Loss of Endothelial Endoglin Promotes High-Output Heart Failure Through Peripheral Arteriovenous Shunting Driven by VEGF Signaling. *Circ Res*. 2020;126(2):243-257. doi:10.1161/CIRCRESAHA.119.315974

244. Tual-Chalot S, Mahmoud M, Allinson KR, et al. Endothelial Depletion of Acvrl1 in Mice Leads to Arteriovenous Malformations Associated with Reduced Endoglin Expression. Kaartinen V, ed. *PLoS ONE*. 2014;9(6):e98646. doi:10.1371/journal.pone.0098646

245. Mahmoud M, Allinson KR, Zhai Z, et al. Pathogenesis of Arteriovenous Malformations in the Absence of Endoglin. *Circulation Research*. 2010;106(8):1425-1433. doi:10.1161/CIRCRESAHA.109.211037

246. Ola R, Künzel SH, Zhang F, et al. SMAD4 Prevents Flow Induced Arteriovenous Malformations by Inhibiting Casein Kinase 2. *Circulation*. 2018;138(21):2379-2394. doi:10.1161/CIRCULATIONAHA.118.033842

247. Fruttiger M. Development of the retinal vasculature. *Angiogenesis*. 2007;10(2):77-88. doi:10.1007/s10456-007-9065-1

248. Tsuji-Tamura K, Morino-Koga S, Suzuki S, Ogawa M. The canonical smooth muscle cell marker TAGLN is present in endothelial cells and is involved in angiogenesis. *Journal of Cell Science*. 2021;134(15):jcs254920. doi:10.1242/jcs.254920

249. Harb R, Whiteus C, Freitas C, Grutzendler J. *In Vivo* Imaging of Cerebral Microvascular Plasticity from Birth to Death. *J Cereb Blood Flow Metab*. 2013;33(1):146-156. doi:10.1038/jcbfm.2012.152

250. Faughnan ME, Mager JJ, Hetts SW, et al. Second International Guidelines for the Diagnosis and Management of Hereditary Hemorrhagic Telangiectasia. *Ann Intern Med*. 2020;173(12):989-1001. doi:10.7326/M20-1443

251. Whitehead KJ, Sautter NB, McWilliams JP, et al. Effect of Topical Intranasal Therapy on Epistaxis Frequency in Patients With Hereditary Hemorrhagic Telangiectasia: A Randomized Clinical Trial. *JAMA*. 2016;316(9):943. doi:10.1001/jama.2016.11724

252. Dupuis-Girod S, Ambrun A, Decullier E, et al. Effect of Bevacizumab Nasal Spray on Epistaxis Duration in Hereditary Hemorrhagic Telangectasia: A Randomized Clinical Trial. *JAMA*. 2016;316(9):934. doi:10.1001/jama.2016.11387

253. Gaillard S, Dupuis-Girod S, Boutitie F, et al. Tranexamic acid for epistaxis in hereditary hemorrhagic telangiectasia patients: a European cross-over controlled trial in a rare disease. *Journal of Thrombosis and Haemostasis*. 2014;12(9):1494-1502. doi:10.1111/jth.12654

254. Geisthoff UW, Seyfert UT, Kübler M, Bieg B, Plinkert PK, König J. Treatment of epistaxis in hereditary hemorrhagic telangiectasia with tranexamic acid - a double-blind placebo-controlled cross-over phase IIIB study. *Thrombosis Research*. 2014;134(3):565-571. doi:10.1016/j.thromres.2014.06.012

255. Sautter NB, Smith TL. Treatment of Hereditary Hemorrhagic Telangiectasia–Related Epistaxis. *Otolaryngologic Clinics of North America*. 2016;49(3):639-654. doi:10.1016/j.otc.2016.02.010

256. Levine CG, Ross DA, Henderson KJ, Leder SB, White RI. Long-term complications of septal dermoplasty in patients with hereditary hemorrhagic telangiectasia. *Otolaryngol--head neck surg*. 2008;138(6):721-724. doi:10.1016/j.otohns.2008.01.005

257. Lund VJ, Darby Y, Rimmer J, Amin M, Husain S. Nasal closure for severe hereditary haemorrhagic telangiectasia in 100 patients. The Lund modification of the Young's procedure: a 22-year experience. *Rhin*. 2017;55(2):135-141. doi:10.4193/Rhin16.315

258. Richer SL, Geisthoff UW, Livada N, et al. The Young's Procedure for Severe Epistaxis from Hereditary Hemorrhagic Telangiectasia. *Am J Rhinol* *Allergy*. 2012;26(5):401-404. doi:10.2500/ajra.2012.26.3809

259. Ruiz-Llorente L, Gallardo-Vara E, Rossi E, Smadja DM, Botella LM, Bernabeu C. Endoglin and alk1 as therapeutic targets for hereditary hemorrhagic telangiectasia. *Expert Opinion on Therapeutic Targets*. 2017;21(10):933-947. doi:10.1080/14728222.2017.1365839

260. Dumortier J, Dupuis-Girod S, Valette PJ, et al. Recurrence of Hereditary Hemorrhagic Telangiectasia After Liver Transplantation: Clinical Implications and Physiopathological Insights. 2019;69(5):9.

261. Hanny Al-Samkari, Raj S. Kasthuri, Joseph G. Parambil, et al. An international, multicenter study of intravenous bevacizumab for bleeding in hereditary hemorrhagic telangiectasia: the InHIBIT-Bleed study. *haematol*. 2020;106(8):2161-2169. doi:10.3324/haematol.2020.261859

262. Brinkerhoff BT, Poetker DM, Choong NW. Long-Term Therapy with Bevacizumab in Hereditary Hemorrhagic Telangiectasia. *N Engl J Med*. 2011;364(7):688-689. doi:10.1056/NEJMc1012774

263. Bose P, Holter JL, Selby GB. Bevacizumab in Hereditary Hemorrhagic Telangiectasia. *N Engl J Med*. 2009;360(20):2143-2144. doi:10.1056/NEJMc0901421

264. Flieger D, Hainke S, Fischbach W. Dramatic improvement in hereditary hemorrhagic telangiectasia after treatment with the vascular endothelial growth factor (VEGF) antagonist bevacizumab. *Ann Hematol*. 2006;85(9):631-632. doi:10.1007/s00277-006-0147-8

265. Dupuis-Girod S, Ginon I, Saurin JC, et al. Bevacizumab in Patients With Hereditary Hemorrhagic Telangiectasia and Severe Hepatic Vascular Malformations and High Cardiac Output. *JAMA*. 2012;307(9). doi:10.1001/jama.2012.250

266. Epperla N, Kapke JT, Karafin M, Friedman KD, Foy P. Effect of systemic bevacizumab in severe hereditary hemorrhagic telangiectasia associated with bleeding: Bevacizumab in HHT. *Am J Hematol*. 2016;91(6):E313-E314. doi:10.1002/ajh.24367

267. Epperla N, Kleman A, Karafin M, Foy P. Re-treatment versus extended treatment strategy of systemic bevacizumab in hereditary hemorrhagic telangiectasia: which is better? *Ann Hematol*. 2018;97(9):1727-1729. doi:10.1007/s00277-018-3324-7

268. Al-Samkari H, Kritharis A, Rodriguez-Lopez JM, Kuter DJ. Systemic bevacizumab for the treatment of chronic bleeding in hereditary haemorrhagic telangiectasia. *J Intern Med*. 2019;285(2):223-231. doi:10.1111/joim.12832

269. Guilhem A, Fargeton AE, Simon AC, et al. Intra-venous bevacizumab in hereditary hemorrhagic telangiectasia (HHT): A retrospective study of 46 patients. de Jesus Perez VA, ed. *PLoS ONE*. 2017;12(11):e0188943. doi:10.1371/journal.pone.0188943

270. Iyer VN, Apala DR, Pannu BS, et al. Intravenous Bevacizumab for Refractory Hereditary Hemorrhagic Telangiectasia–Related Epistaxis and Gastrointestinal Bleeding. *Mayo Clinic Proceedings*. 2018;93(2):155-166. doi:10.1016/j.mayocp.2017.11.013

271. Robert F, Desroches-Castan A, Bailly S, Dupuis-Girod S, Feige JJ. Future treatments for hereditary hemorrhagic telangiectasia. *Orphanet J Rare Dis*. 2020;15(1):4. doi:10.1186/s13023-019-1281-4

272. Graupera M, Potente M. Regulation of angiogenesis by PI3K signaling networks. *Experimental Cell Research*. 2013;319(9):1348-1355. doi:10.1016/j.yexcr.2013.02.021

273. Alsina-Sanchís E, García-Ibáñez Y, Figueiredo AM, et al. ALK1 Loss Results in Vascular Hyperplasia in Mice and Humans Through PI3K Activation. *ATVB*. 2018;38(5):1216-1229. doi:10.1161/ATVBAHA.118.310760

274. Ola R, Dubrac A, Han J, et al. PI3 kinase inhibition improves vascular malformations in mouse models of hereditary haemorrhagic telangiectasia. *Nat Commun*. 2016;7(1):13650. doi:10.1038/ncomms13650

275. Ruiz S, Zhao H, Chandakkar P, et al. Correcting Smad1/5/8, mTOR, and VEGFR2 treats pathology in hereditary hemorrhagic telangiectasia models. *Journal of Clinical Investigation*. 2020;130(2):942-957. doi:10.1172/JCI127425

276. Snodgrass RO, Govindpani K, Plant K, et al. Therapeutic targeting of vascular malformation in a zebrafish model of hereditary haemorrhagic telangiectasia. *Disease Models & Mechanisms*. 2023;16(4):dmm049567. doi:10.1242/dmm.049567

277. Spiekerkoetter E, Tian X, Cai J, et al. FK506 activates BMPR2, rescues endothelial dysfunction, and reverses pulmonary hypertension. *J Clin Invest*. 2013;123(8):3600-3613. doi:10.1172/JCI65592

278. Ruiz S, Chandakkar P, Zhao H, et al. Tacrolimus rescues the signaling and gene expression signature of endothelial ALK1 loss-of-function and improves HHT vascular pathology. *Human Molecular Genetics*. 2017;26(24):4786-4798. doi:10.1093/hmg/ddx358

279. Hessels J, Kroon S, Boerman S, et al. Efficacy and Safety of Tacrolimus as Treatment for Bleeding Caused by Hereditary Hemorrhagic Telangiectasia: An Open-Label, Pilot Study. *JCM*. 2022;11(18):5280. doi:10.3390/jcm11185280

280. Dupuis-Girod S, Fargeton AE, Grobost V, et al. Efficacy and Safety of a 0.1% Tacrolimus Nasal Ointment as a Treatment for Epistaxis in Hereditary Hemorrhagic Telangiectasia: A Double-Blind, Randomized, Placebo-Controlled, Multicenter Trial. *JCM*. 2020;9(5):1262. doi:10.3390/jcm9051262

281. Leber L, Beaudet A, Muller A. Epidemiology of pulmonary arterial hypertension and chronic thromboembolic pulmonary hypertension: identification of the most accurate estimates from a systematic literature review. *Pulm circ*. 2021;11(1):1-12. doi:10.1177/2045894020977300

282. Guignabert C, Bailly S, Humbert M. Restoring BMPRII functions in pulmonary arterial hypertension: opportunities, challenges and limitations. *Expert Opinion on Therapeutic Targets*. 2017;21(2):181-190. doi:10.1080/14728222.2017.1275567

283. Humbert M, Kovacs G, Hoeper MM, et al. 2022 ESC/ERS Guidelines for the diagnosis and treatment of pulmonary hypertension. *Eur Heart J*. 2022;43(38):3618-3731. doi:10.1093/eurheartj/ehac237

284. Guignabert C, Dorfmuller P. Pathology and Pathobiology of Pulmonary Hypertension. *Semin Respir Crit Care Med*. 2013;34(05):551-559. doi:10.1055/s-0033-1356496

285. Rich S, Dantzker DR, Ayres SM, et al. Primary pulmonary hypertension. A national prospective study. *Ann Intern Med*. 1987;107(2):216-223. doi:10.7326/0003-4819-107-2-216

286. Brown LM, Chen H, Halpern S, et al. Delay in Recognition of Pulmonary Arterial Hypertension. *Chest*. 2011;140(1):19-26. doi:10.1378/chest.10-1166

287. Humbert M, Lau EMT, Montani D, Jaïs X, Sitbon O, Simonneau G. Advances in Therapeutic Interventions for Patients With Pulmonary Arterial Hypertension. *Circulation*. 2014;130(24):2189-2208. doi:10.1161/CIRCULATIONAHA.114.006974

288. Mandras S, Kovacs G, Olschewski H, et al. Combination Therapy in Pulmonary Arterial Hypertension—Targeting the Nitric Oxide and Prostacyclin Pathways. *J Cardiovasc Pharmacol Ther*. 2021;26(5):453-462. doi:10.1177/10742484211006531

289. Jain V, Bordes SJ, Bhardwaj A. Physiology, Pulmonary Circulatory System. In: *StatPearls*. StatPearls Publishing; 2022. Accessed March 18, 2023. http://www.ncbi.nlm.nih.gov/books/NBK525948/

290. Humbert M, Guignabert C, Bonnet S, et al. Pathology and pathobiology of pulmonary hypertension: state of the art and research perspectives. *Eur Respir J*. 2019;53(1):1801887. doi:10.1183/13993003.01887-2018

291. Guignabert C, Tu L, Le Hiress M, et al. Pathogenesis of pulmonary arterial hypertension: lessons from cancer. *European Respiratory Review*. 2013;22(130):543-551. doi:10.1183/09059180.00007513

292. Lechartier B, Berrebeh N, Huertas A, Humbert M, Guignabert C, Tu L. Phenotypic Diversity of Vascular Smooth Muscle Cells in Pulmonary Arterial Hypertension. *Chest*. 2022;161(1):219-231. doi:10.1016/j.chest.2021.08.040

293. Montani D, Günther S, Dorfmüller P, et al. Pulmonary arterial hypertension. *Orphanet J Rare Dis*. 2013;8(1):97. doi:10.1186/1750-1172-8-97

294. Sakao S, Taraseviciene-Stewart L, Lee JD, Wood K, Cool CD, Voelkel NF. Initial apoptosis is followed by increased proliferation of apoptosis-resistant endothelial cells. *FASEB j*. 2005;19(9):1178-1180. doi:10.1096/fj.04-3261fje

295. Masri FA, Xu W, Comhair SAA, et al. Hyperproliferative apoptosis-resistant endothelial cells in idiopathic pulmonary arterial hypertension. *American Journal of Physiology-Lung Cellular and Molecular Physiology*. 2007;293(3):L548-L554. doi:10.1152/ajplung.00428.2006

296. Botney MD. Role of hemodynamics in pulmonary vascular remodeling: implications for primary pulmonary hypertension. *Am J Respir Crit Care Med*. 1999;159(2):361-364. doi:10.1164/ajrccm.159.2.9805075

297. Lee SD, Shroyer KR, Markham NE, Cool CD, Voelkel NF, Tuder RM. Monoclonal endothelial cell proliferation is present in primary but not secondary pulmonary hypertension. *J Clin Invest*. 1998;101(5):927-934. doi:10.1172/JCI1910

298. Simonneau G, Montani D, Celermajer DS, et al. Haemodynamic definitions and updated clinical classification of pulmonary hypertension. *Eur Respir J*. 2019;53(1):1801913. doi:10.1183/13993003.01913-2018

299. Humbert M, Sitbon O, Chaouat A, et al. Pulmonary arterial hypertension in France: results from a national registry. *Am J Respir Crit Care Med*. 2006;173(9):1023-1030. doi:10.1164/rccm.200510-1668OC

300. Aldred MA, Morrell NW, Guignabert C. New Mutations and Pathogenesis of Pulmonary Hypertension: Progress and Puzzles in Disease Pathogenesis. *Circ Res*. 2022;130(9):1365-1381. doi:10.1161/CIRCRESAHA.122.320084

301. Larkin EK, Newman JH, Austin ED, et al. Longitudinal analysis casts doubt on the presence of genetic anticipation in heritable pulmonary arterial hypertension. *Am J Respir Crit Care Med*. 2012;186(9):892-896. doi:10.1164/rccm.201205-0886OC

302. Wertz JW, Bauer PM. Caveolin-1 regulates BMPRII localization and signaling in vascular smooth muscle cells. *Biochemical and Biophysical Research Communications*. 2008;375(4):557-561. doi:10.1016/j.bbrc.2008.08.066

303. Tomita S, Nakanishi N, Ogata T, et al. Cavin-1 modulates BMP/Smad signaling through the interaction of Caveolin-1 with BMPRII in pulmonary artery endothelial cells. *European Heart Journal*. 2021;42(Supplement_1):ehab724.1963. doi:10.1093/eurheartj/ehab724.1963

304. Atkinson C, Stewart S, Upton PD, et al. Primary Pulmonary Hypertension Is Associated With Reduced Pulmonary Vascular Expression of Type II Bone Morphogenetic Protein Receptor. *Circulation*. 2002;105(14):1672-1678. doi:10.1161/01.CIR.0000012754.72951.3D

305. Yang X, Long L, Southwood M, et al. Dysfunctional Smad Signaling Contributes to Abnormal Smooth Muscle Cell Proliferation in Familial Pulmonary Arterial Hypertension. *Circulation Research*. 2005;96(10):1053-1063. doi:10.1161/01.RES.0000166926.54293.68

306. Yang J, Davies RJ, Southwood M, et al. Mutations in Bone Morphogenetic Protein Type II Receptor Cause Dysregulation of Id Gene Expression in Pulmonary Artery Smooth Muscle Cells: Implications for Familial Pulmonary Arterial Hypertension. *Circulation Research*. 2008;102(10):1212-1221. doi:10.1161/CIRCRESAHA.108.173567

307. Yang J, Li X, Li Y, et al. Id proteins are critical downstream effectors of BMP signaling in human pulmonary arterial smooth muscle cells. *American Journal of Physiology-Lung Cellular and Molecular Physiology*. 2013;305(4):L312-L321. doi:10.1152/ajplung.00054.2013

308. Zhang S, Fantozzi I, Tigno DD, et al. Bone morphogenetic proteins induce apoptosis in human pulmonary vascular smooth muscle cells. *Am J Physiol Lung Cell Mol Physiol*. 2003;285(3):L740-754. doi:10.1152/ajplung.00284.2002

309. Davies RJ, Holmes AM, Deighton J, et al. BMP type II receptor deficiency confers resistance to growth inhibition by TGF-β in pulmonary artery smooth muscle cells: role of proinflammatory cytokines. *American Journal of Physiology-Lung Cellular and Molecular Physiology*. 2012;302(6):L604-L615. doi:10.1152/ajplung.00309.2011

310. Dunmore BJ, Drake KM, Upton PD, Toshner MR, Aldred MA, Morrell NW. The lysosomal inhibitor, chloroquine, increases cell surface BMPR-II levels and restores BMP9 signalling in endothelial cells harbouring BMPR-II mutations. *Human Molecular Genetics*. 2013;22(18):3667-3679. doi:10.1093/hmg/ddt216

311. Awad KS, Elinoff JM, Wang S, et al. Raf/ERK drives the proliferative and invasive phenotype of BMPR2-silenced pulmonary artery endothelial cells. *American Journal of Physiology-Lung Cellular and Molecular Physiology*. 2016;310(2):L187-L201. doi:10.1152/ajplung.00303.2015

312. Andruska A, Spiekerkoetter E. Consequences of BMPR2 Deficiency in the Pulmonary Vasculature and Beyond: Contributions to Pulmonary Arterial Hypertension. *IJMS*. 2018;19(9):2499. doi:10.3390/ijms19092499

313. Bisserier M, Mathiyalagan P, Zhang S, et al. Regulation of the Methylation and Expression Levels of the BMPR2 Gene by SIN3a as a Novel Therapeutic Mechanism in Pulmonary Arterial Hypertension. *Circulation*. 2021;144(1):52-73. doi:10.1161/CIRCULATIONAHA.120.047978

314. Yu PB, Beppu H, Kawai N, Li E, Bloch KD. Bone Morphogenetic Protein (BMP) Type II Receptor Deletion Reveals BMP Ligand-specific Gain of Signaling in Pulmonary Artery Smooth Muscle Cells. *Journal of Biological Chemistry*. 2005;280(26):24443-24450. doi:10.1074/jbc.M502825200

315. Nakaoka T, Gonda K, Ogita T, et al. Inhibition of rat vascular smooth muscle proliferation in vitro and in vivo by bone morphogenetic protein-2. *J Clin Invest*. 1997;100(11):2824-2832. doi:10.1172/JCI119830

316. Morrell NW, Yang X, Upton PD, et al. Altered growth responses of pulmonary artery smooth muscle cells from patients with primary pulmonary hypertension to transforming growth factor-beta(1) and bone morphogenetic proteins. *Circulation*. 2001;104(7):790-795. doi:10.1161/hc3201.094152

317. Teichert-Kuliszewska K, Kutryk MJB, Kuliszewski MA, et al. Bone Morphogenetic Protein Receptor-2 Signaling Promotes Pulmonary Arterial Endothelial Cell Survival: Implications for Loss-of-Function Mutations in the Pathogenesis of Pulmonary Hypertension. *Circulation Research*. 2006;98(2):209-217. doi:10.1161/01.RES.0000200180.01710.e6

318. Theilmann AL, Hawke LG, Hilton LR, et al. Endothelial *BMPR2* Loss Drives a Proliferative Response to BMP (Bone Morphogenetic Protein) 9 via Prolonged Canonical Signaling. *ATVB*. 2020;40(11):2605-2618. doi:10.1161/ATVBAHA.119.313357

319. Burton VJ, Ciuclan LI, Holmes AM, Rodman DM, Walker C, Budd DC. Bone morphogenetic protein receptor II regulates pulmonary artery endothelial cell barrier function. *Blood*. 2011;117(1):333-341. doi:10.1182/blood-2010-05-285973

320. Johnson JA, Hemnes AR, Perrien DS, et al. Cytoskeletal defects in Bmpr2-associated pulmonary arterial hypertension. *American Journal of Physiology-Lung Cellular and Molecular Physiology*. 2012;302(5):L474-L484. doi:10.1152/ajplung.00202.2011

321. Upton PD, Park JES, De Souza PM, et al. The endothelial protective factors, BMP9 and BMP10, inhibit CCL2 release by human vascular endothelial cells. *Journal of Cell Science*. Published online January 1, 2020:jcs.239715. doi:10.1242/jcs.239715

322. Dannewitz Prosseda S, Tian X, Kuramoto K, et al. FHIT, a Novel Modifier Gene in Pulmonary Arterial Hypertension. *Am J Respir Crit Care Med*. 2019;199(1):83-98. doi:10.1164/rccm.201712-2553OC

323. Thavathiru E, Ludes-Meyers JH, MacLeod MC, Aldaz CM. Expression of common chromosomal fragile site genes, WWOX/FRA16D and FHIT/FRA3B is downregulated by exposure to environmental carcinogens, UV, and BPDE but not by IR. *Mol Carcinog*. 2005;44(3):174-182. doi:10.1002/mc.20122

324. Li M, Vattulainen S, Aho J, et al. Loss of Bone Morphogenetic Protein Receptor 2 Is Associated with Abnormal DNA Repair in Pulmonary Arterial Hypertension. *Am J Respir Cell Mol Biol*. 2014;50(6):1118-1128. doi:10.1165/rcmb.2013-0349OC

325. Aldred MA, Comhair SA, Varella-Garcia M, et al. Somatic Chromosome Abnormalities in the Lungs of Patients with Pulmonary Arterial Hypertension. *Am J Respir Crit Care Med*. 2010;182(9):1153-1160. doi:10.1164/rccm.201003-0491OC

326. Hurst LA, Dunmore BJ, Long L, et al. TNFα drives pulmonary arterial hypertension by suppressing the BMP type-II receptor and altering NOTCH signalling. *Nat Commun*. 2017;8(1):14079. doi:10.1038/ncomms14079

327. Soon E, Crosby A, Southwood M, et al. Bone Morphogenetic Protein Receptor Type II Deficiency and Increased Inflammatory Cytokine Production. A Gateway to Pulmonary Arterial Hypertension. *Am J Respir Crit Care Med*. 2015;192(7):859-872. doi:10.1164/rccm.201408-1509OC

328. Sawada H, Saito T, Nickel NP, et al. Reduced BMPR2 expression induces GM-CSF translation and macrophage recruitment in humans and mice to exacerbate pulmonary hypertension. *Journal of Experimental Medicine*. 2014;211(2):263-280. doi:10.1084/jem.20111741

329. Chester AH, Yacoub MH. The role of endothelin-1 in pulmonary arterial hypertension. *Global Cardiology Science and Practice*. 2014;2014(2):29. doi:10.5339/gcsp.2014.29

330. Giaid A, Yanagisawa M, Langleben D, et al. Expression of Endothelin-1 in the Lungs of Patients with Pulmonary Hypertension. *N Engl J Med*. 1993;328(24):1732-1739. doi:10.1056/NEJM199306173282402

331. Stewart DJ. Increased Plasma Endothelin-1 in Pulmonary Hypertension: Marker or Mediator of Disease? *Ann Intern Med*. 1991;114(6):464. doi:10.7326/0003-4819-114-6-464

332. Davie N, Haleen SJ, Upton PD, et al. ET_A and ET_B Receptors Modulate the Proliferation of Human Pulmonary Artery Smooth Muscle Cells. *Am J Respir Crit Care Med*. 2002;165(3):398-405. doi:10.1164/ajrccm.165.3.2104059

333. Lai YC, Potoka KC, Champion HC, Mora AL, Gladwin MT. Pulmonary Arterial Hypertension: The Clinical Syndrome. *Circ Res*. 2014;115(1):115-130. doi:10.1161/CIRCRESAHA.115.301146

334. Tuder RM, Cool CD, Geraci MW, et al. Prostacyclin synthase expression is decreased in lungs from patients with severe pulmonary hypertension. *Am J Respir Crit Care Med*. 1999;159(6):1925-1932. doi:10.1164/ajrccm.159.6.9804054

335. Hoshikawa Y, Voelkel NF, Gesell TL, et al. Prostacyclin receptor-dependent modulation of pulmonary vascular remodeling. *Am J Respir Crit Care Med*. 2001;164(2):314-318. doi:10.1164/ajrccm.164.2.2010150

336. Kaufmann P, Okubo K, Bruderer S, et al. Pharmacokinetics and Tolerability of the Novel Oral Prostacyclin IP Receptor Agonist Selexipag. *Am J Cardiovasc Drugs*. 2015;15(3):195-203. doi:10.1007/s40256-015-0117-4

337. Kuwano K, Hashino A, Asaki T, et al. 2-{4-[(5,6-Diphenylpyrazin-2-yl)(isopropyl)amino]butoxy}- *N* -(methylsulfonyl)acetamide (NS-304), an Orally Available and Long-Acting Prostacyclin Receptor Agonist Prodrug. *J Pharmacol Exp Ther*. 2007;322(3):1181-1188. doi:10.1124/jpet.107.124248

338. Chen M, Lai Y, Chen R, et al. Efficacy and safety of selexipag, an oral prostacyclin receptor agonist for the treatment of pulmonary hypertension: A meta-analysis. *Pulmonary Pharmacology & Therapeutics*. 2022;72:102100. doi:10.1016/j.pupt.2021.102100

339. Reynolds AM, Holmes MD, Danilov SM, Reynolds PN. Targeted gene delivery of BMPR2 attenuates pulmonary hypertension. *European Respiratory Journal*. 2012;39(2):329-343. doi:10.1183/09031936.00187310

340. Brock M, Samillan VJ, Trenkmann M, et al. AntagomiR directed against miR-20a restores functional BMPR2 signalling and prevents vascular remodelling in hypoxia-induced pulmonary hypertension. *European Heart Journal*. 2014;35(45):3203-3211. doi:10.1093/eurheartj/ehs060

341. Drake KM, Dunmore BJ, McNelly LN, Morrell NW, Aldred MA. Correction of Nonsense *BMPR2* and *SMAD9* Mutations by Ataluren in Pulmonary Arterial Hypertension. *Am J Respir Cell Mol Biol*. 2013;49(3):403-409. doi:10.1165/rcmb.2013-0100OC

342. Sobolewski A, Rudarakanchana N, Upton PD, et al. Failure of bone morphogenetic protein receptor trafficking in pulmonary arterial hypertension: potential for rescue. *Human Molecular Genetics*. 2008;17(20):3180-3190. doi:10.1093/hmg/ddn214

343. Durrington HJ, Upton PD, Hoer S, et al. Identification of a Lysosomal Pathway Regulating Degradation of the Bone Morphogenetic Protein Receptor Type II. *Journal of Biological Chemistry*. 2010;285(48):37641-37649. doi:10.1074/jbc.M110.132415

344. Spiekerkoetter E, Sung YK, Sudheendra D, et al. Low-Dose FK506 (Tacrolimus) in End-Stage Pulmonary Arterial Hypertension. *Am J Respir Crit Care Med*. 2015;192(2):254-257. doi:10.1164/rccm.201411-2061LE

345. Spiekerkoetter E, Sung YK, Sudheendra D, et al. Randomised placebo-controlled safety and tolerability trial of FK506 (tacrolimus) for pulmonary arterial hypertension. *Eur Respir J*. 2017;50(3):1602449. doi:10.1183/13993003.02449-2016

346. Tu L, Desroches-Castan A, Mallet C, et al. Selective BMP-9 Inhibition Partially Protects Against Experimental Pulmonary Hypertension. *Circ Res*. 2019;124(6):846-855. doi:10.1161/CIRCRESAHA.118.313356

347. Szulcek R, Sanchez-Duffhues G, Rol N, et al. Exacerbated inflammatory signaling underlies aberrant response to BMP9 in pulmonary arterial hypertension lung endothelial cells. *Angiogenesis*. 2020;23(4):699-714. doi:10.1007/s10456-020-09741-x

348. Yung LM, Yang P, Joshi S, et al. ACTRIIA-Fc rebalances activin/GDF versus BMP signaling in pulmonary hypertension. *Sci Transl Med*. 2020;12(543):eaaz5660. doi:10.1126/scitranslmed.aaz5660

349. Hoeper MM, Badesch DB, Ghofrani HA, et al. Phase 3 Trial of Sotatercept for Treatment of Pulmonary Arterial Hypertension. *N Engl J Med*. Published online March 6, 2023:NEJMoa2213558. doi:10.1056/NEJMoa2213558

350. Humbert M, McLaughlin V, Gibbs JSR, et al. Sotatercept for the Treatment of Pulmonary Arterial Hypertension. *N Engl J Med*. 2021;384(13):1204-1215. doi:10.1056/NEJMoa2024277

351. Humbert M, McLaughlin V, Gibbs JSR, et al. Sotatercept for the treatment of pulmonary arterial hypertension: PULSAR open-label extension. *Eur Respir J*. 2023;61(1):2201347. doi:10.1183/13993003.01347-2022

352. Walsh LJ, Collins C, Ibrahim H, Kerins DM, Brady AP, O Connor TM. Pulmonary arterial hypertension in hereditary hemorrhagic telangiectasia associated with ACVRL1 mutation: a case report. *J Med Case Reports*. 2022;16(1):99. doi:10.1186/s13256-022-03296-9

353. Yokokawa T, Sugimoto K, Kimishima Y, et al. Pulmonary Hypertension and Hereditary Hemorrhagic Telangiectasia Related to an *ACVRL1* Mutation. *Intern Med*. 2020;59(2):221-227. doi:10.2169/internalmedicine.3625-19

354. Girerd B, Montani D, Coulet F, et al. Clinical Outcomes of Pulmonary Arterial Hypertension in Patients Carrying an *ACVRL1* (*ALK1*) Mutation. *Am J Respir Crit Care Med*. 2010;181(8):851-861. doi:10.1164/rccm.200908-1284OC

355. Davis J, Crampton SP, Hughes CCW. Isolation of Human Umbilical Vein Endothelial Cells (HUVEC). *JoVE*. 2007;(3):183. doi:10.3791/183

356. Asosingh K, Comhair S, Mavrakis L, et al. Single-cell transcriptomic profile of human pulmonary artery endothelial cells in health and pulmonary arterial hypertension. *Sci Rep*. 2021;11(1):14714. doi:10.1038/s41598-021-94163-y

357. Rhodes CJ, Im H, Cao A, et al. RNA Sequencing Analysis Detection of a Novel Pathway of Endothelial Dysfunction in Pulmonary Arterial Hypertension. *Am J Respir Crit Care Med*. 2015;192(3):356-366. doi:10.1164/rccm.201408-1528OC

358. Smadja DM, Melero-Martin JM, Eikenboom J, Bowman M, Sabatier F, Randi AM. Standardization of methods to quantify and culture endothelial colony-forming cells derived from peripheral blood: Position paper from the International Society on Thrombosis and Haemostasis SSC. *J Thromb Haemost*. 2019;17(7):1190-1194. doi:10.1111/jth.14462

359. Paschalaki KE, Randi AM. Recent Advances in Endothelial Colony Forming Cells Toward Their Use in Clinical Translation. *Front Med*. 2018;5:295. doi:10.3389/fmed.2018.00295

360. Salmon RM, Guo J, Wood JH, et al. Molecular basis of ALK1-mediated signalling by BMP9/BMP10 and their prodomain-bound forms. *Nat Commun*. 2020;11(1):1621. doi:10.1038/s41467-020-15425-3

361. Peacock HM, Tabibian A, Criem N, et al. Impaired SMAD1/5 Mechanotransduction and Cx37 (Connexin37) Expression Enable Pathological Vessel Enlargement and Shunting. *ATVB*. 2020;40(4). doi:10.1161/ATVBAHA.119.313122

362. Thomas B, Eyries M, Montagne K, et al. Altered endothelial gene expression associated with hereditary haemorrhagic telangiectasia. *Eur J Clin Invest*. 2007;37(7):580-588. doi:10.1111/j.1365-2362.2007.01824.x

363. Fernandez-Lopez A, Garrido-Martin EM, Sanz-Rodriguez F, et al. Gene expression fingerprinting for human hereditary hemorrhagic telangiectasia. *Human Molecular Genetics*. 2007;16(13):1515-1533. doi:10.1093/hmg/ddm069

364. Kim J, Kim Y, Kim HT, et al. TC1(C8orf4) Is a Novel Endothelial Inflammatory Regulator Enhancing NF-κB Activity. *The Journal of Immunology*. 2009;183(6):3996-4002. doi:10.4049/jimmunol.0900956

365. Atkins GB, Jain MK. Role of Krüppel-Like Transcription Factors in Endothelial Biology. *Circulation Research*. 2007;100(12):1686-1695. doi:10.1161/01.RES.0000267856.00713.0a

366. Townson SA, Martinez-Hackert E, Greppi C, et al. Specificity and Structure of a High Affinity Activin Receptor-like Kinase 1 (ALK1) Signaling Complex. *Journal of Biological Chemistry*. 2012;287(33):27313-27325. doi:10.1074/jbc.M112.377960

367. Kokudo T, Suzuki Y, Yoshimatsu Y, Yamazaki T, Watabe T, Miyazono K. Snail is required for TGFβ-induced endothelial-mesenchymal transition of embryonic stem cell-derived endothelial cells. *Journal of Cell Science*. 2008;121(20):3317-3324. doi:10.1242/jcs.028282

368. Morikawa M, Mitani Y, Holmborn K, et al. The ALK-1/SMAD/ATOH8 axis attenuates hypoxic responses and protects against the development of pulmonary arterial hypertension. *Sci Signal*. 2019;12(607):eaay4430. doi:10.1126/scisignal.aay4430

369. Hoffmann J, Wilhelm J, Olschewski A, Kwapiszewska G. Microarray analysis in pulmonary hypertension. *Eur Respir J*. 2016;48(1):229-241. doi:10.1183/13993003.02030-2015

370. Simões-Correia J, Silva DI, Melo S, et al. DNAJB4 molecular chaperone distinguishes WT from mutant E-cadherin, determining their fate in vitro and in vivo. *Human Molecular Genetics*. 2014;23(8):2094-2105. doi:10.1093/hmg/ddt602

371. Huso TH, Resar LM. The high mobility group A1 molecular switch: turning on cancer – can we turn it off? *Expert Opinion on Therapeutic Targets*. 2014;18(5):541-553. doi:10.1517/14728222.2014.900045

372. Viemann D, Schmolke M, Lueken A, et al. H5N1 Virus Activates Signaling Pathways in Human Endothelial Cells Resulting in a Specific Imbalanced Inflammatory Response. *The Journal of Immunology*. 2011;186(1):164-173. doi:10.4049/jimmunol.0904170

373. Zhang M, Song P, Xu J, Zou MH. Activation of NAD(P)H Oxidases by Thromboxane A $_2$ Receptor Uncouples Endothelial Nitric Oxide Synthase. *ATVB*. 2011;31(1):125-132. doi:10.1161/ATVBAHA.110.207712

374. Faughnan ME, Palda VA, Garcia-Tsao G, et al. International guidelines for the diagnosis and management of hereditary haemorrhagic telangiectasia. *Journal of Medical Genetics*. 2011;48(2):73-87. doi:10.1136/jmg.2009.069013

375. Pahl KS, Choudhury A, Wusik K, et al. Applicability of the Curaçao Criteria for the Diagnosis of Hereditary Hemorrhagic Telangiectasia in the Pediatric Population. *The Journal of Pediatrics*. 2018;197:207-213. doi:10.1016/j.jpeds.2018.01.079

376. Chan NLM, Bourdeau A, Vera S, et al. Umbilical Vein and Placental Vessels from Newborns with Hereditary Haemorrhagic Telangiectasia Type 1 Genotype are Normal despite Reduced Expression of Endoglin. *Placenta*. 2004;25(2-3):208-217. doi:10.1016/S0143-4004(03)00181-4

377. Paschalaki KE, Randi AM. Recent Advances in Endothelial Colony Forming Cells Toward Their Use in Clinical Translation. *Front Med*. 2018;5:295. doi:10.3389/fmed.2018.00295

378. Serth K, Schuster-Gossler K, Cordes R, Gossler A. Transcriptional oscillation of lunatic fringe is essential for somitogenesis. *Genes Dev*. 2003;17(7):912-925. doi:10.1101/gad.250603

379. Luo J, Tang M, Huang J, et al. TGFβ/BMP Type I Receptors ALK1 and ALK2 Are Essential for BMP9-induced Osteogenic Signaling in Mesenchymal Stem Cells. *Journal of Biological Chemistry*. 2010;285(38):29588-29598. doi:10.1074/jbc.M110.130518

380. Roesel CL, Vollmer SV. Differential gene expression analysis of symbiotic and aposymbiotic *Exaiptasia* anemones under immune challenge with *Vibrio coralliilyticus*. *Ecol Evol*. 2019;9(14):8279-8293. doi:10.1002/ece3.5403

381. Medina A, Gilbert MK, Mack BM, et al. Interactions between water activity and temperature on the Aspergillus flavus transcriptome and aflatoxin B 1 production. *International Journal of Food Microbiology*. 2017;256:36-44. doi:10.1016/j.ijfoodmicro.2017.05.020

382. Huylmans AK, Parsch J. Population- and Sex-Biased Gene Expression in the Excretion Organs of *Drosophila melanogaster*. *G3 Genes|Genomes|Genetics*. 2014;4(12):2307-2315. doi:10.1534/g3.114.013417

383. Panov J, Simchi L, Feuermann Y, Kaphzan H. Bioinformatics Analyses of the Transcriptome Reveal Ube3a-Dependent Effects on Mitochondrial-Related Pathways. *IJMS*. 2020;21(11):4156. doi:10.3390/ijms21114156

384. Ricard N, Bidart M, Mallet C, et al. Functional analysis of the BMP9 response of ALK1 mutants from HHT2 patients: a diagnostic tool for novel ACVRL1 mutations. *Blood*. 2010;116(9):1604-1612. doi:10.1182/blood-2010-03-276881

385. Tajer B, Dutko JA, Little SC, Mullins MC. BMP heterodimers signal via distinct type I receptor class functions. *Proc Natl Acad Sci USA*. 2021;118(15):e2017952118. doi:10.1073/pnas.2017952118

386. Snellings DA, Gallione CJ, Clark DS, Vozoris NT, Faughnan ME, Marchuk DA. Somatic Mutations in Vascular Malformations of Hereditary Hemorrhagic Telangiectasia Result in Bi-allelic Loss of ENG or ACVRL1. *Am J Hum Genet*. 2019;105(5):894-906. doi:10.1016/j.ajhg.2019.09.010

387. Brouillard P, Vikkula M. Genetic causes of vascular malformations. *Human Molecular Genetics*. 2007;16(R2):R140-R149. doi:10.1093/hmg/ddm211

388. Snellings DA, Girard R, Lightle R, et al. Developmental venous anomalies are a genetic primer for cerebral cavernous malformations. *Nat Cardiovasc Res*. 2022;1(3):246-252. doi:10.1038/s44161-022-00035-7

389. Bourdeau A, Cymerman U, Paquet ME, et al. Endoglin Expression Is Reduced in Normal Vessels but Still Detectable in Arteriovenous Malformations of Patients with Hereditary Hemorrhagic Telangiectasia Type 1. *The American Journal of Pathology*. 2000;156(3):911-923. doi:10.1016/S0002-9440(10)64960-7

390. Benedito R, Roca C, Sörensen I, et al. The Notch Ligands Dll4 and Jagged1 Have Opposing Effects on Angiogenesis. *Cell*. 2009;137(6):1124-1135. doi:10.1016/j.cell.2009.03.025

391. Kakuda S, Haltiwanger RS. Deciphering the Fringe-Mediated Notch Code: Identification of Activating and Inhibiting Sites Allowing Discrimination between Ligands. *Developmental Cell*. 2017;40(2):193-201. doi:10.1016/j.devcel.2016.12.013

392. Zhang N, Gridley T. Defects in somite formation in lunatic fringe-deficient mice. *Nature*. 1998;394(6691):374-377. doi:10.1038/28625

393. Sparrow DB, Chapman G, Wouters MA, et al. Mutation of the LUNATIC FRINGE Gene in Humans Causes Spondylocostal Dysostosis with a Severe Vertebral Phenotype. *The American Journal of Human Genetics*. 2006;78(1):28-37. doi:10.1086/498879

394. Otomo N, Mizumoto S, Lu HF, et al. Identification of novel LFNG mutations in spondylocostal dysostosis. *J Hum Genet*. 2019;64(3):261-264. doi:10.1038/s10038-018-0548-2

395. Orlova VV, Nahon DM, Cochrane A, et al. Vascular defects associated with hereditary hemorrhagic telangiectasia revealed in patient-derived isogenic iPSCs in 3D vessels on chip. *Stem Cell Reports*. 2022;17(7):1536-1545. doi:10.1016/j.stemcr.2022.05.022

396. Iannucci J, Renehan W, Grammas P. Thrombin, a Mediator of Coagulation, Inflammation, and Neurotoxicity at the Neurovascular Interface: Implications for Alzheimer's Disease. *Front Neurosci*. 2020;14:762. doi:10.3389/fnins.2020.00762

397. Kageyama R, Shimojo H, Isomura A. Oscillatory Control of Notch Signaling in Development. In: Borggrefe T, Giaimo BD, eds. *Molecular Mechanisms of Notch Signaling*. Vol 1066. Advances in Experimental Medicine and Biology. Springer International Publishing; 2018:265-277. doi:10.1007/978-3-319-89512-3_13

398. Holderfield MT, Hughes CCW. Crosstalk Between Vascular Endothelial Growth Factor, Notch, and Transforming Growth Factor-β in Vascular Morphogenesis. *Circulation Research*. 2008;102(6):637-652. doi:10.1161/CIRCRESAHA.107.167171

399. Benjamin D, Sato T, Cibulskis K, Getz G, Stewart C, Lichtenstein L. *Calling Somatic SNVs and Indels with Mutect2*. Bioinformatics; 2019. doi:10.1101/861054

400. Arthur HM, Roman BL. An update on preclinical models of hereditary haemorrhagic telangiectasia: Insights into disease mechanisms. *Front Med*. 2022;9:973964. doi:10.3389/fmed.2022.973964

401. Nigro P, Abe J ichi, Berk BC. Flow Shear Stress and Atherosclerosis: A Matter of Site Specificity. *Antioxidants & Redox Signaling*. 2011;15(5):1405-1414. doi:10.1089/ars.2010.3679

Annex

During my PhD, I have written a book chapter in the form of a minireview with my colleague Mohammad Al Tarras, titled “BMP9/10-ALK1-Endoglin Pathway as a Target of Anti-Angiogenic Therapy in Cancer”. This minireview tackled a side of BMP9/BMP10 signaling that is not directly linked to my main PhD project, but is rather interesting. The minireview is provided in the following pages.

Book Chapter

The BMP9/10-ALK1-Endoglin Pathway as a Target of Anti-Angiogenic Therapy in Cancer

Al Tabosh T[#], Al Tarrass M[#] and Bailly S*

Universite Grenoble Alpes, Inserm, CEA, Biology of Cancer and Infection Laboratory, France

[#]These authors contributed equally to this work

***Corresponding Author:** Bailly S, Universite Grenoble Alpes, Inserm, CEA, Biology of Cancer and Infection Laboratory, F-38000 Grenoble, France

Published **November 26, 2021**

How to cite this book chapter: Al Tabosh T, Al Tarrass M, Bailly S. The BMP9/10-ALK1-Endoglin Pathway as a Target of Anti-Angiogenic Therapy in Cancer. In: Hussein Fayyad Kazan, editor. Immunology and Cancer Biology. Hyderabad, India: Vide Leaf. 2021.

Abstract

The growth and dissemination of solid tumors heavily relies on angiogenesis, making it an attractive therapeutic target in cancer. Tumor angiogenesis is orchestrated by a plethora of secreted factors and signaling pathways. The initial inhibition of the VEGF-pathway, despite successful preclinical studies, yielded only modest clinical benefits in patients, promoting the search

for other anti-angiogenic targets. The BMP9/10-ALK1-endoglin pathway is an important regulator of vascular development. This pathway has been investigated by multiple groups as a therapeutic target for tumor angiogenesis inhibition. For that, various pharmacological and genetic means were used to target different components of this pathway. Here, we recapitulate the outcome of most cellular, preclinical and clinical studies targeting BMP9/10-ALK1-endoglin pathway as an attempt to block tumor angiogenesis.

Introduction

Angiogenesis, the formation of new blood vessels from pre-existing ones, is active during physiological development to provide the growing tissues with an adequate supply of oxygen and nutrients while removing metabolic wastes. In adulthood, the vascular tree generally reaches a quiescent state, with few exceptions including wound healing and the female menstrual cycle. This vascular quiescence is tightly regulated by a variety of pro-angiogenic and anti-angiogenic factors that coordinate angiogenic processes in a spatiotemporal manner [1]. Vascular endothelial growth factor (VEGF), basic fibroblastic growth factor (bFGF), angiogenin, thrombospondin (TSP), angiopoietins, and transforming growth factor-β (TGF-β) are all examples of angiogenic factors that control the ON-OFF angiogenic switch [2]. In solid malignancies, dysregulation of the angiogenic switch towards the pro-angiogenic phenotype promotes the development of a highly vascularized niche that supports tumor growth and provides an escape route for metastatic dissemination [3]. Therefore, inhibition of tumor angiogenesis is considered an important therapeutic strategy in cancer treatment [4].

The main goal of anti-angiogenic therapies is to abrogate the formation of new blood vessels within the tumor, in an attempt to deprive cancer cells from oxygen and nutrients, and consequently inhibit tumor growth and progression. Moreover, tumor induced angiogenesis is associated with the formation of aberrant vascular network characterized by acidosis, interstitial hypertension and hypoxia. This abnormal microenvironment

endangers the efficacy and proper delivery of therapeutics to solid tumors [5]. Therefore, the development of anti-angiogenic therapies and combining them with cytotoxic drugs constitutes an important aspect in cancer therapies.

Targeting VEGF signaling has been demonstrated as the prime antiangiogenic target in the clinic for the last two decades. Anti-VEGF therapies, including blocking antibodies against VEGF (bevacizumab), kinase inhibitors (sunitinib, imatinib, sorafenib, axitinib and regorafenib), and decoy receptors, have been included in the first line therapies against advanced and metastatic cancers [6]. Unfortunately, in contrast to the promising results from preclinical studies, the use of this monotherapy has yielded only modest therapeutic benefit in some tumor types, failed in others and was associated with the generation of resistant and more aggressive tumors [7,8]. Hence, alternative and/or complementary therapeutics directed at novel targets of vascular development are urgently needed.

Members of the Transforming growth β (TGF-β) superfamily of signaling molecules have been previously described as important modulators of vasculogenic and angiogenic processes. Among them, BMP9 and BMP10, which bind with high affinity to a signaling complex of receptors composed of activin receptor-like-kinase-1 (ALK1) and endoglin [9] which are mostly expressed on endothelial cells, play an essential role in vascular development [10]. This signaling complex is composed of two type I receptors (ALK1), two type II receptors (BMPRII, ActRIIA or ActRIIB) and the co-receptor endoglin. Both type I and type II receptors possess Serine/Threonine kinase activities. Binding of BMP9/10 to this receptor complex leads to the phosphorylation of ALK1 by the constitutively active type II receptor. Consequently, activated ALK1 phosphorylates transcription factors known as Smads that modulate target gene expression [9,11,12]. Endoglin is a homodimeric cell-surface co-receptor that lacks enzymatic activity and functions as a co-receptor in association with ALK1, enhancing ALK1 signaling [13]. ALK1 and endoglin display highly similar expression patterns, being mostly restricted to endothelial cells. Complete genetic ablation of either ALK1 or endoglin in mice results in

embryonic lethality due to impairment of blood vessel development [14]. In addition, heterozygous loss-of-function mutations in either gene in humans give rise to two closely related forms of the vascular disorder hereditary hemorrhagic telangiectasia (HHT) [15].

Interestingly, an elevated expression level of both ALK1 and endoglin was reported in the angiogenic tumor endothelium [16,17] and the BMP9/10-ALK1-endoglin pathway was proposed to be involved in resistance to anti-VEGF therapy in tumors [18]. In addition, BMP9 is known to regulate the development of lymphatic vessels [19,20], which has implications for metastatic spread of tumor cells through lymphatic vasculature [21]. As a result, the BMP9/10-ALK1-endoglin signaling pathway emerged as an interesting candidate target for anti-angiogenic cancer therapies. Consequently, extensive *in vitro* and *in vivo* studies have been performed in the past two decades to investigate the implication of this pathway in tumor angiogenesis, using multiple cancer models. Most preclinical studies revealed promising anti-angiogenic responses, giving rise to several clinical trials aiming to improve the overall survival of cancer patients. Here, we provide a brief overview of the cellular, preclinical and clinical studies targeting BMP9/10-ALK1-endoglin pathway as an attempt to block tumor angiogenesis.

Targeting ALK1 as an Anti-Angiogenic Therapy in Cancer

Different biological compounds have been designed/identified to interfere with ALK1 signaling including the BMP type-I receptor inhibitors LDN-193189 [22], OD16 and OD29 [23], and the miRNA miR-199b-5p [24], all of which have demonstrated effective inhibition of ALK1 signaling. However, the specificity of designed drugs and crosstalk with other pathways make it difficult to predict the final outcome of such inhibitors. For this reason, targeting ALK1 have been majorly studied in the context of tumor angiogenesis through highly specific designed products such as ALK1-Fc fusion ligand trap (dalantercept/ACE-041) developed by Acceleron Pharma Inc [25], and PF-03446962

(fully human antibody that targets extracellular domain of ALK1) developed by Pfizer [26], both of which have been implicated in independent clinical trials.

Preclinical Studies

ALK1 Ligand Trap

The characterization of the ALK1-Fc fusion protein has demonstrated its ability to specifically trap BMP9 and BMP10, but not any other ligand of the TGF-β family [27]. In vitro studies showed that dalantercept, and its mouse counterpart RAP-041, inhibited BMP9 and BMP10 induced Smad1/5 phosphorylation and downstream signaling (e.g, id1 gene expression), without affecting TGF-β induced Smad2 phosphorylation [27,28]. Moreover, functional assays showed that dalantercept blocks cord formation and endothelial sprouting *in vitro* in human umbilical vein endothelial cells (HUVEC), as well as FGF induced neovascularization and VEGF-induced vessel formation *in vivo* in a chick chorioallantoic membrane (CAM) assay [27]. The anti-tumor effects of ALK-1 Fc were primarily investigated through the application of RAP-041 in rat insulin promoter – SV40 large T antigen (RIP1-Tag2) model of pancreatic neuroendocrine tumorigenesis. Results showed an impaired tumor growth already after 2 weeks [28] and a decrease in the number of hepatic micro metastasis compared to the control cohort after a prolonged 4-week treatment [29]. Similar results have been obtained by blocking metastatic dissemination in the transgenic spontaneous mouse mammary tumor virus (MMTV)-polyoma middle T antigen (PyMT) and the syngeneic transplantable E0771 breast cancer models [30]. Likewise, dalantercept reduced tumor burden in MCF-7 mammary adenocarcinoma orthotopic model [27]. On the other hand, in another study of poorly/non-metastatic melanoma, breast, head and neck cancer, no effect was observed on primary tumor growth at the experimental endpoint following the use of RAP-041 as a monotherapy [31].

ALK1 Antibody

The ALK1 antibody (PF-03446962) directly binds to the extracellular domain of ALK1 (residues 42-56) with a high affinity, but doesn't bind to other closely related ALKs, such as ALK2/3/4/5/or ALK7, thus reducing potential off-target effects. *In vitro* studies demonstrated that PF-03446962 prevented binding of BMP9 to endothelial cells (ECs), inhibited BMP9-induced Smad1 phosphorylation, and BMP responsive element (BRE)-luciferase transcriptional reporter activity [32]. Moreover, the monoclonal antibody efficiently blocked serum-induced Smad1 phosphorylation, migration, endothelial sprouting, as well as tube formation in HUVECs [32,33]. Similarly, a reduction in tumor growth and inhibition of both microvascular and lymphatic vessel density has been reported in MDA-MB-231 human breast cancer xenografts when using PF-03446962 [33].

Although both strategies are directed to block the signaling through ALK1, the modes of action of dalantercept and PF-03446962 are distinct, one blocking the ligands the other blocking the receptor. Both approaches demonstrated that ALK1-targeting induces changes in the vascular network and subsequent alterations in the tumor microenvironment, described through in-depth vasculature characterization using several approaches such as monitoring pericyte coverage, vascular perfusion, as well as sprouting and leakiness of the vessels [30-34], all of which are critical factors that describe what is known by "vascular normalization". In the context of tumor anti-angiogenic therapies, the vascular normalization hypothesis states that antiangiogenic therapy aims to restore the balance between pro- and antiangiogenic factors back towards equilibrium. As a result, vessel structure and function become more normal: vessels are more mature with enhanced perivascular coverage, blood flow is more homogeneous, vessel permeability and hypoxia are reduced, and importantly the delivery of systemically administered anticancer therapies into tumors is more uniform [35]. Nevertheless, contradicting data have been described when assessing the functionality of the tumor-associated vasculature following administration of either RAP-041 or PF-03446962. For instance, PF-03446962

quantitatively disrupted vascular normalization in M24met/R xenograft tumors [33], while ALK1-Fc treatment that increased coverage of tumor endothelial cells by NG2-expressing cells (i.e. pericytes) [31]. Hu-lowe et al [33] displayed that flow rates were only affected in large, functional blood vessels, whereas smaller ones were unaffected. Contradictory to this result, Hawinkels et al [31] described a slight increase in perfusion. These results demonstrate that targeting the same receptor by two different approaches in different tumor models yields different results, and suggests more investigation of the underlying mechanisms following ALK1 activation.

Alk1+/- Mice

Other means of targeting ALK1 signaling as a therapeutic approach in cancer angiogenesis include genetic approaches using heterozygote mice. Cunha et al reported that blunted ALK1 expression using RIP1-Tag2; $Alk1^{+/-}$ mice showed a significant retardation in tumor progression through the angiogenic switch, reduced de novo tumor growth, and impaired angiogenesis in comparison to RIP1-Tag2; $Alk1^{+/+}$ mice, consistent with results of using RAP-041 which has been addressed in this same work [28,29].

Combinatory Treatments

Combinatorial treatments of ALK1-blocking agents with other targeted therapies have also shown promising results in targeting both tumor angiogenesis and progression. For instance, combined use of ALK1-Fc fusion along with chemotherapy (Doxorubicin or Cisplatin) has shown increased cytotoxic effect and impaired tumor growth in melanoma, head and neck cancer, and breast cancer models [31]. Likewise, in experimental breast carcinomas, RAP-041-induced blunted vessel density was further diminished in combined therapy group (RAP-041 + Docetaxel), accompanied by a significant reduction in the metastatic count in the lungs [30]. Moreover, Dual targeting of VEGF and BMP9/10 signals using a newly designed ALK1FLT1-Fc (ALK-Fc fused to VEGFR1-Fc) trap significantly inhibited both angiogenesis and growth of human

BxPC3 pancreatic tumor xenografts [36]. Of note, co-administration of RAP-041 and VEGFR2 neutralizing antibody DC101 showed no additional therapeutic benefit in MMTV-PyMT breast cancer model [30]. Interestingly, tumors described previously as resistant to VEGF inhibitors showed a significant decrease in tumor burden and associated vasculature when exposed to PF-03446962, through a mechanism suggesting disruption of vascular normalization phenotype induced by bevacizumab [33]. It was also shown that combinatorial use of dalantercept with the VEGFR2 tyrosine kinase inhibitor sunitinib leads to tumor stasis in renal cell carcinoma [37].

Clinical Trials

The results obtained from preclinical studies of the two ALK1 targeting agents in different cancer models prompted several clinical trials to assess safety, pharmacokinetics, pharmacodynamics, and anti-tumor efficacy in patients with advanced cancer, either as monotherapy or in combination with other antiangiogenic approaches. Phase I clinical trials in patients with different tumors, including non-small lung cancer carcinoma, hepatocellular carcinoma (HCC), persistent or recurrent ovarian carcinoma and related malignancies, as well as relapsed/refractory multiple myeloma showed that both dalantercept and PF-03446962 were generally well tolerated, gave promising and motivating responses, and had a manageable safety profile distinct from that of anti-VEGF therapy [26,38-40]. None of the patients enrolled in these clinical trials displayed the most severe adverse events (AE) reported following bevacizumab treatment (gastrointestinal perforation, impaired wound healing, and serious bleeding). Commonly observed AE upon dalantercept administration were peripheral oedema, fatigue and anemia, whilst fatigue, nausea and thrombocytopenia (not associated with bleeding) were typical of PF-03446962 infusion [25,26]. Moreover, several patients enrolled in these trials developed telangiectases, which are often observed in HHT patients, demonstrating an on-target effect of blocking ALK1 receptor signaling. Though safe, independent phase II clinical trials utilizing dalantercept as monotherapy in patients with recurrent/persistent endometrial carcinoma, ovarian

carcinoma, and squamous cell carcinoma of the head and neck revealed insufficient single agent activity with limited efficacy that did not reach the intended primary endpoint [41-43]. Similarly, phase II clinical trials assessing the efficacy of PF-03446962 in pre-treated patients with refractory urothelial cancer and advanced malignant pleural mesothelioma demonstrated no or limited activity as single drug [44,45].

Acceleron Pharma Inc has recruited patients to test efficacy of combining dalantercept with sorafenib and axitinib in advanced HCC and renal cell carcinoma (RCC), respectively. Results from the dose-escalation and expansion cohorts evaluating the combination of dalantercept plus axitinib in advanced RCC showed that the combination of these two therapies is well tolerated and associated with a clinical response [46]. However, the phase II trial of this combination in RCC patients showed that the addition of dalantercept to axitinib did not appear to improve treatment-related outcomes in previously treated patients with advanced RCC reporting 1 treatment related death and a lower objective response rate in the combination group (19%) in comparison to placebo plus axitinib (24.6%). Likewise, combinatorial phase Ib study of dalantercept and sorafenib showed no improvement in antitumor activity in patients with HCC [47]. In a similar fashion, Pfizer also tested the combination of PF-03446962 with regorafenib in patients with refractory metastatic colorectal cancer, however the combined therapy was associated with unacceptable toxicity and did not demonstrate notable clinical activity in these patients [48].

Targeting Endoglin as an Anti-Angiogenic Therapy in Cancer

Another proposed anti-tumorigenic target within the ALK1 signaling pathway is endoglin (CD105). Several lines of evidence support the rationale for targeting endoglin as a novel anti-angiogenic therapy in cancer. Endoglin is highly expressed on the tumor-associated vascular and lymphatic endothelium, and its expression holds prognostic significance in certain tumors [17]. In addition, gene expression profiling of circulating endothelial cells (CEC), which are elevated in the blood of

cancer patients and are thought to contribute to tumor angiogenesis, revealed an increase of endoglin expression of CEC-enriched samples from metastatic patients compared to healthy subjects [49]. Moreover, a soluble form of endoglin, which is shed following cleavage of the membrane-bound form by matrix metalloproteinase 14 [50], is detected in the serum of patients with different solid tumors [17]. Last but not least, anti-VEGF was shown to increase endoglin expression on tumor-endothelial cells [51], in line with suggestions implicating the ALK1 signaling pathway in resistance to anti-VEGF therapies.

With that, several groups focused on targeting endoglin to suppress tumor angiogenesis, either by directly blocking endoglin using an antibody raised against it or by sequestering its ligands through an endoglin ligand trap composed of the extracellular region of endoglin fused to an immunoglobulin Fc domain (Eng-Fc).

Preclinical Studies

Endoglin Antibody

In vitro, TRC105, a chimeric antibody that binds human endoglin with high avidity, triggered the apoptosis of HUVECs through antibody-dependent cellular cytotoxity [52]. Preclinically, SN6j, a parental antibody of TRC105, showed promising anti-tumorigenic effects without significant side effects. Antibody treatment reduced microvessel density and angiogenesis in multiple metastatic tumor models and suppressed tumor metastasis, leading to prolonged survival of the tumor-bearing mice [53]. In addition, combination of SN6j with the chemotherapeutic agent cyclophosphamide synergistically enhanced antitumor efficacy [54].

Endoglin Ligand Trap and Genetic Targeting

Endoglin ligand traps also triggered anti-angiogenic responses both *in vitro* and *in vivo*. Exogenous treatment or expression of HUVECs with Eng-Fc efficiently inhibited spontaneous and VEGF-induced sprouting on matrigel and in 3D collagen matrices [50]. *In vivo*, Eng-Fc blocked angiogenesis by

suppressing VEGF-induced vessel formation or sprouting in CAM assay and angioreactors respectively. The ligand trap also successfully decreased tumor burden in a colon-26 adenocarcinoma model [55]. Contrary to these findings, one group exploring the impact of single or dual genetic targeting of ALK1 and endoglin on tumor angiogenesis reported no effect of genetic ablation of one copy of the *Eng* gene on tumor angiogenesis and growth in a mouse model of pancreatic neuroendocrine tumors [56]. On the other hand, reducing Acvrl1 gene dosage in the same model decreased tumor vasculature and delayed tumor growth. Interestingly, dual targeting of Acvrl1 and Eng, through genetic ablation of one copy of each gene, resulted in a synergistic reduction of overall tumor burden, suggesting a beneficial impact of combinatorial targeting of ALK1 and endoglin. The different effects of endoglin targeting on tumor angiogenesis could be explained by the different levels of target inhibition when using antibodies versus genetic ablation of a single *Eng* allele or by inherent differences between disease models rendering some more responsive to therapy than others.

Clinical Trials

The encouraging preclinical results led to some phase I clinical studies assessing TRC105 safety, pharmacokinetics and anti-tumor efficacy in patients with advanced or metastatic solid tumors [57,58]. In these studies, TRC105 resulted in a short-term stable disease in some patients with two showing exceptional ongoing responses after 18 and 48 months. The safety assessment of TRC105 identified well-tolerated adverse events at clinically relevant doses mostly comprising infusion reactions, low-grade headaches and anemia that is probably caused by suppression of endoglin-expressing proerythroblasts. Interestingly, some patients receiving TRC105 developed mucocutaneous telangiectases [58] or epistaxis [57], well known symptoms of the vascular disorder HHT caused by endoglin or ALK1 mutations, demonstrating on-target effect of TRC105. Finally, TRC105 treatment induced a significant induction of VEGF levels in patients of one study, which could be a potential compensatory mechanism for the anti-angiogenic effect of TRC105 [57]. This further encouraged combination therapies

comprising TRC105 and anti-VEGF treatments, which is feasible due to the distinct identified safety profile of TRC105 compared to anti-VEGF therapies.

These studies were followed by a phase II clinical trial assessing the tolerability and efficacy of TRC105 administration on 13 heavily pre-treated patients with urothelial carcinoma. TRC105 was once again well-tolerated, but its anti-tumor activity was not satisfactory with only 2 patients achieving stable disease for 4 months and a median overall survival of 8.3 months [59]. However, in this study TRC105 seemed to have a positive impact on immune subsets, notably regulatory T cells, suggesting potential benefit for combining TRC105 with immunotherapy. In support of that, enhanced therapeutic effects were recently reported when combining TRC105 with PD1 inhibition in four preclinical cancer models [60].

Another phase II study aimed to investigate the efficacy of TRC105 administration in HCC patients that have previously progressed on sorafenib. Evidence of clinical activity was not enough to proceed [61], but combination therapy with sorafenib in HCC was tested in a following phase I trial [61]. The combination of both agents was well-tolerated using the recommended single agent doses and encouraging activity triggered the launch of a phase II study. A few other clinical trials assessed the combination of TRC105 with other VEGF-targeting agents such as bevacizumab [62,63] and axitinib [64]. The combination of TRC105 with bevacizumab was well-tolerated [62]. Despite initial reports showing clinical response, TRC105 addition to bevacizumab failed to improve progression-free survival in patients with refractory metastatic RCC [63]. Following this trial, TRC105's efficacy was assessed with axitinib instead of bevacizumab in metastatic RCC patients. This combination therapy was also well-tolerated and provided encouraging evidence of activity leading to further investigations [64].

Targeting BMP9 and BMP10 as an Anti-Angiogenic Therapy in Cancer

Most preclinical studies addressing the role of the ALK1 signaling pathway in tumor angiogenesis relied on the pharmacological targeting of ALK1 or endoglin, either using neutralizing antibodies or soluble forms of ALK1 or endoglin. However, these approaches globally suppress the signaling pathway without considering potential specific roles of BMP9 versus BMP10 in tumor angiogenesis. By following tumor growth and dissemination in a syngeneic orthotopic mammary cancer model genetically deficient in *Bmp9*, *Bmp10* or both, we showed that deletion of *Bmp9*, but not *Bmp10*, increases tumor vascular density and decreases vessel normalization, leading to enhanced tumor growth and metastasis [65]. In addition, mice deficient in both *Bmp9* and *Bmp10* did not show any added therapeutic benefit compared to *Bmp9*-deficient mice. These results suggest that BMP10 targeting can be omitted, and specific targeting of BMP9 rather than ALK1 or endoglin could be more suitable in this model. Interestingly, this study also highlighted BMP9 as an angiogenic quiescence factor that promotes vessel normalization. In this case, activating the BMP9 pathway rather than blocking it can provide new means for cancer therapy, especially when combined with chemo- or immunotherapies [65]. In line with the role of BMP9 as a vascular quiescence factor, Bmp9 deficiency in a pancreatic neuroendocrine tumor model led to hyperbranching and increased metastases, despite a contradictory decrease in tumor growth [56]. On the other hand, blocking BMP9 through a monoclonal anti-BMP9 antibody showed anti-tumor activity and an increase in the normalization of tumor blood vessels in a model of RCC [66]. All in all, targeting different components, and sometimes even the same element, within a signaling pathway can yield different or opposing outcomes in different models.

Conclusion

The BMP9/10-ALK1-endoglin pathway is an important regulator of vascular development that recently captivated the attention of

the scientific and medical community as a target for inhibiting tumor angiogenesis and growth [67]. Several groups attempted to block different components of this pathway (ALK1, endoglin or BMP9) using distinct pharmacological and genetic means either alone or in combination with chemo- or antiangiogenic therapy. Despite the encouraging reported effects of blocking this pathway on tumor angiogenesis and growth in most preclinical models tested, single agent therapies in patients with different solid malignancies generated only modest effects. In this regard, combinatorial clinical trials integrating BMP9/10-ALK1-endoglin and other pathways targeting agents are still ongoing with the hope of better potential.

Targeting the tumor vasculature to "starve a tumor to death" instead of targeting tumor cells with chemotherapeutic drugs was conceived over four decades ago and has led to the development of antiangiogenic drugs approved in cancer since now two decades. However, antiangiogenic therapies so far have not fulfilled expectations and provide only transitory improvements. More recent work is now proposing the opposite, that is to promote angiogenesis in order to increase influx of chemotherapeutic drugs into tumor cells [68]. It will be interesting in the future to see how the BMP9/10-ALK1-endoglin pathway will fit into this new hypothesis.

References

1. Ricard N, Bailly S, Guignabert C, Simons M. The quiescent endothelium: signalling pathways regulating organ-specific endothelial normalcy. Nat Rev Cardiol. 2021; 18: 565–580.
2. Ribatti D, Nico B, Crivellato E, Roccaro AM, Vacca A. The history of the angiogenic switch concept. Leukemia. 2007; 21: 44–52.
3. Bergers G, Benjamin LE. Tumorigenesis and the angiogenic switch. Nat Rev Cancer. 2003; 3: 401–410.
4. Marmé D. Tumor Angiogenesis: A Key Target for Cancer Therapy. Oncol Res Treat. 2018; 41: 164.
5. Munn LL. Aberrant vascular architecture in tumors and its importance in drug-based therapies. Drug Discov Today. 2003; 8: 396–403.

6. Meadows KL, Hurwitz HI. Anti-VEGF Therapies in the Clinic. Cold Spring Harbor Perspectives in Medicine. 2012; 2: a006577–a006577.
7. Crawford Y, Ferrara N. Tumor and stromal pathways mediating refractoriness/resistance to anti-angiogenic therapies. Trends in Pharmacological Sciences. 2009; 30: 624–630.
8. Kieran MW, Kalluri R, Cho YJ. The VEGF pathway in cancer and disease: responses, resistance, and the path forward. Cold Spring Harb Perspect Med. 2012; 2: a006593.
9. David L, Mallet C, Mazerbourg S, Feige JJ, Bailly S. Identification of BMP9 and BMP10 as functional activators of the orphan activin receptor-like kinase 1 (ALK1) in endothelial cells. Blood. 2007; 109: 1953–1961.
10. Desroches-Castan A, Tillet E, Bouvard C, Bailly S. BMP9 and BMP10 : Two close vascular quiescence partners that stand out. Developmental Dynamics. 2021.
11. Townson SA. Specificity and Structure of a High Affinity Activin Receptor-like Kinase 1 (ALK1) Signaling Complex. Journal of Biological Chemistry. 2012; 287: 27313–27325.
12. Shi Y, Massagué J. Mechanisms of TGF-β Signaling from Cell Membrane to the Nucleus. Cell. 2003; 113: 685–700.
13. Kim SK, Henen MA, Hinck AP. Structural biology of betaglycan and endoglin, membrane-bound co-receptors of the TGF-beta family. Exp Biol Med (Maywood). 2019; 244: 1547–1558.
14. Tual-Chalot S, Oh SP, Arthur HM. Mouse models of hereditary hemorrhagic telangiectasia: recent advances and future challenges. Front. Genet. 2015; 6.
15. Dupuis-Girod S, Bailly S, Plauchu H. Hereditary hemorrhagic telangiectasia: from molecular biology to patient care: Hereditary hemorrhagic telangiectasia. Journal of Thrombosis and Haemostasis. 2010; 8: 1447–1456.
16. Seki T, Yun J, Oh SP. Arterial endothelium-specific activin receptor-like kinase 1 expression suggests its role in arterialization and vascular remodeling. Circ Res. 2003; 93: 682–689.
17. Bernabeu C, Lopez-Novoa JM, Quintanilla M. The emerging role of TGF-β superfamily coreceptors in cancer. Biochimica

et Biophysica Acta (BBA) - Molecular Basis of Disease. 2009; 1792: 954–973.
18. Hu-Lowe DD. Targeting Activin Receptor-Like Kinase 1 Inhibits Angiogenesis and Tumorigenesis through a Mechanism of Action Complementary to Anti-VEGF Therapies. Cancer Res. 2011; 71: 1362–1373.
19. Niessen K, Zhang G, Ridgway JB, Chen H, Yan M. ALK1 signaling regulates early postnatal lymphatic vessel development. Blood. 2010; 115: 1654–1661.
20. Levet S. Bone morphogenetic protein 9 (BMP9) controls lymphatic vessel maturation and valve formation. Blood. 2013; 122: 598–607.
21. Duong T, Koopman P, Francois M. Tumor lymphangiogenesis as a potential therapeutic target. J Oncol. 2012; 2012: 204946.
22. Cuny GD. Structure-activity relationship study of bone morphogenetic protein (BMP) signaling inhibitors. Bioorg Med Chem Lett. 2008; 18: 4388–4392.
23. Ma J. Inhibiting Endothelial Cell Function in Normal and Tumor Angiogenesis Using BMP Type I Receptor Macrocyclic Kinase Inhibitors. Cancers (Basel). 2021; 13: 2951.
24. Lin X. MiR-199b-5p Suppresses Tumor Angiogenesis Mediated by Vascular Endothelial Cells in Breast Cancer by Targeting ALK1. Front Genet. 2019; 10: 1397.
25. Bendell JC. Safety, pharmacokinetics, pharmacodynamics, and antitumor activity of dalantercept, an activin receptor-like kinase-1 ligand trap, in patients with advanced cancer. Clin Cancer Res. 2014; 20: 480–489.
26. Simonelli M. Phase I study of PF-03446962, a fully human monoclonal antibody against activin receptor-like kinase-1, in patients with hepatocellular carcinoma. Ann Oncol. 2016; 27: 1782–1787.
27. Mitchell D. ALK1-Fc inhibits multiple mediators of angiogenesis and suppresses tumor growth. Mol Cancer Ther. 2010; 9: 379–388.
28. Cunha SI. Genetic and pharmacological targeting of activin receptor-like kinase 1 impairs tumor growth and angiogenesis. J Exp Med. 2010; 207: 85–100.

29. Eleftheriou NM. Compound genetically engineered mouse models of cancer reveal dual targeting of ALK1 and endoglin as a synergistic opportunity to impinge on angiogenic TGF-β signaling. Oncotarget. 2016; 7: 84314–84325.
30. Cunha SI. Endothelial ALK1 Is a Therapeutic Target to Block Metastatic Dissemination of Breast Cancer. Cancer Res. 2015; 75: 2445–2456.
31. Hawinkels LJAC. Activin Receptor-like Kinase 1 Ligand Trap Reduces Microvascular Density and Improves Chemotherapy Efficiency to Various Solid Tumors. Clin Cancer Res. 2016; 22: 96–106.
32. van Meeteren LA. Anti-human activin receptor-like kinase 1 (ALK1) antibody attenuates bone morphogenetic protein 9 (BMP9)-induced ALK1 signaling and interferes with endothelial cell sprouting. J Biol Chem. 2012; 287: 18551–18561.
33. Hu-Lowe DD. Targeting activin receptor-like kinase 1 inhibits angiogenesis and tumorigenesis through a mechanism of action complementary to anti-VEGF therapies. Cancer Res. 2011; 71: 1362–1373.
34. Cunha SI, Pietras K. ALK1 as an emerging target for antiangiogenic therapy of cancer. Blood. 2011; 117: 6999–7006.
35. Goel S, Wong AHK, Jain RK. Vascular Normalization as a Therapeutic Strategy for Malignant and Nonmalignant Disease. Cold Spring Harb Perspect Med. 2012; 2: a006486.
36. Akatsu Y. Dual targeting of vascular endothelial growth factor and bone morphogenetic protein-9/10 impairs tumor growth through inhibition of angiogenesis. Cancer Sci. 2017; 108: 151–155.
37. Wang X. Inhibition of ALK1 signaling with dalantercept combined with VEGFR TKI leads to tumor stasis in renal cell carcinoma. Oncotarget. 2016; 7: 41857–41869.
38. Goff LW. A Phase I Study of the Anti-Activin Receptor-Like Kinase 1 (ALK-1) Monoclonal Antibody PF-03446962 in Patients with Advanced Solid Tumors. Clin Cancer Res. 2016; 22: 2146–2154.

39. Doi T. A phase I study of the human anti-activin receptor-like kinase 1 antibody PF-03446962 in Asian patients with advanced solid tumors. Cancer Med. 2016; 5: 1454–1463.
40. Bendell JC. Safety, pharmacokinetics, pharmacodynamics, and antitumor activity of dalantercept, an activin receptor-like kinase-1 ligand trap, in patients with advanced cancer. Clin Cancer Res. 2014; 20: 480–489.
41. Burger RA. Phase II evaluation of dalantercept in the treatment of persistent or recurrent epithelial ovarian cancer: An NRG Oncology/Gynecologic Oncology Group study. Gynecol Oncol. 2018; 150: 466–470.
42. Makker V. Phase II evaluation of dalantercept, a soluble recombinant activin receptor-like kinase 1 (ALK1) receptor fusion protein, for the treatment of recurrent or persistent endometrial cancer: an NRG Oncology/Gynecologic Oncology Group Study 0229N. Gynecol Oncol. 2015; 138: 24–29.
43. Jimeno A. A phase 2 study of dalantercept, an activin receptor-like kinase-1 ligand trap, in patients with recurrent or metastatic squamous cell carcinoma of the head and neck. Cancer. 2016; 122: 3641–3649.
44. Necchi A. PF-03446962, a fully-human monoclonal antibody against transforming growth-factor β (TGFβ) receptor ALK1, in pre-treated patients with urothelial cancer: an open label, single-group, phase 2 trial. Invest New Drugs. 2014; 32: 555–560.
45. Wheatley-Price P. A Phase II Study of PF-03446962 in Patients with Advanced Malignant Pleural Mesothelioma. CCTG Trial IND.207. J Thorac Oncol. 2016; 11: 2018–2021.
46. Voss MH. The DART Study: Results from the Dose-Escalation and Expansion Cohorts Evaluating the Combination of Dalantercept plus Axitinib in Advanced Renal Cell Carcinoma. Clin Cancer Res. 2017; 23: 3557–3565.
47. Abou-Alfa GK. A Phase Ib, Open-Label Study of Dalantercept, an Activin Receptor-Like Kinase 1 Ligand Trap, plus Sorafenib in Advanced Hepatocellular Carcinoma. Oncologist. 2019; 24: 161-e170.
48. Clarke JM. A phase Ib study of the combination regorafenib with PF-03446962 in patients with refractory metastatic

colorectal cancer (REGAL-1 trial). Cancer Chemother Pharmacol. 2019; 84: 909–917.
49. Smirnov DA. Global Gene Expression Profiling of Circulating Endothelial Cells in Patients with Metastatic Carcinomas. Cancer Res. 2006; 66: 2918–2922.
50. Hawinkels LJAC. Matrix Metalloproteinase-14 (MT1-MMP)–Mediated Endoglin Shedding Inhibits Tumor Angiogenesis. Cancer Res. 2010; 70: 4141–4150.
51. Bockhorn M. Differential vascular and transcriptional responses to anti-vascular endothelial growth factor antibody in orthotopic human pancreatic cancer xenografts. Clin Cancer Res. 2003; 9: 4221–4226.
52. Seon BK. Endoglin-targeted cancer therapy. Curr Drug Deliv. 2011; 8: 135–143.
53. Uneda S. Anti-endoglin monoclonal antibodies are effective for suppressing metastasis and the primary tumors by targeting tumor vasculature. Int J Cancer. 2009; 125: 1446–1453.
54. Takahashi N, Haba A, Matsuno F, Seon BK. Antiangiogenic therapy of established tumors in human skin/severe combined immunodeficiency mouse chimeras by anti-endoglin (CD105) monoclonal antibodies, and synergy between anti-endoglin antibody and cyclophosphamide. Cancer Res. 2001; 61: 7846–7854.
55. Castonguay R. Soluble Endoglin Specifically Binds Bone Morphogenetic Proteins 9 and 10 via Its Orphan Domain, Inhibits Blood Vessel Formation, and Suppresses Tumor Growth. Journal of Biological Chemistry. 2011; 286: 30034–30046.
56. Nikolas M Eleftheriou, Jonas Sjölund, Matteo Bocci, Eliane Cortez, Se-Jin Lee. et al. Compound genetically engineered mouse models of cancer reveal dual targeting of ALK1 and endoglin as a synergistic opportunity to impinge on angiogenic TGF-β signaling. Oncotarget. 2016; 7: 84314–84325.
57. Karzai FH. A phase I study of TRC105 anti-endoglin (CD105) antibody in metastatic castration-resistant prostate cancer. BJU Int. 2015; 116: 546–555.

58. Rosen LS. A Phase I First-in-Human Study of TRC105 (Anti-Endoglin Antibody) in Patients with Advanced Cancer. Clinical Cancer Research. 2012; 18: 4820–4829.
59. Apolo AB. A Phase II Clinical Trial of TRC105 (Anti-Endoglin Antibody) in Adults With Advanced/Metastatic Urothelial Carcinoma. Clin Genitourin Cancer. 2017; 15: 77–85.
60. Schoonderwoerd MJA. Targeting Endoglin-Expressing Regulatory T Cells in the Tumor Microenvironment Enhances the Effect of PD1 Checkpoint Inhibitor Immunotherapy. Clin Cancer Res. 2020; 26: 3831–3842.
61. Duffy AG. Phase I and Preliminary Phase II Study of TRC105 in Combination with Sorafenib in Hepatocellular Carcinoma. Clin Cancer Res. 2017; 23: 4633–4641.
62. Gordon MS. An open-label phase Ib dose-escalation study of TRC105 (anti-endoglin antibody) with bevacizumab in patients with advanced cancer. Clin Cancer Res. 2014; 20: 5918–5926.
63. Dorff TB. Bevacizumab alone or in combination with TRC105 for patients with refractory metastatic renal cell cancer. Cancer. 2017; 123: 4566–4573.
64. Toni K Choueiri, M Dror Michaelson, Edwin M Posadas, Guru P Sonpavde, David F McDermott, et al. An Open Label Phase Ib Dose Escalation Study of TRC105 (Anti-Endoglin Antibody) with Axitinib in Patients with Metastatic Renal Cell Carcinoma. Oncologist. 2019; 24: 202–210.
65. Marie Ouarné, Claire Bouvard, Gabriela Boneva, Christine Mallet, Johnny Ribeiro, et al. BMP9, but not BMP10, acts as a quiescence factor on tumor growth, vessel normalization and metastasis in a mouse model of breast cancer. J Exp Clin Cancer Res. 2018; 37: 209.
66. Verena Brand, Christian Lehmann, Christian Umkehrer, Stefan Bissinger, Martina Thier, et al. Impact of selective anti-BMP9 treatment on tumor cells and tumor angiogenesis. Molecular Oncology. 2016; 10: 1603–1620.
67. Sherwood LM, Parris EE, Folkman J. Tumor Angiogenesis: Therapeutic Implications. New England Journal of Medicine. 1971; 285: 1182–1186.
68. Rivera LB, Bergers G. CANCER. Tumor angiogenesis, from foe to friend. Science. 2015; 349: 694–695.